AD-A087 433 JOHNS HOPKINS UNIV LAUREL MD APPLIED PHYSICS LAB F/G 8/14
THE INVESTIGATION OF THE MAGNETOSPHERIC DYNAMICS IN CONJUNCTION--ETC(U)
DEC 79 C MENG N00017-72-C-4401
UNCLASSIFIED AFGL-TR-80-0070 NL

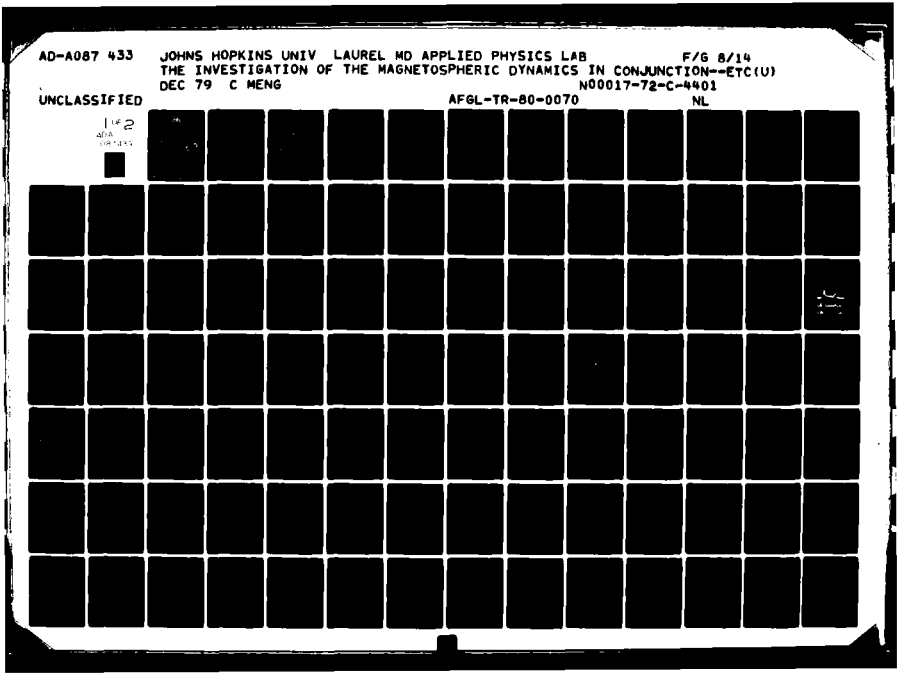

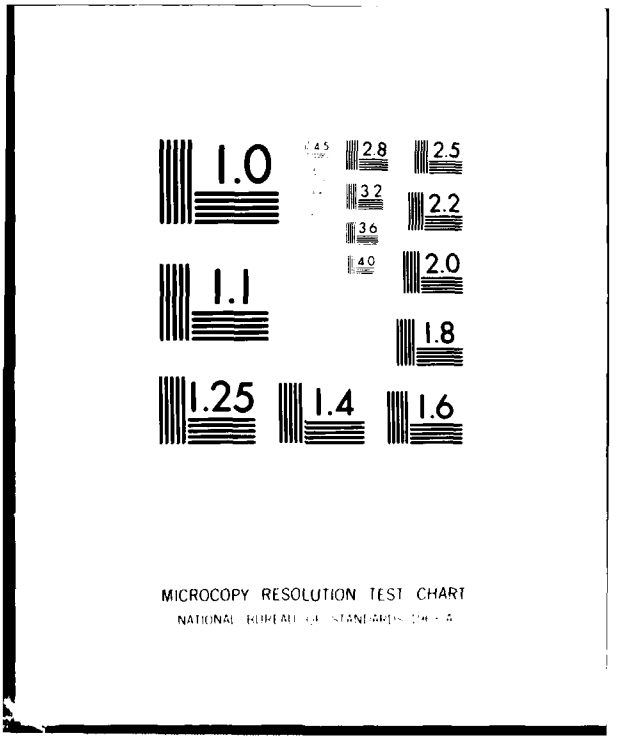
1.0
2.8
2.5
3.2
2.2
3.6
4.0
2.0
1.1
1.8
1.25
1.4
1.6
MICROCOPY RESOLUTION TEST CHART
NATIONAL BUREAU OF STANDARDS

12 B.S.

(18) AFGL-TR-80-0076 (19)

(6) THE INVESTIGATION OF THE MAGNETOSPHERIC DYNAMICS IN CONJUNCTION WITH THE SCATHA SATELLITE OBSERVATIONS.

(10) Ching-I. Meng

Applied Physics Laboratory
Johns Hopkins Road
Laurel, Maryland 20810

(9) Final Report.
1 Oct [redacted]78 - 30 Sep [redacted]79,

(11) Dec [redacted]79 (12) 138

(16) 6781 (17) 00

Approved for public release; distribution unlimited.

(15) N9017-72-C-4401

AIR FORCE GEOPHYSICS LABORATORY
AIR FORCE SYSTEMS COMMAND
UNITED STATES AIR FORCE
HANSCOM AFB, MASSACHUSETTS 01731

Extract number is per the author Ming I. Wang

DISCLAIMER NOTICE

THIS DOCUMENT IS BEST QUALITY PRACTICABLE. THE COPY FURNISHED TO DTIC CONTAINED A SIGNIFICANT NUMBER OF PAGES WHICH DO NOT REPRODUCE LEGIBLY.

UNCLASSIFIED

SECURITY CLASSIFICATION OF THIS PAGE (When Date Entered)

REPORT DOCUMENTATION PAGE	READ INSTRUCTIONS BEFORE COMPLETING FORM
1. REPORT NUMBER: AFGL-TR-80-0070	2. GOVT ACCESSION NO.: AD-A087433
3. RECIPIENT'S CATALOG NUMBER	
4. TITLE (and Subtitle): The investigation of the magnetospheric dynamics in conjunction with the SCATHA satellite observations	5. TYPE OF REPORT & PERIOD COVERED: Final 10/1/78-9/30/79
	6. PERFORMING ORG. REPORT NUMBER
7. AUTHOR(s): Ching-I. Meng	8. CONTRACT OR GRANT NUMBER(s): MIPR No FY71217900005 N00017-72-C-4401
9. PERFORMING ORGANIZATION NAME AND ADDRESS: Applied Physics Laboratory, Johns Hopkins Road, Laurel, Maryland 20810	10. PROGRAM ELEMENT, PROJECT, TASK AREA & WORK UNIT NUMBERS: 62101F 678100
11. CONTROLLING OFFICE NAME AND ADDRESS: Air Force Geophysics Laboratory, Hanscom Air Force Base, Massachusetts 01731, Monitor/Arthur Wendel, Lt./PHG	12. REPORT DATE: December 1979
	13. NUMBER OF PAGES: 135
14. MONITORING AGENCY NAME & ADDRESS(if different from Controlling Office)	15. SECURITY CLASS. (of this report): Unclassified
	15a. DECLASSIFICATION/DOWNGRADING SCHEDULE

16. DISTRIBUTION STATEMENT (of this Report)

Approved for public release; distribution unlimited.

17. DISTRIBUTION STATEMENT (of the abstract entered in Block 20, if different from Report)

18. SUPPLEMENTARY NOTES

19. KEY WORDS (Continue on reverse side if necessary and identify by block number)

Auroral oval, Geomagnetic disturbance, Magnetosphere, Magnetospheric substorm

20. ABSTRACT (Continue on reverse side if necessary and identify by block number)

This task consists of two parts. The first part concerns (a) the collection and analysis of ground-based and satellite data for the purpose of monitoring the magnetospheric conditions in support of the SCATHA satellite activity at Air Force Geophysics Laboratory, and (b) the technical support in the study of the particle and field data returned by SCATHA satellite. The second part is to analyze observations of auroral phenomena made by satellites of the USAF Defense Meteorological Satellite Program. The effort at APL/JHU for the first part of this task was majorly in the role of providing supports to the SCATHA

DD FORM 1 JAN 73 1473 EDITION OF 1 NOV 65 IS OBSOLETE

UNCLASSIFIED

SECURITY CLASSIFICATION OF THIS PAGE (When Date Entered)

activity and for the second part of DMSP observations was in the understanding of polar region auroral phenomena. Therefore, this final report is divided into a summary of efforts supporting SCATHA and scientific results from analyzing DMSP data. The former consists of (1) a short description of why and how the ground-based magnetic data can be used in monitoring the magnetospheric conditions and (2) a list of data collected together with a guide for using these data. The latter contains (1) a list and abstracts of all scientific reports and journal articles published or submitted for publication during this reporting period, with at least partial sponsorship attributed to AFGL, and (2) an article concerning a possible diurnal variation of the auroral oval size.

I. INTRODUCTION

This task consists of two parts. The first part concerns (a) the collection and analysis of ground-based and satellite data for the purpose of monitoring the magnetospheric conditions in support of the SCATHA satellite activity at Air Force Geophysics Laboratory, and (b) the technical support in the study of the particle and field data returned by SCATHA satellite. The second part is to analyze observations of auroral phenomena made by satellites of the USAF Defense Meteorological Satellite Program. The effort at APL/JHU for the first part of this task was majorly in the role of providing supports to the SCATHA activity and for the second part of DMSP observations was in the understanding of polar region auroral phenomena. Therefore, this final report is divided into a summary of efforts supporting SCATHA and scientific results from analyzing DMSP data. The former consists of (1) a short description of why and how the ground-based magnetic data can be used in monitoring the magnetospheric conditions and (2) a list of data collected together with a guide for using these data. The latter contains (1) a list and abstracts of all scientific reports and journal articles published or submitted for publication, during this reporting period, with at least partial sponsorship attributed to AFGL, and (2) an article concerning a possible diurnal variation of the auroral oval size.

II. USING GROUND BASED MAGNETOGRAM TO MONITOR MAGNETOSPHERIC CONDITIONS

Since the beginning of the satellite *in situ* measurements after the International Geophysical Year, it has been increasingly clear that the magnetosphere becomes intermittently unstable and explosively releases a large amount of energy into the polar upper atmosphere. This particular magnetospheric phenomenon is called the *magnetospheric substorm*. It is manifested as an activity or disturbance of various polar upper atmospheric phenomena, such as intense auroral displays and particle precipitations. Highly active conditions in the polar upper atmosphere result from a successive occurrence of such an elementary activity, the polar substorm, which lasts typically of order one to three hours.

The magnetospheric structure and its relation to the polar upper atmosphere provide the basic frame of reference in describing various magnetospheric phenomena and their associated polar geophysical phenomena.

The process that provides the particles for the auroral oval during quiet conditions is considerably disturbed and intensified during a magnetospheric substorm. As a result, quiet auroral arcs lying along the auroral oval are activated during the substorm and called the auroral substorm.

The geomagnetic field is also greatly disturbed by motions of the energetic charged particles which appear during substorms. Electric currents are generated by the gyration, oscillation and drift motions of these protons and electrons, resulting in magnetic disturbances in middle and low latitudes, as well as in the magnetosphere. Their asymmetric distribution (with respect to the dipole axis) and the resulting electric field appears to play the key role in the magnetospheric substorm; this electric field in the magnetosphere is communicated to the ionosphere (which is the base of the magnetosphere) and generates electric currents there. In particular, a concentrated electric current, which is called the auroral electrojet, is induced along the auroral oval and causes intense geomagnetic disturbances. The magnetic disturbance generated by the auroral electrojet and the motions of the protons in the magnetosphere (i.e. the ring current) is called the polar magnetic substorm which is one of the manifestations of the magnetospheric substorms.

In order to accurately monitor the changing distribution of the magnetic disturbance vectors over the entire earth during the lifetime of a substorm, a network of magnetometers distributed adjacent to the flow pattern of the polar electrojet which causes polar magnetic substorms is required. In addition to the high latitude observations, the magnetic disturbances detected in the mid-latitudes can also be used to monitor the magnetospheric substorm activity based on the knowledge of the three-dimensional model current system connecting the magnetosphere and ionosphere discussed by Akasofu and Meng (*J. Geophys. Res., 74,* 293, 1969). In any case, for a good Universal Time coverage detecting the geomagnetic activity, the network of ground-based magnetic observations should have a nearly even distribution in longitude. High latitude stations of the network in the auroral zone provide the information of the auroral electrojet activity which is usually more intense in the midnight sector; and the chain of mid-latitude observatories reveals intensities of field aligned currents, connecting the magnetospheric current system with the ionospheric current systems, and the ring current in the inner magnetosphere which is an accurate measure of the

magnetic storm activity. Thus, the magnetospheric condition can be determined from observations of a network of ground-based geomagnetic observatories.

The magnetic disturbance observed on the earth's surface during magnetospheric substorms can be interpreted simply as due to three-dimensional magnetospheric electric current systems: (1) A partial ring current near the magnetospheric equator on the dayside, (2) field aligned currents flowing into the ionosphere in the morning sector and flowing out of the ionosphere in the evening side, (3) a very intense westward auroral electrojet along the nightside auroral oval as shown in Figure 1. The magnetic disturbance vectors observed during an intense magnetospheric substorm on a magnetic polar plot are illustrated in Figure 2. The largest disturbance was detected along the auroral oval at $\sim 65^\circ$ gm lat near midnight meridian. The auroral zone magnetometer stations on the dayside, however, are not significantly affected by the substorm activity. In the middle and low latitudes below $\sim 60^\circ$ gm lat, a systematic magnetic disturbance pattern was observed. A generally southward disturbance was detected in the afternoon sector, an eastward disturbance in the evening sector, and a westward disturbance in the late morning sector. The magnetic variations observed by a worldwide network of magnetometer stations are shown in Figures 3, 4 and 5, grouped by their longitudes. It is rather clear that the magnetic disturbance was very consistent in each local time sector from $\sim 60^\circ$ to equator. A detailed description of this magnetospheric substorm has been published in the *Journal of Geophysical Research, 74,* 293, 1969. Based on this type of study, the magnetic variations observed by mid-latitude stations can also be used to monitor the magnetospheric substorm activity. However, the onset time of each magnetospheric substorm cannot be determined from the mid-latitude magnetograms.

III. GROUND BASED DATA SET TO SUPPORT SCATHA OBSERVATIONS

This section describes the available data set collected at the Applied Physics Laboratory, The Johns Hopkins University, to complement and support the study of the SCATHA satellite data. The ground-based geomagnetic data are discussed here and the next section describes various satellite data during the SCATHA operational period. The SCATHA satellite was launched on January 30, 1979 and placed into the final orbit on February 7, 1979. Except for a few minor misfunctions, almost all of the instruments are operating normally.

In order to speed up the analysis of the SCATHA observations, the ground-based magnetic disturbance information is needed in the same pace as the data processing of the SCATHA satellite. Usually, the magnetograms disseminated through the World Data Center are delayed by at least 6 months to one year. It is rather fortunate that the SCATHA satellite is operating during the period of the International Magnetospheric Study. Some of the geomagnetic data over North America can be obtained with a rather short time delay of about 2 to 4 weeks. And the geomagnetic data from 5 networks of geomagnetic observatories are collected for determing the geomagnetic condition. The first one is the Alaskan meridional chain of magnetometers along the magnetic longitude of approximately 260° between ~ 80° and 60° geomagnetic latitude consisting of nine stations, named Eureka (80°N, 85.7°W), Isachsen (78.8°N, 104°W), Sach Harbor (72°N, 125.3°W), Cape Parry (70.2°N, 124.7°W), Inuvik (68.25°N, 133.3°W), Arctic Village (68.13°N, 145.6°W), Fort Yukon (66.57°N, 147.48°W), College (64.88°N, 148.05°W) and Talkeetna (63.3°N, 150.1°W). The second network is the Canadian Fort Churchill meridional chain along the magnetic longitude of about 326° from ~ 73° to 65° geomagnetic latitude; the stations are Pelly Bay, Rankin Inlet, Eskimo Point, Back, Gillam and Island Lake. The third network is an east-west chain connecting two above-mentioned meridional networks along the auroral zone at geomagnetic latitudes of about 67° and 68°. It consists of Fort Yukon, Normal Wells, Fort Simpson, Fort Smith, Lynn Lake and Gillam. The distribution of these three high-latitude networks is shown in Figure 6 and they are ideally located to monitor the auroral electrojet activity over North America. Data from two mid-latitude magnetometer networks are also used to monitor the geomagnetic activity. They are: (1) the U. S. International Magnetospheric Study chain from Pacific Ocean to Atlantic Ocean consisting of seven stations, namely Guam, Wake Island, Honolulu, Tahiti, Tucson, San Juan and Eusebro; and (2) the Air Force Geophysics Laboratory chain across the U. S. Continent along about 54° geomagnetic latitude with seven stations. They are: Newport, WA (55.2° gm lat; 299.6° gm long); Rapid City, SD (54.1°; 317.3°); Camp Douglas, WI (56.3°; 334.2°); Mt. Clemens, MI (55.8°; 344.8°), Sudbury, MA (55.8°; 1.9°); Lompoc, CA (40.2°; 300.6°); Tampa, FL (40.7°; 344.9°). Figure 7 illustrates the spatial distribution of these networks which are very effective in measuring

magnetic storm activities, the intensity of ring current, the configuration of the field-aligned currents and the partial ring currents associated with the development of the magnetospheric substorms.

Data from most of the IMS magnetometer stations (as shown in Figure 8) are transmitted in real-time by the ground station and linked with NOAA's Space Environment Laboratory at Boulder, Colorado via the NOAA geosynchronous weather satellites. These data are available to scientific community through the Data Center at Boulder only with one week delay. The data from AFGL's magnetometer network are linked with the Air Force Geophysics Laboratory in real-time by telephone lines and these digital magnetic field data are processed about once a week. All of these data obtained by above-mentioned 5 magnetometer networks since January 1979 are routinely collected at APL/JHU for supporting the SCATHA project.

This data base, with the ground-based geomagnetic observations from American Continent and Pacific Ocean covering only 1/3 of the earth in longitude, can only provide effective geomagnetic activity monitoring for less than 3/4 of a universal-time day; the blind spot of the above-mentioned networks in determining the geomagnetic activity is from about 18 UT to 06 UT when Europe is in the midnight sector. In order to expand the longitudinal (i.e. universal-time) coverage of monitoring capability of magnetic activity of the data set, recently we began to obtain the magnetograms from three more auroral zone stations (Abisko, Leirvogur and Narsscrssuaq) in Europe. The addition of these stations enables us to monitor the geomagnetic activity (auroral electrojet activity) between 20 and 06 UT.

Magnetograms from these IMS magnetometer networks and individual observatories provide us with information for determining the occurrence and development of each magnetospheric substorm. However, these data are not suitable to be used to scan the general magnetospheric conditions on a daily basis. For this purpose, the 3-hour geomagnetic planetary index Kp and the hourly storm-time variation index Dst are collected. The Kp index is a measure intended to express the degree of geomagnetic activity over the whole earth. For this purpose, local geomagnetic activities at twelve selected observations (Table 1) in moderately high geomagnetic latitudes up to 63° are combined and synthesized into the Kp index at Institut für Geophysik at Göttingen (Germany) for the IUGG; Association of Geomagnetism and

Aeronomy. The Kp index ignores the composition of the disturbance field. Therefore, the interpretation of Kp is not always straightforward, but the high Kp values are mainly due to the field of polar magnetic disturbances. The storm-time variation (Dst) index is derived from the first term of Fourier analysis of the mid-latitude geomagnetic storm field. It represents the component of the disturbance field axially symmetric with respect to the earth dipole axis. The Dst field is due mainly to external sources and its vector lines are nearly parallel to the earth's surface. Studies of ground magnetic records alone cannot give the unique location of the electric current systems responsible for the Dst disturbance. In the past it was often tacitly assumed that in low latitudes the Dst field is produced by axially symmetric ring current in the magnetosphere. Satellite *in situ* observations have now established that the variation of the Dst field is associated with the changes of the proton belt (ring current) in the inner magnetosphere. The 3-hour Kp index and the hourly Dst index are routinely obtained for the purpose of monitoring the gross magnetospheric conditions and Appendix 1 consists of these indices for the first 6 months (February to July, 1979) of the SCATHA mission.

Based on the above-mentioned data set, the special geomagnetic activity and the magnetospheric conditions during the first 6 months of SCATHA satellite operation are selected. Table 2 lists five geomagnetically quiet days of each month; and the daily sum of 8 Kp indices is given in parenthesis after the corresponding date. The quietest days during these 6 months are February 13, 14, March 14, April 20, and July 31. Table 3 gives the five disturbed days of each month. Periods of geomagnetic storm and their approximate intensity are given in Table 4. In order to understand the magnetospheric dynamics, detailed studies of the isolated well-defined magnetospheric substorm are required and Table 5 lists the isolated substorms identified from the Alaskan chain of magnetometers.

IV. SATELLITE DATA TO SUPPORT SCATHA STUDY

SCATHA satellite, just like any other satellites, is capable of making only one-point *in situ* measurements of the space environment at any time. And due to the motion of a satellite, it is usually very difficult to determine whether the observed variation is the consequence of the temporal

changes of the magnetosphere or the motion of the satellite. Therefore, besides the basic SCATHA data set, information of simultaneous measurements of various parameters by other satellites at the different parts of the magnetosphere are also needed in the study of the magnetospheric dynamics. Since SCATHA is in a near-synchronous orbit, data from other synchronous satellites at different longitudes are very essential. Various data from four geosynchronous satellites are collected at APL/JHU.

GOES-1,2,3 (Geosynchronous Operational Environmental Satellite) are the NASA-developed, NOAA-operated weather watching spacecraft. These spin-stabilized satellites carried a space environment monitor system to measure proton, electron, and solar x-ray fluxes and magnetic fields, in addition to their primary meteorological packages. GOES-1 is stationed over the Indian Ocean, GOES-2 over the U. S. Continent, and GOES-3 over the Pacific Ocean. The magnetic field data, in the format shown by Figure 9, since May 1978 are routinely acquired by us from NOAA. The particle data are also available to us from Dr. D. J. Williams of NOAA by request.

The fourth geosnychronous satellite which provides useful measurements in supporting SCATHA's mission is the ESA-GEOS 2 satellite. It was launched on July 14, 1978 and parked between 0° and 35°E. This satellite is the first spacecraft in an equatorial geostationary orbit dedicated completely to scientific measurements. It can serve as a reference platform for the magnetospheric observations and also makes correlative measurements with the SCATHA satellite. Its payload consists of instruments to measure: (1) DC and AC electric and magnetic field, (2) gradient of the magnetic field, (3) thermal and suprathermal plasma parallel and perpendicular to the magnetic field, (4) energy spectra, angular distribution and composition of positive ions, (5) angular distribution and energy spectra of energetic electrons and protons. Daily summaries of these experiments from 15 August 1978 onward are available; and APL/JHU receives them routinely for the SCATHA analysis usage. These data summaries provide status information on the environmental conditions encountered along the geostationary orbit. Figure 10 is an example of GEOS-2 daily summary. The format and content of the summary are described in the following.

Format and Content of GEOS-2 Daily Summaries

The data are plotted on a time scale of 1 cm/hour. The length of one plot is 24 cm and 00.00 hours UT occurs in the middle of the time scale. For every 24 hour interval two sheets are produced. One which contains the data from the wave-field experiments on GEOS-2 and one which contains the data from the particle experiments.

The wave-field data sheet contains from top to bottom the following parameters plotted versus time:

1) The V-component of the magnetic field (V being the local vertical direction).
2) The D-component of the magnetic field (D being directed toward the east, perpendicular to V and the spin axis direction of the earth).
3) The H-component of the magnetic field (completing the VDH triad).
4) The standard variation of the total magnetic vector.

The coordinate transformation used for the generation of the VDH components is unfortunately not applicable in eclipse conditions. The data in these traces for the period 1 September-16 October 1978 in the interval 20.30-22.30 UT should therefore be disregarded.

5) The measured DC electric field direction with respect to the satellite sun line.

Since 5 August an anomaly has developed in conjunction with the solar array of the spacecraft. Apparently as a consequence of a short circuit between one string of cells and structure, we observe a spin periodic variation of the potential of the zero volt reference of all experiments. The potential of all experiments with respect to spacecraft structure therefore varies between 0 Volts during one half of the spin period and +12 V during the second half. Such voltage excursions cannot be suppressed by the existing common mode rejection of the differential amplifiers used for electric field measurements. Electric field data from the double probe experiment are therefore only available for one half spin period. The data can in principle be interpolated but the necessary correction software has not yet been developed and therefore the 5th trace from top in the wave/field data should be disregarded until further notice.

6) Total ULF magnetic RMS power in plane perpendicular to the S/C spin axis below 5 Hz and parallel to the S/C spin axis below 1.5 Hz.

7) The RMS power (0-80 db) in the magnetic domain in various frequency ranges

   a) 2.5 - 5.0 kHz
   b) 1.2 - 2.5 kHz
   c) 0.6 - 1.3 kHz
   d) 0.2 - 0.6 kHz

8) The RMS power (0-80 db) in the electric domain in various frequency ranges

   a) 5.0 - 10.0 kHz
      2.5 - 5.0 kHz
      1.2 - 2.5 kHz
      0.6 - 1.2 kHz
      0.2 - 0.6 kHz

These AC electric field data are not available. Reason is the solar array anomaly.

9) The plasma density derived from the output of the plasma resonance sounder.

The particle data sheet contains from top to bottom the following parameters plotted versus time:

1) Electron countrates in the energy range 50 - 500 eV obtained by integrating the results from 2 electrostatic analyzers, one viewing parallel the other close to perpendicular to the satellite spin axis.

2) This trace gives data from the ion mass spectrometer. The curve represents average mass detector counts per sample at hydrogen. No correction has been made for background spacecraft potential or variation in geometric factor with energy. The curve will often have a sawtooth appearance which is a result of mode changes from thermal mode (about 0 - 110 ev range)

to survey mode 25 eV - 16.4 keV). Generally thermal mode fluxes are larger than survey mode so that as a rough rule the upper envelope of the trace is proportional to average flux in about 0 - 110 eV range and lower envelope to average flux in 25 eV - 16.4 keV range.

3) The energy flux of electron in the 0.5 - 20 keV range arriving parallel to the satellite spin axis.
(erg sec^{-1} cm^{-2} sr^{-1}).

4) Electron fluxes in the energy range 0.5 - 20 keV obtained by integrating the results from an electrostatic analyzer, viewing parallel to the spin axis.
(part. cm^{-2} sec^{-1} sr^{-1}).

5) Electron countrates in the energy range 20 to 250 keV obtained from two solid state detectors one looking close to parallel and one close to perpendicular to the spin axis.

6) Proton countrates in the energy range 20 keV to 3.3 MeV obtained from two solid state detectors one looking close to parallel and one close perpendicular to the spin axis.

The data points which appear in the various traces are computed averages over approximately 3 minutes. Only in the case of the mass spectrometer the averaging period is approximately 6 minutes.

Space environmental data from three other satellites are also gathered at APL/JHU to support the SCATHA operation. They are the ESA-GEOS-1 satellite, ISEE-1 and 2 satellites and IMP-8 satellite. GEOS-1 was launched on 20 April 1977. As a result of a malfunction in the separation mechanism between the 2nd and 3rd stage of the vehicle, it was not placed into the planned geostationary orbit, instead it achieved an eccentric orbit with the apogee of 38,000 km ($\sim$ 7 R_e), the perigee of 2050 km and periodicity of 12 hours. The instrument onboard GEOS-1 is identical to GEOS-2 described earlier. The daily summaries of GEOS-1 measurements are obtained from GEOS project office and their format and content are the same as GEOS-2 shown in Figure 10. ISEE-1 and 2, the mother-daughter pair of satellites were launched into a highly eccentric orbit with apogee of about 21.5 R_e and perigee of 281 km. They carried the complete particle and field instrumentational

package. The complete set of data from the low energy particle experiment on both satellites are available at APL/JHU. Since Dr. Ching-I. Meng is the co-investigator of this experiment, other ISEE satellite data can also be obtained through the principal investigator of other experiments. IMP-8 is another satellite that can provide useful data to support the SCATHA mission. It has a nearly circular orbit at about 30 R_e and with a period of about 12 days. Both magnetic field data and energetic (E > 15 keV) particle data are available at APL/JHU.

In addition to those high altitude satellites monitoring the simultaneous space environment in the different locations of the magnetosphere, the low altitude satellite observations are also useful to study the coupling between the magnetosphere and ionosphere while they are conjugate with SCATHA. The field aligned current data from TRIAD satellite and auroral imagery from DMSP satellites are routinely collected and analyzed; and the complete data set are archived at APL/JHU.

In conclusion, the simultaneous space environmental data at different locations of the geospace to support the SCATHA mission are available from high altitude satellites, GOES-1,2,3, ESA-GEOS-1 and 2, ISEE-1 and 2 and IMP-8 and low altitude satellites TRIAD and DMSP satellites. Appendix 2 is an example of the data set collected at APL/JHU for supporting SCATHA mission during a quiet and disturbed day.

V. SCIENTIFIC RESULTS

The following is a list of journal articles that were published or submitted for publication during this reporting period. They are at least partially sponsored by the Air Force Geophysics Laboratory under this task.

1. Meng, C.-I., Conjugate low energy electron observations made by ATS-6 and DMSP-32 satellites, Quantitative Modelling of Magnetospheric Processes, ed. by W. P. Olson, *AGU Geophysical Monograph Series, Vol. 21*, 96, 1979.

2. Meng, C.-I., Polar cap variations and the interplanetary magnetic field, *Dynamics of the Magnetosphere*, ed. by S. I. Akasofu, (in press), 1979.

3. Meng, C.-I., Diurnal variation of the auroral oval size and the minimum oval, *J. Geophys. Res.*, *84*, 5319, 1979.

4. Lui, A. T. Y. and C.-I. Meng, Relevance of southward magnetic fields in the neutral sheet to anisotropic distribution of energetic electrons and substorm activity, with A. T. Y. Lui, *J. Geophys. Res.*, *84*, 5817, 1979.

5. Carbary, J. F., S.-I. Akasofu, C.-I. Meng, J. P. Sullivan and R. P. Lepping, Association of the AE-index with the solar wind poynting flux incident on the magnetosphere, *J. Geophys. Res.*, (submitted), 1979.

6. Fairfield, D. H., C.-I. Meng, Magnetosheath, bow shock and upstream phenomena, *IMP Book*, (in press), 1979.

The abstracts of these articles are reproduced in the following.

CONJUGATE LOW ENERGY ELECTRON OBSERVATIONS MADE BY ATS-6 AND DMSP-32 SATELLITES

Ching-I. Meng

The Johns Hopkins University
Applied Physics Laboratory
Laurel, Maryland 20810

Abstract. Coordinated simultaneous observations of low energy electrons at conjugate locations by using two satellites are presented. The geosynchronous ATS-6 measures the plasma sheet electrons near the magnetospheric equator, and the polar-orbiting DMSP-32 measures the auroral electron precipitation above the ionosphere. It is found that the particle characteristics of precipitated auroral electrons of diffuse auroras in the evening sector are nearly identical to those of the trapped plasma sheet electrons in the conjugate magnetospheric equator. This property of conjugate electrons reveals that the conjugate latitude of ATS-6 in the evening sector is at about 65.7° corrected geomagnetic latitude.

POLAR CAP VARIATIONS AND THE INTERPLANETARY MAGNETIC FIELD

Ching-I. Meng

The Johns Hopkins University
Applied Physics Laboratory
Laurel, Maryland 20810

Abstract. This paper reviews research involved with direct and inferred determinations of the polar cap size and location, as well as their relationships with the interplanetary magnetic field. "Polar cap" is defined here as the region of open geomagnetic field lines encircled by the auroral oval. The first part of the paper reports the progress in the observation and understanding of polar cap size variations as related to changes of the interplanetary magnetic field magnitude and direction obtained by scaling the global auroral distributions from DMSP auroral pictures. Some new results on configurational changes of the auroral oval (i.e., the polar cap) with different orientations of the interplanetary magnetic field are also discussed. There are indications of the dawn-dusk and sunward-tailward displacements of the auroral oval in association with the interplanetary magnetic field B_y and B_x components, respectively. It is obvious from this review that a better understanding of the interaction between the terrestrial magnetosphere and the interplanetary magnetic field requires further efforts, both observational and theoretical.

DIURNAL VARIATION OF THE AURORAL OVAL SIZE AND THE MINIMUM OVAL

Ching-I. Meng

The Johns Hopkins University
Applied Physics Laboratory
Laurel, Maryland 20810

Abstract. An examination of the equatorial boundary of the auroral oval (as defined by quiet-time auroral electron precipitations) reveals a periodic variation of its latitudinal location. The period of oscillation is 24-hours and the amplitude is about 4° with the highest latitude detected during the first 12 hours of each UT day. This diurnal variation seen in the evening and morning sectors of the auroral oval is in phase as is the diurnal variation of the northern and southern hemispheres. The observed latitudinal variation is attributed to UT diurnal variation of the auroral oval size in association with the daily procession of the geomagnetic pole. The auroral oval is smaller when the northern geomagnetic pole is near the local midnight around 0600 UT; it is larger when the northern geomagnetic pole is near the local noon around 1800 UT. The equatorward edges of the evening sector of the quiet auroral oval (1900-2100 MLT) are located at about 72° CGL and 69° CGL, respectively. Furthermore, the minimum auroral oval does not progressively contract towards the smaller size as geomagnetic quiescence continues.

RELEVANCE OF SOUTHWARD MAGNETIC FIELDS IN THE NEUTRAL SHEET TO ANISOTROPIC DISTRIBUTION OF ENERGETIC ELECTRONS AND SUBSTORM ACTIVITY

A. T. Y. Lui
C.-I. Meng

The Johns Hopkins University
Applied Physics Laboratory
Laurel, Maryland 20810

Abstract. The implications of southward magnetic fields at the magnetotail neutral sheet to the development of streaming anisotropy of energetic electrons and magnetospheric substorm activity are examined. Magnetic field and energetic particle measurements from the IMP-6 spacecraft, the AE index, and global auroral images from DMSP spacecraft are utilized in this study. Criteria are developed to identify events of southward magnetic fields at the neutral sheet which imply the presence of X-type magnetic neutral lines. Several features of the observations suggest that the southward magnetic fields and the implied X-type neutral lines are associated with magnetic bubbles in the neutral sheet region. It is found that the signatures of magnetic bubbles are sometimes detected in association with tailward streaming and flux enhancement of energetic electrons (47 keV $< E <$ 350 keV). A cigar-shaped anisotropy in the energetic electron distribution is frequently but not always observed before the onset of tailward streaming of energetic electrons. The tailward streaming is magnetic field-aligned and occurs in the form of bursts, suggesting that the generating process is activated somewhat quasi-periodically and is not in a steady state. Signatures of magnetic bubbles are also detected without any substantial enhancement or detectable tailward streaming of energetic electrons. By comparing IMP-6 observations with the AE index and global auroral images from DMSP spacecraft, it is found that signatures of magnetic bubbles in the neutral sheet are observed during substorms as well as during quiet geomagnetic conditions, indicating that magnetic bubbles are intrinsic features of the neutral sheet in the magnetotail regardless of substorm activity.

ASSOCIATION OF THE AE-INDEX WITH THE SOLAR WIND POYNTING FLUX INCIDENT ON THE MAGNETOSPHERE

J. F. Carbary[1], S.-I. Akasofu[2], C.-I. Meng[1],
J. P. Sullivan[3] and R. P. Lepping[4]

[1]The Johns Hopkins University
Applied Physics Laboratory
Laurel, Maryland 20810

[2]Geophysical Institute
University of Alaska
Fairbanks, Alaska 99701

[3]Center for Space Research
Massachusetts Institute of Technology
Cambridge, Massachusetts 02139

[4]Laboratory for Extraterrestrial Physics
NASA/Goddard Space Flight Center
Greenbelt, Maryland 20771

Abstract. The power transmitted to the magnetosphere from the solar wind should be equivalent to the incident electromagnetic power modified by an efficiency function which may depend on the interaction between the interplanetary and terrestrial magnetic fields. The transmitted power drives various currents within the magnetosphere and generates the various types of geomagnetic activity. Since geomagnetic activity can occur on time scales of minutes and the lifetime of a substorm is only about an hour or two, we have used 5-minute averages of IMP 8 solar wind plasma and interplanetary magnetic field data to investigate the connection between the transmitted Poynting flux and geomagnetic activity as reflected in the AE(11) index. We find that during periods of geomagnetic activity the transmitted power coincides with auroral electrojet activity, sometimes on time scales of several minutes. During periods of relative geomagnetic quiescence, there appears to be little relation between the transmitted power flux and the AE index. This study suggests that geomagnetic activity may depend on more than a simple northward or southward orientation of the IMF.

The article entitled "Diurnal Variation of the Auroral Oval Size" is reproduced here as part of this final report to indicate our continuous effort in studying (1) the coupling between the magnetosphere and ionosphere as well as (2) the space environment monitoring analysis by using USAF satellite.

DIURNAL VARIATION OF THE AURORAL OVAL SIZE

Ching -I. Meng

The Johns Hopkins University
Applied Physics Laboratory
Laurel, Maryland 20810

JANUARY 1979

Submitted to the Journal of Geophysical Research

ABSTRACT

An examination of the equatorial boundary of the auroral oval (as defined by quiet-time auroral electron precipitations) reveals a periodic variation of its latitudinal location. The period of oscillation is 24-hours and the amplitude is about 4°. This diurnal variation seen in the evening and morning sectors of the auroral oval is in phase as is the diurnal variation of the northern and southern hemispheres. The observed latitudinal variation is attributed to UT diurnal variation of the auroral oval size in association with the daily precession of the geomagnetic pole. The auroral oval is smaller when the northern geomagnetic pole is near the local midnight around 0600 UT; it is larger when the northern geomagnetic pole is near the local noon around 1800 UT. The equatorial edges of the evening sector of the quiet auroral oval (1900-2100 MLT) are located at about 72° CGL and 69° CGL, respectively, which correspond to the minimum auroral oval.

I. INTRODUCTION

In the past twenty years, various types of satellite observations have revealed that the terrestrial magnetosphere is open in the sense that some of the geomagnetic field lines extend into interplanetary space and connect with the magnetic field lines of solar origin. The auroral oval in the polar ionosphere separates the region of the closed field lines from the open geomagnetic field lines of the polar cap. It has been known for many years that the size of the auroral oval, determined from ground-based all-sky camera data, is not fixed *(Feldstein and Starkov, 1967)*. During geomagnetically quiet periods, the auroral oval contracts poleward to near about 70° geomagnetic latitude at midnight for $K_p \approx 1$. The auroral oval expands equatorward in geomagnetically disturbed times with the equatorial edge of the midnight oval below 50° geomagnetic latitude during large magnetic storms. Inverse linear relationships between the latitudinal location of the auroral oval and the geomagnetic activity were reported (see review by *Akasofu and Chapman, 1972)*. In addition to the geomagnetic activity, the size of the auroral oval is also controlled by the interplanetary magnetic field (see review by *Meng, 1979)*. Using the idea of reconnection between the interplanetary magnetic field and the geomagnetic field, *Akasofu (1975)* suggested that the variation of the auroral oval size is determined by the difference between the dayside merging rate (which increases the flux of open geomagnetic lines) and the nightside tailfield reconnection rate (which decreases the flux of open field lines). The reduction or enlargement of the oval size occurs when the value of this difference is negative or positive, respectively.

Images from polar orbiting satellites have made possible the study of auroral display over most parts of the polar region. Many authors (e.g., *Lui et al., 1975; Holzworth and Meng, 1975; Berkey and Kamide, 1976; Sheehan and Carovillano, 1978; Pike and Dandekar, 1979; Meng, 1979)* have used such satellite photographs to examine auroral oval size variations. These global observations of auroral displays confirmed the earlier studies of the auroral oval variations in conjunction with

the geomagnetic activity and the interplanetary magnetic field orientation, and a gradual contraction of the auroral oval during quiet geomagnetic conditions. The purpose of this work is (1) to examine the auroral oval variation during prolonged, extremely quiet geomagnetic periods when the auroral emissions were too weak to be detected by the DMSP auroral images, and (2) to determine the minimum size of the auroral oval by using the precipitating auroral electron data from DMSP satellites.

II. ANALYSIS

The Defense Meteorological Satellite Program (DMSP) is a USAF operational system which consists of two satellites in 830-km sun synchronous circular polar orbits along the dawn-dusk and noon-midnight meridians *(Pike, 1975)*. In addition to meteorological instruments, some of the dawn-dusk satellites launched since 1974 also carried low energy electron detectors to monitor the auroral electron precipitations below 20 keV. A dawn-dusk DMSP satellite traverses the auroral oval four times each orbit in 101 minutes and crosses the morning and evening parts of the oval over both northern and southern polar regions. The data set in this study was selected on the basis of an extended geomagnetically quiet period with the daily sum of K_p less than 6 or 7 for consecutive days. Locations of the equatorial edge of the auroral oval precipitation region were tabulated during these extremely quiet days. This edge corresponds to the equatorial boundary of the diffuse auroras and the earthward edge of the plasma sheet *(Lui et al., 1975; Meng, 1976; Lui et al., 1977; Meng et al., 1979)*.

The identification of the equatorial edge of the auroral oval precipitation is generally uncomplicated and unambiguous. Thus, it is used here to monitor the "size" of the auroral oval, instead of the less well defined poleward boundary of the auroral oval. Figure 1 illustrates the precipitating electron profiles of a typical polar region crossing during an extremely quiet period when the daily sum of K_p was 2- on January 21, 1978. Carrying a 16-channel auroral electron detector measuring precipitations between 50 eV to 20 keV, the DMSP-36 (F2) satellite entered the northern polar region from the morning side and traversed the auroral oval at the $\sim$ 0700 Magnetic Local Time (MLT) meridian and the $\sim$ 2020 MLT meridian. It reached its highest latitude over the polar cap at 86° Corrected Geomagnetic Latitude (CGL) at about 1002 UT. The intense precipitations detected near about 0958 UT and 1008 UT were associated with the morning and evening parts of the auroral oval, respectively. The equatorial edge of the auroral oval is easily defined by a sharp decrease of two orders of magnitude of the precipitating electron fluxes near or below 1 keV.

The ambiguity in defining the poleward boundary of the auroral oval is demonstrated by this example. The satellite traversed the equatorial boundaries of the morning and evening auroral oval at about 0957 UT and 1008 UT, corresponding to geomagnetic coordinates of approximately 73.2° CGL, 0700 MLT and 69.5 CGL, 2020 MLT, respectively. The so-defined equatorial boundary is in excellent agreement with that determined from a detailed analysis of the particle precipitation characteristics, such as the electron spectrum. Detected for about one minute near 0956 UT the less intense precipitations below the defined morning auroral oval are associated with the energetic electrons executing the gradient $\vec{B}$ drift along the constant-B contours near the magnetospheric equator. Characteristics of the low energy electron precipitations observed during the extremely quiet times will be discussed elsewhere.

III. RESULTS

The latitudinal variations of the equatorial boundary of the auroral oval detected by the DMSP-36 (F2) satellite during three extended quiet periods from November 1977 to January 1979 are described. Figure 2 illustrates the observation from November 20 to 26, 1977. The top curve with solid dots and triangles represents the equatorial location of the evening auroral oval detected between the 1900 MLT meridian and the 2100 MLT meridian. The lower curve with open circles and triangles indicates the equatorial location of the morning auroral oval monitored between the 0300 MLT and the 0700 MLT meridians. The local time limitation to the evening and morning parts of the auroral oval was used to minimize the following two effects: (1) the asymmetric latitudinal distribution of the oval with respect to the magnetic pole, and (2) the satellite sampling pattern being fixed with respect to the geomagnetic latitude and local time coordinates of a sun-synchronous satellite. During the 6 days in November, the auroral electron data over the polar region were essentially continuous over both hemispheres. The gaps shown in the latitudinal variation were mostly due to the satellite's crossing of the oval at the local times outside the ranges used for this study. The dots and circles correspond to the northern auroral oval observations and triangles indicate the southern oval observations.

The geomagnetic activity is indicated on the top of the diagram by the 3-hour K_p index and the daily sum of K_p. During the first two days (November 20 and 21, 1977) the K_p's were about 1 except for a few isolated occasions and the daily sums of K_p were 8+ and 9. From 1200 UT of November 22 to 1200 UT of November 25, the geomagnetic activity was very low with K_p's of 0 or 1 for about 72 hours and the daily sum of K_p was 6+, 4+ and 4 for November 22, 23 and 24, respectively. During this quiet period, the equatorial edge of the evening auroral oval precipitation was located between about 68° CGL and 71° CGL. Very intense geomagnetic activity occurred after 1200 UT on November 25 and the 3-hour K_p index increased to 5 at the end of that day. The evening oval moved from about 71° CGL to 59° CGL within 13 hours. From this example, it is clear that the equatorial boundary of the morning auroral oval was located between 68° CGL and 73° CGL during quiet periods and moved equatorward to about 60° CGL with increasing activity.

The latitudinal variations of the equatorial edge of the auroral oval in Figure 2 reveal several salient features.

(1) *Coherent variations of the auroral oval latitude over the northern and southern polar regions.* The observations between the northern and southern auroral ovals were made by the same satellite at intervals about 30 to 40 minutes apart. Whenever successive monitorings between the alternative hemispheres were available, the locations of the equatorial oval boundary were rather consistent as shown by the continuity between dots (or circles) and triangles without significant indications of large disparity ($\gtrsim 1°$) between different hemispheres.

(2) *Consistent variations between evening (1900 to 2100 MLT) and morning (0300 to 0700 MLT) parts of the auroral oval.* The changes of the upper (evening) and lower (morning) curves were very coherent in both poleward and equatorward movements, indicating a nearly simultaneous variation at both sectors of the auroral oval. (Observations of the evening and morning ovals were separated by approximately 10 minutes over the same hemisphere and about 50 minutes between the opposite hemispheres.) The coherent variations between these two local time segments of the oval were independent of geomagnetic activity; the consistency was observed in activity-related latitudinal variations such as equatorward expansion of the oval with increasing K_p, as well as in other variations which are not related to K_p changes.

(3) *Diurnal variation of the auroral oval latitude.* The most outstanding latitudinal variation of the auroral oval shown in Figure 2 is a periodic oscillation of about 24 hours. The higher latitudes above 70° CGL were reached by the equatorial edge of the oval during the first 12 hours of each UT day, and the equatorial edge was at lower latitudes below 69° CGL in the second half of a UT day. From about 1200 UT of November 20 to 1200 UT of November 25, five complete cycles of this UT diurnal variation of the oval latitude were detected at both evening and morning parts of the auroral oval.

In order to determine whether these features exist during other quiet periods, several events were examined. Figure 3 illustrates another extended quiet period two weeks after the previous example. The geomagnetic activity was low from December 7 to December 10, 1977 with the daily sum of K_p being 6, 3, 6- and 7-, respectively. The equatorial boundary of the auroral oval located between 68° and 73° CGL clearly showed a diurnal variation similar to the previous example. The moderate geomagnetic activity (K_p = 2-, 2) on December 9 caused the evening auroral oval to move down to 65° CGL. On December 11, the oval was near 58° CGL during intense activity with a K_p of 5+. It is interesting that during these four consecutive quiet days the location of the equatorward edge of the auroral oval did not show a progressively poleward shift towards higher latitude in addition to the diurnal variation. This will be discussed later.

Figure 4 is an example of the latitudinal variation of the auroral oval observed in late January 1978. The daily sum of K_p index was 6, 2-, 5- and 3 for January 20, 21, 22 and 23, 1978. These are the geomagnetically quietest consecutive days during the past five years. The 3-hour K_p was 0 or 1 from 0900 UT of January 20 to 1500 of January 24, 1978. The diurnal variation of the auroral oval latitude was observed from January 21 to 24. On January 20, a suddenly enhanced activity (K_p = 2) interfered with the diurnal variation between 0600 and 0900 UT while the oval shifted equatorward to about 68° CGL. On the quietest day (ΣK_p = 2-), the maximum of the diurnal latitudinal variation of the evening oval was at about 72° CGL and the minimum at about 69° CGL.

IV. CONCLUSION AND DISCUSSION

From the examples shown and others examined, one concludes that the equatorial boundary of the auroral oval, determined from the DMSP satellites auroral electron measurements, exhibits a periodic oscillation of its latitudinal location during geomagnetic quiescence. The period of this oscillation is 24 hours and the amplitude is about 4°, with the maximum observed within the first 12 hours of each UT day. This diurnal variation of the equatorward edge was in phase over the evening (1900 to 2100 MLT meridians) and morning (0300 to 0700 MLT meridians) parts of the auroral oval as well as over northern and southern polar regions. The latitudinal peak and valley of the variation were at approximately 72° CGL and 69° CGL, respectively.

It is important to explore the detected diurnal variation of the oval latitude. The first possibility to be considered is that the corrected geomagnetic coordinate *(Gustafsson, 1970)* used by the USAF in the DMSP observations may not represent the true distribution of the earth's magnetic field, namely, a largely displaced magnetic pole between the model field and the true field. The offset of this coordinate system could cause a UT dependence of the auroral oval location. But, in this case, the UT diurnal variations of the evening and morning parts of the auroral oval (and also between opposite hemispheres) should be out of phase. However, the observed in phase diurnal variations between the opposite segments of the auroral oval and between the opposite hemispheres deny this possibility. Furthermore, the inaccuracy of the corrected geomagnetic coordinate system cannot be as large as a few degrees in latitude around the auroral oval region *(Gustafsson,* Private Communication).

Another possibility is that the dawn-dusk DMSP satellites in sun-synchronous circular polar orbit (fixed with respect to the geographic pole) sample only a fixed local time segment of the auroral oval during any UT interval. This might produce an apparent diurnal variation of certain phenomenon in association with the rotation of the geomagnetic pole. However, the data used in this study, limited between 1900 and 2100 MLT for the evening oval and 0300 to 0700 MLT for the morning oval, should reduce the orbital effect drastically, if not completely.

The most likely explanation of the observed UT dependence of the auroral oval latitude is actual diurnal variation of the auroral oval size. As the size of the auroral oval changes with the UT, the latitudinal variation of the oval location should be in phase between the evening and morning sectors of the auroral oval as well as between northern and southern hemispheres, just as detected. Based on these quiet time observations, it is believed that the auroral oval indeed executes a diurnal variation of its size as the geomagnetic pole rotates around the geographic pole. The auroral oval is at its smallest size around 0600 UT while the northern geomagnetic pole is near the local midnight; the largest oval occurs around 1800 UT when the northern geomagnetic pole is near the local noon. The radii of the maximum and minimum size ovals differ by about 4° in colatitude. It is important to substantiate this diurnal variation of the auroral oval size. A conclusive way would be to determine the latitude of the auroral oval at a certain fixed magnetic local time meridian from the simultaneous DMSP auroral pictures. Unfortunately, the auroral pictures of the intervals examined in this report either are unavailable or show no significant auroral emissions. During geomagnetically very quiet periods, the optical emissions of the auroral oval become very weak, often below the threshold of the DMSP detector. This type of auroral picture without auroras was frequently ignored and not logged into the DMSP data stream.

Even though the diurnal variation of the auroral oval size cannot be confirmed by simultaneous DMSP optical auroral observations, some previous studies support this implication. From statistical examination of 150 days of the USAF Q index (auroral oval size) determined from DMSP northern hemispheric observations, *P. E. Argo* (Private Communication, *April 1978)* noticed a slight dependence of the averaged Q on the UT. Between 0400 to 0800 UT, $< Q >$ was about 5.5 compared with about 2.5 at other UT. The Q index is determined by

$$Q = \frac{1}{0.9} \left[\theta_{eq} - 18 - 5.1 \cos (t - 12°)\right]$$

where θ_{eq} is the co-latitude (in CGL) of the equatorward edge of auroral oval scaled from the DMSP auroral picture at the magnetic local time 't' *(Starkov, 1969)*. Thus, a variation of about 3.0 in Q is equivalent to a change of the auroral oval latitude by 3.33° which is consistent with the 4° amplitude of the diurnal variation observed here. From a much smaller data set (162 noon-midnight orbit auroral pictures), *Sheehan and Carovillano (1978)* also noticed a slight indication of the UT dependence of the auroral oval latitude measured at 0100 MLT meridian.

In addition to establishing a clear UT diurnal variation of the auroral oval size, the observations of extended, extremely quiet periods also reveal that the evening sector of the smallest auroral oval is located at about 72° CGL before 1200 UT and at about 69° after 1200 UT. The oval did not move toward the higher latitudes as the geomagnetic quiescence continued. Thus, it appears that such auroral oval locations correspond to the ground-state (or the quasi-ground-state) of the magnetosphere during extremely quiet geomagnetic conditions. The diurnal variation of the auroral oval size by about 4° in radius reveals that the area of the polar cap (i.e., the flux of open geomagnetic field lines) varies by about 30%. This change of the polar cap size undoubtedly is caused by the three-dimensional interaction between the interplanetary magnetic field and the diurnal precession of the earth's dipole. The nature and physics of this three-dimensional interaction have not been clearly understood, and the detailed mechanism producing the observed diurnal variation of the auroral oval size is beyond the scope of this report. However, based on observation, which were not discussed here, it has been noticed that the diurnal variation of the polar cap and its phase relation with the UT are not effected by the different sectors (i.e., toward or away) of the interplanetary magnetic field.

ACKNOWLEDGEMENTS

This work was supported in part by the Air Force Office of Scientific Research, Air Force Systems Command, under Grant 79-0010 to The Johns Hopkins University and the Air Force Geophysics Laboratory under Task ZU40 of Contract N00017-72-C-4401 between The Johns Hopkins University and the Department of the Navy. It was also supported by the Atmospheric Sciences Section of the National Science Foundation Grant ATM75-02621 A01 through contract from the University of California, Berkeley, to The Johns Hopkins University.

REFERENCES

Akasofu, S. I. and S. Chapman, Solar Terrestrial Physics, *Oxford University Press*, 1972.

Akasofu, S. I., The roles of the north-south component of the interplanetary magnetic field on large scale auroral dynamics observed by the DMSP satellite, *Planet. Space Sci.*, *23*, 2349, 1975.

Berkey, T. F. and Y. Kamide, On the distribution of global auroras during intervals of magnetospheric quiet, *J. Geophys. Res.*, *81*, 4701, 1976.

Feldstein, Y. I. and G. V. Starkov, Dynamics of auroral belt and polar geomagnetic disturbances, *Planet. Space Sci.*, *15*, 209, 1967.

Gustafsson, G., A revised corrected geomagnetic coordinate system, *Ark. Geofys.*, *5*, 595, 1970.

Holzworth, R. H. and C.-I. Meng, Mathematical representation of the auroral oval, *Geophys. Res. Lett.*, *2*, 377, 1975.

Lui, A. T. Y., C. D. Dnger and S.-I. Akasofu, The equatorward boundary of the diffuse aurora and auroral substorms as seen by the ISIS 2 auroral scanning plotometer, *J. Geophys. Res.*, *80*, 3603, 1975.

Lui, A. T. Y., D. Venkatesan, C. D. Anger, S.-I. Akasofu, W. J. Heikkila, J. D. Winningham and J. R. Burrows, Simultaneous observations of particle precipitations and auroral emissions by the ISIS 2 satellite in the 19-24 MLT sector, *J. Geophys. Res.*, *82*, 2210, 1977.

Meng, C.-I., Polar cap variations and the interplanetary magnetic field, *Space Sciences Rev.*, (in press), 1979.

Meng, C.-I., Simultaneous observations of low-energy electron precipitation and optical auroral arcs in the evening sector by the DMSP 32 satellite, *J. Geophys. Res.*, *81*, 2771, 1976.

Meng, C.-I., B. Mauk and C. E. McIlwain, Electron precipitation of evening diffuse aurora and its conjugate electron fluxes near the magnetospheric equator, *J. Geophys. Res.*, *84*, (in press), 1979.

Pike, C. P., (editor), Defense meteorological satellite program auroral-ionospheric interpretation guide, *Air Force Surveys in Geophysics, No. 306 (AFCRL-TR-75-0191)*, AFGL, Hanscom AFB, Massachusetts, 1975.

Pike, C. P. and B. S. Dandekar, Auroral oval dynamics from DMSP photographs, *J. Geophys. Res.*, (submitted), 1979.

Sheehan, R. E. and R. L. Carovillano, Characteristics of the equatorward auroral boundary near midnight determined from DMSP images. *J. Geophys. Res.*, *83*, 4749, 1978.

Starkov, G. V., Analytical representation of the equatorial boundary of the oval auroral zone, *Geomagn. Aeron.*, *9*, 614, 1969.

FIGURE CAPTIONS

FIGURE 1 Polar region electron precipitation profile detected by the DMSP-36 (F2) satellite on January 21, 1978. Only three-energy channels, out of a total of 16, are shown, namely 110 eV, 1.06 keV and 8.99 keV. The profiles cover the complete northern polar region. The satellite entered the polar region along ~ 0700 magnetic local time meridian and departed from ~ 2000 MLT meridian. The intense precipipitations near 0958 UT and 1008 UT correspond to transversals of the morning and the evening parts of the auroral oval, respectively. The equatorial edge of the auroral oval is defined by a sharp decrease of the ~ 1 keV electron precipitation at about 0957 and 1008 UT.

FIGURE 2 Latitudinal variation of the location of the auroral oval equatorial boundary from November 20 to 26, 1977. The top curve is for the evening auroral oval (detected between 1900-2100 MLT) and the lower curve is for the morning auroral oval (between 0300-0700 MLT). The dots and circles correspond to the measurement made over the northern polar region; triangles were made over the southern polar regions. The geomagnetic activity is represented by the 3-hour K_p index and the daily sum of K_p on the top of the graph. Please note that this period corresponds to a prolonged geomagnetic quiescence. The diurnal variation of the auroral oval latitude is clearly demonstrated; and it is coherent over the morning and evening ovals as well as over opposite hemispheres (see text).

FIGURE 3 Same as Figure 2, but observed from December 7 to 11, 1977.

FIGURE 4 Same as Figure 2, but observed from January 19 to 24, 1978. Please note that this is the geomagnetically quietest period in the past five years.

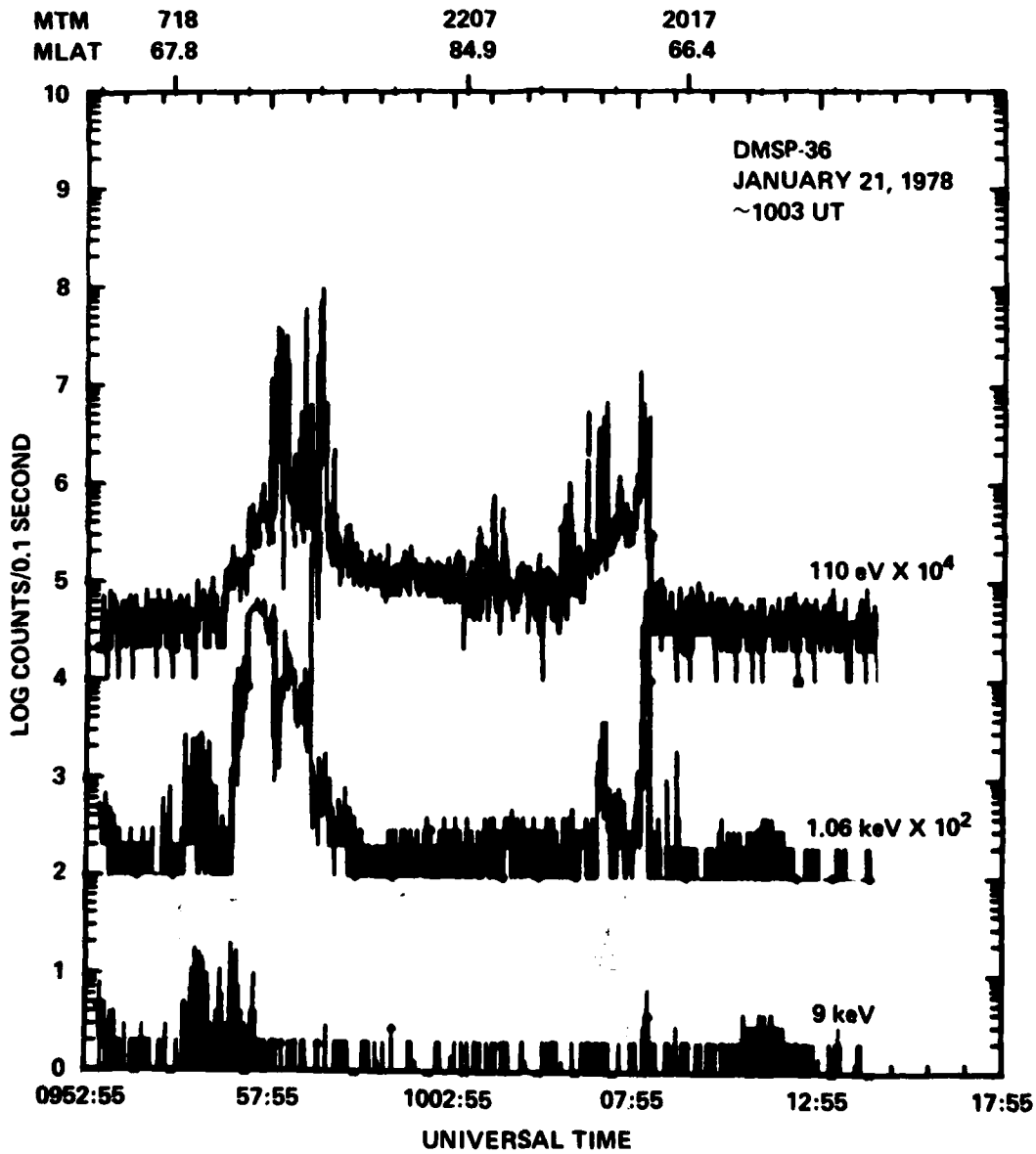
MTM 718 2207 2017
MLAT 67.8 84.9 66.4
DMSP-36
JANUARY 21, 1978
~1003 UT
110 eV X 10^4
1.06 keV X 10^2
9 keV
LOG COUNTS/0.1 SECOND
0
1
2
3
4
5
6
7
8
9
10
0952:55
57:55
1002:55
07:55
12:55
17:55
UNIVERSAL TIME

FIGURE 1

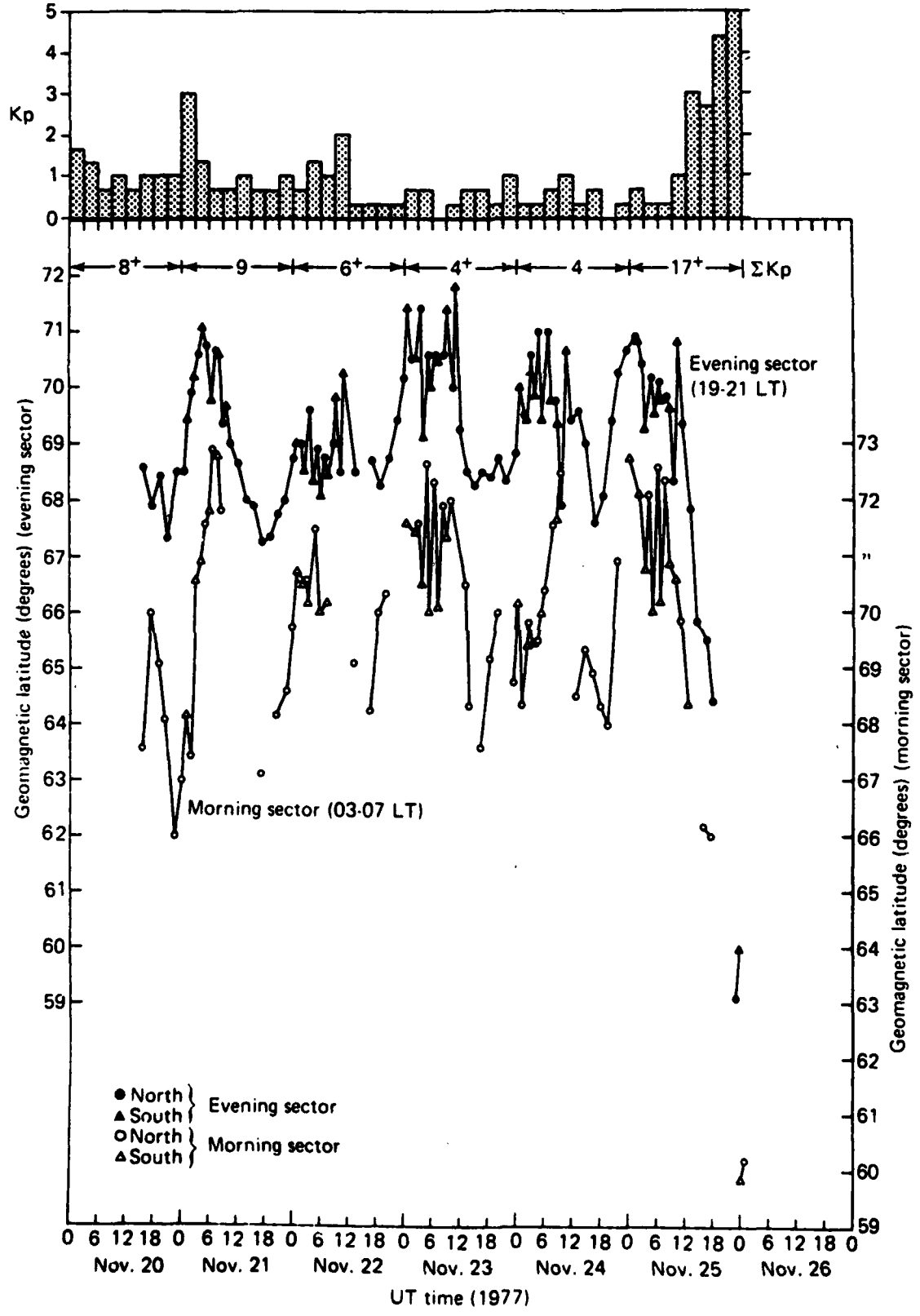
Kp
8+
9
6+
4+
4
17+
ΣKp
Evening sector
(19-21 LT)
Morning sector (03-07 LT)
Geomagnetic latitude (degrees) (evening sector)
Geomagnetic latitude (degrees) (morning sector)
● North
▲ South
Evening sector
○ North
△ South
Morning sector
Nov. 20
Nov. 21
Nov. 22
Nov. 23
Nov. 24
Nov. 25
Nov. 26
UT time (1977)

FIGURE 2

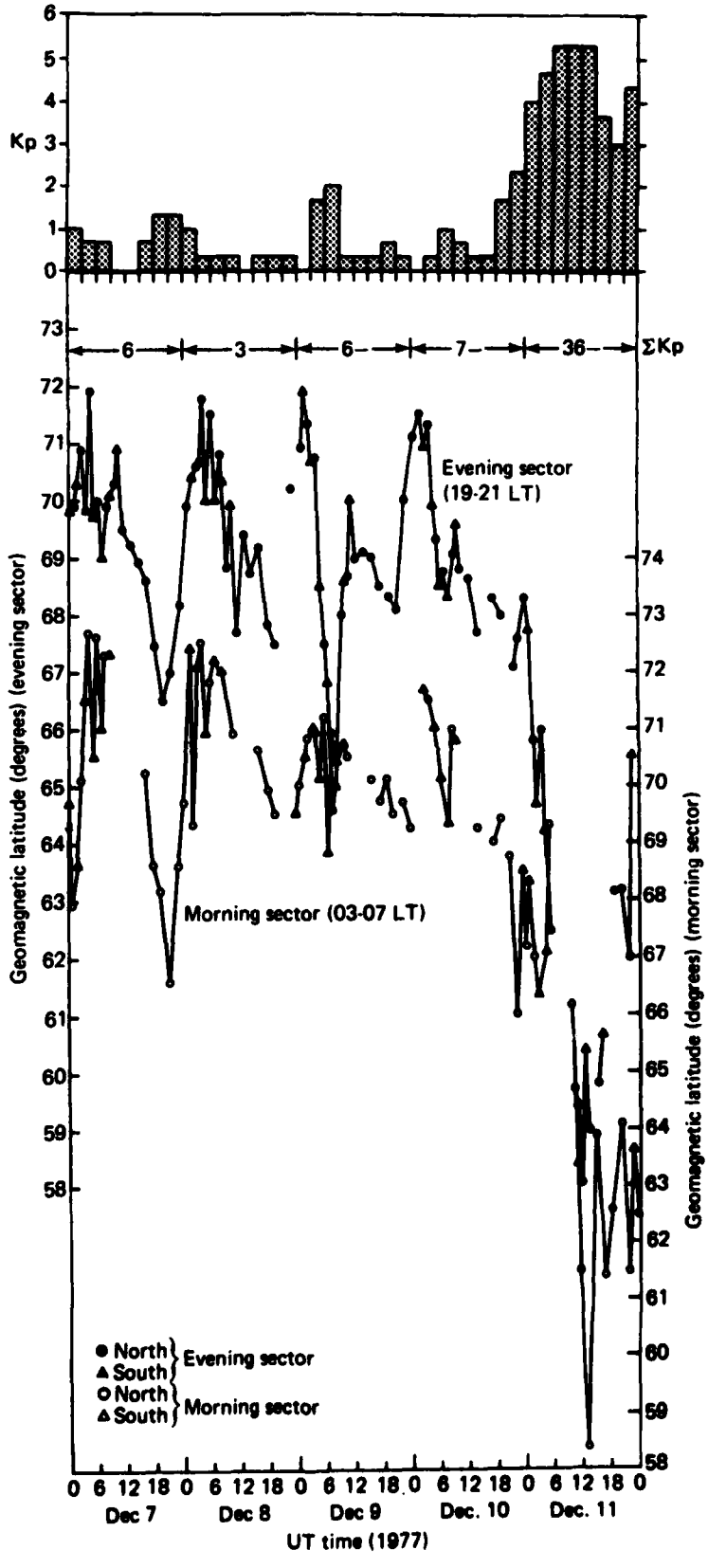
Kp
6
5
4
3
2
1
0
73
6
3
6
7
36
ΣKp
72
71
70
69
68
67
66
65
64
63
62
61
60
59
58
Evening sector
(19-21 LT)
Morning sector (03-07 LT)
Geomagnetic latitude (degrees) (evening sector)
Geomagnetic latitude (degrees) (morning sector)
74
73
72
71
70
69
68
67
66
65
64
63
62
61
60
59
58
● North
▲ South
Evening sector
○ North
△ South
Morning sector
0 6 12 18 0 6 12 18 0 6 12 18 0 6 12 18 0 6 12 18 0
Dec 7
Dec 8
Dec 9
Dec. 10
Dec. 11
UT time (1977)

FIGURE 3

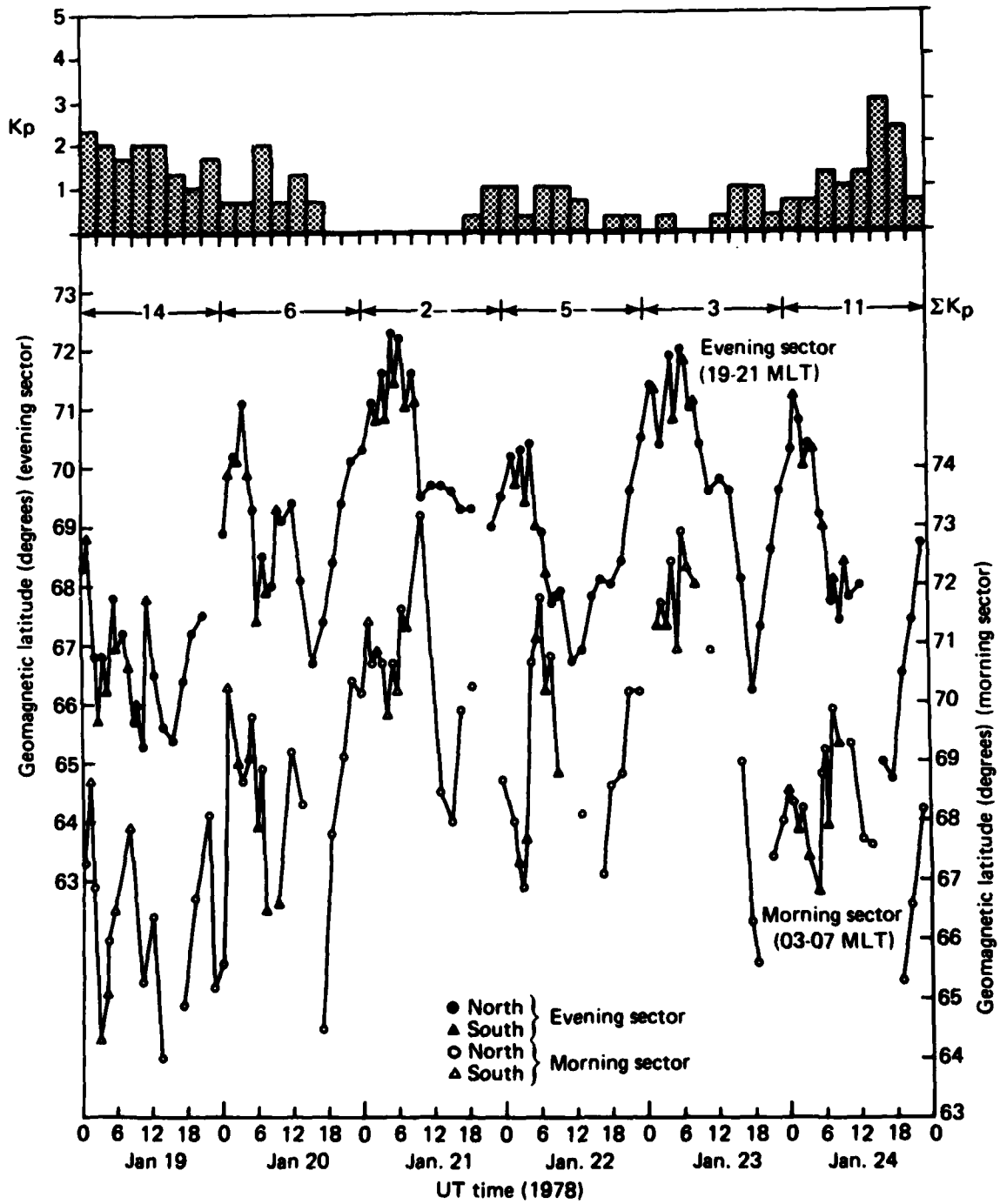
Kp
5
4
3
2
1
14
6
2
5
3
11
ΣKp
Evening sector
(19-21 MLT)
Morning sector
(03-07 MLT)
Geomagnetic latitude (degrees) (evening sector)
Geomagnetic latitude (degrees) (morning sector)
73
72
71
70
69
68
67
66
65
64
63
74
● North
▲ South
Evening sector
○ North
△ South
Morning sector
0 6 12 18 0 6 12 18 0 6 12 18 0 6 12 18 0 6 12 18 0 6 12 18 0
Jan 19
Jan 20
Jan. 21
Jan. 22
Jan. 23
Jan. 24
UT time (1978)

FIGURE 4

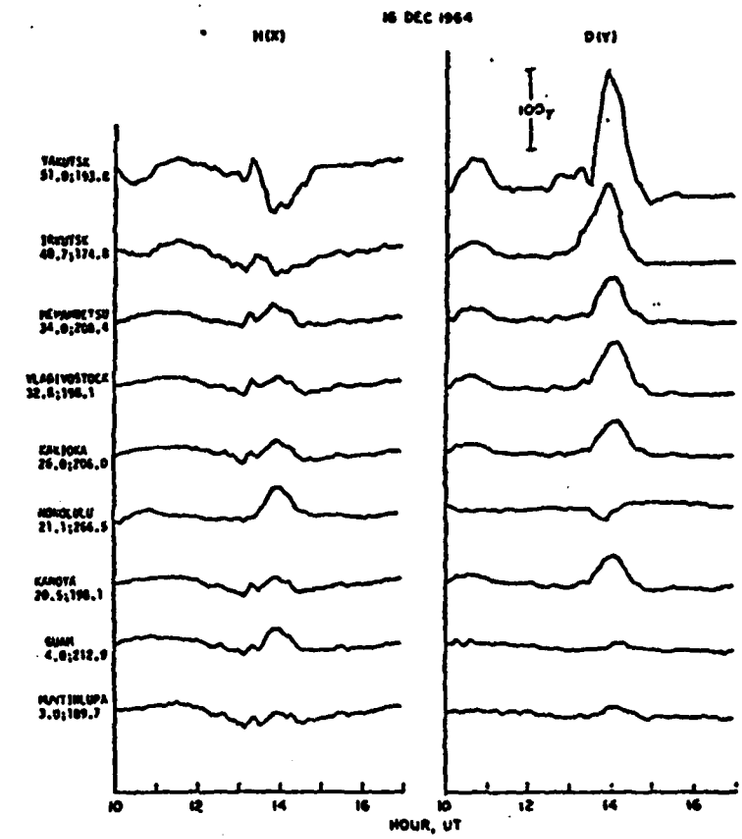

The *H* and *D* component magnetic records below dipole latitude 60°, Pacific sector.

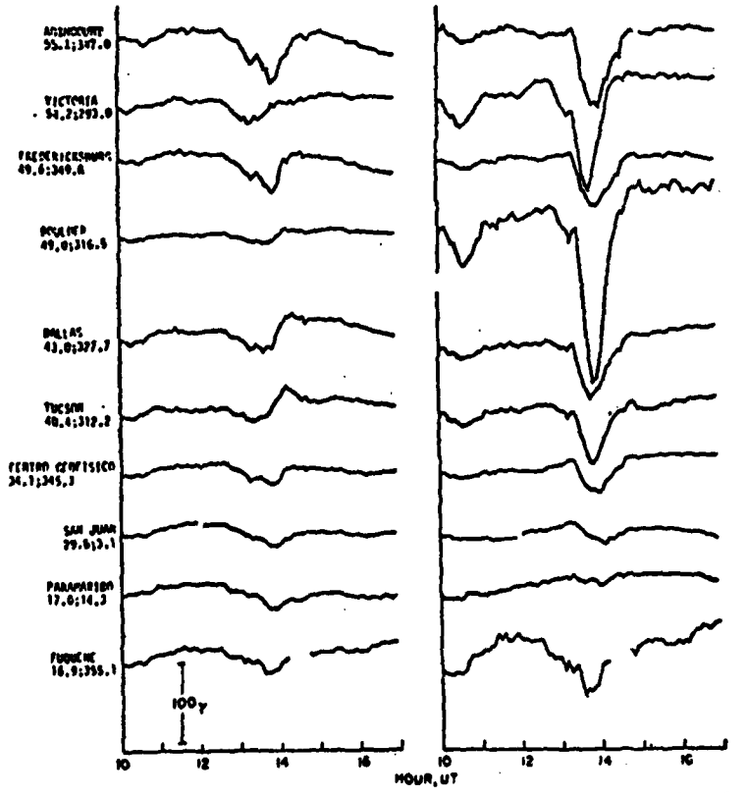

The *H* and *D* component magnetic records below dipole latitude 60°, America sector.

FIGURE 5

TABLE 1

Observatory	dp lat	Observatory	dp lat
Meanook (Canada)	61.8°N	Rude Skov (Denmark)	55.9°N
Sitka (Alaska)	60.0°N	Wingst (Germany)	54.6°N
Lerwick (Scotland)	62.5°N	Witteveen (Holland)	54.1°N
Eskdalemuir (Scotland)	58.5°N	Hartland (England)	54.6°N
Lövo (Sweden)	58.1°N	Agincourt (Canada)	55.1°N
Fredericksburg (USA)	49.6°N	Amberley (New Zealand)	47.7°S

TABLE 2

QUIET DAYS

FEBRUARY 1979

13 (ΣK_p = 4+), 14 (4+), 17 (10-), 20 (12+), 10 (13+)

MARCH 1979

14 (5-), 21 (9+), 12 (11+), 7 (12+), 20 (13-)

APRIL 1979

20 (4-), 19 (12-), 11 (12), 18 (13-)

MAY 1979

17 (6), 16 (10+), 6 (12+), 31 (13), 4 (13+)

JUNE 1979

5 (8), 3 (8), 28 (8+), 1 (9+), 18 (12+)

JULY 1979

31 (4+), 25 (6), 2 (8-), 11 (8+), 24 (11+)

TABLE 3

DISTURBED DAYS

FEBRUARY 1979

21 (ΣK_p = 41), 22 (34), 23 (33), 27 (28), 26 (29-)

MARCH 1979

29 (45-), 10 (40), 28 (36-), 22 (31), 6 (33)

APRIL 1979

25 (54-), 5 (38+), 29 (39+), 22 (39-), 4 (34+)

MAY 1979

25 (37+), 22 (36), 26 (32), 19 (30+), 24 (28)

JUNE 1979

7 (30), 6 (25+), 22 (29-), 23 (26+), 16 (24+)

JULY 1979

7 (30-), 29 (29), 6 (25-), 27 (27+), 20 (24+)

TABLE 4

MAGNETIC STORMS

FEBRUARY 1979	
21 to 22	Dst ≈ 100 γ
MARCH 1979	
10 to 12	Dst ≈ 130 γ
29 to 30	Dst ≈ 120 γ
APRIL 1979	
3 to 5	Dst ≈ 200 γ
21 to 23	Dst ≈ 90 γ
25 to 26	Dst ≈ 150 γ
MAY 1979	
None	
JUNE 1979	
None	

TABLE 5

DAYS OF ISOLATED (WELL-DEFINED) MAGNETOSPHERIC SUBSTORMS

(ALASKAN CHAIN)

FEBRUARY 1979	
4	(1000 UT to 1200 UT)
7	(1140 UT to 1315 UT)
8	(1000 UT to 1140 UT)
9	(1400 UT to 1700 UT)
MARCH 1979	
4	(1100 UT to 1530 UT)
5	(1000 UT to 1120 UT)
8	(1140 UT to 1315 UT)
22	(1000 UT to 1230 UT)
APRIL 1979	
13	(1150 UT to 1430 UT)
17	(1000 UT to 1300 UT)
MAY 1979	
5	(0900 UT to 1020 UT)
29	(1100 UT to 1420 UT)
JUNE 1979	
17	(1040 UT to 1300 UT)
26	(1030 UT to 1240 UT)
29	(1040 UT to 1200 UT)
JULY 1979	
21	(0940 UT to 1100 UT)

FIGURE 1

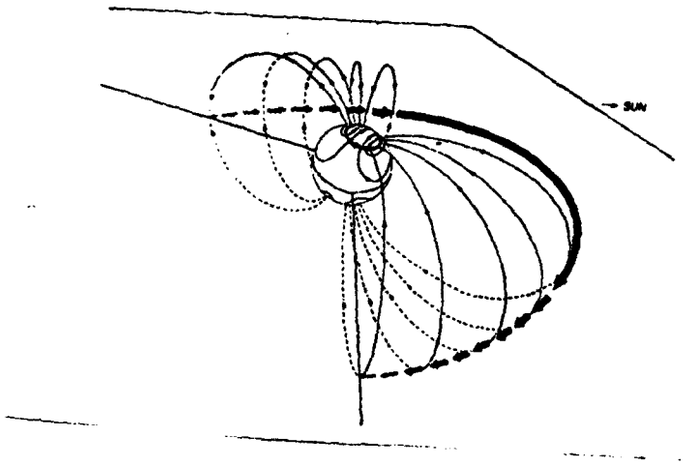

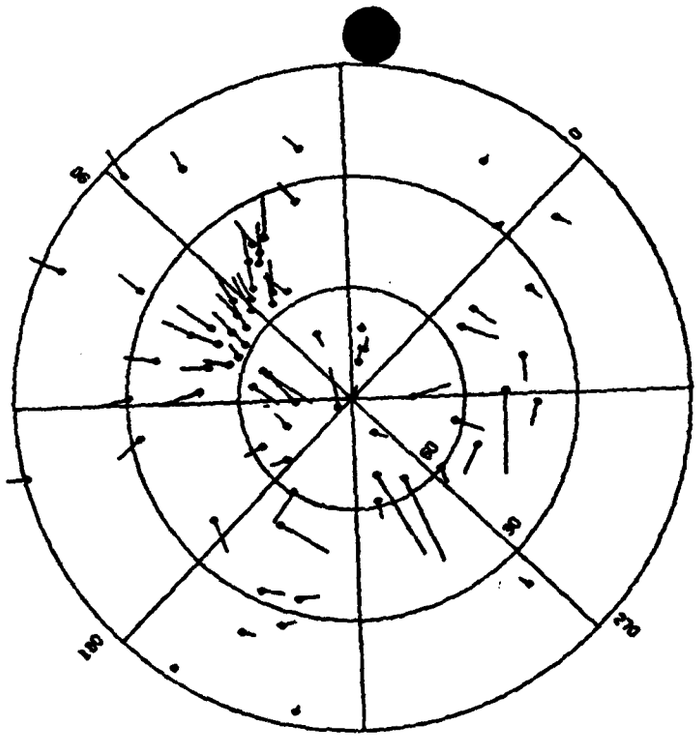

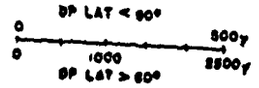

The distribution of the magnetic disturbance vectors at 1400 UT, December 16, 1964;

FIGURE 2

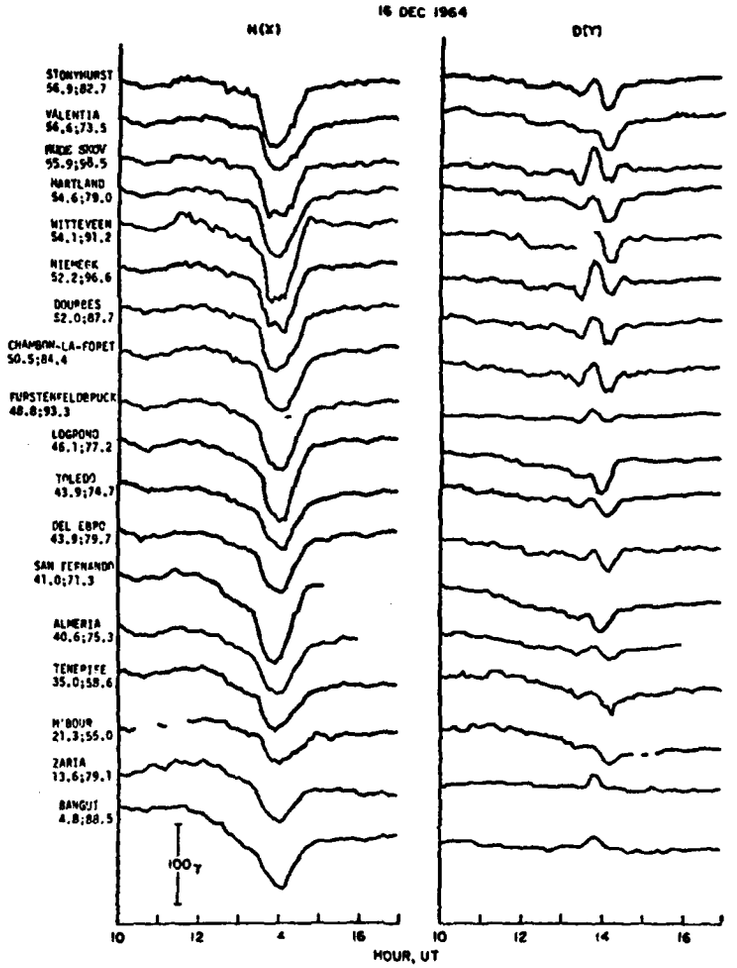

The *H* and *D* component magnetic records below dipole latitude 60°, West Europe sector.

FIGURE 3

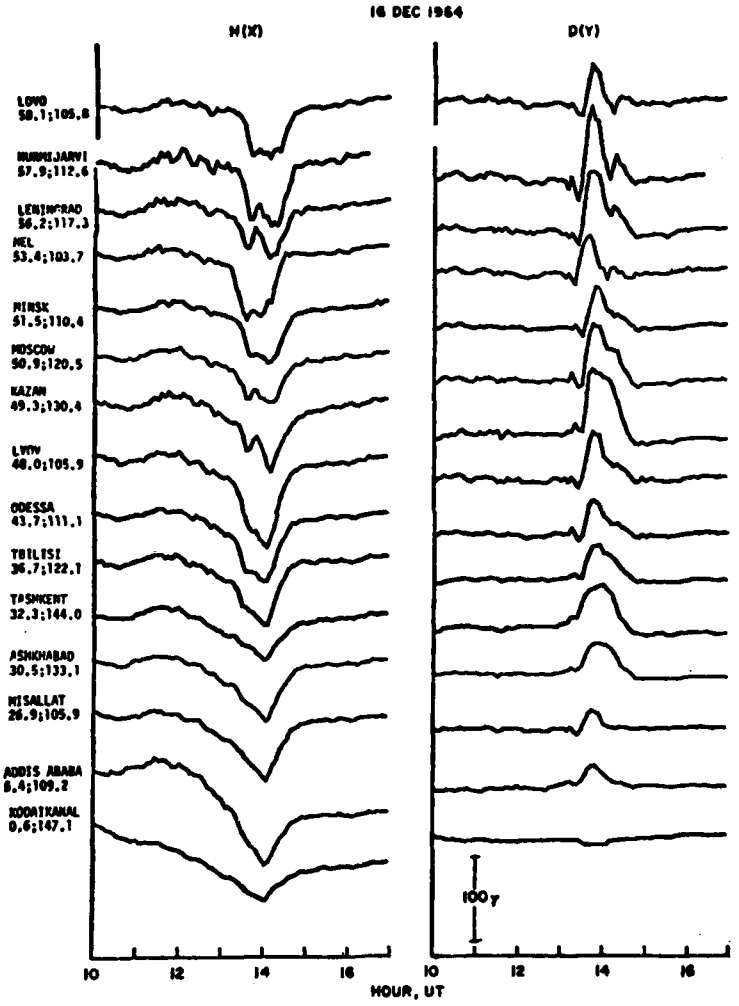

The *H* and *D* component magnetic records below dipole latitude 60°, East Europe sector.

FIGURE 4

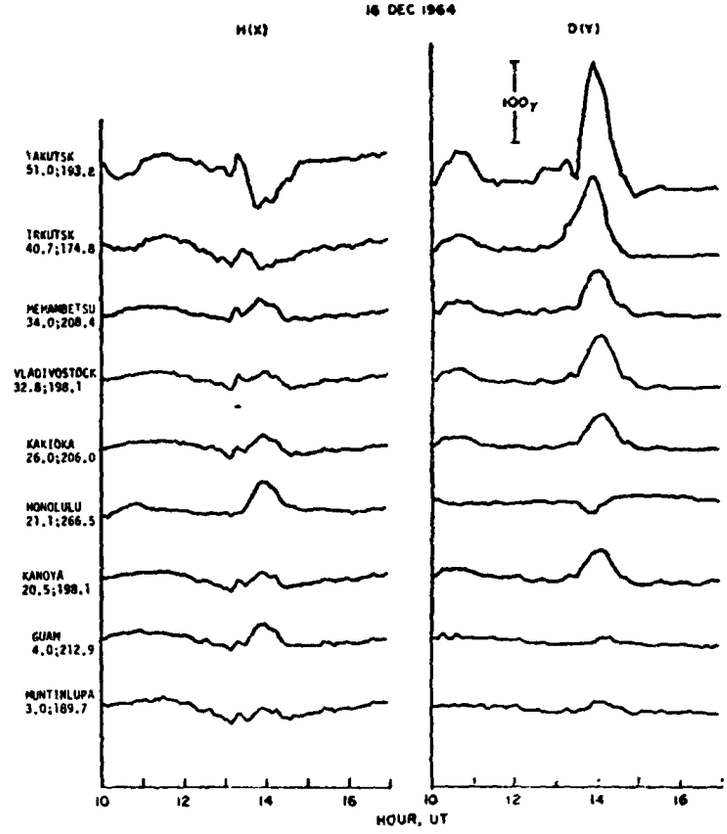

The *H* and *D* component magnetic records below dipole latitude 60°, Pacific sector.

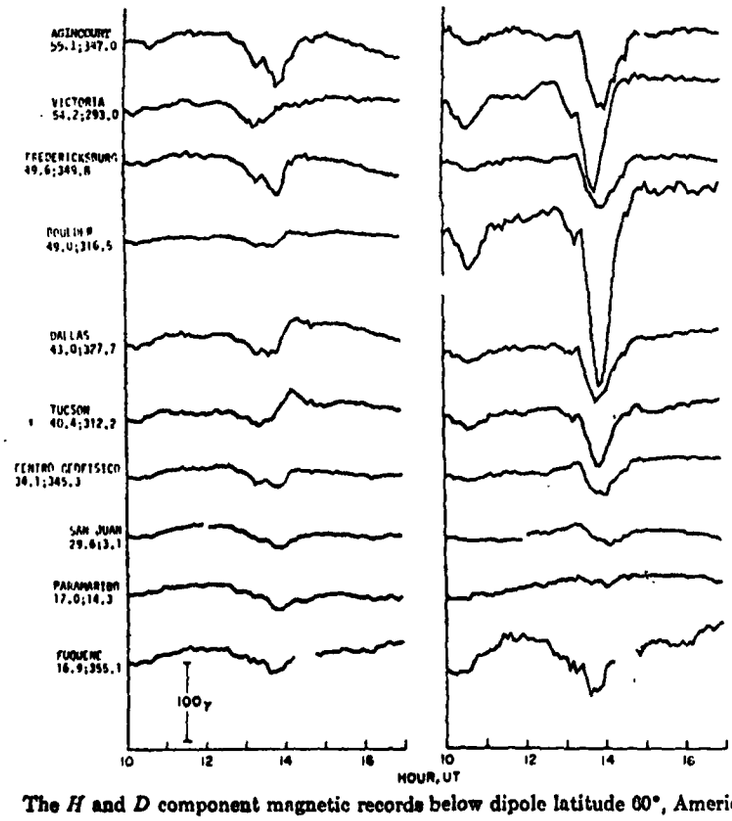

The *H* and *D* component magnetic records below dipole latitude 60°, America sector.

FIGURE 5

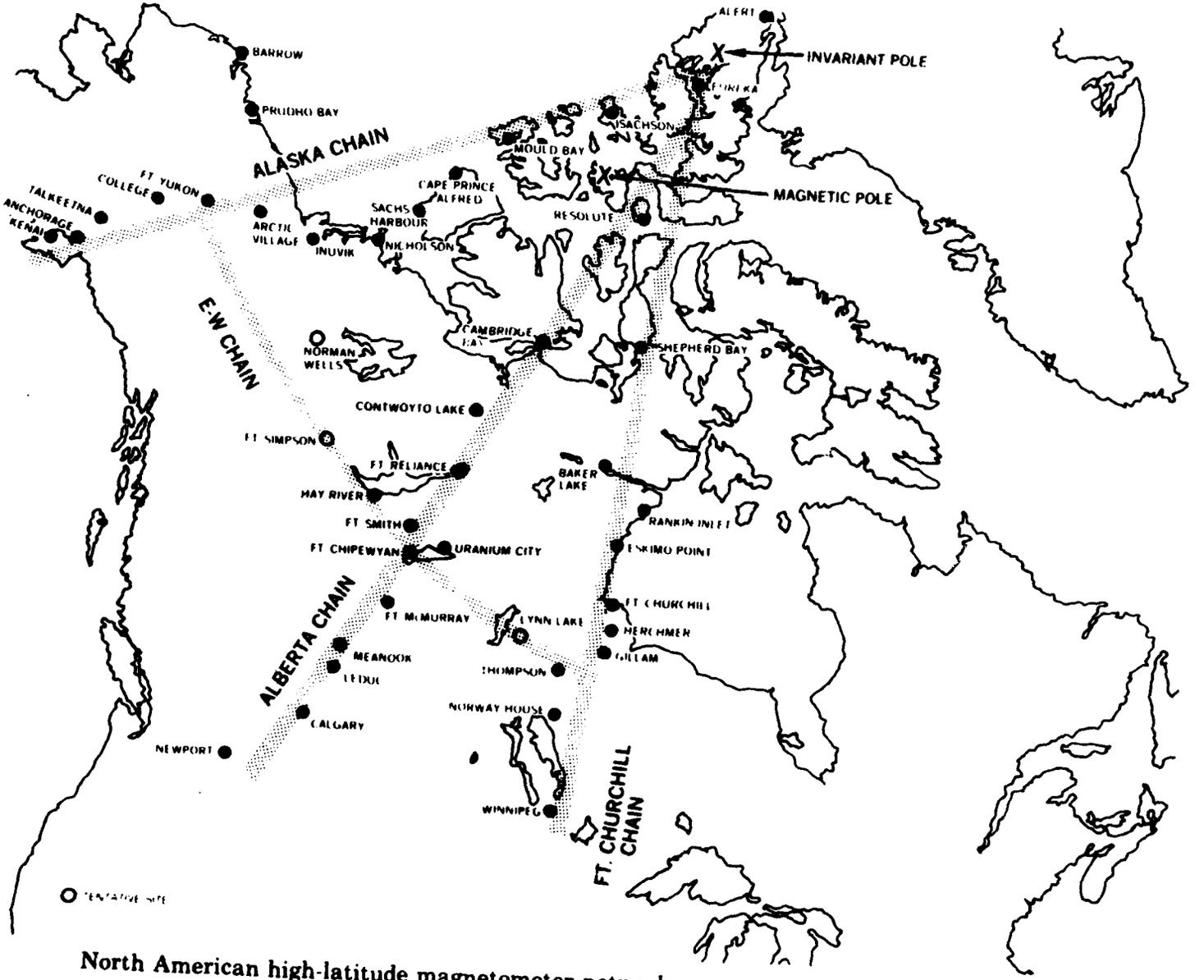

North American high-latitude magnetometer network.

FIGURE 6

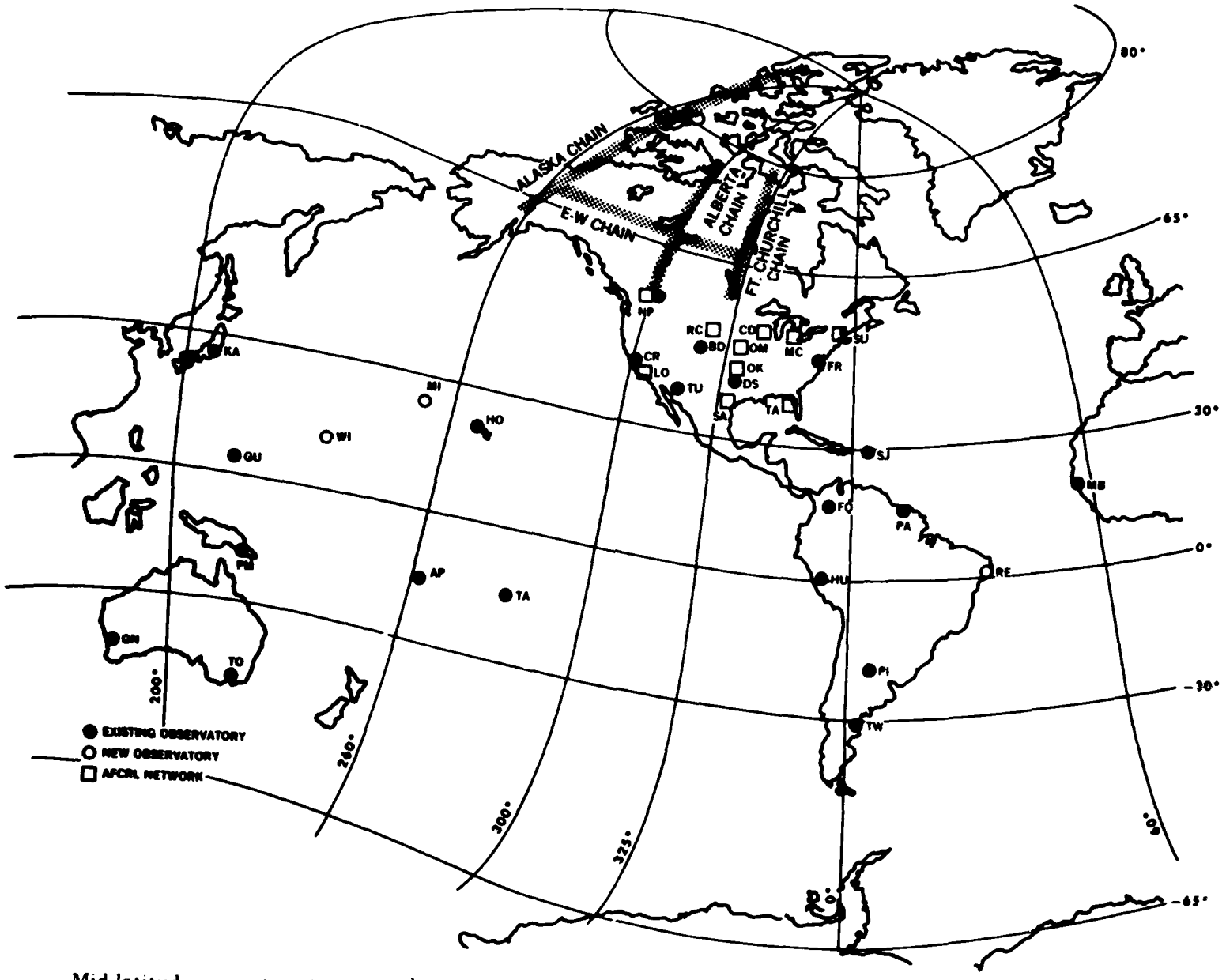

Mid-latitude magnetometer network.

FIGURE 7

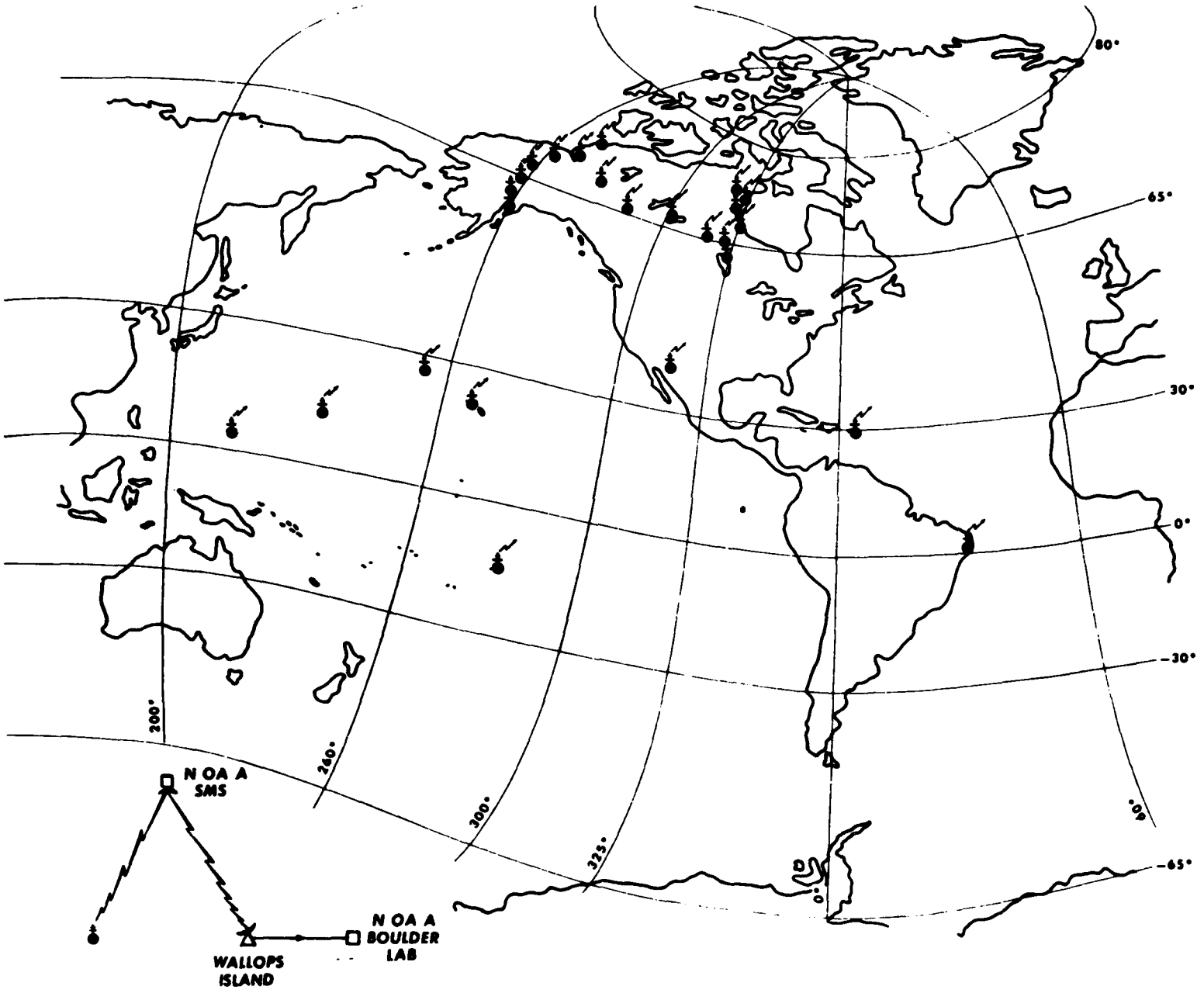

North American magnetometer observatories with satellite telemetry relay links.

FIGURE 8

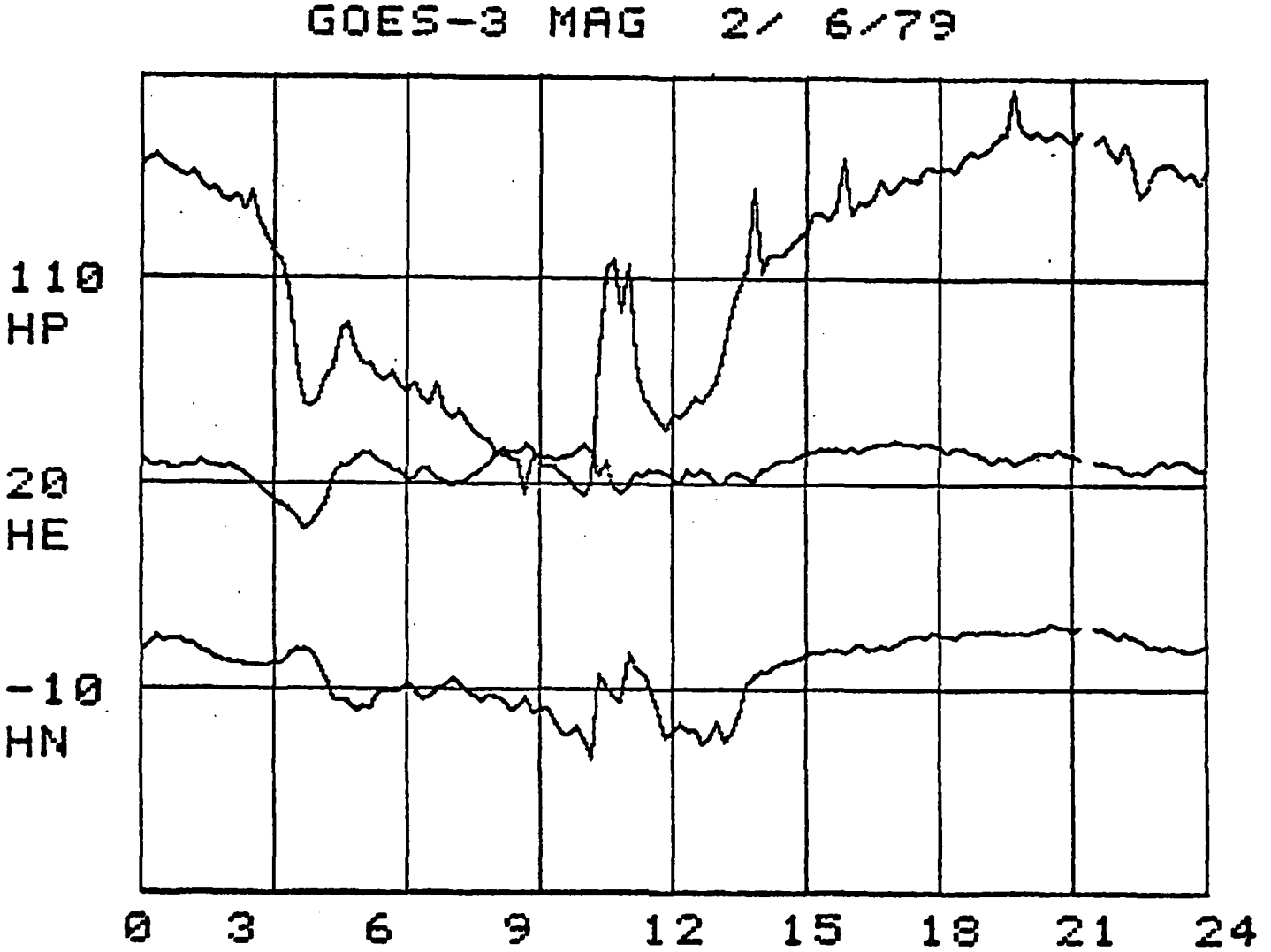

FIGURE 9

EUROPEAN SPACE AGENCY

EUROPEAN SPACE OPERATIONS CENTRE

Daily Summaries of GEOS-2

Particle Data

Wave/Field Data

Period covered in this issue: 12 Jan 1979 12.00GMT ...
.... 2 Feb 1979 12.00GMT

Note for users of GEOS-2 Daily Summaries:

Longitude/distance data not available on the summaries for the period 26 Jan 1979 00.00GMT .... 2 Feb 1979 12.00GMT.
Please extrapolate from preceding data.

FIGURE 10

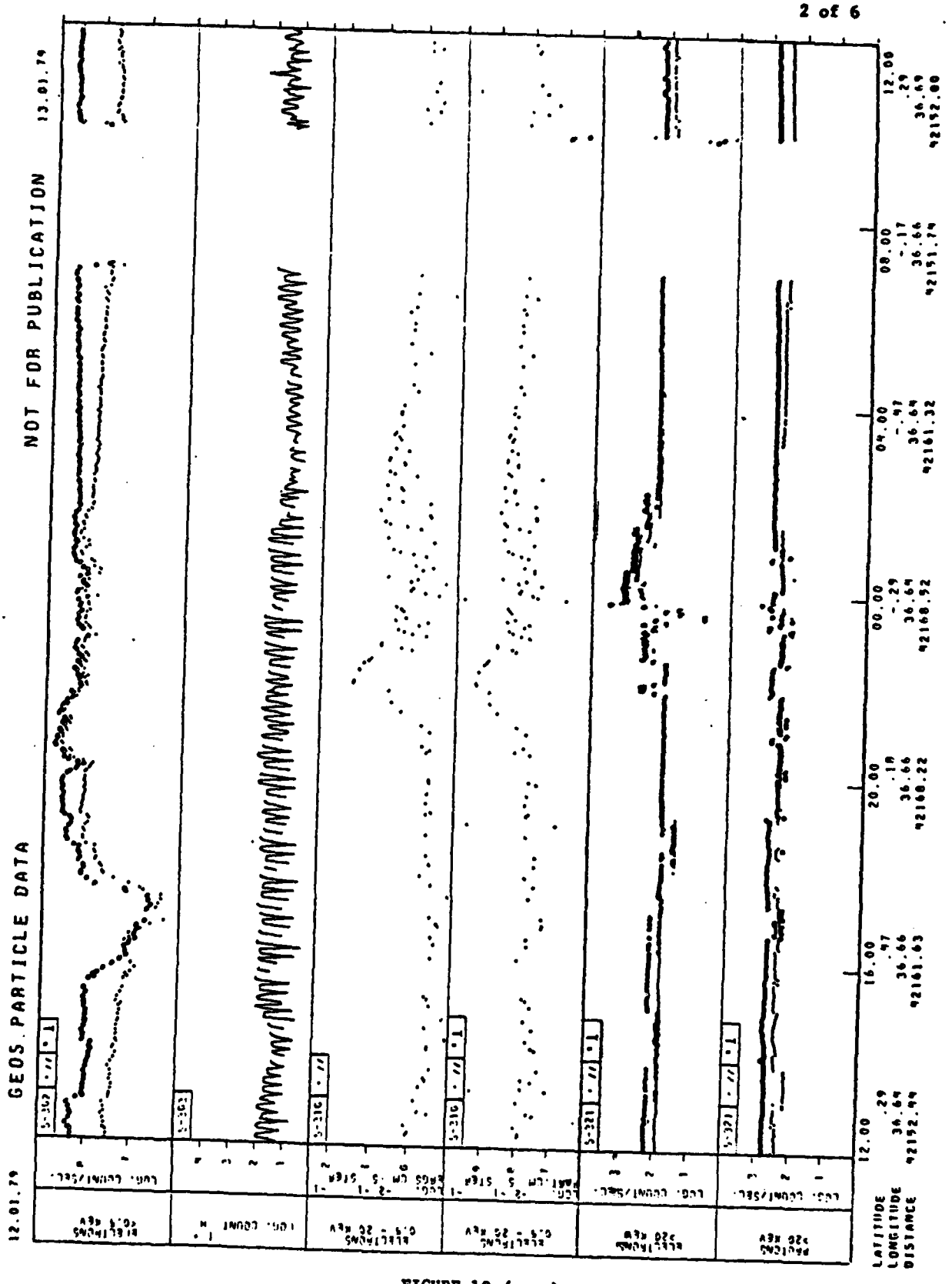

FIGURE 10 (cont)

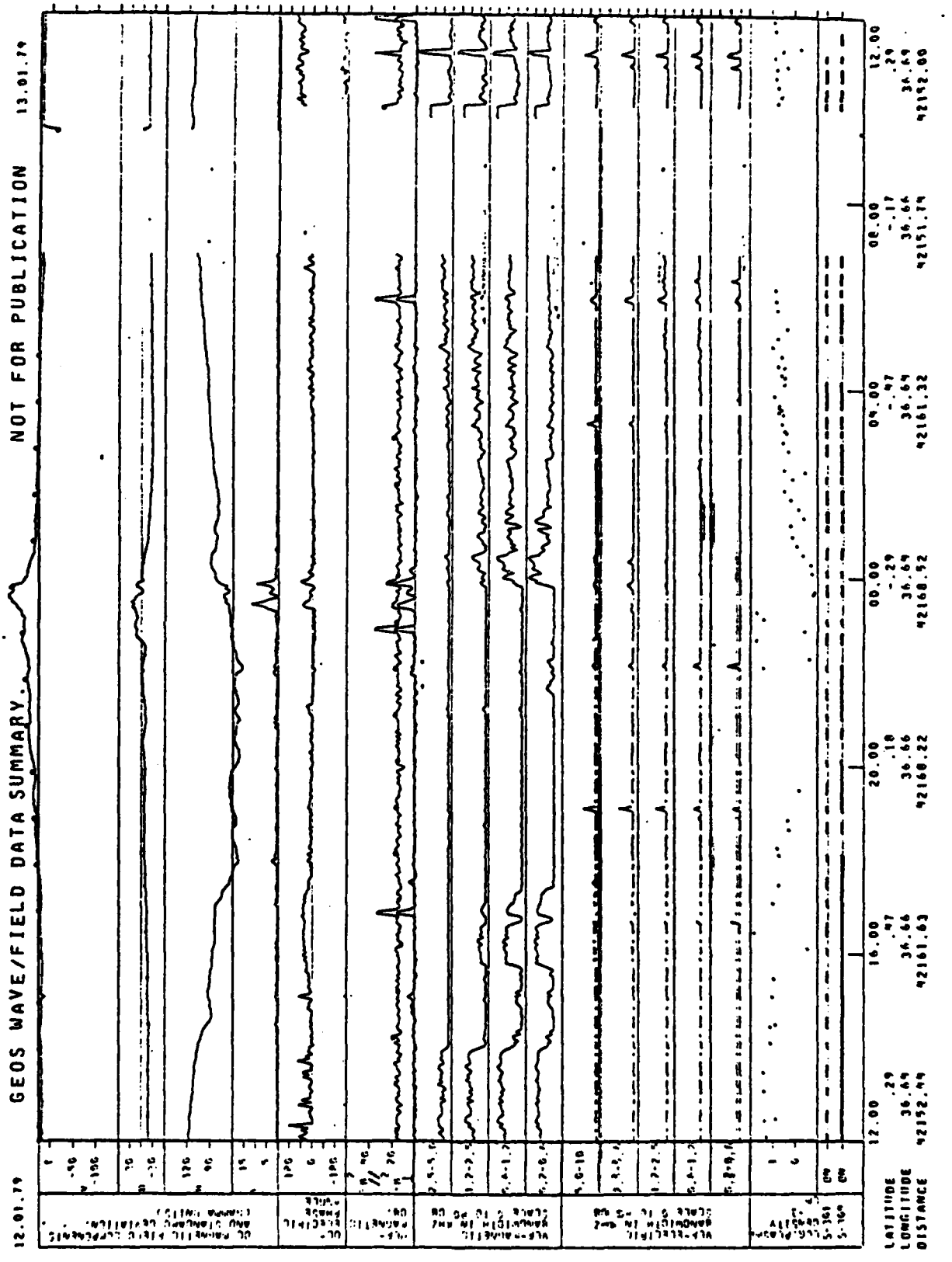

FIGURE 10 (cont)

Note for Users of GEOS Wave/Field Data

Since early December 1977 an offset in the GEOS magnetometer renders the values for the DC Magnetic Field suspect. Absolute values as displayed should therefore be treated with caution!

On 3rd April 1978 an inversion manoeuvre was started to move the satellites + z-axis (spin-axis) from pointing south to pointing north. This manoeuvre will be executed in two stages, and between 3rd and 10th April the satellite will assume an intermediate attitude. (Target attitude: RA = 291°, Dec = 12°) During this week, the duration of data acquisition is of shorter duration than normal.

FIGURE 10 (cont)

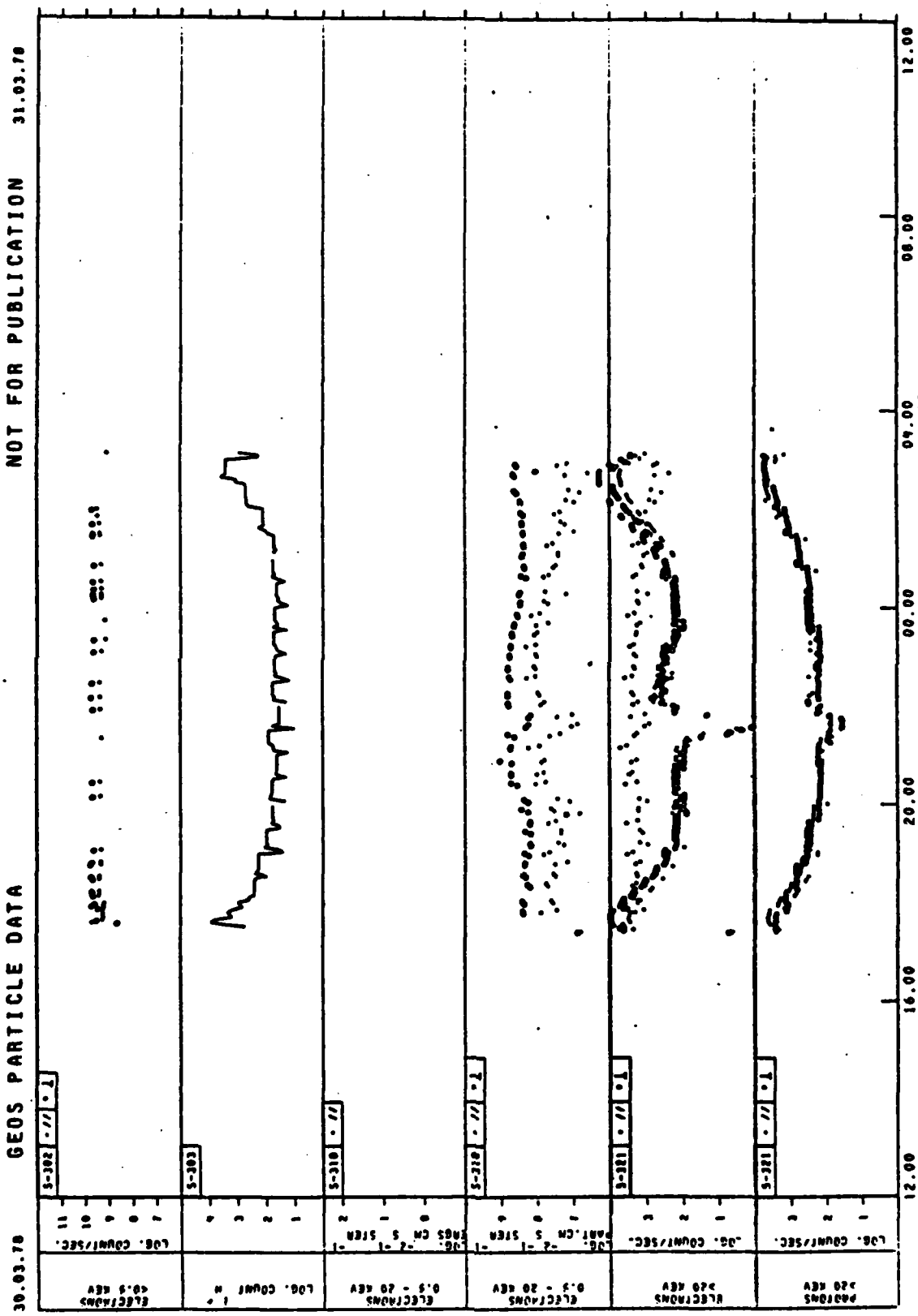

FIGURE 10 (cont)

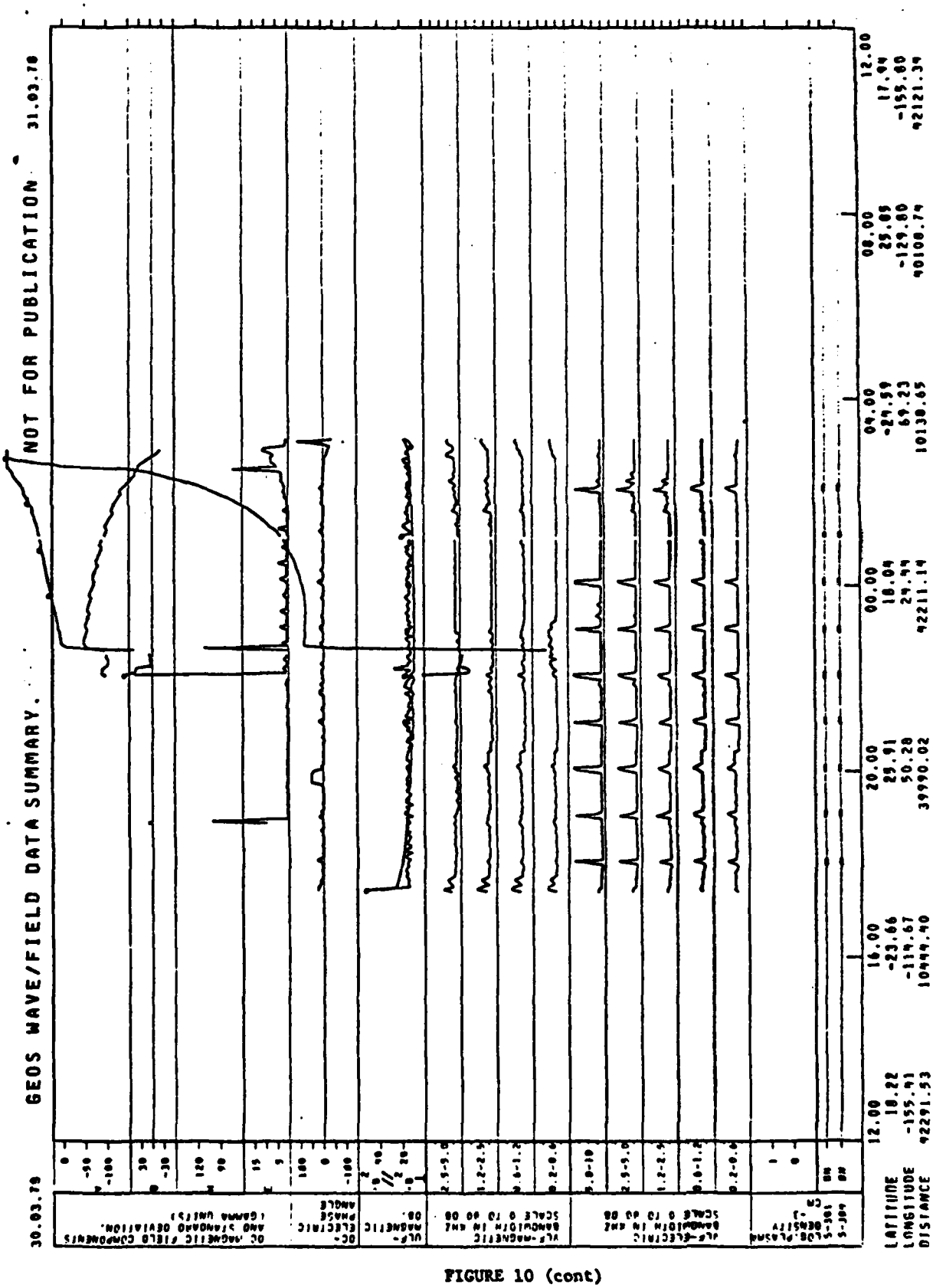

FIGURE 10 (cont)

APPENDIX 1

Kp and Dst Indices

February to July 1979

FEBRUARY 1979

Day	Three-Hourly Indices Kp									Three-Hourly Indices Kn								Ap	as				Cp
		1	2	3	4	5	6	7	8	Sum	1	2	3	4	5	6	7	8		N	S	M		
1	Q7	2+	2+	2	2+	1+	1-	1-	2-	13+	2+	2-	2-	2	1+	1-	0+	2-	6	13	18	16	6 C	0.3
2		3+	3+	3-	3-	2-	2-	2+	2	18+	2+	2+	2	2+	2-	2-	3-	2	18	18	19	18	19	0.5
3	Q8A	2	2-	0+	0+	1+	2	4	3+	15	2-	1	0+	0+	1+	2-	4+	3	9	28	13	7	26	0.5
4		4-	4-	3	3+	3+	4+	3	2+	27-	4-	3+	3-	3	3+	4+	3-	2+	19	29	32	29	32	1.0
5		4-	2+	3-	3	2-	0+	0+	2	16	3	2+	2+	3	2	0+	0+	2-	9	12	12	17	7 K	0.5
6		2+	4	3	3-	3	2	3-	4	24-	2+	3	3-	3	3	2+	3	3+	16	22	25	22	25	0.9
7	Q6	2-	1	1-	2-	2-	2	2	2+	13	1+	1+	1+	1+	2-	2	2+	1-	6	8	14	9	14 C	0.3
8	Q9A	3-	2+	2-	3-	1+	2+	2+	2+	18-	2+	2-	2-	3-	1+	3-	2+	2	9	16	16	16	16	0.6
9		3-	2+	2	3-	2+	2+	2-	2	18	2+	2-	2-	2	2+	3-	1+	2+	9	14	17	15	16	0.5
10	Q5	2	2-	2-	1+	2	1+	2-	2-	13+	2-	1	1	1-	2-	2-	2	1+	6	11	12	10	13 C	0.3
11		4	4	2-	2+	2	1-	2	3-	19+	4-	3+	2-	2	2-	1-	2-	3-	12	24	14	20	13	0.7
12		4+	4	4-	4-	4	2+	1+	1-	23+	3+	3+	3+	4+	4-	2+	2-	1-	17	30	20	33	17	0.9
13	Q1	0+	0+	1	1	1-	0+	0+	0+	4+	0+	0+	1-	1	0+	0+	0	0	3	4	4	6	3 CK	0.0
14	Q2	0+	0	0	1	0	1-	1-	2-	4+	0	0	0	1-	0+	1-	1-	2-	2	5	4	3	5 CK	0.0
15		1+	2	4-	3	3	3	2	1-	19-	1+	2-	3-	3	2+	3	2	1+	11	16	19	19	17	0.6
16	Q8A	1+	3+	2	2+	2	1-	1	0+	13	2+	2+	2+	2	2-	0+	1	0+	7	11	13	20	9 KK	0.3
17	Q3	0+	1-	1+	1+	1	2	1+	2-	10-	0+	1-	1	1	1+	2	2	2	5	9	6	4	10 C	0.2
18		2-	4+	4-	4	3-	2+	4+	4+	27+	2+	4	4-	4+	3	3-	4-	4-	22	37	42	46	38	1.1
19		4+	3	3-	2+	4	2+	3-	2	23+	3+	3-	2	2+	4-	3-	3-	2	15	27	26	23	25	0.9
20	Q4	2-	2-	2-	1-	1-	1+	2	3-	12+	2-	1+	1	0+	1-	2-	2+	3-	6	12	12	10	13 C	0.3
21	Q6	2+	5+	7-	5	4+	3+	4+	4-	41	1+	4+	3+	4+	4	3+	4	3+	29	76	93	66	102	1.7
22	Q2	4+	4-	5-	5	5	3-	3+	3+	34	4+	4+	4	4+	4+	4+	3+	4-	33	46	58	54	58	1.3
23	Q3	5	5	5-	4	4	2	3+	4	33	3-	4+	4-	3+	4-	3	3+	4-	31	45	57	45	38	1.3
24		3+	3	3-	3+	3	4-	3+	3+	26-	3	2+	2	3-	3	3+	3	3+	17	21	21	22	21	0.9
25		2+	4	4-	2	3-	2-	3-	3+	22+	2+	3	3-	2	3-	2	3-	3	14	25	19	23	22	0.8
26	Q5	4-	4-	3-	3-	3+	4+	4+	4	29-	3	3	3-	3-	3+	4	4	4-	22	48	37	23	55	1.1
27	Q4	4-	5-	3	3+	4-	3+	2+	2	28	3-	4-	3-	3-	3	3	2	2+	24	32	22	32	23	1.2
28		4-	2	2-	3	4-	4+	4-	3-	29-	3+	2-	1+	3-	4-	4	3+	3	17	35	23	18	48	0.9
																		Mean	19	24.6	23.3	23.0		0.78

Day	Three-Hourly Indices Kn								Three-Hourly Indices Ks								S	So	Prov Rz	IMF	
	1	2	3	4	5	6	7	8	1	2	3	4	5	6	7	8					
1	2	2-	1+	2	1	1-	0+	2-	3-	2-	2	2+	2-	1-	1-	2-	191.4	185.8	116	T	T
2	2+	2	2	2	2-	2-	3-	2-	3-	2+	2	2+	2-	2-	3-	2	191.1	185.6	127	T	TA
3	1+	1+	0	0+	1+	2-	4	3	2-	1-	1-	0+	1+	2-	3-	3	193.3*	187.4*	148	T	T
4	3+	3	3-	3-	3+	3-	3-	2	4-	3+	3-	3	3+	4	3-	2+	193.1	187.7	123	TA	A
5	3-	2+	2+	3+	2+	0	0	2	3	2	2+	3-	2-	1-	1-	2-	203.1	197.4	134	A	A
6	2	3	2+	3+	3+	2+	3	3+	3-	3+	3-	3-	3-	2+	3	4-	212.4	206.5	146	A	A
7	1	1-	1-	1	2-	2-	2	2+	1+	2-	2-	1+	2-	2+	3-	3	209.0	203.4	144	T	T
8	2+	1+	1+	2+	1+	3-	2+	2	2+	2	2	3	1+	3-	2+	2	213.0*	207.2*	142	T	T
9	2+	2-	2-	2	2+	2+	2-	2+	3-	2	2-	2	2+	3-	1+	2+	206.2	198.7	139	T	T
10	1+	1-	1	1-	1+	2-	2	1+	2	1+	1+	1-	2	2-	2+	1+	203.7*	196.4*	137	T	A
11	3	3+	1+	2	1+	1-	2	3-	4-	3+	2-	2	2	1-	1+	2+	207.6*	202.2*	137	A	*
12	3	3	3+	4-	4-	3-	1+	1-	3+	4-	3+	4-	3+	2+	2-	1-	208.4	199.4	138	A	T
13	0+	0	1-	1	0+	0+	0	0	0+	1-	1-	1+	1-	0+	0	0+	208.4	199.4	152	A	A
14	0	0	0	1-	0	1	1-	2-	0+	0	0	1-	0+	1-	1-	1+	209.4*	204.2*	163	A	A
15	1-	2-	3	3	2+	3	2	1	2-	2-	3-	3	2+	3	2+	2-	210.3*	205.0*	161	A	A
16	2-	2+	2	2	2	0+	1	0+	3-	3-	3-	2	2-	1-	1	0+	214.3	209.2	190	A	-
17	0+	1-	1	1	1+	2	2	2-	1-	1-	1+	1+	2-	2-	2-	2+	218.3	213.1	168	A	A
18	2-	4	3+	4-	3	2+	4	4-	3-	4	4	4	3	3-	3+	3+	243.3	237.7	162	AT	A
19	3+	3-	2	2	4-	3-	3-	2	3	2+	2+	2+	4-	3-	3-	2	243.4	237.8	156	T	A
20	2-	1+	1	0+	1-	2	2	3-	2	2-	1-	1-	1-	1+	2+	3-	235.3*	230.1*	169	A	A
21	1+	4	4-	5-	4-	5	4-	5-	1+	5-	5+	4+	4	4-	7-	6-	230.2	225.1	171	TA	A
22	4	3	4	5-	4+	4+	3	4-	4+	4	4	4	4+	4+	4-	4	228.3	223.3	169	A	-
23	4+	4	3+	3+	4-	3+	3	4-	5	5-	4	4-	3+	3-	3+	4-	288.2	196.8	127	TA	-
24	3	2+	2+	3-	3	3+	3	3+	3	3-	2	2+	3-	3+	3	3+	186.7	182.8	99	T	A
25	2	3+	3	2	3-	2	2+	3	2+	3	3-	2	3-	2-	3-	3	178.9	167.5	88	TA	A
26	3+	3	3-	3-	4-	4	4	4-	3	3	2+	2+	3+	4-	4+	4-	169.4	166.8	108	T	T
27	4-	4-	3	2+	3-	3-	2	2+	4-	4-	3-	3	3	3	2	2+	165.9	162.7	97	T	T
28	3+	1+	1+	3-	3+	4-	3+	3-	4-	2	2-	2+	4-	4	3+	3+	166.8	163.6	95	T	-
																	Mean	204.1	199.1	136.8	

MARCH 1979

Day		Three-Hourly Indices Kp									Three-Hourly Indices Km								Ap	GS				Cp
		1	2	3	4	5	6	7	8	Sum	1	2	3	4	5	6	7	8		N	S	M		
1		4	3+	2+	2+	2+	2+	3-	2	21+	3+	2+	2-	2+	2	2+	3-	2	12	25	18	25	19	0.7
2		4	4	3	4-	3+	3-	3	4-	27+	3+	3	3-	3	3	3-	3+	3	20	32	26	32	27	1.8
3		4-	1+	3-	2	3-	3+	3	3-	21+	3	1+	2	2-	2+	3	3-	2+	13	23	16	17	23	0.7
4		4	3+	3+	5-	4+	3	3+	5	31	3+	3-	3-	4	4-	3+	3+	4+	27	47	37	38	47	1.2
5		3	4	3+	3	2-	1+	3-	2	21	3	3+	3-	3	1+	1	3-	2+	13	21	24	38	19	0.8
6	05	3+	3+	4	5-	5-	5-	4+	4	33	3-	3	3	5-	4+	4	4	4-	28	42	38	35	46	1.3
7	05A	3-	2	1+	0+	0+	1	2-	2	12+	2+	3-	1+	0+	0+	1+	2-	2+	7	15	9	13	12	0.3
8	06A	2	2	1+	3-	2	1	1+	2-	14	2	1+	1	2+	2	1	1+	1+	7	13	10	12	11	0.3
9		3+	2-	3+	4-	3	2+	3-	3+	23+	3-	1-	3	4-	3-	2	2+	4-	15	21	21	23	19	0.8
10	02	5	5-	4+	4+	4	4+	6+	7	48	5-	4-	3	4-	5-	4+	5+	6	34	91	63	54	101	1.6
11		5+	3+	3+	3	3+	3-	2-	0	23-	4-	3-	3-	3-	3-	2+	1+	0	16	36	13	29	19	1.0
12	04	1	2-	3-	2-	0+	1+	2+	0+	11+	1-	1	2	1	1-	1+	2+	1-	6	7	7	8	7	CK 0.3
13	08A	1+	3	3-	2	1+	2	0+	1-	13+	2-	2+	2+	2	1+	1+	0+	1-	7	9	9	12	6	CC 0.4
14	01	1-	1-	0+	0+	0+	0+	1	1	5-	0+	0+	0	0	0	0	1-	1	3	4	2	2	4	CC 0.0
15	09A	1-	1+	1	1	2+	3-	3-	3-	14+	1-	2-	1+	1	2+	3-	3-	3-	8	15	14	9	20	0.4
16	08A	3	3-	2+	3	3	2+	1+	2	20-	3-	3-	2-	2+	3-	2	2-	2+	11	21	15	22	15	0.6
17		3	3	4-	4	3	3-	2	3-	26	3	3	4	4-	3-	2	2	3	21	32	35	46	22	1.1
18	07A	2+	3-	2	2	3-	1+	0+	0	13+	2+	2+	1+	2	3-	1+	0+	0	7	13	9	14	9	C 0.3
19		0	0+	3-	3+	3+	3+	3	2-	18-	0+	1-	2+	3-	3	3	3-	2-	11	20	17	14	24	0.6
20	03	1+	2	2	2-	1+	1+	1+	2-	13-	1+	2-	2-	1	1+	1+	1+	2-	6	10	8	9	9	CK 0.3
21	02	0	0+	2-	1	1+	1	2+	2-	9+	0+	1-	2-	1-	1+	1+	2+	2	6	9	8	8	10	C 0.2
22	04	1-	1-	4	6-	7-	7-	4-	3	31	1-	1+	4-	5	6-	6+	4-	3	45	45	74	33	85	1.5
23		4-	3+	3	2-	2	2+	2+	2+	21-	3	3+	3-	2	2	2	2+	2+	12	29	17	26	21	0.7
24		2+	3-	4	3+	2+	2+	3-	4-	23+	2+	2+	4-	3	2	2	3	3+	15	27	27	29	25	0.8
25		3+	4	4-	3+	3	3+	3+	4+	28+	3	3+	3+	3+	3-	3-	3	4-	21	34	32	34	33	1.1
26		4+	4-	4-	3+	4-	5-	4	4-	31	4	3+	3+	3	3+	4	4-	4-	26	42	39	33	48	1.2
27		1+	3	3	3+	3+	4-	4-	4	25+	3+	3-	3	3	3+	3+	4-	4-	18	26	31	16	41	1.0
28	03	4	4-	4	5+	4-	5-	3	5+	30-	3+	3	3+	5-	5-	4+	3	5	30	58	43	37	57	1.4
29	01	6	5	6+	5+	5+	6	7-	5-	45-	6+	4	5	5-	4	5	6-	4+	66	87	74	72	89	1.7
30		5	4+	3	1+	2+	2-	2	2-	21+	5-	4-	2+	1+	2	1+	1+	2	16	19	14	23	12	0.9
31		3	3+	2-	2-	3	3+	3+	5+	25-	3	3-	2	2-	3-	3	3+	4+	19	31	22	17	36	1.0
																		Mean	19	28.9	24.9	27.2		0.81

Day	Three-Hourly Indices Kn								Three-Hourly Indices Ks								S	Sa	Prov Rz	IMF	
	1	2	3	4	5	6	7	8	1	2	3	4	5	6	7	8					
1	3	2+	2-	2+	2	2	3-	2	3+	2+	2-	3-	2	3-	3-	2+	171.6	160.5	116	TA	-
2	3+	3	2+	3	3	2+	3	3	3	3	3-	3	3	3-	3+	3+	173.7	178.7	138	TA	T
3	3	1	2+	1+	3-	3+	3-	2+	3-	2-	2-	2-	2-	3	2+	3-	176.3	173.3	141	T	TA
4	3+	3-	3	4+	4-	3+	3+	4+	4-	3-	3-	4	4-	4-	4-	5-	184.4	181.4	142	T	T
5	3-	3+	3-	3	1+	1	2+	2+	3	3+	3-	3-	1	1-	3-	2+	183.8*	180.1*	135	T	T
6	3-	3	3+	4+	4	4	4	3+	3-	3	3	5-	5-	4	4	4-	185.2	182.4	144	TA	A*
7	2+	3-	1+	1-	0+	1+	2-	2	2+	2+	2-	0+	1-	1	1+	3-	185.9*	183.1*	146	T	T
8	2-	1+	1	2+	2	1	1+	1+	2+	1	1-	2+	2	1	1-	1+	181.4	178.9	143	TA	A*
9	3-	1	3	4-	3	2	3-	4-	2+	0+	3-	3+	2+	2	2	4	184.8	181.4	146	T	T
10	4+	4-	3+	4-	5	4	5	6-	5-	4-	3-	4-	4	5-	6-	6+	183.8	180.4	140	TA	A*
11	4+	3-	3	3-	3	2+	2-	0	5-	3	3-	3-	3-	2+	1+	0	184.1*	181.7*	156	T	A
12	1-	1+	2+	1+	1-	1+	3-	1-	1	1-	1+	1	1-	1+	2+	1	191.8	188.7	178	A	A
13	1+	2	2+	2	1+	1+	0+	1-	2-	2+	2+	2-	1+	1+	0+	1-	188.6	186.3	169	A	A
14	0+	0+	0	0	0	0	1+	1	0+	0+	0+	0	0	0	1-	1	191.5	189.4	159	A	A*
15	1	2-	1+	1+	3-	3-	2+	3-	1-	2	2-	1	2	2+	3-	3-	183.3	181.3	155	T	A
16	3-	2+	2	3-	3-	2	1+	2+	3-	3-	2-	2+	3	2-	2-	2+	185.4*	183.5*	138	A	A
17	3	3-	4+	4-	3-	2+	2	3	3+	3+	5+	4-	2+	2-	2-	3	179.5	177.7	142	A	A
18	2	3-	2-	2	3-	2-	1-	0	2+	2	1+	2-	2+	1+	0+	0+	188.3*	186.6*	142	A	A
19	0	1	1-	1-	1	1	3-	2-	0+	0+	2-	3-	3	3	2+	2-	179.8	177.6	138	A	A
20	1	2	2-	1+	1+	1+	1+	2-	2-	1+	1+	1	1+	2-	1+	2	185.6	184.1	128	T	AT
21	0+	0+	1+	1-	2-	1+	2+	2	1-	1	2-	1-	1+	1	2	2	183.5	182.2	134	A	A
22	1-	1	4-	5+	6-	5+	4-	3	1	2-	4	5	6-	6	4	3	182.4	181.1	148	T	T
23	3	3-	2+	2	2	2	2+	2+	3	3-	3	2	2-	2	3-	2+	189.6	188.5	139	AT	T
24	2	2	4-	3	2	2	3	3	2+	3-	3+	3	2+	2+	3-	3+	189.4	188.3	118	T	T
25	3	3	3+	3	3-	3-	3	3+	3	4-	3+	3+	3	3-	3	4-	189.1	188.2	114	T	T*
26	4	3	3+	3-	3+	4	4-	3+	4+	3+	3+	3	4-	4	4-	4	201.8	200.2	114	T	T
27	1+	3-	3	3	3	3+	3+	4-	1+	2+	3-	3	4-	4+	4	4-	188.7	187.9	117	T	T
28	3+	3-	3+	3-	5-	4+	3-	5-	3+	3	3+	5-	5-	4+	3	6-	189.2	188.6	114	T	T
29	5	4	4-	5	4+	5-	5+	5-	6-	4+	5-	4+	4	5+	6	4+	192.8	191.4	118	A	A
30	4+	4-	2+	1+	2+	2-	2-	2+	5-	4-	2	1+	2	1+	1+	2-	187.8	186.6	127	A	A
31	3-	3-	2	2-	2+	3	3+	4	3	3-	2	2-	3-	3	4-	5-	201.8*	201.4*	147	T	-
																Mean	185.8	184.8	137.8		

APRIL 1979

Day		Three-Hourly Indices Kp									Three-Hourly Indices Km								Ap	oo				Cp
		1	2	3	4	5	6	7	8	Sum	1	2	3	4	5	6	7	8		N	S	M		
1		4+	5-	3	4	4+	3+	2+	4+	32+	4	4	3-	4	4-	3+	2	5+	33	34	46	41	39	1.3
2		4+	5	3+	4-	4-	5-	4-	4-	34	6	4+	3	3	3	4+	3	3	36	59	96	56	58	1.4
3		3	2+	3-	3-	3-	5+	7-	8	33+	3	2+	3	3-	2+	5-	6-	7-	54	32	31	45	19	1.6
4	05	7-	6+	5+	5+	5-	2	2-	2+	34+	6-	5+	5	5-	5-	1+	2-	2-	47	88	93	188	81	1.5
5	02	4+	4	5-	6	7-	6+	4-	3-	38+	5-	4+	4+	5	5	5	3	3	92	48	71	36	75	1.6
6		4-	3-	3	1+	3-	3+	2+	2	21	3	2+	2+	1	2-	2	2	2-	12	61	24	68	18	0.7
7	GG A	2+	3	3	3+	2-	2+	2+	3+	21+	2	2	2+	3-	1	2	2-	3	12	22	15	17	21	0.7
8		3+	3-	2+	2	2-	2+	3	3+	21+	3-	3-	2+	2-	1+	2	3	3	12	19	16	17	19	0.7
9	Q6A	4	3+	1	1-	1+	2-	2-	1+	15	4-	3	2-	1	1	1-	1	1-	9	25	18	22	22	0.5
10	Q8A	1	3-	3+	2+	3	3	3-	2	28	1	3+	3	2	3-	2+	2	2	12	12	15	9	16	K 0.7
11	Q3K	1+	1	1+	1+	1+	3	1+	2	12	1-	1+	1	1	1+	2	1	1+	6	12	10	17	6	CK 0.3
12		2	3	3	3+	2+	3	3	4	24+	1+	3-	3-	3	2	2+	2+	3+	15	28	18	11	26	0.9
13	Q9A	2+	2+	2+	3-	3+	3+	2-	2+	20+	2	2	2	2-	3	3-	2-	2	11	25	16	28	14	0.6
14		2+	2+	2	3-	3-	4-	3-	5-	23	2-	2	2-	2	2-	3-	3-	4	15	18	14	21	12	0.9
15		4	3	2	3-	4+	3+	3-	3+	25+	4-	3	1	2+	3	3	2+	3-	18	34	19	35	28	1.8
16		4	5-	3+	3	2+	3-	2	1	23	4-	4	3-	2	2-	2	2-	1	16	34	25	32	27	0.9
17	Q5A	3	3-	3	2+	2	2-	3-	2+	20-	3-	2+	2+	3-	2-	1+	3-	2	11	17	16	14	28	0.6
18	Q4	2	2	1+	2+	1	1	1+	2-	13-	2-	1+	1+	2+	1	0+	1-	2-	6	16	13	17	13	0.3
19	Q2	1	2	2-	1	1	2+	1+	1+	12-	1+	2+	2-	1	0+	2	1-	1-	6	11	7	8	18	CC 0.2
20	Q1	1-	0	1-	0+	0+	1-	1-	0+	4-	0+	0	0+	0	0	0	0+	0+	2	9	6	12	3	CC 0.0
21		1	2-	2+	3-	4	4+	4	5	25	1-	2-	2	2+	4-	3+	4-	5-	21	8	18	4	13	C 1.1
22	Q4	6-	6-	4	5	4+	5	5-	4+	39-	5-	4	3+	4	3	4	4+	4-	45	59	52	53	58	1.5
23		5	5	3+	3+	3+	3+	3-	2	28	5-	4+	3	3	3+	3	2	1+	23	52	39	48	43	1.1
24		3+	3+	1+	2+	2+	2	2-	4	22+	3+	3	3-	2	2	2+	2-	3	14	24	25	26	24	0.8
25	D1	8-	8	8-	7	7	5	6-	6-	54-	7-	6-	7-	6	6+	5-	4+	5	126	189	66	27	146	1.9
26	G7A	4	2+	1	2	1	3-	3	3	19	4-	3-	1+	1+	1+	1+	2+	2+	12	51	66	183	15	0.7
27		3+	3+	3	3-	3+	5	5-	5	36+	4-	4-	2+	3	3	4-	4-	5-	27	26	17	18	26	1.2
28		5-	4	5+	4+	4-	3+	4	4	33+	4+	4-	4-	4-	3-	3-	3+	4-	31	45	58	48	48	1.3
29	D3	4	5+	5+	4+	4+	5+	5	6-	39+	4+	4	5-	4-	4-	4-	4+	5-	47	43	36	36	45	1.5
30		5+	4+	3+	4+	4+	3	3	3-	30+	5-	4	4-	4-	4-	2	3-	2-	26	66	52	75	43	1.2
																		Mean	25	35.7	31.4	33.8		0.96

Day	Three-Hourly Indices Kn								Three-Hourly Indices Ks								S	So	Prov Rz	IMF	
	1	2	3	4	5	6	7	8	1	2	3	4	5	6	7	8					
1	3+	4-	3	4-	4-	3+	2+	5+	4	4	3-	4	4-	3+	2	5+	282.8°	282.6°	131	T	-
2	4+	5-	3	3	3+	4+	3+	3	4	4+	3	3	3	4+	3	3	203.6	203.4	134	T	-
3	3-	2-	3-	3-	3-	5-	6-	7-	3	2+	3	3-	2+	5-	6-	7-	194.2	194.2	135	T	-
4	6-	5	4+	4+	4	2-	1+	2	6-	5+	5	5-	5-	1+	2-	2-	183.3	183.5	138	T	-
5	4	4+	4+	5+	6	6	4-	3-	5-	4+	4+	5	5	5	3	3	179.1	179.3	139	TA	-
6	3	2+	3-	2-	2+	3	3-	2+	3	2+	2+	1	2-	2	2	2-	175.9	176.3	91	A	A
7	2	3-	3-	3-	2	2+	2+	3	2	2	2+	3-	1	2	2-	3	166.4	166.7	77	AT	T
8	3-	2+	2	2+	2-	2+	3	3+	3-	3-	2+	2-	1+	2	3	3	168.5°	169.8°	69	T	T°
9	3+	3	1+	1-	1+	2	2	2-	4-	3	2-	1	1	1-	1	1-	169.1	169.6	61	TA	T
10	1-	3	3	2+	2+	2+	3-	2+	1	3+	3	2	3-	2+	2	2	172.3	173.8	87	TA	-
11	1	1	1+	1+	1+	3-	2-	2	1-	1+	1	1	1+	2	1	1+	169.2°	170.8°	109	A	A°
12	2-	2+	3	3-	2+	3+	3-	4-	1+	3-	3-	3	2	2+	2+	3+	173.6	174.5	107	A	-
13	2	2-	3-	2	3	3-	2-	2	2	2	2	2-	3	3-	2-	2	174.8	175.8	113	A	A
14	2	2	2	2+	3-	3-	3	4+	2-	2	2-	2	2-	3-	3-	4	169.9	170.9	116	TA	A°
15	3+	3-	2-	3-	4-	3	3-	3+	4-	3	1	2+	3	3	2+	3-	166.9	168.1	117	A	A
16	4-	4-	3	3-	2+	2	3-	1	4-	4	3-	2	2-	2	2-	1	178.5	171.7	119	A	A°
17	3-	2	3	3-	2	1+	3-	2-	3-	2+	2+	3-	2-	1+	3-	2	166.7	168.8	107	TA	T°
18	2-	2	1+	2+	1+	1	2-	2	2-	1+	1+	2+	1	0+	1-	2-	157.3	158.7	98	AT	A
19	1	2+	2-	1+	1	2+	1	1+	1+	2+	2-	1	0+	2	1-	1-	158.8	159.4	79	A	A
20	1-	0	0+	0	0	0+	1-	1-	0+	0	0+	0	0	0	0+	0+	156.6	156.1	68	A	A
21	1	1+	3-	3-	4-	3+	4	4+	1-	2-	2	2+	4-	3+	4-	5-	159.9	161.5	68	TA	TA
22	5-	4	3+	4+	4-	4	4-	4-	5-	4	3+	4	3	4	4+	4-	158.8°	159.7°	79	T	T
23	4+	4	3+	3	3+	3	3-	2+	5-	4+	3	3	3+	3	2	1+	160.5	162.3	79	T	T
24	3	3-	3	3-	2+	2	1+	4	3+	3	3-	2	2	2+	2-	3	168.8	161.9	88	T	T°
25	6+	7-	7	6+	6	4	4+	5-	7-	6-	7-	6	6+	5-	4+	5	170.5	172.5	85	T	T
26	3+	2	1+	2	1+	2+	3-	3-	4-	3-	1+	1+	1+	1+	2+	2+	179.7	182.8	118	T	T
27	3	3+	3+	3-	3	5-	4+	4	4-	4-	2+	3	3	4-	4-	5-	192.4°	195.1°	125	T	T
28	4+	4-	5-	4+	3+	3	3+	4-	4+	4-	4-	4-	3-	3-	3+	4-	189.4°	192.1°	132	T	T
29	3+	4+	5-	4	3+	5-	4	5-	4+	4	5-	4-	4-	4+	4+	5-	183.8	185.7	132	T	T
30	4+	4	3+	4	4-	3-	3-	3-	5-	4	4-	4-	4-	2	3-	2-	182.5°	185.2°	120	TA	A
																Mean	173.8	175.8	162.8		

MAY 1979

Day	Three-Hourly Indices Kp									Three-Hourly Indices Km								Ap	aa				Cp
		1	2	3	4	5	6	7	8	Sum	1	2	3	4	5	6	7	8		N	S	M	
1		3+	4+	4-	3+	1+	3-	3	4	25+	3+	4	3	3	1+	2-	3-	1+	13	32	23	31 22	1.3
2		4-	4+	4-	2+	2+	3-	2	1	21+	4-	3+	3-	2+	2	2+	3-	1	14	22	17	26 15	0.9
3	01	2+	2-	1-	1+	2	2-	2	2	14-	2+	2-	1-	1+	2-	1+	2-	2	6	12	6	7 11 CC	0.3
4	23	2+	1	1-	1+	1	2-	3	2+	13+	2+	1-	0+	1+	1	1+	3-	3	7	16	7	8 15 CC	0.3
5	04	2	2	1+	2	1+	3-	2	1+	15-	2	2-	2-	2+	2-	2	2-	1	7	13	12	13 13 CC	0.3
6	01	1+	1	2-	1+	2	2	1	2	12+	1-	1	2-	2-	2-	2-	1-	2-	4	13	6	9 11 CC	0.1
7		2	1+	1+	3	4-	3-	3	2	19	2-	1-	1+	3-	3+	3-	3-	2	11	20	16	21 25	0.6
8	04	1	2+	1	2-	2	2	1+	2	15+	1-	2-	3-	2-	2-	2-	1+	2	8	16	9	16 11 C	0.4
9		1	2+	3-	3+	1+	3	4	2+	22	1	2+	3-	3	3	3-	3+	2	14	25	20	27 28	0.8
10	04	3-	1	1	1+	2	3	2	2-	14-	1	1-	1	1	2	1-	2	2-	7	14	11	8 17 C	0.4
11		3-	3+	4+	3	4	4	3	3+	27-	2+	2+	4	3-	3+	3	2+	3	13	34	23	27 31	1.0
12		3+	2+	2-	3-	3	2+	2	2	18+	2+	2+	2-	3-	2+	2-	2	2-	9	15	10	12 16	0.5
13	04	2	2	2+	2-	2+	3-	2	1+	16+	2-	2-	2+	2-	2-	2	2-	1+	4	16	9	14 14 C	0.4
14		3	2+	2	2+	4-	3+	2+	2	21	2	2+	2-	2	3	3-	2	2	11	23	12	13 23	0.6
15		2+	2+	1-	2+	3+	3	2+	2+	21-	2+	3-	3-	2+	3-	2+	2	2+	11	21	14	17 22	0.8
16	02	1	2+	2	1-	0+	1-	2	1+	11+	2	2	2+	1	0+	0+	1+	1	6	15	7	13 9 CC	0.2
17	01	3-	1	1+	1-	1-	3+	1-	0	8+	1+	1+	1+	1-	0+	0	0+	0+	3	8	2	4 5 CC	0.1
18		2-	1-	1-	1+	2+	2+	4+	4-	17	1+	1-	1-	1+	2+	2	3	3+	11	20	9	6 24	0.6
19	00	4-	4	4-	4-	4	3+	4+	4-	31-	4-	4-	3	3+	4-	3+	3	3+	24	33	34	32 36	1.1
20		3+	4	3-	2+	2+	2+	2+	3	22-	2+	4-	3	2+	2+	2+	2+	3	15	24	25	21 29	0.7
21		1-	1-	2-	2	4-	3-	4	3+	20-	1	1-	2+	2-	3+	2+	4-	3	13	21	24	12 33	0.7
22	01	4+	4-	4-	5-	3+	5	5+	5	35	4+	4-	4-	4	3-	4	4	4+	24	56	24	33 57	1.4
23		3+	3	1	1	1-	1-	4-	3+	17-	3	3-	2-	1	1-	1-	3	1+	11	20	11	14 16	0.5
24	01	4-	3+	4-	4	4	3+	4+	5	31+	3	3	4+	3+	4-	3	3+	4-	27	38	25	34 39	1.2
25	02	4+	5+	4	3+	4+	5-	5	4-	35-	4-	4+	3+	3+	3+	4	4	3+	34	62	42	44 56	1.4
26	04	5-	4+	4-	3+	4	5-	3	3	30+	4	4	3+	3-	4-	4-	3-	3-	25	43	32	38 36	1.2
27		3	4-	4-	3+	3+	3-	3	3-	25+	3	3	3+	3	3-	3-	3-	2+	17	3.	26	28 29	0.9
28		3	2	2-	2+	2	3	4	2+	18+	3-	2-	2+	1-	2-	2+	3	2+	11	28	11	18 29	0.6
29		2	1	1+	2-	2-	2+	4-	7	23-	2-	1	1+	2-	2	2	5-	6-	33	52	18	9 61	1.3
30		3+	4-	3	2-	2-	2-	1	1-	17-	3+	4-	2	2-	1+	1+	1-	1-	12	16	10	27 8	0.5
31	04	4+	4	3+	2+	2-	2	3-	1-	11	0+	1-	1	3-	2-	2-	2-	0+	6	14	6	7 13 CC	0.3
																		Mean	14	25.2	16.6	20.9	0.60

Day	Three-Hourly Indices Ka								Three-Hourly Indices Ka								S	So	Prov Rz	IMF	
	1	2	3	4	5	6	7	8	1	2	3	4	5	6	7	8					
1	3	4	3	2+	2-	3-	3-	3+	4-	4-	3	3	1-	1	2+	4-	177.6	186.4	148	T	+
2	4	3	3	2+	2	2+	3-	1+	3+	3+	3-	2+	2-	3-	3-	1	176.4	179.2	186	T	-
3	2+	1+	1-	1+	2	2-	2	2	3-	2	1-	1	2-	1-	1+	2	161.6	164.3	183	T	-
4	2	1-	1-	1+	1	2-	3-	3-	2+	1-	0+	1+	1-	1-	1-	3	173.1	176.3	132	AT	-
5	2	2-	2-	2	2-	3-	2	1+	2	2-	2-	3-	1+	1+	1+	1-	166.6	169.6	113	T=	T
6	1	1	2-	2-	2+	2	1+	2	3+	1	1+	1+	1+	1	0+	1	168.1*	171.1*	122	A	A
7	2	1	1+	3	4-	3-	3-	2+	1+	1-	1+	2+	3	2	3-	2+	174.7	178.0	148	A	A
8	1-	2+	3	2	2+	2+	2-	2+	0+	2-	3-	2+	1	1	1	2+	179.0*	182.4*	165	A	A*
9	1+	3-	3	3+	3	3	3+	2+	1-	2	2+	3	3	2	3+	2	177.9	181.2	162	A	A
10	1+	1	1+	2-	2	3	3-	2	1	1-	1	1	2-	2	1+	1+	171.3	174.7	145	A	-
11	2+	2+	4+	3-	4-	3+	3-	3+	2	2	4-	2+	3	3-	2	3-	175.1	178.6	148	TA	T
12	2+	2+	2-	3	3-	2+	2+	2	3-	2+	2-	2	2	1+	1+	1+	180.4	184.2	156	A	A
13	2	2-	2+	2	2+	3-	2	2-	1+	1+	2	1	1+	2-	1+	1	182.8	186.6	163	T	T
14	2	2+	2	2	3+	3	2+	2	2-	2	2-	2	2+	2+	1+	2	176.1	182.0	203	T	A
15	2+	3-	3-	2+	3	2+	2+	3-	2	3-	3-	2	2+	2+	2-	2	176.0	182.0	267	A	A
16	2-	2	2+	1+	1-	1-	2-	1+	2+	2	2	1-	3+	0+	1-	1-	172.4	176.4	187	T	A
17	1+	1+	1+	1-	1-	2+	1-	0+	1+	1	1+	1-	0+	0	0+	0	183.5	187.7	164	T	A
18	1+	1-	1	2-	3-	2+	3+	3+	1+	1-	0+	1	1+	1+	2+	1	167.3*	171.3*	148	T	T
19	4	4-	3	4-	4-	4-	3	4-	4+	4-	3	3+	3+	3	3-	4-	157.7	161.5	159	T	T
20	2+	4-	3	3-	3-	3-	3-	3-	3-	4	3-	2	2+	2	2-	2	152.0	156.6	187	T	-
21	1	1	2-	2	3+	2+	3+	3	1	0+	2+	1+	3+	2+	4	3+	151.9	155.7	114	T	-
22	4+	3+	4-	4	3	4	4	4	5-	4	4-	4	2+	4	4+	4+	152.7*	156.5*	111	T	T
23	3+	3	2-	1+	1	1	3-	3	3	3-	2-	1-	1-	1	3+	3-	152.0	156.0	117	AT	A
24	3	3	4	3+	4-	3	3+	4-	3	3	4+	4-	4-	3	3	4-	155.2*	159.2*	115	T	T
25	4-	4+	3+	3	3+	4	4-	3+	4-	4+	4-	4-	3+	4	4+	4-	149.4*	153.3*	124	T	T
26	4	4-	3+	3	4-	4	3-	3-	4	4	4-	3-	4-	4-	3-	3-	145.2	149.1	123	T	*
27	3-	3	3	3	3	3-	3-	2+	3+	3+	3+	3	3-	3-	3-	2	145.5	149.4	119	T	T
28	3-	2-	2+	1-	2	3-	3+	3-	3-	2-	1+	0+	2-	2-	3-	2	144.3	148.2	111	TA	T
29	2	1+	1+	2-	2	3-	5+	6+	2-	1	1	2	2	1+	4-	4+	140.1	144.2	113	A	A
30	4-	4-	3	2+	2	2	1	1-	3	4-	3-	1	1	1-	1-	1-	154.1	158.4	98	-	A
31	2+	1	1+	1	2+	2+	2	1-	1	1-	0+	2	1-	2+	1+	1	170.1	174.6	122	AT	AT
																Mean	155.2	159.2	134.5		

JUNE 1979

Day	Three-Hourly Indices Kp									Three-Hourly Indices Km								Ap	aa				Cp
		1	2	3	4	5	6	7	8	Sum	1	2	3	4	5	6	7	8		N	S	M	
1	04	1-	1	1	1	1-	1+	1	3-	9+	1	1	1+	1-	0+	1+	1-	2-	5	14	4	7 12	CC	0.2
2	06	2-	2-	1-	2	1+	1	1-	3-	12-	1+	2	1-	2-	1	1	0+	2+	6	16	4	11 10	CC	0.3
3	02	1-	0+	0+	1	1+	1+	1+	2-	8	1	0	0+	0+	:	1	1+	2-	6	11	6	9 15	CC	0.1
4	07	1+	2-	2-	2	2	1+	2	1-	13-	1+	1+	2-	2	2-	1	1+	0+	6	16	0	11 13	KK	0.3
5	01	1	1	2-	1	1+	1-	1-	1-	8	1-	1-	1	1-	1+	1-	1-	0+	4	14	4	13 6	CK	0.1
6	02	1	1+	1-	3-	4-	3	7	6	25+	1-	2-	1-	2+	3	3-	5+	5	34	51	28	9 70		1.3
7	01	4-	5	5-	2-	3	4+	4+	3+	30	4-	5-	4-	2-	3-	3+	3	3	26	43	25	37 33		1.2
8		3	3-	2+	3-	3-	3	4-	3-	23-	1	3-	2+	2	2	2+	3-	2+	16	28	14	28 23		0.8
9		2+	3-	2+	3+	3+	4-	4-	3-	24	2+	3-	2+	3-	2+	3	3+	3-	15	29	20	21 29		0.9
10		2+	3-	3	3	3	3+	3+	2+	23	2+	2+	3	3	2+	3-	3-	2	14	29	20	22 26		0.8
11		2+	3	2+	2	3	3-	2-	2	19	2-	3-	2+	2-	2+	2	1+	2-	10	22	12	15 18		0.6
12	09A	2	2+	2-	1-	1	1-	3	2	13+	2	2+	2-	1	1-	1-	2	2-	7	13	5	9 18	CK	0.3
13		1+	1	0+	1+	3-	3	2+	3-	15-	1+	0+	0+	1+	2+	2+	2-	2+	8	15	9	6 19	CC	0.4
14		2+	2+	2-	2-	2-	2+	2-	1+	15	2-	2+	2-	2	1+	2-	1+	1	7	18	7	13 12	CC	0.4
15		1	2+	3-	1+	3-	2+	3-	3	18	1-	2	3-	2-	2	2-	2+	2+	13	16	10	10 16	C	0.5
16	09*	3-	3-	3+	2+	4	3-	4-	3	26+	3-	3	3+	3-	4-	3-	3	3	16	29	22	19 33		0.9
17		2+	3+	2+	2	4-	4	3	2	23-	3-	3	2	2	3-	4-	3-	2-	14	28	24	28 34		0.8
18	05	1+	2+	2-	1+	1	2-	2-	1+	12+	1+	2+	2-	1	1-	1-	1+	1-	6	16	6	10 11	C	0.3
19	08	1+	3-	2	1+	1+	1+	1+	2-	13	1+	3-	2	2-	1+	1	1	1+	6	15	7	11 11	CC	0.3
20		2-	1	2	1	2+	2+	3-	3-	16-	2-	1	2	1+	2+	2	3-	2+	8	21	10	7 24		0.4
21		2-	2+	3	2+	3	3+	4	4-	23+	2-	2+	3+	2+	1-	1-	-	1+	15	34	21	14 42		0.9
22	03	4	2	3+	3-	4-	4+	5+	3+	29-	4-	2-	3-	3-	1	4-	4	4-	24	36	29	25 39		1.2
23	04*	3	4-	4	4-	3-	3-	3-	4	26+	3	4-	4-	3+	2-	3-	3-	4-	19	30	22	25 28		1.0
24		3-	3+	3	2	2-	1+	2	2	18	3-	3	3	2-	1+	1+	1+	2+	10	16	13	17 12		0.5
25		2+	3-	2+	2	2-	1+	3	2-	17	2-	3-	3-	2	2-	1+	3-	1+	9	18	15	15 18		0.5
26		0+	1	2-	2	5	4+	4+	4	23-	0+	1	1+	3-	4-	3+	3+	4-	28	39	23	9 53		1.1
27		3	3-	2+	3-	3-	3-	1+	0+	16-	3-	3-	2+	2+	3-	2+	1	0+	10	17	16	15 18		0.6
28	03	0+	1	2	1-	1-	1-	2-	1+	8+	0+	1-	2	1+	0+	1-	1	1+	4	9	4	5 8	CK	0.1
29	08A	1+	0+	0+	1+	2	2	3+	2+	13	1+	1-	0+	1+	2-	2	3	2	7	17	12	8 21	<	0.3
30		2	2-	2-	2-	2-	4-	2+	3	18-	2	2	2-	2-	1+	3-	1+	3-	18	22	8	9 22		0.5
																		Mean	12	22.9	13.5	10.4		0.56

Day	Three-Hourly Indices Ka								Three-Hourly Indices Ka								S	So	Prov Rz	IMF	
	1	2	3	4	5	6	7	8	1	2	3	4	5	6	7	8					
1	1+	1+	1+	1	0+	2-	1	2+	0+	1-	1	0	0	1	0+	1+	184.2	189.5	121	T	T
2	1+	2	1	2	1+	1+	1	3-	1+	2+	0+	1+	3+	0+	0	2	201.0*	206.0*	152	T	T
3	1	0+	0+	1-	1+	1+	1+	2	1	0	0	0	1	1-	1	1+	210.0*	216.1*	161	T	T
4	2-	2-	2	2	2+	2-	2	1	1-	1	1	2-	1+	0+	1-	0	222.4*	228.0*	178	A	A
5	1	1+	1+	1	2-	1	1+	1	0	0+	1-	0+	1-	0+	0	0	223.5	230.2	207	-	-
6	1	2-	1	3-	4-	3	6	5+	0	2-	0+	2-	2	2-	4+	5-	231.2	238.1	226	A	A
7	4-	5-	4-	2	3	4-	3+	3+	4	5-	4	1+	2	3-	3-	3-	231.2	238.1	222	-	-
8	3-	3-	2+	2+	3-	3	3	3-	3	3-	2+	2-	1+	1+	2+	2	235.6	242.7	228	TA	A
9	2+	3	3-	3	3-	3+	3+	3-	2+	2+	2	3-	2-	3-	3	2+	240.8*	247.4*	231	TA	A*
10	2	2+	3	3	3	3	3-	3-	2+	3-	3	3-	2-	2	2+	1	232.7	239.9	205	A	A
11	2	3-	2+	2	3-	3-	2-	2+	2-	2+	2	1+	2-	1+	1+	1	222.7	229.6	186	TA	A
12	2+	2+	2	1+	1	1	2+	2+	1+	2	1+	0+	1-	0+	2-	1+	202.8	208.3	199	A	A
13	1+	0+	1-	2-	3-	3-	2	2+	1	0+	0+	1+	2-	2-	1+	2+	187.7	193.7	172	A	A
14	2	3-	2+	2+	1+	2+	2-	2-	2-	2+	1	1+	1+	1+	0+	3+	179.9	185.7	149	A	A
15	1-	2+	3-	2	3-	2+	2+	3-	1-	2-	2+	1+	1+	1+	2+	2	178.5	176.8	127	T	T
16	2+	3	3+	3	4-	3-	3	3-	3	3-	3	2+	3	3-	3	3	162.3	167.5	103	T	T
17	2+	3	2+	2	3	4-	3	2	3-	3	2-	2+	2	3+	3-	2-	153.2	158.1	122	-	T
18	2-	2+	2-	1+	1+	1+	2-	1	1+	2-	1+	0+	0+	0+	1	0+	147.7	152.6	126	AT	T
19	1+	3	2-	2-	1+	1+	1+	1+	1+	3-	2+	2-	1	1-	0+	1	141.5	146.2	118	T	T
20	1+	1	2+	2	3-	3-	3-	3-	2	1-	2-	1-	2-	1+	3-	2	148.7	151.9	111	-	T
21	2	2+	3+	2+	3	3	3+	3+	1+	2+	3	2	3-	2+	4-	3+	144.1	148.9	124	T	T
22	4-	2-	3	3-	3	4-	4	4-	4-	2	2+	3-	3+	3+	4-	4-	136.6	141.1	108	A	A
23	3-	4-	4	3+	3	3-	3-	3+	3+	4	4-	3	2-	3-	2+	4-	134.6	139.8	96	T	T
24	2+	3	3	2-	2-	1+	2-	2+	3-	3	3	2-	1+	1+	1+	2+	136.7	141.2	98	A	A
25	2	3	3-	2	2-	2-	2+	2-	2-	3-	2+	2	2-	1-	3-	1	143.1	147.8	128	T	T*
26	1-	1+	1+	2+	4	3+	3+	4-	0	1	2-	3-	4-	3	3+	3+	148.6	153.7	132	-	T
27	3	3-	3-	3-	3	2+	1+	1-	2+	3-	2	2-	3-	2	1-	0	153.3	158.5	112	TA	T
28	1-	1	2+	1	1-	1+	1+	2-	0	0+	1+	0	0	0+	1-	1-	153.9	159.1	128	T	T
29	1+	1-	1-	2-	2	3-	3	2	1	0+	0	1	1	1+	3	2-	161.4	166.9	124	TA	T*
30	2+	2	2-	2+	2-	3+	2	3	2	2	2-	1+	1-	2-	1-	2+	170.9*	176.7*	154	T	T
																Mean	148.3	186.8	150.5		

JULY 1978

Day	Three-Hourly Indices Kp									Three-Hourly Indices Km								Ap	aa			Cp
		1	2	3	4	5	6	7	8	Sum	1	2	3	4	5	6	7	8		N	S	M	
1	03	2	2-	3-	2-	1+	2+	2-	1+	19-	2	2	3-	2+	1+	2-	1+	1	7	17	9	13	1.4
2	03	2-	1-	0+	1-	1	1	1+	1	8-	2-	1-	0	1-	1	2+	1-	1-	4	9	3	6	0.1
3		1-	1-	2+	4+	4-	3	3	3	21-	1-	0+	3	4	3	3-	2+	3-	14	31	11	16	2.8
4		3	3+	3	2-	1+	1-	1	1+	15-	3-	3+	3+	1+	1+	3+	1	1+	9	23	7	12	2.1
5		1-	2-	2+	2+	2+	3	3	2+	18-	1-	1+	2-	2+	2-	3-	2+	2	9	18	16	18	3.5
6	01	1	2	3-	4	3-	2+	4	4	25-	1	2+	3-	3+	2+	2	5-	3+	22	42	21	26	4.7
7	01	4	4	3	2+	5+	5+	3+	2+	34-	4-	3	3-	2	4+	4-	3-	2	27	55	33	25	4.3
8		2	2+	2+	2	2+	3	2+	2+	19-	2	2+	2-	2	2-	2+	2	2+	9	22	8	15	2.5
9	09<	1	2-	1+	1	1+	1	1+	1+	12	1	2-	1	1+	2-	3-	1-	1+	4	15	9	9	1.6
10	07	1	2-	1-	1-	2	1+	2+	2	12-	0+	2-	1-	1	2-	1	2-	2-	4	12	4	4	0.7
11	04	1	1+	1+	1+	1-	1-	1	1	8+	1	1	2	2	1-	0+	1	1	4	6	4	7	1.1
12		1-	1	0+	1	3-	4	4	2+	16	1+	1	1-	1+	2	3+	3+	2-	11	24	12	4	0.6
13		3-	3-	2+	2+	4+	5-	3	2-	23	2+	3-	2+	2+	3+	3+	2	1	15	26	17	17	2.9
14		2	1+	1	2+	3-	2-	5-	4+	25	2	2-	1	2	2+	1+	4-	4-	14	26	14	9	1.5
15		4-	4-	3	3-	3-	3-	3	2+	26-	1+	3	3-	4-	2+	2+	3	3-	15	32	21	21	3.4
16		3	2+	3-	3+	2	2+	3	3+	22	3	2+	3-	2	2-	1+	3-	1	11	24	12	15	2.4
17		3+	3	2-	3-	3	2+	2+	4+	23-	1-	3	2-	3	3	2	2+	4	16	31	14	22	4.1
18		3+	3	3+	3+	3-	2+	3-	4-	24-	2	3-	3	3-	3-	2	2	3+	15	28	15	21	4.0
19		4-	3+	2+	1	2+	2-	2-	3	19	4-	3+	2	1	2+	1+	2-	1	11	23	14	12	2.5
20	04*	1	2+	2	4	5-	5	3+	4	24+	1	2+	2	3+	4-	3-	3-	4-	14	31	22	18	3.2
21		2+	2+	2-	3-	2	2	3-	3-	19+	2+	3-	2+	3-	2-	3-	2	3-	7	17	15	16	2.5
22	06	2-	2-	2-	1	1	2-	2+	1	12	2-	2-	2	1+	1+	1+	1+	1-	4	15	4	10	1.9
23	08	1-	2+	1+	1	1+	1+	2	2	12	1-	3-	2	1	1+	1+	1+	2	4	13	5	9	1.3
24	05	2+	2-	1	1-	2-	1+	1	2-	11-	2+	2-	1+	1-	1+	1	1-	1+	4	14	4	9	1.2
25	02	1+	1+	1-	0+	0+	1-	1-	1-	6	2-	1+	1	1+	0	3+	2+	1-	3	8	3	7	0.1
26		1-	1	2-	1+	1+	2-	5-	6-	18	0+	1	2	2-	1+	1+	4	5	17	28	21	8	1.9
27	04	5+	4+	2-	3	2+	5-	3	3	27+	4	4	2-	3-	2+	3+	2+	1-	21	39	17	25	3.1
28		4+	3	2+	1-	1-	2-	2	3	18-	4-	3-	1-	1+	1	2-	1+	1-	13	21	7	15	2.6
29	02	3-	3-	3+	3	4	4	5	4+	29	1-	3	3+	3	1+	3+	4-	4-	24	43	25	28	5.2
30		3	2	2-	3	3-	2+	2	1	16-	3-	2	2-	1-	1+	2	2-	1	9	28	17	21	3.5
31	01	2+	1+	1-	1-	0+	0+	0+	0+	4+	0	1	0+	0+	0+	0+	0+	0	1	5	4	5	0.3
																		Mean	12	22.9	12.8	17.8	2.59

Day	Three-Hourly Indices Kn								Three-Hourly Indices Ks								S	So	Prov Rz	IMF	
	1	2	3	4	5	6	7	8	1	2	3	4	5	6	7	8					
1	2	2-	3	3-	2-	2+	2-	1+	2	2	2	2-	1+	1-	1	0+	180.2	184.3	158	T	T
2	2-	1-	3+	1	2-	1	1+	1+	2-	1-	0	1	1	0	0+	0+	196.3*	206.9*	164	AT	T*
3	1	1-	4+	5-	3+	3	2+	3	0+	0+	3-	3+	2+	2	2	2	208.4	212.4	205	A	-
4	3-	3+	3+	2-	2-	1-	2-	2	3	3+	3+	1	0+	0+	1+	1-	213.9	218.1	219	TA	A
5	1	2-	2	3-	2	3	3-	2+	1-	1+	2-	2	1	2-	2	2-	197.9	204.5	232	TA	A
6	1	2+	3	4-	3-	2+	5	4-	1+	2	2+	3-	2	2-	4+	3	234.4	211.3	240	TA	A
7	4	3+	3	2+	4+	4	3	3-	1	3-	2	2-	4+	4-	3-	1+	223.4	207.2	223	AT	A
8	2+	2+	2+	2+	2+	3-	3-	3-	2-	2	1+	1+	1+	1+	1+	2	199.9	216.7	219	A	A
9	1+	2-	1+	1+	2-	3-	1	2-	1-	2-	0+	1+	1+	2+	3+	1	191.4*	197.9*	191	TA	A
10	1-	2	1	1+	2	2-	2+	2+	0+	2-	0+	3+	1	3+	1	1	179.8	185.9	163	A	A
11	1+	1+	2+	2+	1-	1-	1+	1+	1-	1-	2-	1+	0+	0	0+	1-	172.7	179.6	155	AT	1*
12	1-	1	1-	1	3+	4-	3	2	0+	1-	0+	3+	1+	3+	3+	1+	164.7	178.1	149	T	TA
13	1-	3-	2+	3-	3	4-	2+	1+	2+	3-	2	2	3+	3+	2	1-	156.2	151.4	142	T	T
14	2	1+	1+	2+	3-	2	4-	4	2	2	1-	1+	2-	1-	3+	4-	149.9*	194.7*	127	TA	-
15	3+	3	3-	3-	3-	3-	3	3	1+	3	3-	2+	2	2+	4-	4-	148.3	151.1	121	T	T
16	3-	2+	3-	2+	2	2	3-	3+	3+	2+	1+	2-	1+	0+	2	3-	139.0	143.6	114	T	T
17	3-	3	2-	4-	3+	3-	3+	4	3-	3	2	3	1-	2-	1+	4	138.1	142.7	109	TA	T
18	3	3	3	3-	3+	2+	2+	3+	3+	2+	3	2+	3-	2-	2	4-	136.7	141.2	110	T	T
19	4-	3	2+	1+	3-	2	2	3	4	3+	2	1+	2-	1-	1	1	139.5	143.6	135	AT	T
20	1	2+	2+	4-	4-	3-	3	4-	1	2+	2-	3+	3+	3-	3-	4-	141.9	146.6	158	T	T
21	2+	3	2	3	2	2	2-	2	2+	3-	2-	2+	2-	1+	2+	3	139.2*	143.7*	151	T	T
22	2	2-	2	2-	1	1	2-	1	1+	2-	2-	1	3+	3+	1-	3+	150.9	155.7	152	T	T
23	1-	3-	2	1+	2-	2-	2-	2+	0+	3-	2+	0+	1-	1	1+	1+	158.0*	163.1*	154	T	*
24	2+	2-	1	1	2-	1+	1	2-	1-	2	1+	0+	1	1-	0+	1-	163.4	168.6	143	T	T
25	2-	1+	1+	0+	0+	1	0+	1	1+	1+	1-	1	0	0	0	0+	159.4	164.5	144	A	A
26	1-	1+	2+	2+	1+	1+	4+	5	3	1-	2-	1+	1	1	4	5+	160.5	165.6	142	T	T
27	5-	4	2	3+	3-	4	3-	3	5	4-	1+	2-	2	2+	2	2	154.3*	159.1*	148	TA	T*
28	4-	3-	1-	1+	1+	2	2	3	4-	3-	0+	2+	0+	1	1	2	153.3	158.1	132	T	T
29	3-	3	4-	3+	4-	4	4	4	2+	3	2	2+	1+	1+	3+	1+	152.3	156.7	148	A	A
30	1	2+	2-	3	3-	2+	2	1+	2+	2	1+	2+	2+	2-	2-	1+	159.5	162.3	158	A	A
31	0+	1	0+	1-	0+	0+	1	2	2	1-	0+	0+	0	3	0	0	148.8	152.4	144	A	TA
																Mean	169.9	171.4	159.9		

NASA/GODDARD SPACE FLIGHT CENTER

HOURLY EQUATORIAL DST VALUES(PROVISIONAL)

FEBRUARY 1979

UNIT=GAMMAS G.M.T.

DAY	1	2	3	4	5	6	7	8	9	10	11	12	13	14	15	16	17	18	19	20	21	22	23	24
1	-36	-34	-29	-29	-21	-15	-14	-13	-9	-15	-19	-20	-22	-20	-19	-14	-12	-12	-13	-12	-12	-12	-13	-20
2	-22	-22	-26	-27	-24	-24	-24	-20	-20	-21	-20	-23	-29	-31	-26	-18	-15	-17	-20	-17	-16	-20	-29	-36
3	-35	-30	-28	-26	-26	-22	-19	-18	-18	-15	-10	-9	-8	-10	-9	-11	-13	-12	2	6	16	15	9	0
4	-3	-13	-17	-12	-4	1	-6	-14	-14	-15	-13	-9	-3	-5	-20	-14	-22	-29	-26	-25	-26	-36	-44	-49
5	-47	-42	-40	-38	-38	-38	-34	-32	-31	-30	-35	-32	-34	-35	-34	-30	-29	-29	-27	-23	-20	-14	-14	-10
6	-8	-10	-13	-27	-31	-31	-25	-22	-33	-37	-33	-29	-30	-28	-27	-21	-19	-21	-20	-19	-20	-25	-25	-19
7	-17	-16	-16	-15	-14	-10	-8	-6	-3	3	4	2	0	1	-1	-5	-10	-10	-11	-8	-4	-8	-15	-13
8	-15	-24	-27	-23	-22	-23	-24	-20	-18	-14	-10	-8	-7	-4	-3	-5	-11	-12	-12	-13	-9	-4	-2	-9
9	-16	-10	-10	-16	-17	-16	-16	-13	-12	-18	-17	-15	-17	-14	-10	-7	-9	-10	-13	-13	-10	-10	-12	-14
10	-14	-16	-15	-13	-12	-10	-10	-10	-10	-12	-10	-8	-5	-5	-6	-10	-11	-10	-8	-6	-6	-5	-8	-11
11	-8	-3	2	-12	-2	6	1	-2	-3	-7	-6	-1	-1	-2	-1	-2	-4	-7	-9	-10	-13	-16	-26	-34
12	-36	-37	-37	-42	-48	-51	-58	-54	-48	-49	-40	-37	-37	-34	-28	-25	-16	-11	-7	-6	-4	-4	-4	-4
13	-4	-3	2	3	-3	-8	-8	-9	-10	-9	-7	-7	-10	-10	-9	-7	-5	-5	-4	-5	-4	-1	-1	1
14	0	2	2	3	1	1	2	1	-2	-3	-3	1	5	5	6	6	6	5	4	5	4	4	6	3
15	6	4	1	4	8	6	4	2	1	-5	-24	-23	-14	-15	-15	-17	-16	-18	-20	-16	-12	-9	-6	-5
16	-7	-7	-5	-11	-16	-16	-15	-10	-6	-2	-3	-10	-12	-9	-4	-4	-6	-7	-6	-4	-2	0	-3	-6
17	-5	-3	-2	-1	0	2	6	9	11	13	10	7	7	6	6	9	13	13	13	10	7	10	13	14
18	9	11	12	33	30	25	29	26	9	20	12	8	13	10	9	5	3	1	-3	0	-2	0	-7	-11
19	-11	-9	-9	-13	-10	-9	-8	-8	-3	-1	-1	-3	-2	-12	-18	-6	0	-3	-11	-9	-7	-3	-3	-6
20	-8	-11	-11	-9	-10	-13	-9	-1	2	2	1	-2	-4	-5	-3	-5	-5	-7	-11	-13	-17	-12	-10	-18
21	-20	-17	-14	7	4	-18	-40	-66	-90	-68	-49	-53	-38	-37	-30	-22	-1	-28	-27	-64	-93	-98	-92	-78
22	-90	-86	-76	-65	-62	-62	-70	-76	-81	-76	-67	-45	-22	-25	-41	-32	-52	-40	-42	-33	-33	-23	-25	-5
23	-14	-7	-22	-39	-36	-31	-32	-40	-43	-37	-32	-31	-23	-19	-18	-12	-15	-19	-18	-15	-25	-41	-50	-47
24	-45	-45	-45	-44	-40	-41	-40	-33	-31	-30	-30	-32	-33	-27	-25	-26	-30	-33	-38	-38	-31	-30	-34	-37
25	-34	-35	-40	-39	-39	-41	-34	-29	-33	-31	-28	-26	-22	-22	-18	-11	-10	-13	-16	-14	-21	-27	-32	-32
26	-35	-43	-39	-34	-35	-38	-45	-41	-37	-37	-37	-35	-32	-31	-27	-26	-34	-33	-43	-55	-57	-57	-66	-72
27	-66	-61	-66	-66	-61	-67	-61	-64	-58	-47	-43	-45	-42	-38	-38	-39	-35	-41	-41	-36	-34	-30	-37	-36
28	-41	-40	-41	-35	-34	-35	-34	-28	-24	-13	-12	-25	-25	-33	-28	-31	-41	-46	-48	-57	-59	-56	-47	-48

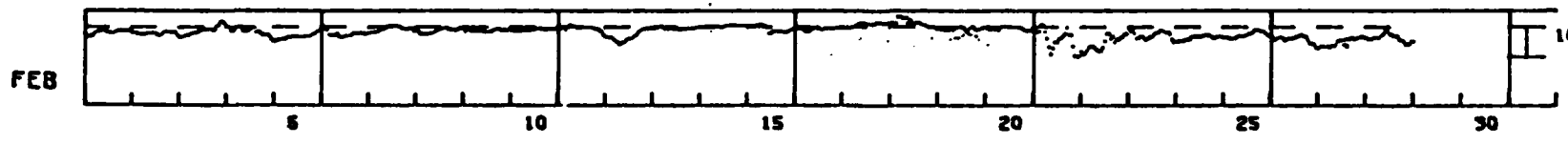

NASA/GODDARD SPACE FLIGHT CENTER

HOURLY EQUATERIAL DST VALUES(PROVISIONAL)

MARCH 1979

UNIT=GAMMAS G.M.T.

DAY	1	2	3	4	5	6	7	8	9	10	11	12	13	14	15	16	17	18	19	20	21	22	23	24
1	-31	-27	-30	-24	-25	-22	-23	-28	-28	-20	-18	-22	-26	-26	-29	-34	-37	-36	-27	-25	-22	-23	-21	-16
2	-18	-22	-29	-29	-33	-32	-33	-23	-22	-17	-19	-25	-32	-34	-35	-36	-37	-30	-23	-17	-24	-23	-16	-18
3	-22	-21	-16	-12	-12	-11	-12	-13	-10	-9	-10	-10	-11	-20	-28	-30	-29	-25	-26	-22	-27	-35	-37	-32
4	-26	-28	-28	-23	-20	-15	-19	-7	-12	-35	-62	-69	-42	-48	-66	-59	-49	-42	-44	-37	-28	-23	-27	-30
5	-20	-24	-29	-42	-45	-40	-35	-32	-37	-41	-30	-27	-27	-28	-30	-30	-25	-20	-18	-13	-13	-8	-3	-2
6	-10	-8	-13	-21	-21	-19	-22	-25	-24	-38	-52	-57	-70	-67	-71	-71	-64	-66	-62	-59	-62	-56	-45	-36
7	-37	-40	-41	-35	-38	-38	-36	-34	-33	-32	-31	-32	-32	-32	-30	-29	-26	-26	-24	-23	-26	-30	-29	-28
8	-24	-20	-21	-22	-24	-26	-25	-24	-23	-25	-25	-20	-20	-20	-18	-16	-15	-16	-17	-15	-13	-13	-14	-14
9	-16	-18	-16	-15	-15	-15	-14	-13	-2	-13	-20	-19	-14	-8	-12	-16	-16	-10	-5	3	-8	-16	-12	4
10	1	2	-11	-16	-5	-11	-19	-26	-22	-26	-20	-19	-32	-27	-24	-24	-15	-4	-11	-31	-44	-71	-110	-129
11	-125	-120	-103	-98	-95	-88	-85	-80	-74	-65	-62	-55	-48	-49	-50	-55	-54	-54	-51	-48	-44	-41	-38	-37
12	-36	-35	-34	-32	-31	-29	-32	-33	-32	-28	-25	-23	-19	-18	-17	-17	-17	-19	-13	-14	-12	-8	-8	-10
13	-10	-8	-5	-12	-15	-18	-18	-12	-19	-15	-10	-10	-7	-10	-11	-14	-15	-12	-8	-5	-6	-8	-8	-11
14	-11	-9	-5	-3	7	5	6	7	6	6	7	6	5	6	2	1	2	1	3	6	6	7	6	6
15	6	5	8	12	14	17	24	28	30	27	26	23	28	26	24	16	8	12	17	15	17	15	23	21
16	11	10	9	4	3	8	5	1	-5	-1	-5	-2	0	3	3	4	3	2	8	9	7	12	17	20
17	19	11	19	26	21	12	2	10	10	-7	-15	-14	-15	-15	-19	-18	-18	-22	-18	-15	-8	-7	-8	-14
18	-12	-10	-8	-7	-6	-8	-4	-1	-2	-3	-4	-3	-2	0	0	2	1	-2	4	6	4	3	4	4
19	6	7	6	8	10	9	6	1	-5	-10	-21	-24	-13	-10	-9	-9	-9	-7	-2	3	2	-1	3	4
20	7	3	0	-2	0	3	5	5	8	10	11	9	7	5	7	7	-1	1	2	4	3	12	16	14
21	14	14	12	14	15	15	13	14	15	16	17	15	15	17	20	19	14	17	14	14	15	16	16	18
22	16	16	14	9	10	14	15	17	33	47	37	-14	-22	-13	-26	-50	-74	-57	-47	-48	-37	-30	-22	-20
23	-20	-21	-23	-24	-23	-25	-19	-16	-19	-21	-23	-23	-20	-21	-24	-23	-21	-23	-21	-21	-22	-20	-14	-10
24	-9	-14	-16	-13	-11	-13	-18	-18	-28	-38	-30	-29	-31	-32	-31	-24	-19	-21	-20	-16	-16	-14	-9	-12
25	-8	-9	-14	-13	-10	-8	-8	-11	-16	-18	-15	-24	-22	-22	-28	-27	-30	-39	-39	-43	-33	-31	-23	-24
26	-36	-36	-39	-35	-28	-29	-27	-24	-32	-27	-22	-23	-26	-43	-46	-49	-46	-37	-43	-54	-47	-46	-40	-32
27	-26	-25	-28	-25	-23	-21	-22	-34	-39	-36	-27	-25	-35	-39	-36	-36	-37	-51	-53	-48	-54	-48	-45	-38
28	-35	-44	-39	-33	-31	-31	-31	-34	-29	-25	-21	-21	-43	-35	-34	-37	-43	-44	-40	-33	-31	-35	-43	-49
29	-45	-53	-46	-42	-48	-50	-64	-75	-88	-79	-60	-60	-68	-66	-65	-66	-78	-82	-103	-97	-108	-121	-112	-115
/30	-96	-82	-80	-77	-70	-76	-76	-77	-69	-64	-60	-59	-57	-56	-57	-60	-60	-58	-45	-38	-35	-33	-32	-32
31	-26	-20	-26	-34	-36	-32	-30	-34	-33	-26	-22	-26	-24	-22	-25	-33	-41	-47	-38	-35	-35	-39	-35	-40

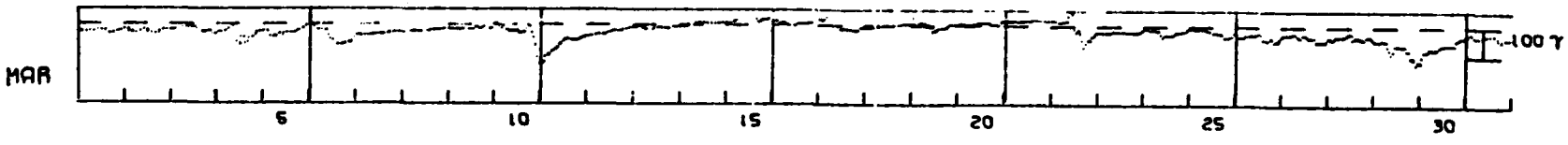

NASA/GODDARD SPACE FLIGHT CENTER

HOURLY EQUATORIAL DST VALUES(PROVISIONAL)

APRIL 1979

UNIT=GAMMAS

DAY	1	2	3	4	5	6	7	8	9	10	11	12	13	14	15	16	17	18	19	20	21	22	G.M.T. 23	G.M.T. 24
1	-46	-54	-47	-53	-44	-38	-31	-36	-34	-36	-44	-44	-40	-47	-56	-49	-48	-49	-46	-43	-39	-33	-21	-32
2	-20	-56	-65	-78	-60	-65	-71	-55	-40	-34	-35	-37	-44	-53	-56	-55	-53	-55	-56	-52	-49	-45	-39	-40
3	-41	-39	-38	-35	-32	-30	-27	-28	-25	-18	-10	-11	-12	-4	-1	2	-38	-58	-77	-82	-91	-103	-118	-160
4	-154	-171	-191	-197	-188	-183	-167	-156	-136	-128	-118	-112	-105	-101	-95	-92	-92	-86	-82	-77	-69	-65	-59	-58
5	-57	-57	-33	-31	-13	-1	7	-14	-16	2	-32	-36	-3	6	23	-13	-20	-24	-29	-32	-38	-41	-35	-29
6	-30	-37	-40	-41	-39	-41	-41	-39	-36	-28	-27	-28	-31	-29	-29	-25	-19	-19	-15	-13	-12	-14	-15	-13
7	-11	-12	-18	-21	-19	-17	-10	-7	-8	-12	-13	-4	-5	-4	-14	-12	-13	-9	-9	-12	-12	-10	-15	-9
8	-13	-13	-11	-6	-3	-1	3	7	9	3	-5	-10	-6	-3	-1	2	6	0	-2	-3	-6	-10	-13	-12
9	-13	-15	-25	-23	-23	-16	-12	-13	-8	-5	-5	-4	-1	0	-1	-1	1	2	3	4	6	8	10	13
10	13	10	8	8	5	-12	-5	-5	-4	-9	-10	-7	-9	-4	-1	0	3	-5	-9	-15	-16	-13	-8	-2
11	1	4	6	13	14	14	14	12	10	11	9	10	7	6	9	10	10	9	5	3	7	6	2	2
12	7	6	5	13	17	16	8	10	15	6	14	4	9	9	4	0	-1	5	5	-5	-9	-5	-5	-5
13	1	3	4	2	2	3	4	3	6	7	11	9	8	-4	-1	2	-2	-5	-7	-5	-2	-3	-1	-2
14	-1	-2	0	4	8	6	10	12	10	12	14	11	14	18	18	16	9	6	2	7	13	12	-12	-11
15	-10	-12	-9	-18	-15	-13	-10	-8	-4	-2	4	4	3	-1	-9	-13	-11	-6	-5	-4	0	-4	-4	-7
16	-3	-8	-19	-29	-42	-31	-18	-17	-21	-16	-12	-10	-11	-15	-18	-19	-17	-16	-18	-18	-8	-2	3	1
17	-2	-5	-5	-3	-1	-1	-3	-1	-1	0	-2	-4	-5	-2	-2	-4	-8	-8	-4	-6	-4	1	0	-4
18	-7	-6	-3	-2	4	7	10	11	9	6	3	7	10	9	7	7	8	10	10	7	5	7	7	3
19	3	3	10	5	2	6	8	5	6	9	10	8	7	10	11	9	7	5	7	10	10	7	8	9
20	9	11	11	10	10	7	6	11	13	13	12	11	10	10	11	12	13	15	16	20	23	22	24	24
21	22	20	20	22	21	23	23	21	18	23	34	34	27	17	3	-8	-12	-12	-13	-19	-26	-40	-62	-54
22	-53	-67	-65	-86	-73	-63	-50	-48	-45	-42	-36	-46	-41	-38	-42	-43	-56	-54	-58	-54	-48	-56	-62	-60
23	-66	-58	-48	-47	-53	-44	-35	-37	-32	-31	-27	-30	-35	-38	-36	-39	-39	-40	-37	-33	-29	-30	-27	-22
24	-25	-26	-26	-27	-30	-30	-21	-21	-22	-21	-19	-20	-21	-21	-21	-20	-21	-21	-24	-24	-25	-24	-22	-19
25	33	12	-46	-56	-52	-100	-109	-65	-108	-95	-101	-115	-142	-136	-148	-134	-132	-124	-112	-100	-94	-79	-82	-76
26	-69	-68	-69	-68	-64	-58	-53	-52	-50	-46	-45	-48	-49	-43	-40	-39	-39	-40	-42	-45	-42	-64	-62	-38
27	-35	-35	-36	-40	-31	-25	-22	-21	-29	-38	-32	-30	-31	-27	-31	-26	-30	-46	-49	-37	-48	-61	-74	-60
28	-56	-71	-77	-64	-58	-50	-53	-43	-59	-68	-51	-52	-53	-53	-51	-51	-52	-45	-41	-43	-37	-38	-46	-50
29	-38	-28	-29	-18	-19	-43	-43	-42	-41	-52	-52	-48	-44	-41	-48	-48	-46	-49	-51	-54	-63	-61	-59	-66
30	-51	-48	-52	-47	-40	-36	-40	-39	-31	-36	-34	-33	-33	-34	-38	-38	-34	-28	-29	-29	-28	-23	-22	-21

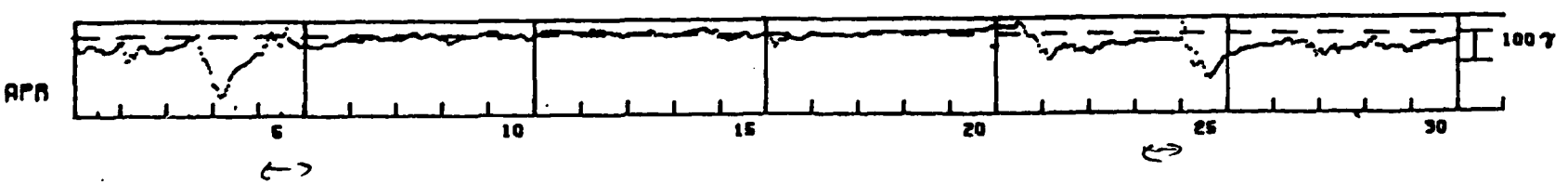

NASA/GODDARD SPACE FLIGHT CENTER

HOURLY EQUATORIAL DST VALUES(PROVISIONAL)

MAY 1979

UNIT=GAMMAS

DAY	1	2	3	4	5	6	7	8	9	10	11	12	13	14	15	16	17	18	19	20	21	22	23	G.M.T. 24
1	-18	-15	-16	-18	-21	-22	-22	-26	-24	-18	-16	-9	-6	-4	-5	-7	-9	-9	-18	-24	-24	-27	-26	-27
2	-35	-40	-37	-40	-35	-30	-29	-32	-32	-30	-25	-23	-26	-24	-23	-22	-23	-20	-21	-21	-21	-18	-15	-11
3	-8	-6	-9	-10	-10	-7	-8	-5	-6	-6	-7	-10	-11	-12	-16	-15	-11	-9	-10	-11	-7	-9	-6	-8
4	-16	-14	-11	-9	-8	-8	-6	-4	-4	-4	-6	-5	-3	-4	-3	-2	-5	-4	-4	-3	-15	-13	-14	-10
5	-2	-3	-6	-7	-7	-11	-7	-6	-6	-4	-1	2	3	5	6	5	4	5	5	12	19	21	21	19
6	17	14	12	9	9	9	7	7	7	5	8	11	12	14	16	13	12	9	7	8	10	13	13	12
7	12	6	5	8	12	13	15	17	15	8	10	9	6	0	-3	-1	4	-2	-5	-6	1	2	1	3
8	7	7	7	8	9	9	5	0	4	12	19	20	21	22	26	23	20	18	15	17	19	20	18	19
9	18	23	22	20	15	16	20	23	21	23	17	16	15	20	16	16	16	6	-6	-5	-6	-2	-1	3
10	5	6	9	9	11	11	14	14	12	14	17	21	22	21	24	20	22	18	15	14	12	15	15	15
11	17	21	18	16	21	27	19	-2	-6	3	10	9	5	2	-6	-2	-9	-10	-10	-10	-5	-15	-14	-7
12	-6	-2	5	8	10	6	7	8	7	7	14	16	14	14	10	11	11	7	4	8	12	13	11	10
13	9	12	12	10	12	12	13	12	16	20	22	23	26	23	21	18	13	15	18	22	26	26	22	20
14	19	20	17	13	9	10	13	15	15	14	17	17	14	12	10	9	8	6	6	7	9	12	14	15
15	15	11	17	21	17	12	10	6	7	11	12	12	13	10	8	4	6	6	5	7	4	5	6	5
16	6	7	4	4	6	8	8	6	11	13	13	15	14	16	17	19	17	16	14	15	14	13	11	12
17	13	13	13	14	13	12	11	8	6	8	9	7	7	6	7	10	11	11	15	20	23	22	24	25
18	25	26	29	32	35	33	32	36	36	35	33	31	31	19	17	23	26	26	17	13	13	2	-16	-18
19	-10	-7	-20	-17	-21	-26	-19	-12	-11	-15	-29	-26	-18	-21	-20	-20	-20	-16	-15	-13	-27	-24	-24	-18
20	-13	-18	-23	-27	-28	-21	-18	-12	-10	-8	-4	-9	-14	-15	-12	-12	-14	-16	-21	-19	-16	-21	-16	-11
21	-7	-3	-1	-4	0	3	4	5	-1	-3	0	-1	0	1	-6	-8	-11	-18	-24	-29	-20	-24	-30	-33
22	-42	-41	-31	-39	-37	-34	-31	-39	-47	-50	-50	-39	-38	-41	-35	-33	-33	-28	-40	-34	-32	-42	-33	-25
23	-29	-36	-32	-27	-28	-25	-22	-16	-15	-11	-9	-12	-13	-14	-16	-16	-16	-16	-16	-18	-19	-20	-24	-31
24	-38	-40	-38	-29	-26	-23	-36	-30	-26	-15	-20	-24	-15	-21	-21	-15	-18	-21	-21	-29	-20	-24	-26	-19
25	-19	-13	-9	-13	-26	-25	-26	-21	-19	-22	-15	-14	-19	-22	-27	-26	-29	-39	-40	-41	-32	-33	-33	-30
26	-39	-40	-26	-21	-26	-26	-23	-21	-14	-12	-8	-9	-13	-16	-14	-12	-13	-11	-12	-15	-15	-13	-18	-14
27	-12	-11	-5	-9	-15	-22	-21	-16	-21	-22	-14	-10	-11	-13	-17	-21	-22	-20	-19	-21	-19	-21	-20	-16
28	-11	-6	-3	-1	0	-1	-2	-3	-3	-4	1	2	5	1	-1	3	-1	0	-1	-1	-3	-8	-13	-12
29	-6	-2	-1	-5	-7	-5	-2	-1	4	8	11	7	4	2	1	4	2	2	2	24	61	83	23	81
30	41	37	26	20	14	5	8	7	7	7	13	11	7	5	6	8	9	9	8	10	11	10	7	5
31	3	4	5	6	8	12	12	10	13	15	25	23	20	21	16	20	17	14	12	10	10	10	9	9

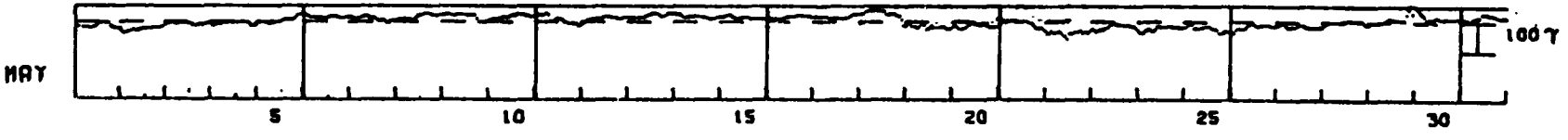

NASA/GODDARD SPACE FLIGHT CENTER

HOURLY EQUATORIAL DST VALUES (PROVISIONAL)

JUNE 1979

UNIT=GAMMAS

DAY	1	2	3	4	5	6	7	8	9	10	11	12	13	14	15	16	17	18	19	20	21	22	GMT 23	GMT 24
1	3	3	4	2	-1	-4	-4	-3	1	3	3	2	1	2	0	-1	-4	-5	1	1	0	-2	-5	-6
2	-6	-6	-6	-1	-1	1	3	3	0	2	3	7	11	10	5	4	4	4	6	6	4	2	2	3
3	10	12	13	14	14	11	10	11	12	12	11	11	11	11	11	12	14	14	11	10	12	14	14	11
4	7	3	7	7	10	9	5	1	-1	-5	-6	-3	-1	0	0	5	9	10	13	7	9	15	19	22
5	23	23	22	21	20	22	21	19	21	22	20	17	14	14	20	22	24	26	28	30	30	27	27	26
6	27	27	24	23	22	19	17	17	19	24	27	31	28	23	19	11	13	16	22	53	48	28	19	41
7	37	25	22	7	-13	-34	-38	-35	-32	-27	-25	-25	-25	-27	-22	-21	-27	-28	-27	-22	-19	-18	-20	-15
8	-9	-14	-11	-13	-14	-11	-16	-12	-10	-12	-10	-10	-13	-17	-16	-14	-8	-4	-1	-3	-3	-5	-1	0
9	2	-3	-6	-11	-10	-5	-4	-2	-2	-2	-9	-7	-8	-10	-12	-14	-10	-6	-6	-6	-11	-13	-4	1
10	2	4	5	-3	-10	-11	-10	-12	-18	-15	-15	-13	-15	-15	-17	-15	-9	-4	-6	-8	-8	-8	-6	-9
11	-5	-4	-5	-6	-5	-4	-5	-11	-8	-5	-4	-6	-6	-7	-9	-15	-12	-5	-2	1	2	-2	-2	-2
12	-4	-7	-8	-7	-6	-5	-8	-10	-8	-6	-3	-5	-5	0	3	3	7	4	5	5	11	8	8	5
13	6	4	3	1	1	1	6	2	6	9	7	5	6	6	2	-5	-7	-3	4	5	4	4	2	1
14	0	-5	-5	-5	0	4	1	0	-4	-4	4	8	7	7	10	7	6	7	15	20	17	12	12	13
15	11	13	10	9	6	3	8	7	7	5	4	2	-1	-3	-2	0	0	1	-1	0	0	1	3	2
16	-4	-2	-2	-7	-6	-14	-17	-18	-17	-14	-12	-5	-1	-5	-14	-15	-13	-10	-11	-19	-20	-21	-25	-27
17	-26	-19	-15	-17	-14	-11	-11	-4	-6	-3	-3	-2	-1	-1	-4	-12	-27	-23	-12	-8	-6	-7	-2	1
18	2	1	0	0	0	-1	-2	1	3	4	3	2	2	1	1	-2	-2	-2	-3	-5	-7	-3	1	2
19	3	7	7	3	-3	-8	-10	-7	-5	-4	-4	-6	-5	-5	-6	-8	-11	-14	-11	-8	-6	-9	-8	-9
20	-5	-12	-13	-11	-7	-8	-6	-1	2	-1	0	2	7	15	20	23	21	18	17	8	4	3	3	3
21	3	5	5	5	6	-6	-14	-21	-11	-8	-4	-3	-6	-10	-5	-1	-4	-14	-12	-22	-22	-26	-27	-25
22	-18	-17	-12	-10	-10	-17	-6	-9	-7	-5	1	0	-6	-10	-9	-13	-23	-34	-44	-40	-39	-46	-43	-28
23	-22	-19	-17	-28	-35	-32	-38	-36	-26	-23	-17	-18	-18	-20	-19	-17	-21	-24	-21	-16	-17	-30	-25	-22
24	-19	-15	-20	-26	-29	-25	-25	-25	-19	-17	-14	-18	-15	-14	-13	-15	-12	-13	-13	-15	-14	-8	-10	-13
25	-10	-9	-6	-5	-11	-13	-10	-12	-10	-7	-8	-8	-3	1	-1	-2	-4	-4	-2	-6	-12	-10	-8	-8
26	-5	-5	-3	-7	-3	-6	-6	-3	-6	-1	4	4	2	10	5	-2	-4	-11	-5	-20	-23	-31	-41	-45
27	-32	-25	-20	-32	-34	-31	-27	-21	-19	-21	-19	-13	-9	-15	-18	-18	-21	-23	-22	-25	-24	-20	-16	-16
28	-14	-12	-12	-14	-12	-12	-11	-7	-11	-5	-7	-6	-8	-5	-4	-4	-5	-6	-10	-10	-10	-4	1	4
29	-2	-3	-1	-1	0	-1	-2	-2	0	0	4	6	5	5	10	8	6	3	5	7	6	3	0	-7
30	-9	-6	-8	-6	-6	-8	6	-11	-10	-7	-4	-3	-3	-5	-4	0	5	6	4	-3	-5	0	11	6

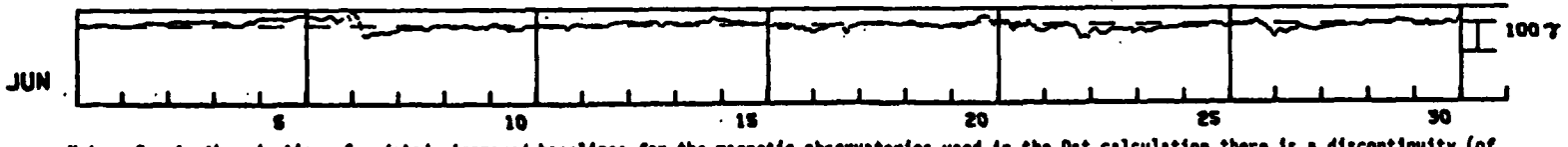

Note: Due to the adoption of updated, improved baselines for the magnetic observatories used in the Dst calculation there is a discontinuity (of about 10 nT) in the reference level of the provisional Dst between the last hourly interval of May (distributed last month) and the first hour of June. Revised provisional Dst values based on the new baselines will be provided upon request. However, the baseline changes have no significant effects on relative values of Dst over period of one month or less. The final Dst values for 1979 will be published after the end of the year based on baselines further updated. The revision of baselines is related to the circumstance that during periods of high solar activity, accurate baseline determinations are more difficult than during years of low solar activity.

NASA/GODDARD SPACE FLIGHT CENTER

HOURLY EQUATORIAL DST VALUES(PROVISIONAL)

JULY 1978

UNIT=GAMMAS

DAY	1	2	3	4	5	6	7	8	9	10	11	12	13	14	15	16	17	18	19	20	21	22	G.M.T. 23	G.M.T. 24
1	15	12	8	8	8	9	13	18	23	26	17	14	13	12	11	11	9	6	6	9	9	9	12	12
2	10	10	14	10	11	10	13	12	13	15	16	16	15	20	26	31	34	33	33	32	31	37	33	33
3	31	29	25	26	25	24	37	82	73	62	49	36	36	28	21	16	8	5	2	4	9	[illegible]	5	7
4	9	8	5	7	12	2	-13	-16	-16	-13	-8	-8	-12	-16	-15	-11	-14	-10	-9	-9	-5	-2	4	4
5	0	-1	-2	0	3	2	2	5	5	7	10	10	10	9	5	4	5	11	13	17	11	9	13	15
6	19	20	17	15	13	12	11	6	7	4	2	1	6	6	-1	-4	-4	-2	-1	13	25	22	24	27
7	14	9	11	15	15	13	12	10	5	8	13	13	11	5	-20	-31	-23	-9	-12	-8	-1	-5	1	6
8	2	4	-3	-7	-5	-1	2	-4	-5	-6	3	5	7	4	1	-5	-11	-7	-3	-2	1	1	9	11
9	14	15	12	15	13	8	7	3	3	7	10	12	4	-5	-14	-19	-14	-14	-9	-5	-2	0	7	8
10	3	4	0	13	13	9	11	9	5	13	15	13	12	14	10	10	7	4	7	9	8	3	5	8
11	12	12	13	18	19	16	9	13	10	12	11	11	7	12	16	17	18	15	15	15	17	17	20	20
12	19	19	16	15	15	21	21	19	20	23	25	24	22	33	35	37	25	20	14	3	1[illegible]	12	15	13
13	3	-1	-[illegible]	-5	-5	-2	0	1	8	11	18	13	16	14	8	-4	3	-2	-8	-10	-7	-6	-6	-7
14	-8	-8	-5	-4	2	6	12	16	19	21	18	18	12	8	0	0	0	-1	1	-2	-12	-4	8	8
15	1	-5	-10	-7	-6	-5	-4	-9	-4	-1	4	2	2	-2	-11	-16	-21	-17	-8	-8	-10	-3	-2	-6
16	-6	-10	-8	-12	-12	-11	-4	-4	-1	4	11	12	10	5	3	-1	0	2	3	6	8	13	14	4
17	2	2	0	2	4	5	7	9	11	17	13	11	12	18	12	10	7	9	14	20	21	15	11	6
18	-8	-2	-3	-6	-10	-8	-11	-5	-3	2	7	-1	-6	-4	-8	-8	-7	-9	-10	-16	-9	-1	6	8
19	13	9	7	5	2	1	5	9	7	6	10	14	16	10	6	7	9	6	5	5	6	8	13	15
20	16	16	11	12	13	12	13	11	3	4	6	9	5	-2	-2	0	-9	-17	-25	-20	-13	-16	-19	-8
21	-1	-4	-1	1	-5	-10	-6	-7	-4	1	4	5	10	9	4	-1	-5	-2	2	3	0	-2	1	2
22	2	-2	-7	-7	-4	-1	5	7	4	4	9	11	12	16	20	22	23	16	15	9	4	-1	3	8
23	10	13	13	15	17	8	6	7	10	12	12	5	1	3	3	4	6	7	11	11	7	1	7	9
24	14	16	13	11	9	10	7	3	3	6	11	14	16	10	7	5	7	10	7	5	3	0	1	2
25	-1	0	4	7	9	13	20	19	19	15	15	16	18	14	8	8	7	9	12	15	19	22	25	23
26	21	20	17	19	24	23	23	18	14	15	19	20	19	18	12	11	8	5	10	12	-1	-18	-41	-67
27	-77	-81	-82	-59	-51	-42	-36	-34	-31	-21	-12	-7	-10	-17	-20	-13	-7	2	-2	-5	-2	-4	-6	-11
28	-16	-22	-18	-17	-12	-7	-7	-10	-9	-7	-4	-3	-6	-10	-15	-12	-6	-6	3	6	11	30	36	32
29	38	23	16	18	24	29	43	61	48	28	24	29	27	20	22	19	9	2	-4	9	17	18	12	21
30	12	1	-1	2	5	4	5	9	13	8	0	2	1	-4	-11	-18	-22	-20	-18	-14	-8	-9	-5	-6
31	-7	-8	-9	-9	-9	-8	-5	-3	-1	-1	-3	-2	2	2	-4	-5	-6	-7	-6	-4	1	3	6	4

NOTE: Because of problems in the scale value and the baseline at the Honolulu Magnetic Observatory, data from only three observatories (San Juan, Kakioka and Hermanus) were used in the derivation of the above Dst values. It appears that the problems developed toward the end of June. Therefore the provisional Dst values for June may not be accurate near the end of that month.

APPENDIX 2

Quiet Day

February 13, 1979

$\Sigma Kp = 4+$

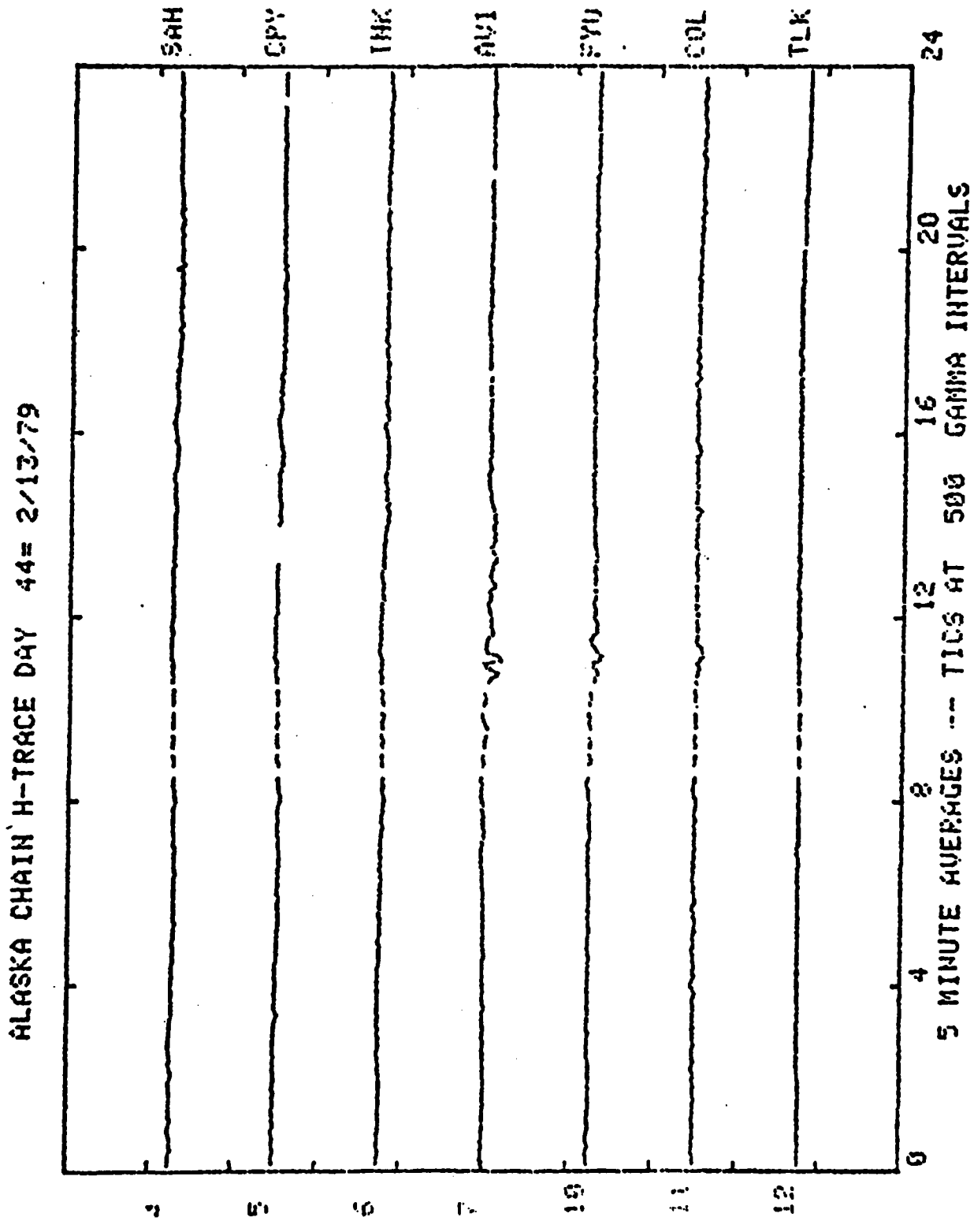
ALASKA CHAIN H-TRACE DAY 44= 2/13/79
SAH
CPV
IHK
AU1
FYU
COL
TLK
0
4
8
12
16
20
24
5 MINUTE AVERAGES -- TICS AT 500 GAMMA INTERVALS

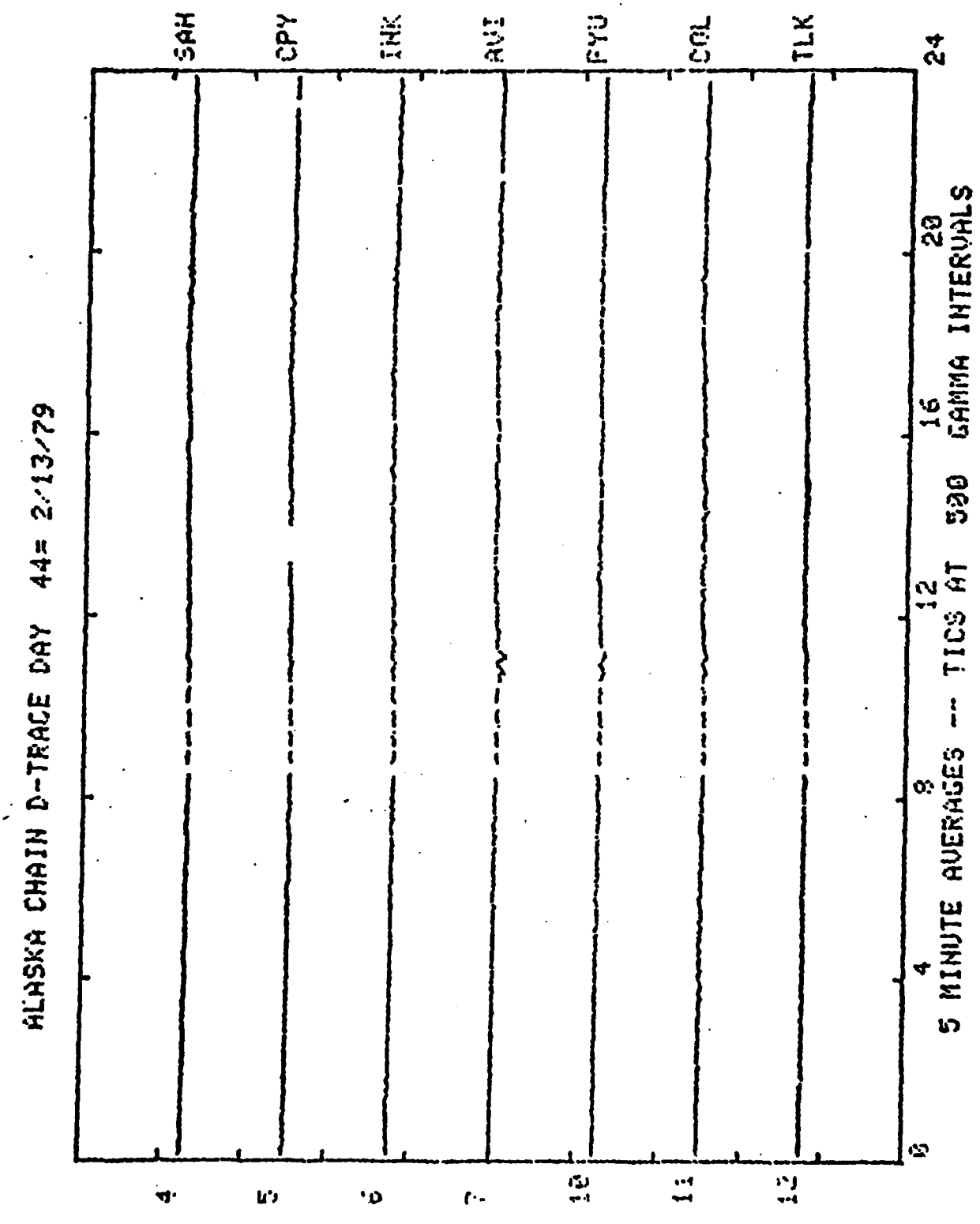
ALASKA CHAIN D-TRACE DAY 44= 2/13/79
SAH
CPY
INK
AUI
FYU
COL
TLK
0
4
8
12
16
20
24
5 MINUTE AVERAGES -- TICS AT 500 GAMMA INTERVALS

Appendix 2
Quiet Day

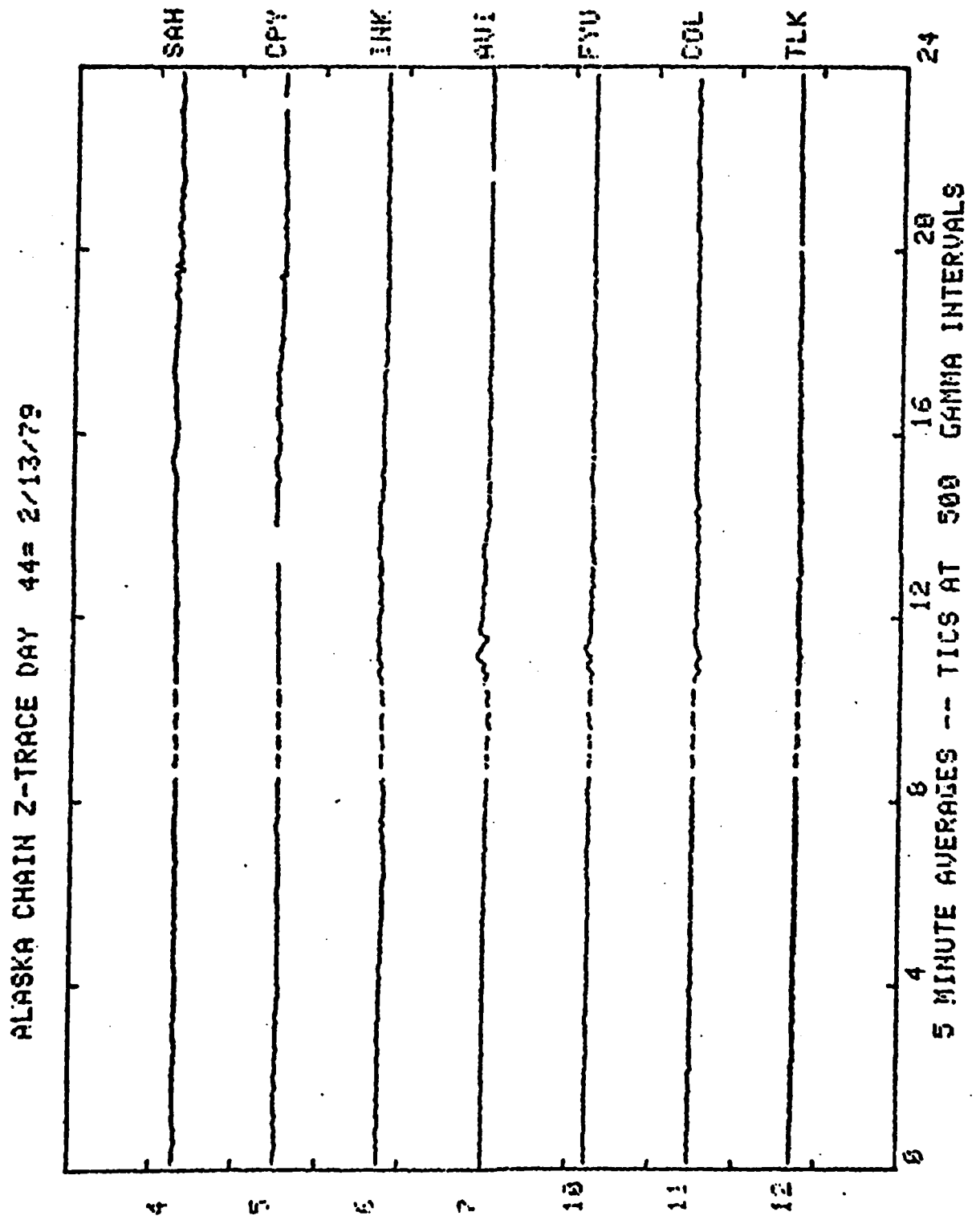

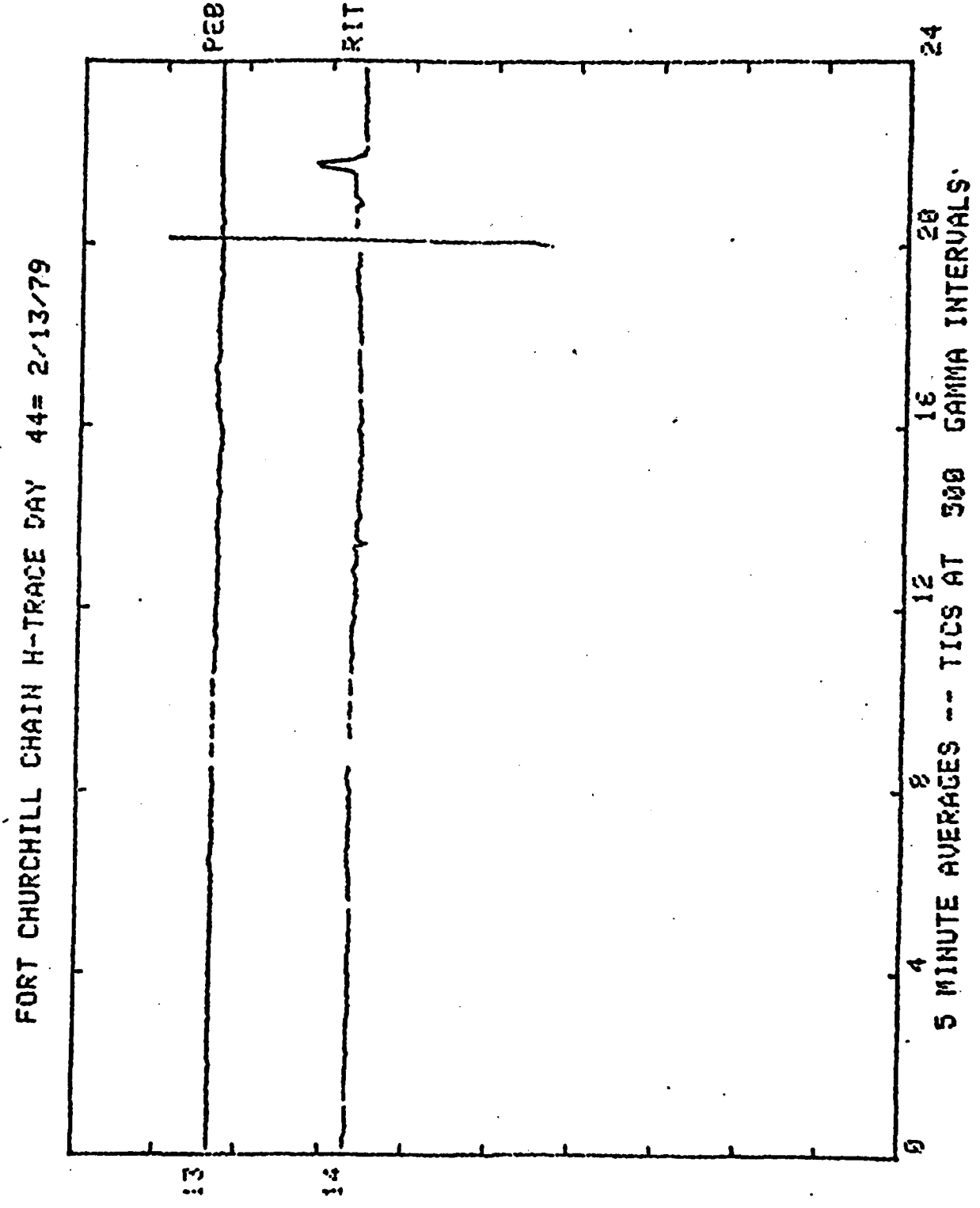
FORT CHURCHILL CHAIN H-TRACE DAY 44= 2/13/79
PEB
RIT
13
14
0
4
8
12
16
20
24
5 MINUTE AVERAGES -- TICS AT 300 GAMMA INTERVALS

Appendix 2
Quiet Day

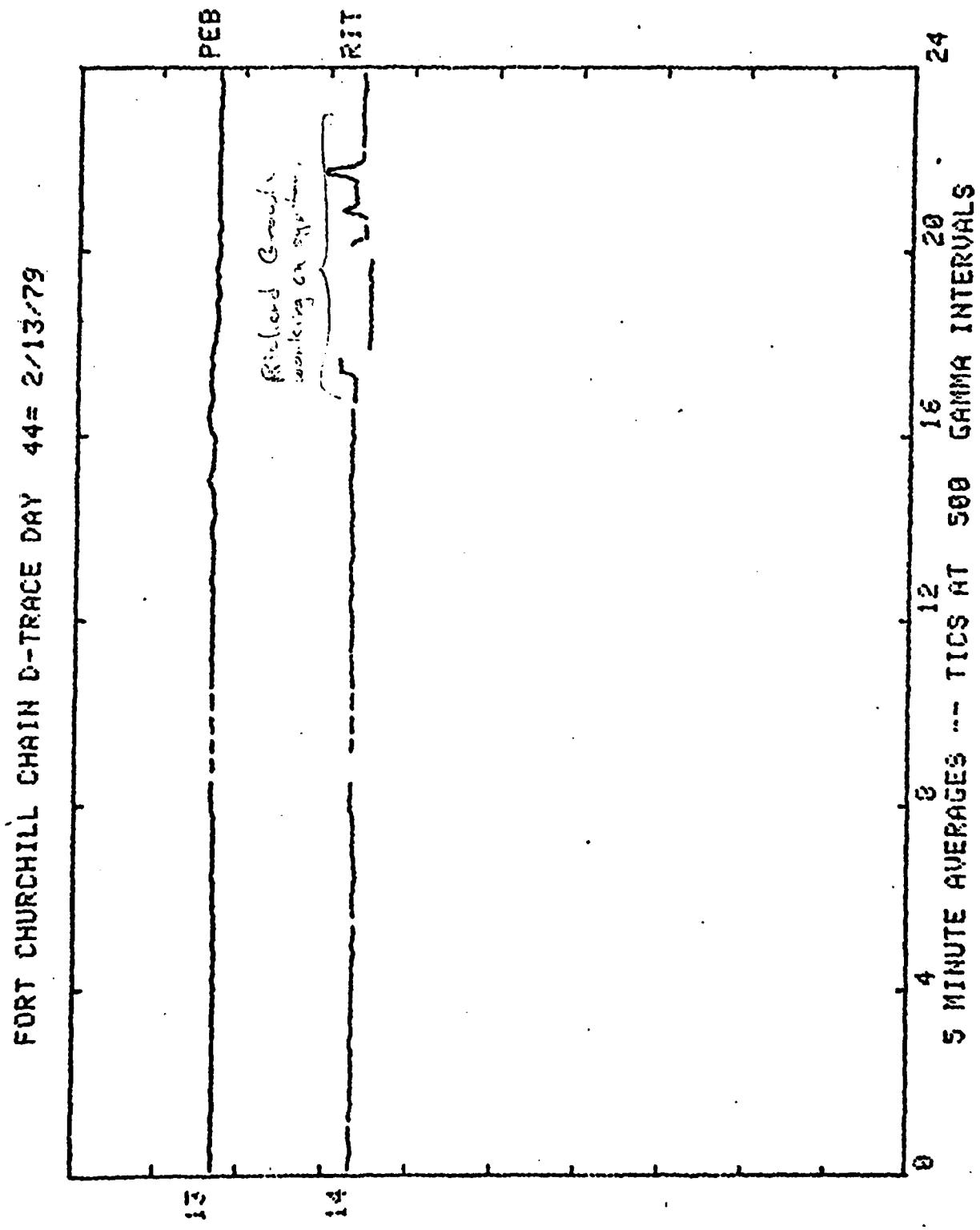

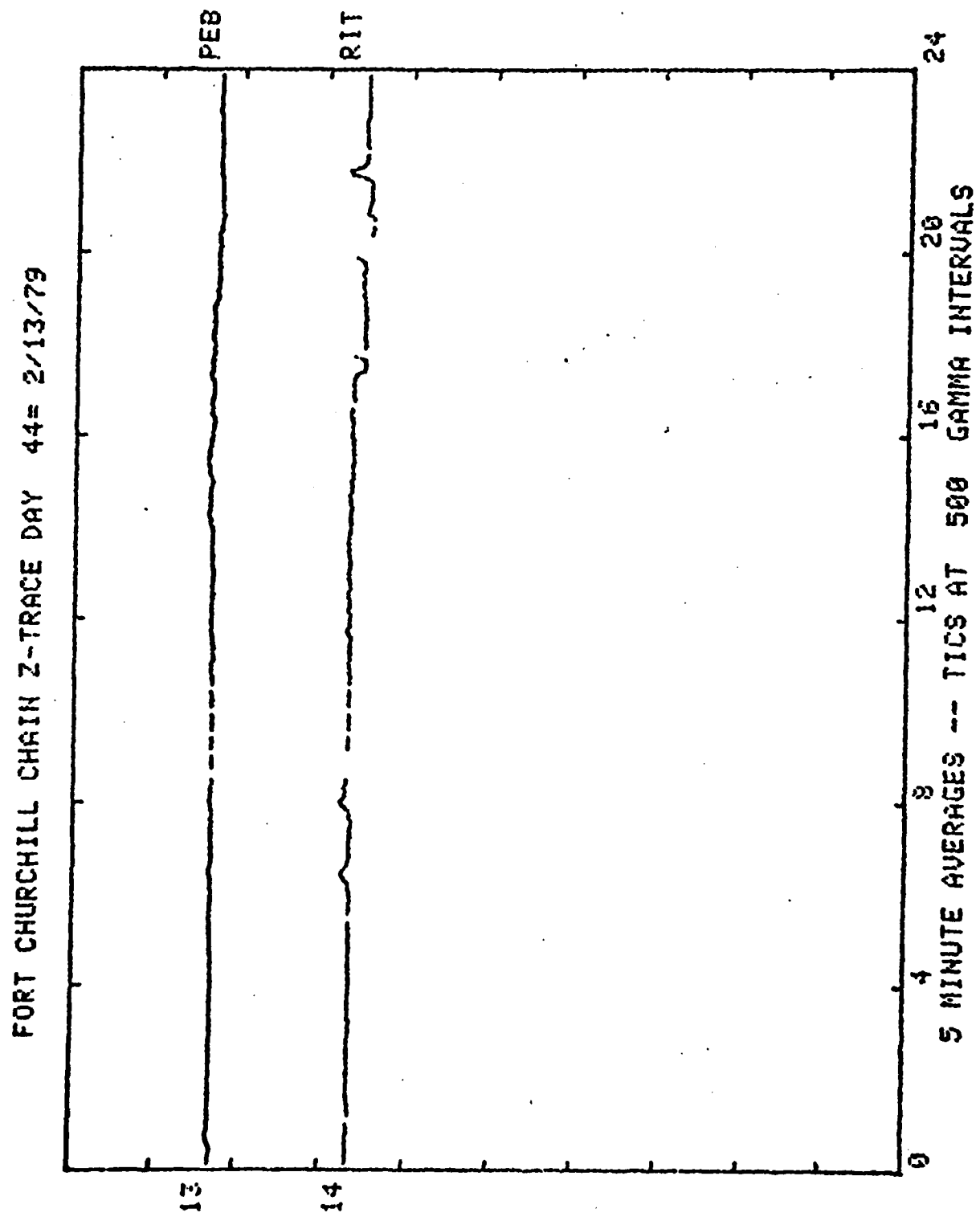
FORT CHURCHILL CHAIN Z-TRACE DAY 44= 2/13/79
PEB
RIT
13
14
0
4
8
12
16
20
24
5 MINUTE AVERAGES -- TICS AT 500 GAMMA INTERVALS

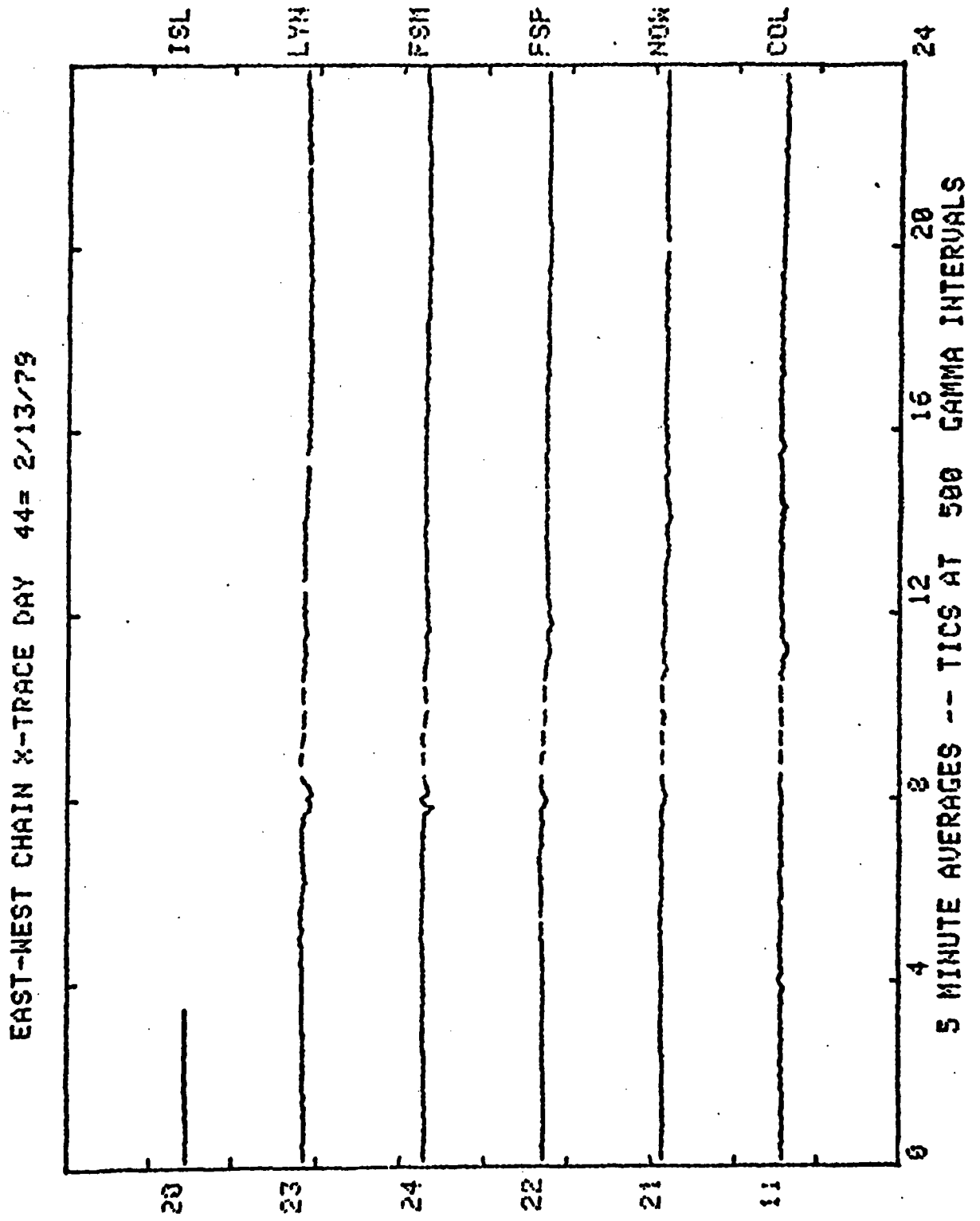
EAST-WEST CHAIN X-TRACE DAY 44= 2/13/79
ISL
LYN
FSM
FSP
NOR
COL
0
4
8
12
16
20
24
5 MINUTE AVERAGES -- TICS AT 500 GAMMA INTERVALS
23
23
24
22
21
11

Appendix 2
Quiet Day

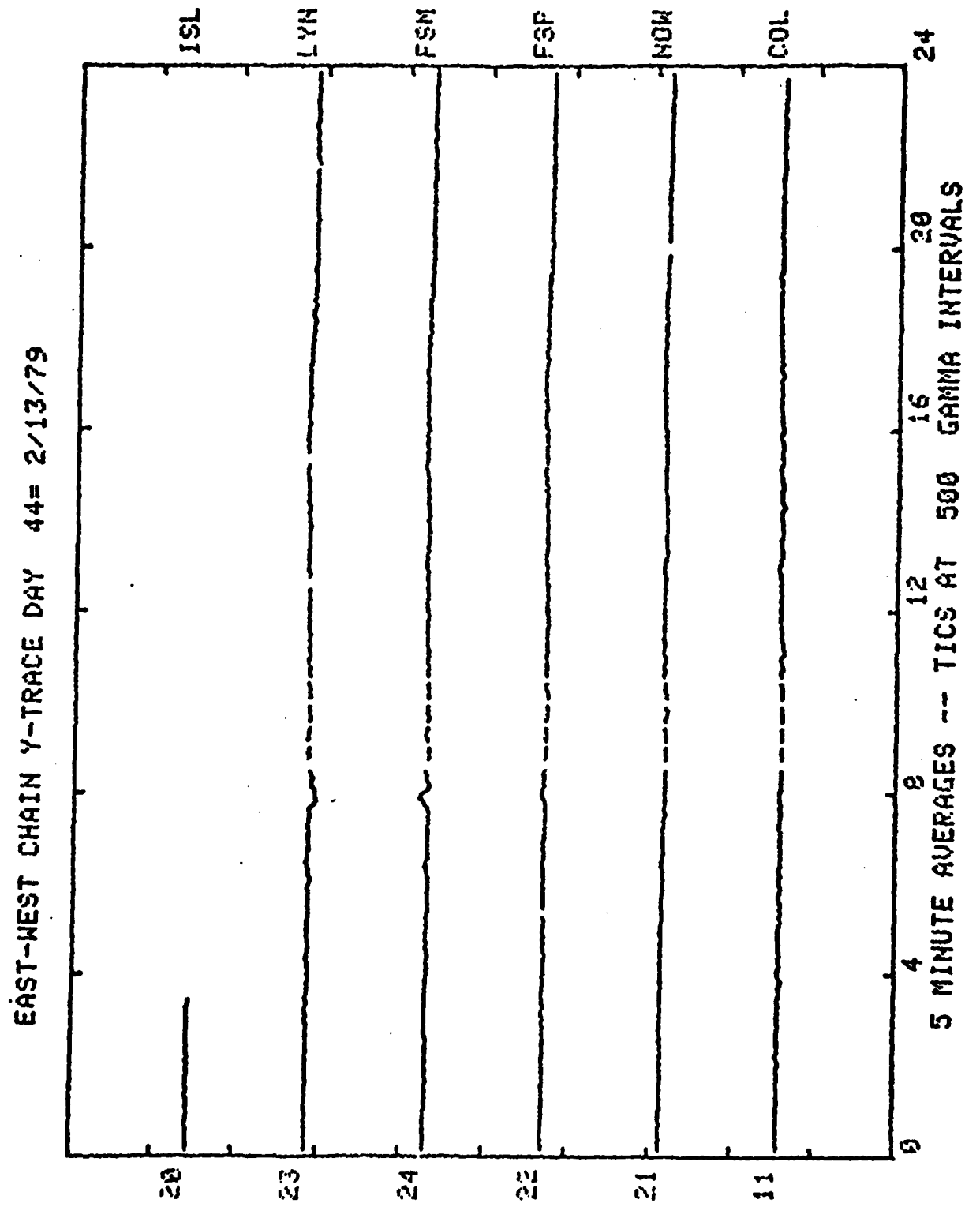

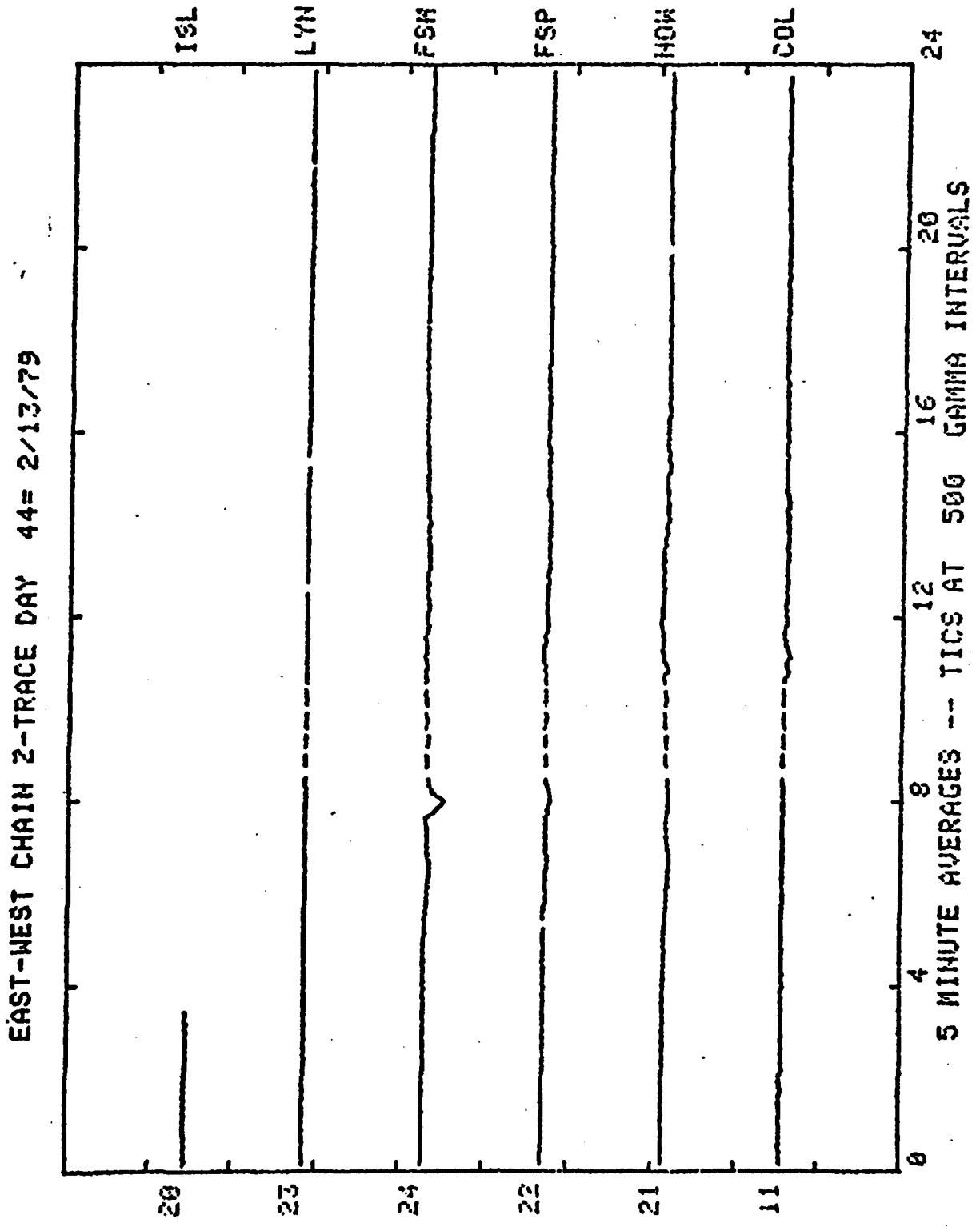
EAST-WEST CHAIN 2-TRACE DAY 44= 2/13/79
ISL
LYN
FSM
FSP
HOW
COL
0
4
8
12
16
20
24
5 MINUTE AVERAGES -- TICS AT 500 GAMMA INTERVALS
20
23
24
22
21
11

Quiet Day

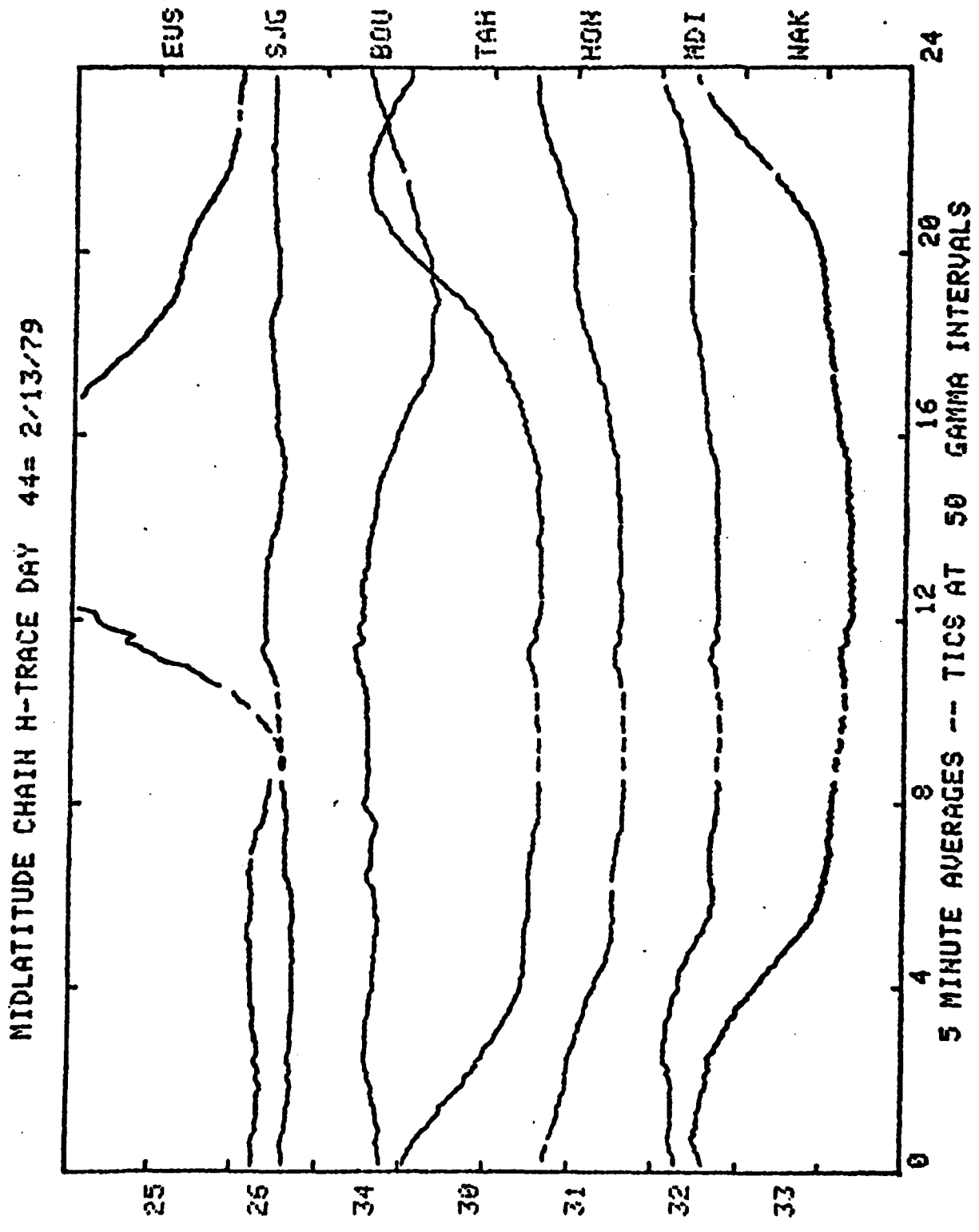
MIDLATITUDE CHAIN H-TRACE DAY 44= 2/13/79
EUS
SJG
BOU
TAH
HON
ADI
NAK
25
26
34
30
31
32
33
0
4
8
12
16
20
24
5 MINUTE AVERAGES -- TICS AT 50 GAMMA INTERVALS

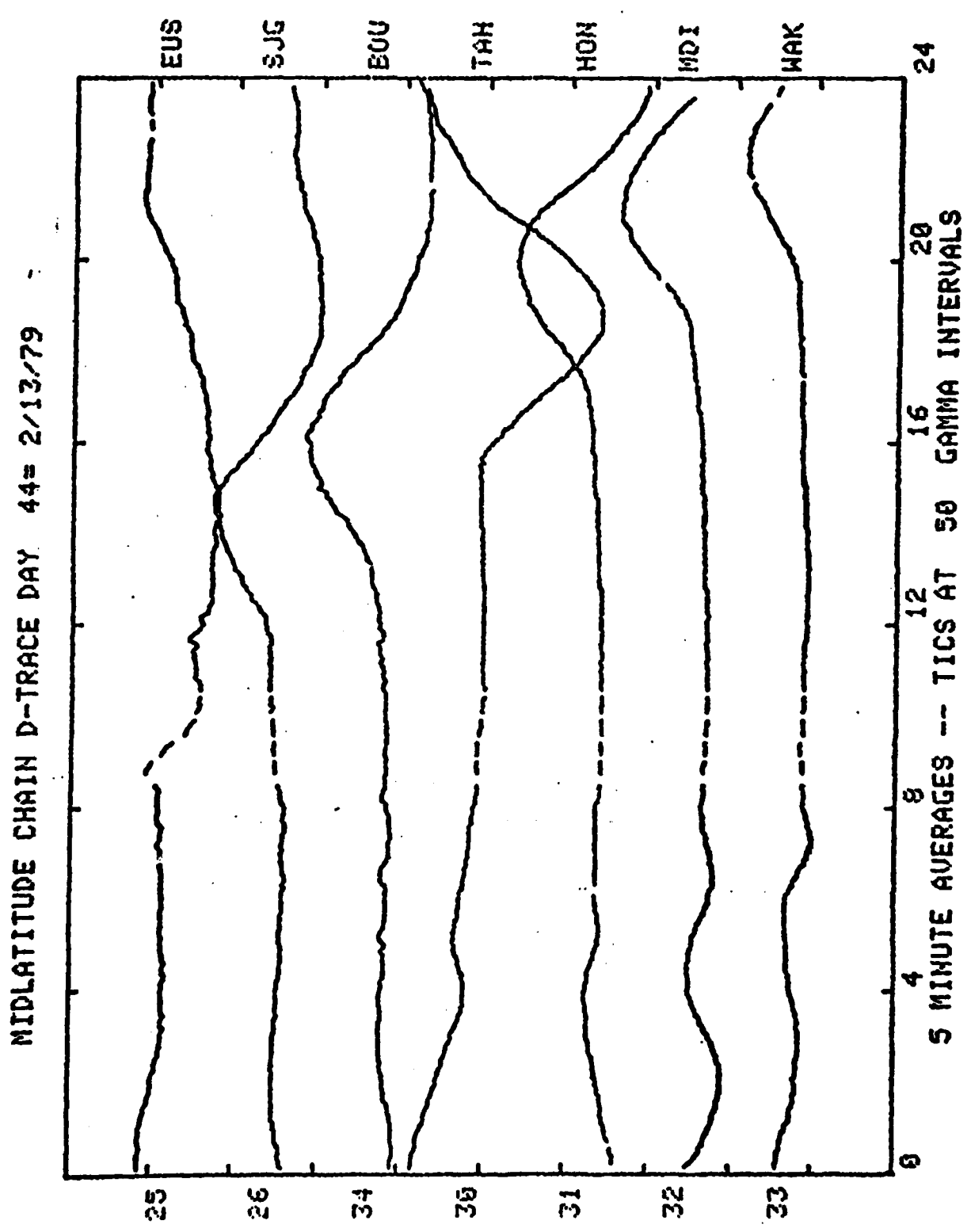
MIDLATITUDE CHAIN D-TRACE DAY 44= 2/13/79
EUS
SJG
BOU
TAH
HON
MDI
WAK
25
26
34
30
31
32
33
0
4
8
12
16
20
24
5 MINUTE AVERAGES -- TICS AT 50 GAMMA INTERVALS

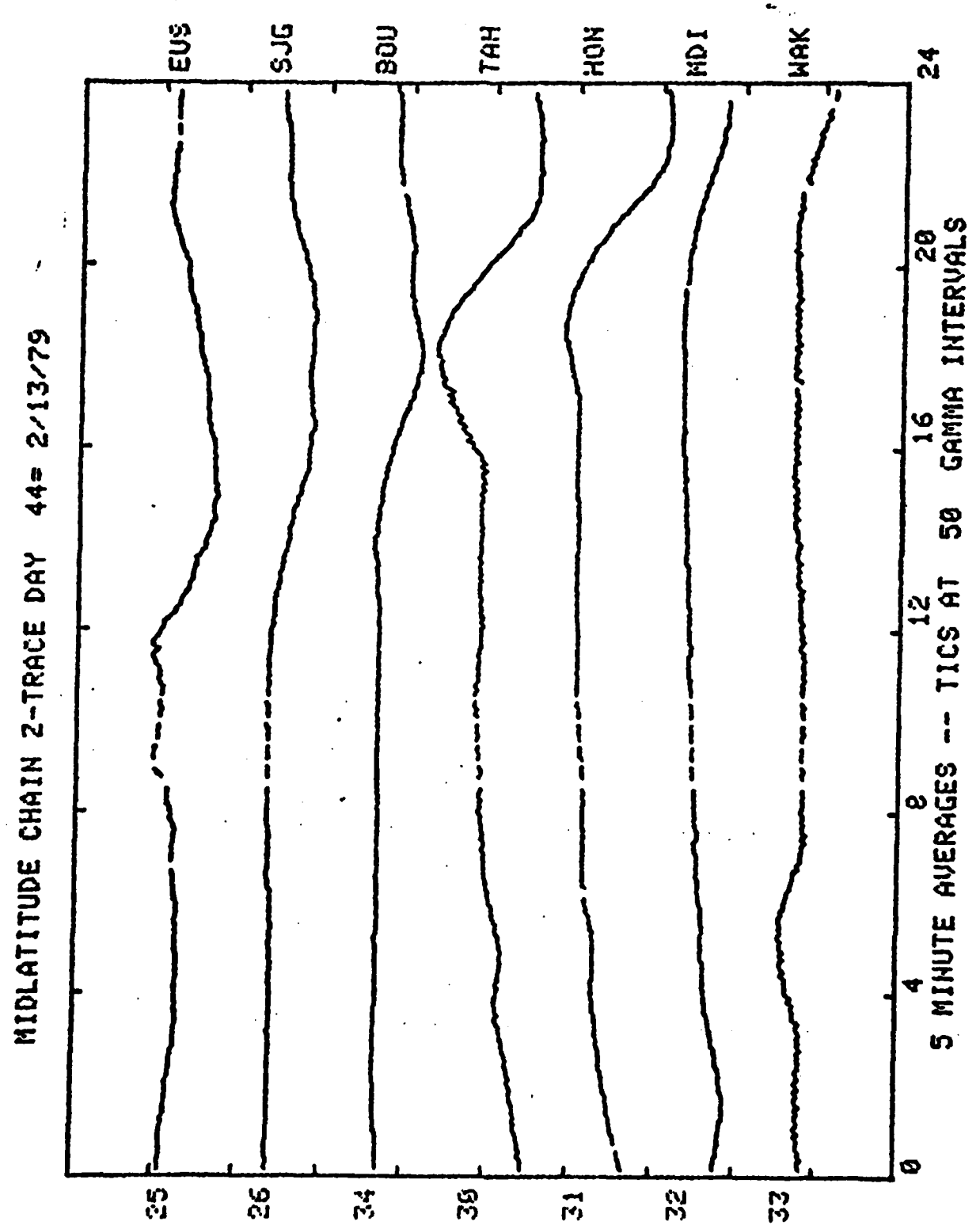
MIDLATITUDE CHAIN 2-TRACE DAY 44= 2/13/79
EUS
SJG
BOU
TAH
HON
MDI
WAK
25
26
34
30
31
32
33
0
4
8
12
16
20
24
5 MINUTE AVERAGES -- TICS AT 50 GAMMA INTERVALS

Appendix 2
Quiet Day

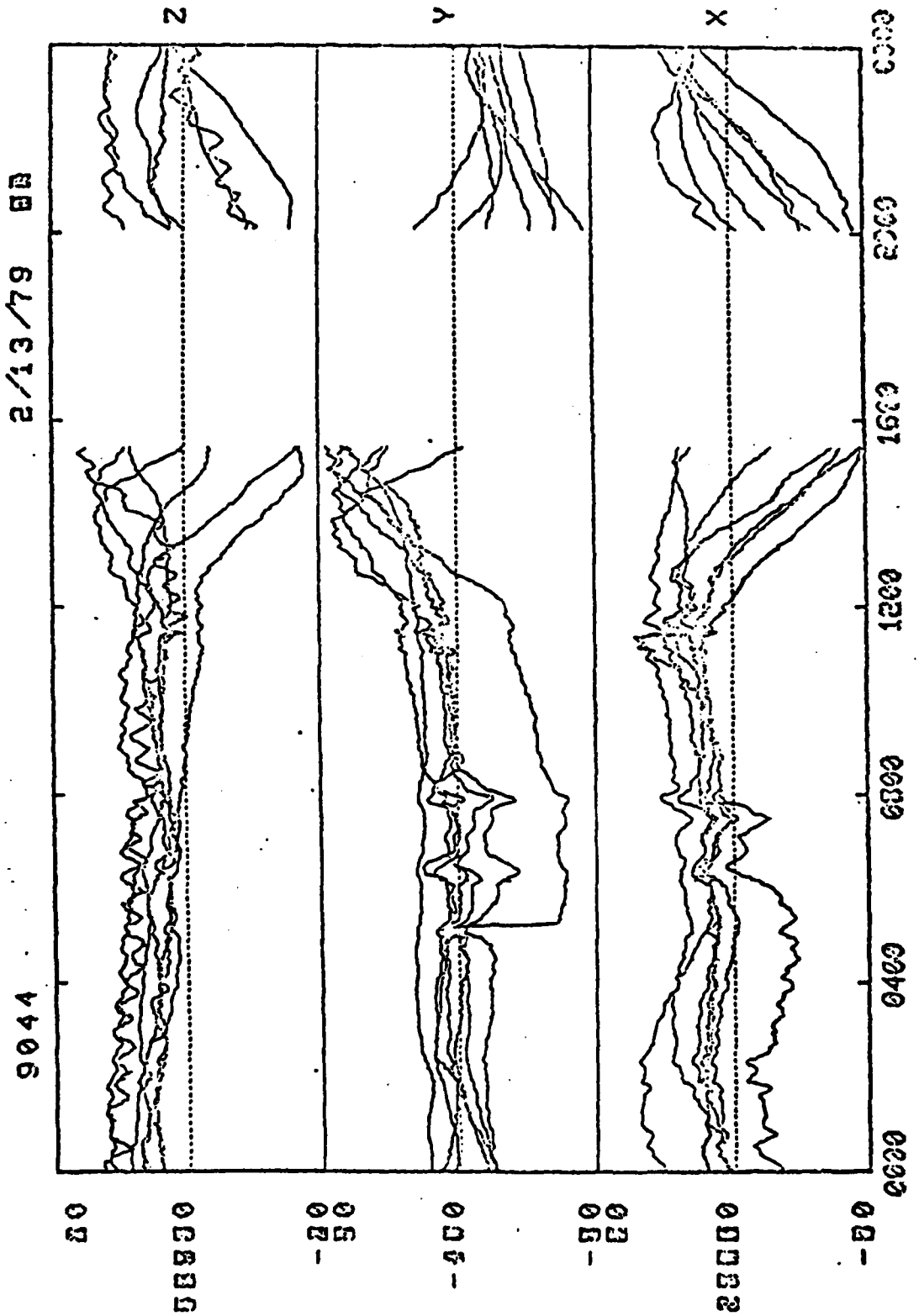

Appendix 2
Quiet Day

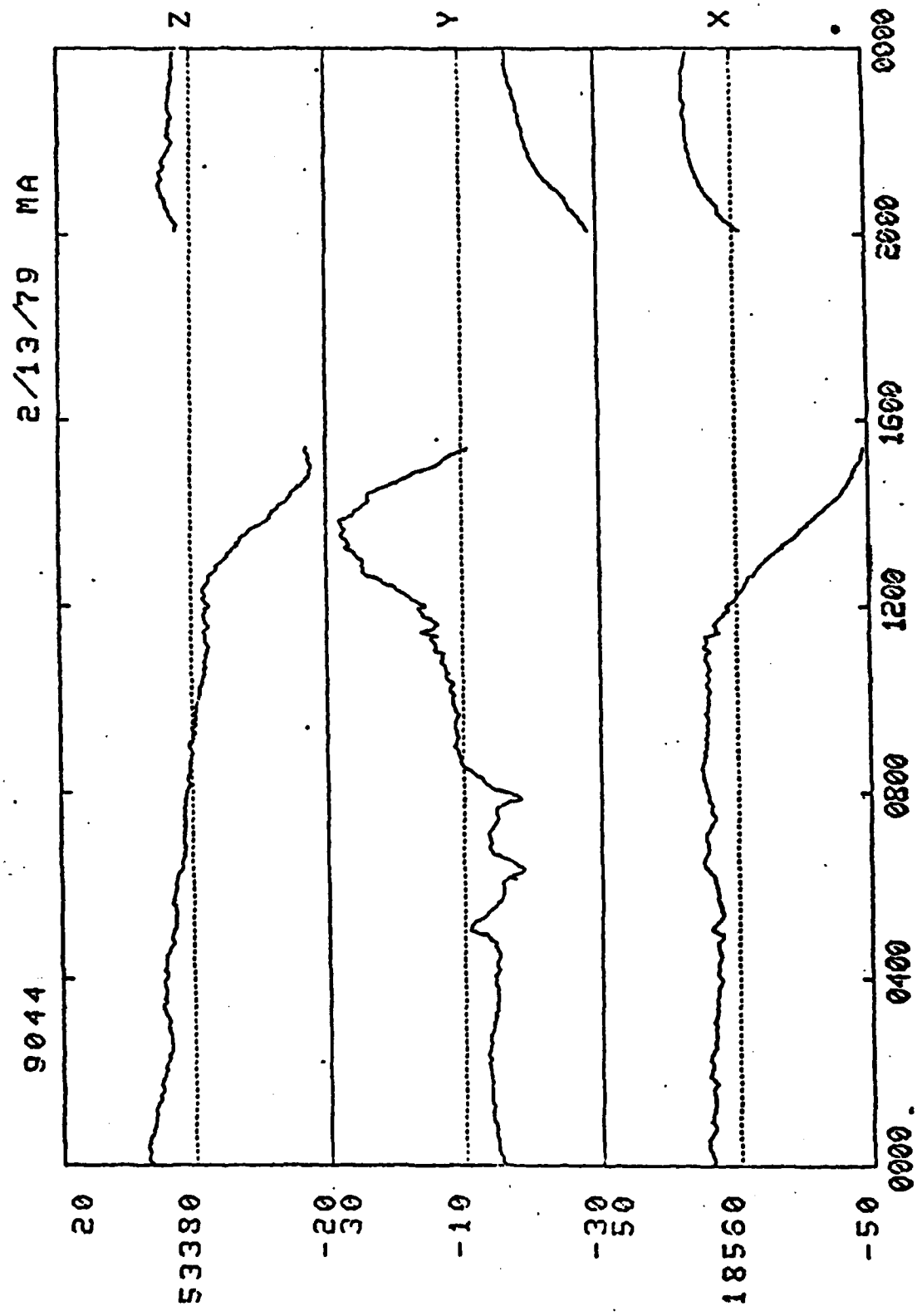

Appendix 2
Quiet Day

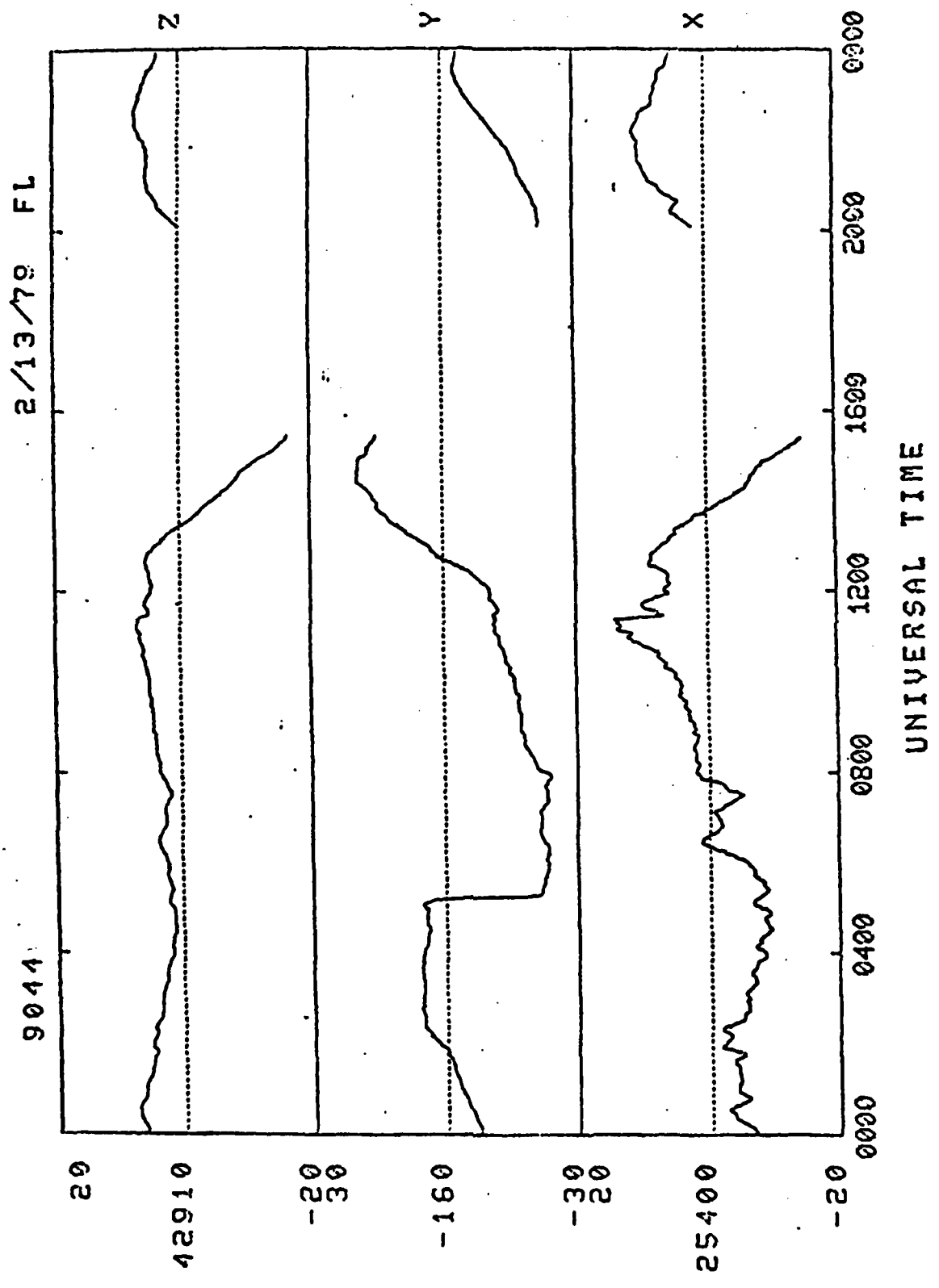

Appendix 2
Quiet Day

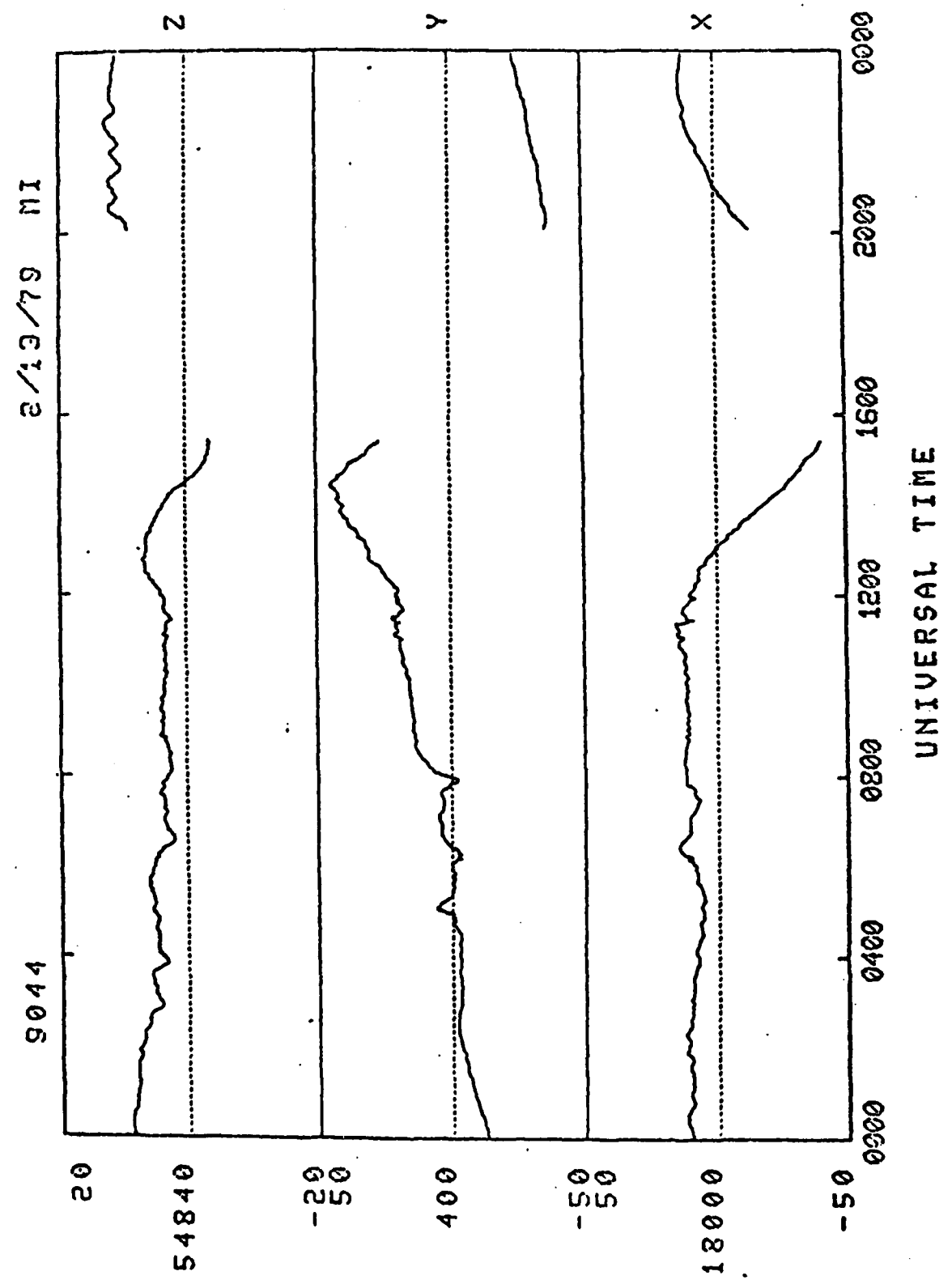

Appendix 2
Quiet Day

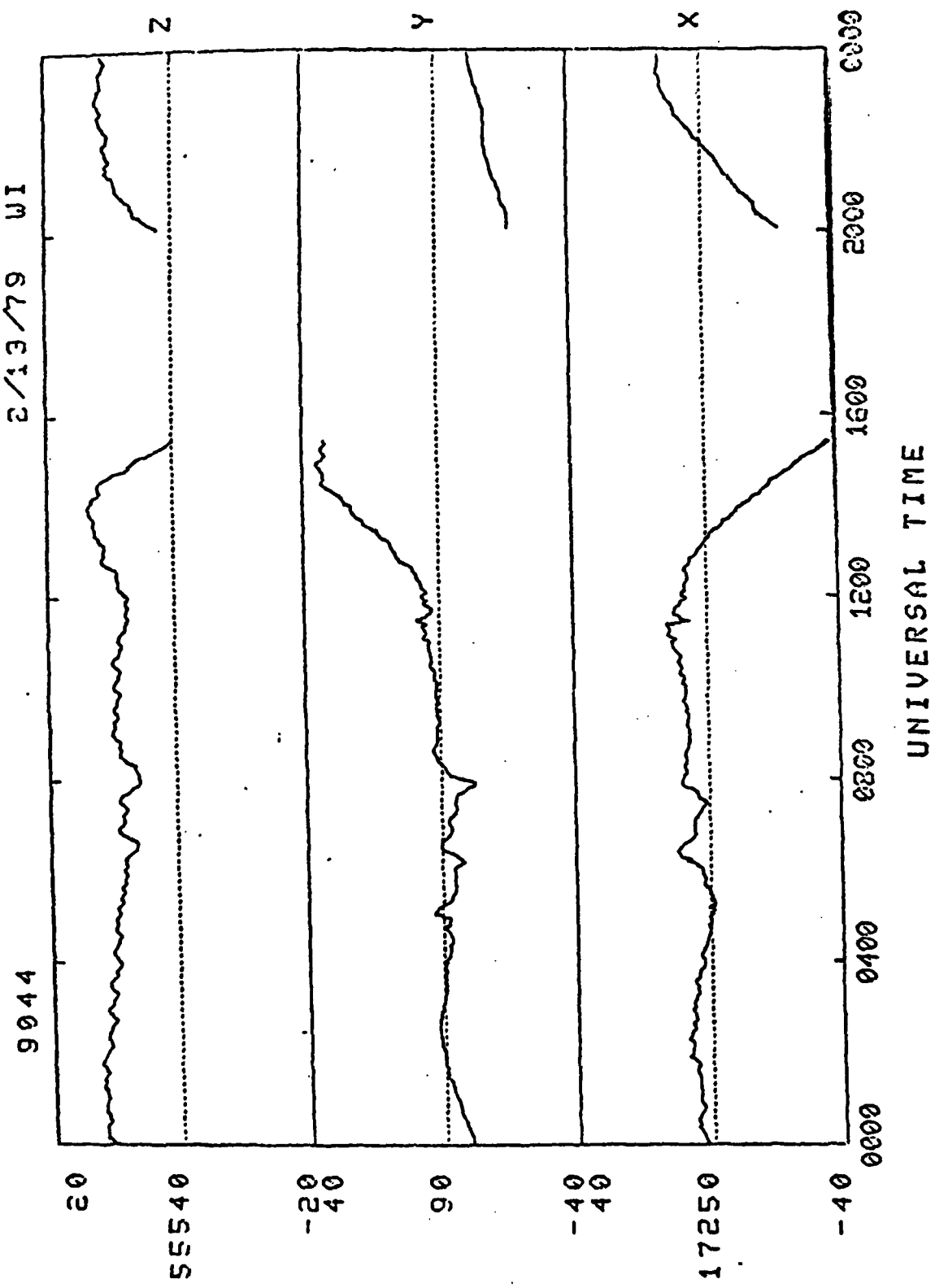

Appendix 2
Quiet Day

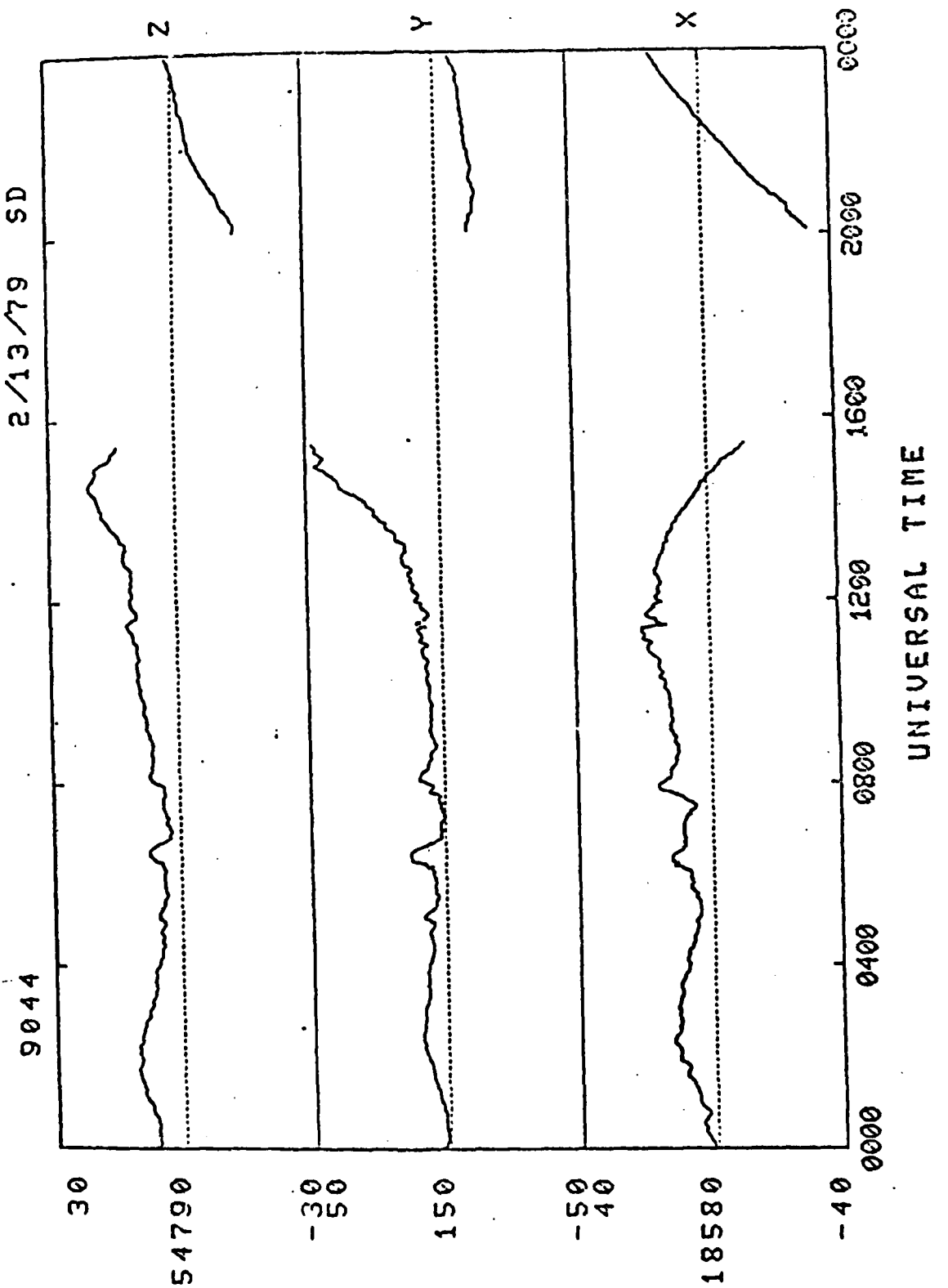

Appendix 2
Quiet Day

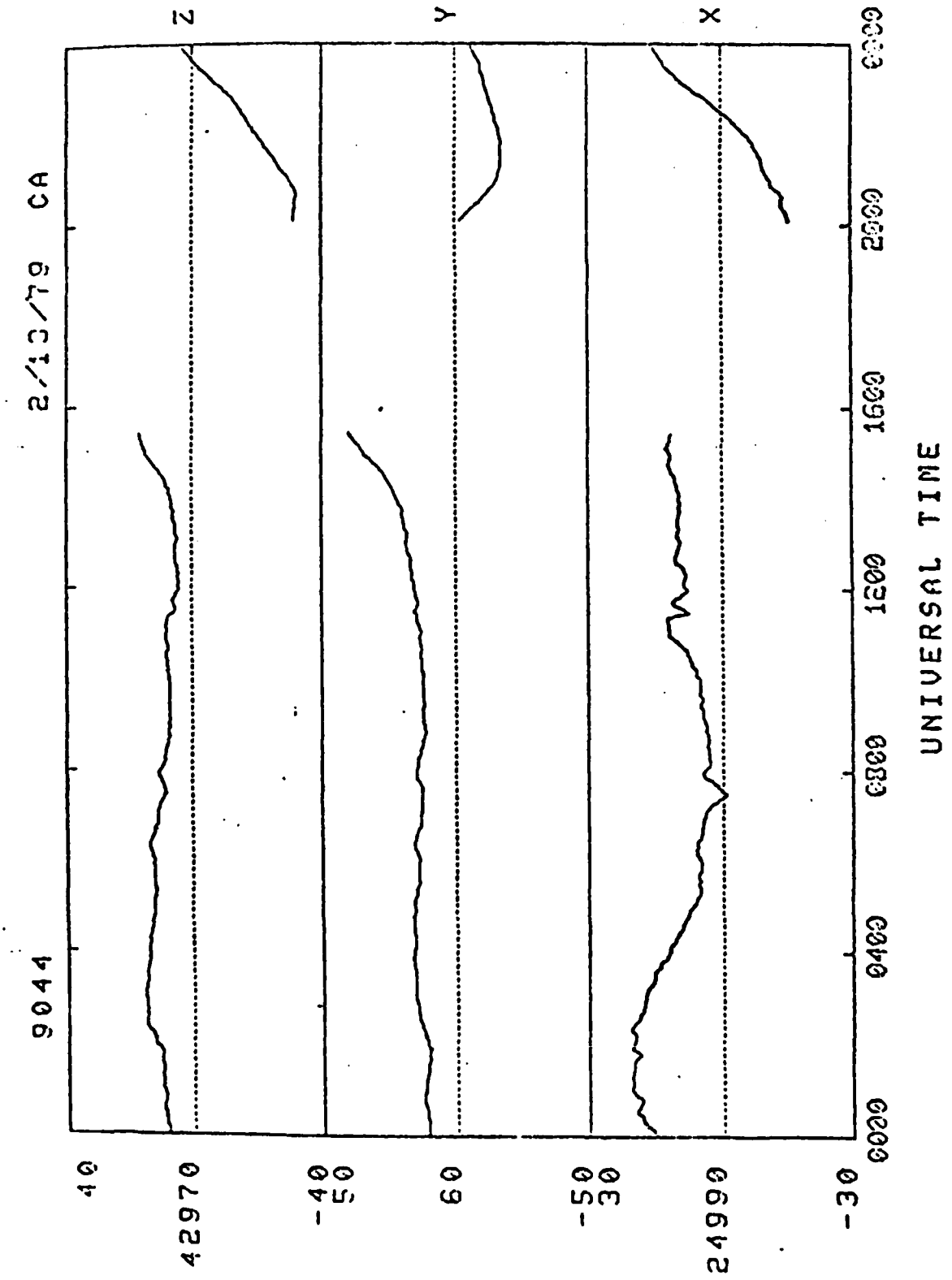

AD-A087 433 JOHNS HOPKINS UNIV LAUREL MD APPLIED PHYSICS LAB F/G 8/14
THE INVESTIGATION OF THE MAGNETOSPHERIC DYNAMICS IN CONJUNCTION--ETC(U)
DEC 79 C MENG N00017-72-C-4401

UNCLASSIFIED AFGL-TR-80-0070 NL

2 OF 2
AD A087433

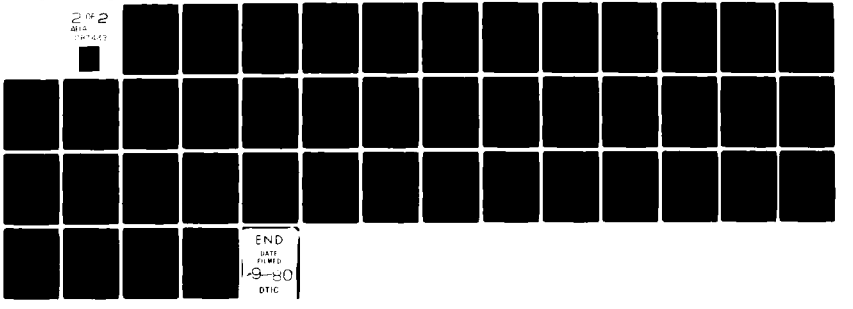

END
DATE FILMED
9-80
DTIC

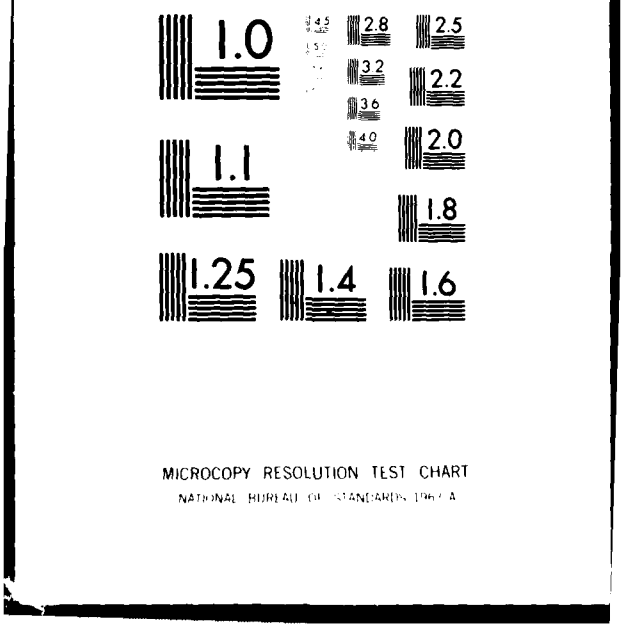
1.0
2.8
2.5
3.2
2.2
3.6
4.0
2.0
1.1
1.8
1.25
1.4
1.6
MICROCOPY RESOLUTION TEST CHART
NATIONAL BUREAU OF STANDARDS 1963-A

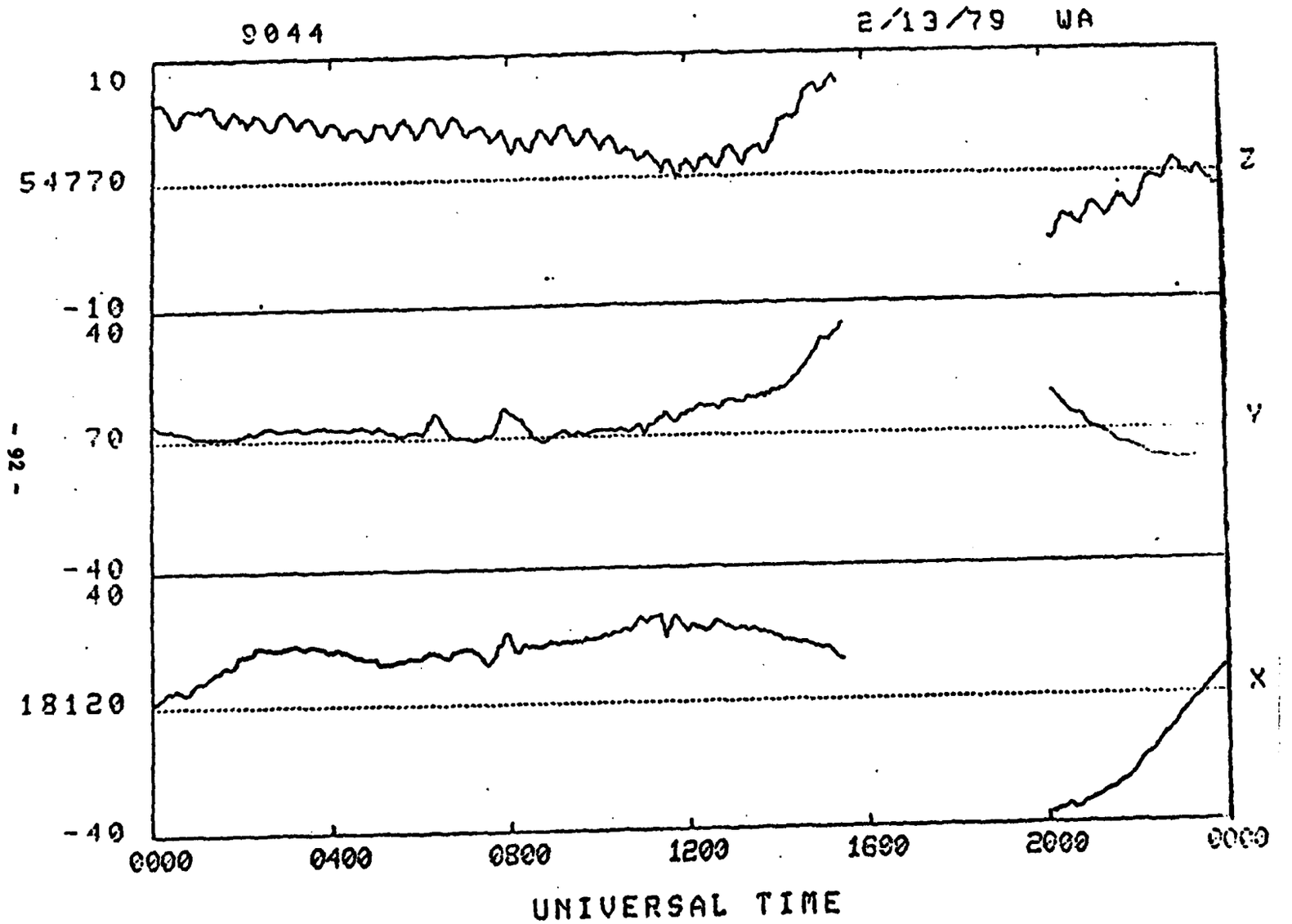

Appendix 2
Quiet Day

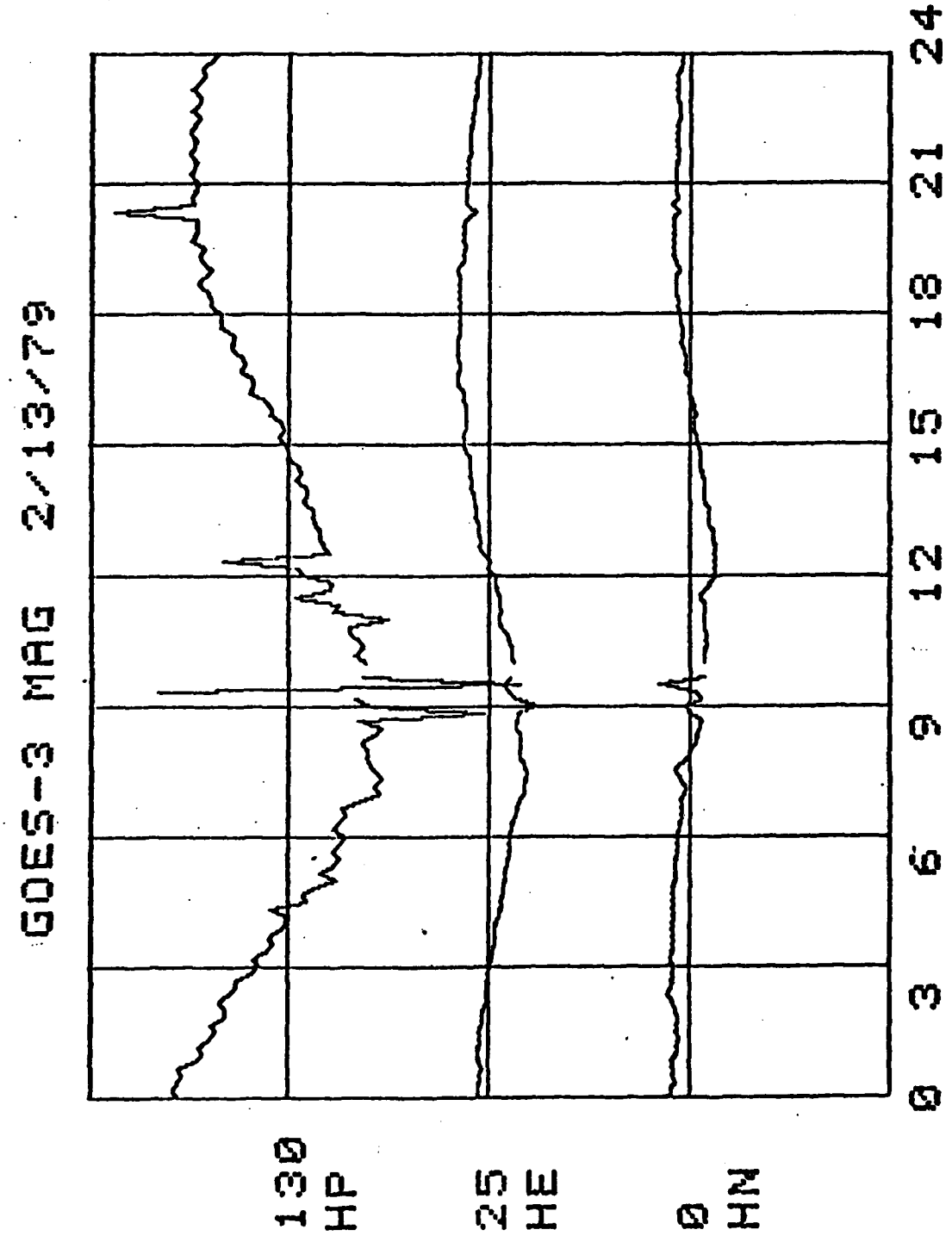
GOES-3 MAG 2/13/79
0 3 6 9 12 15 18 21 24
139 HP
25 HE
0 HN

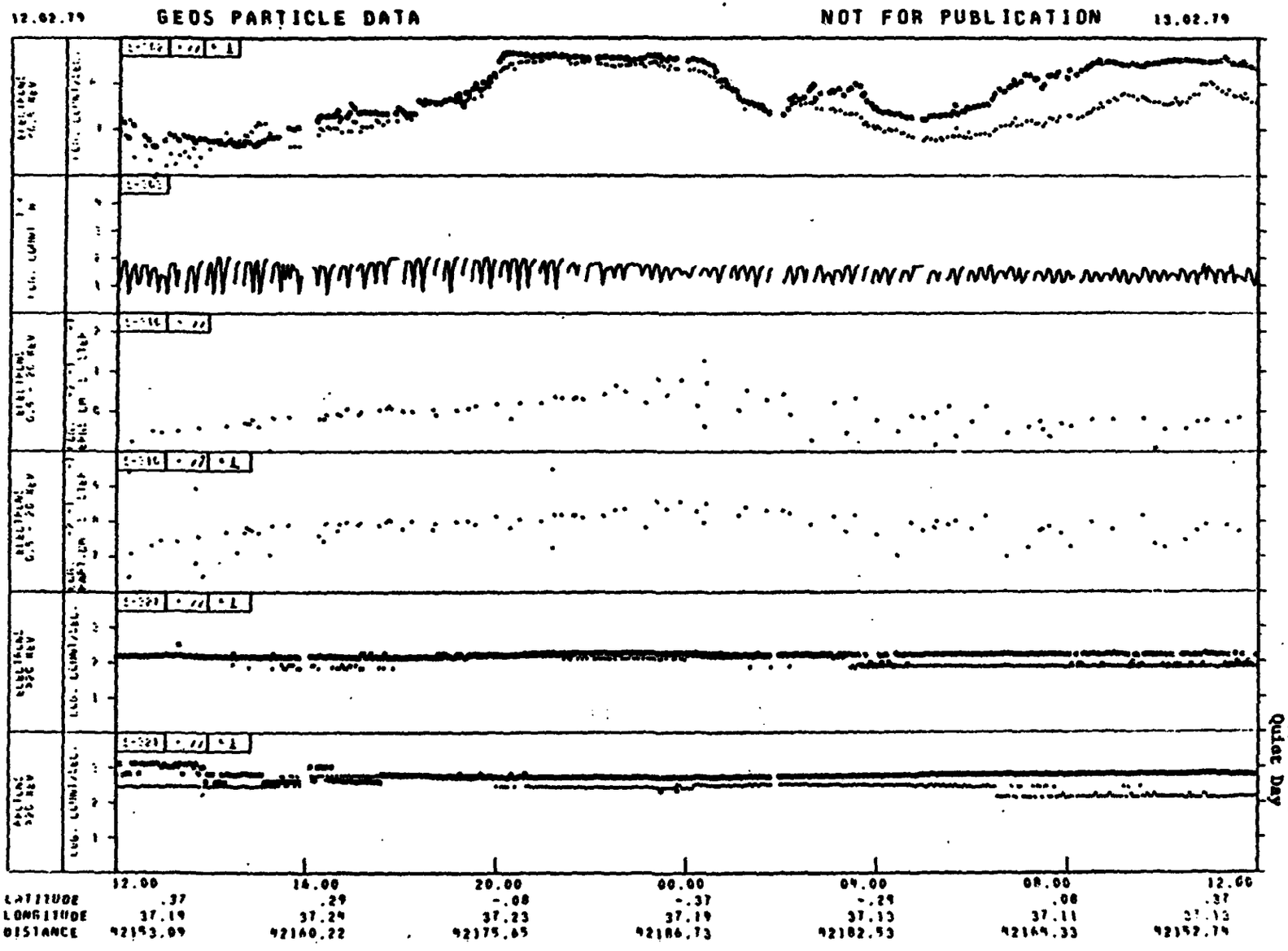

Appendix 2
Quiet Day

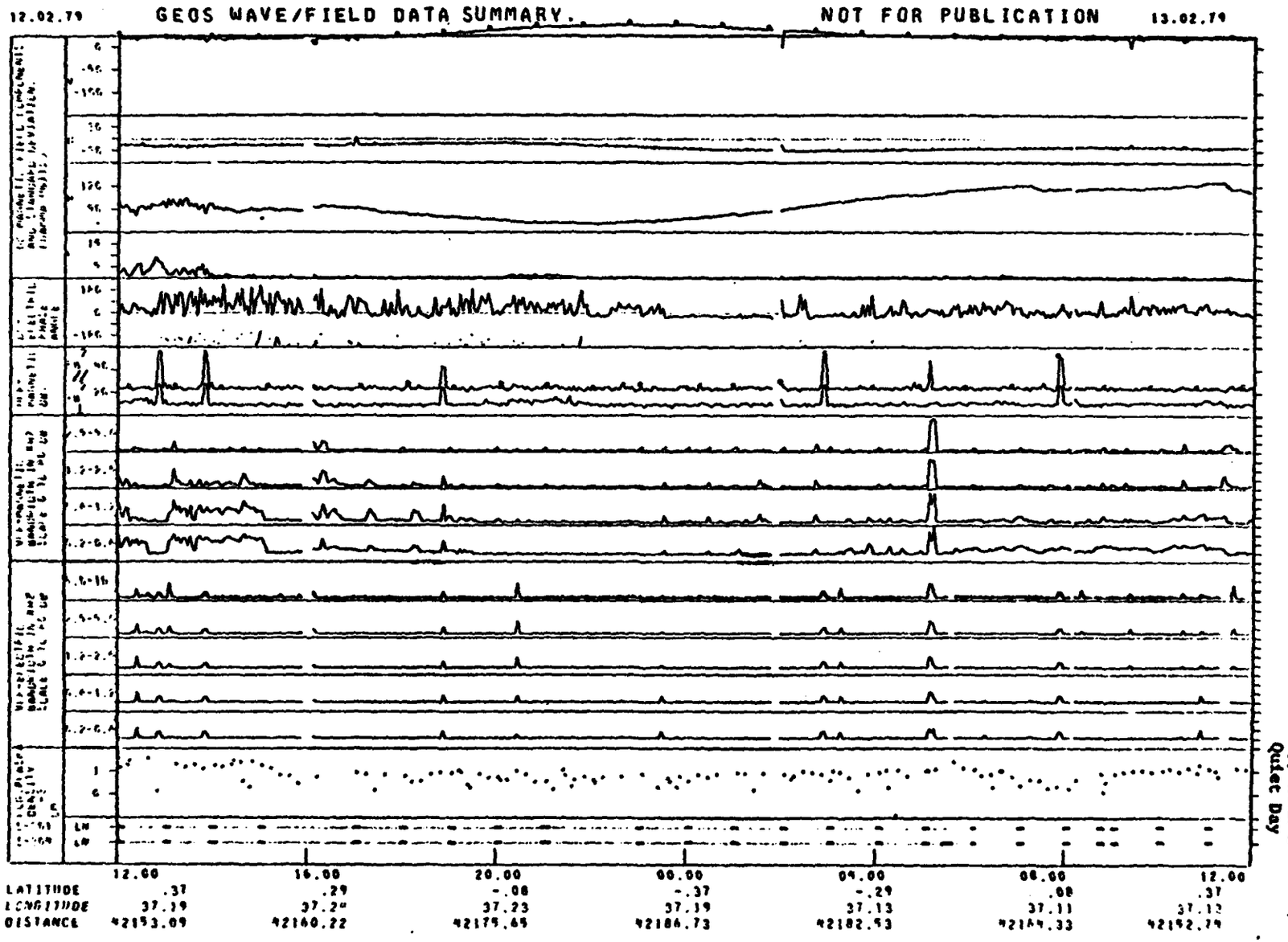

Appendix 2
Quiet Day

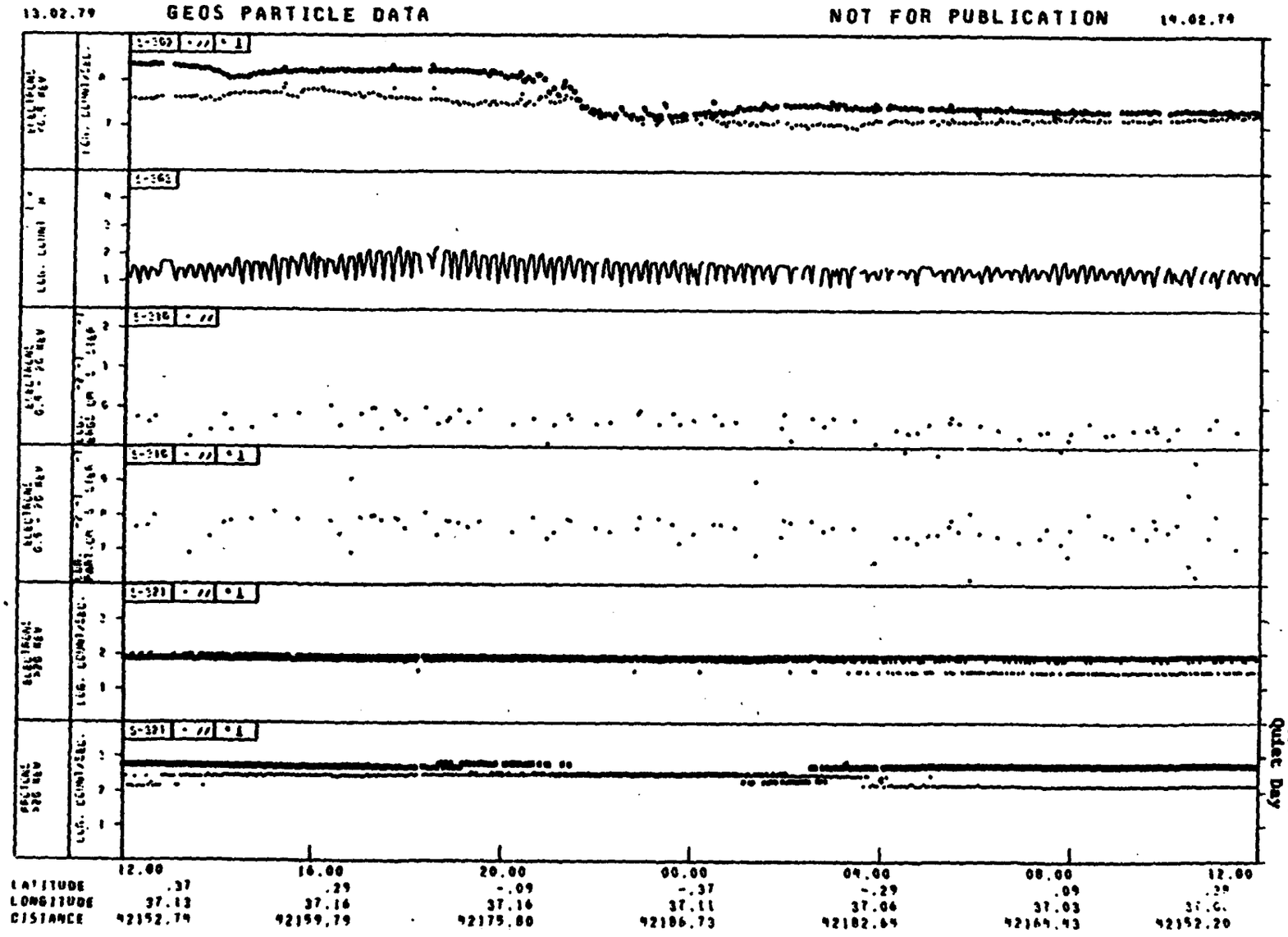

Appendix 2
Quiet Day

Appendix 2
Quiet Day

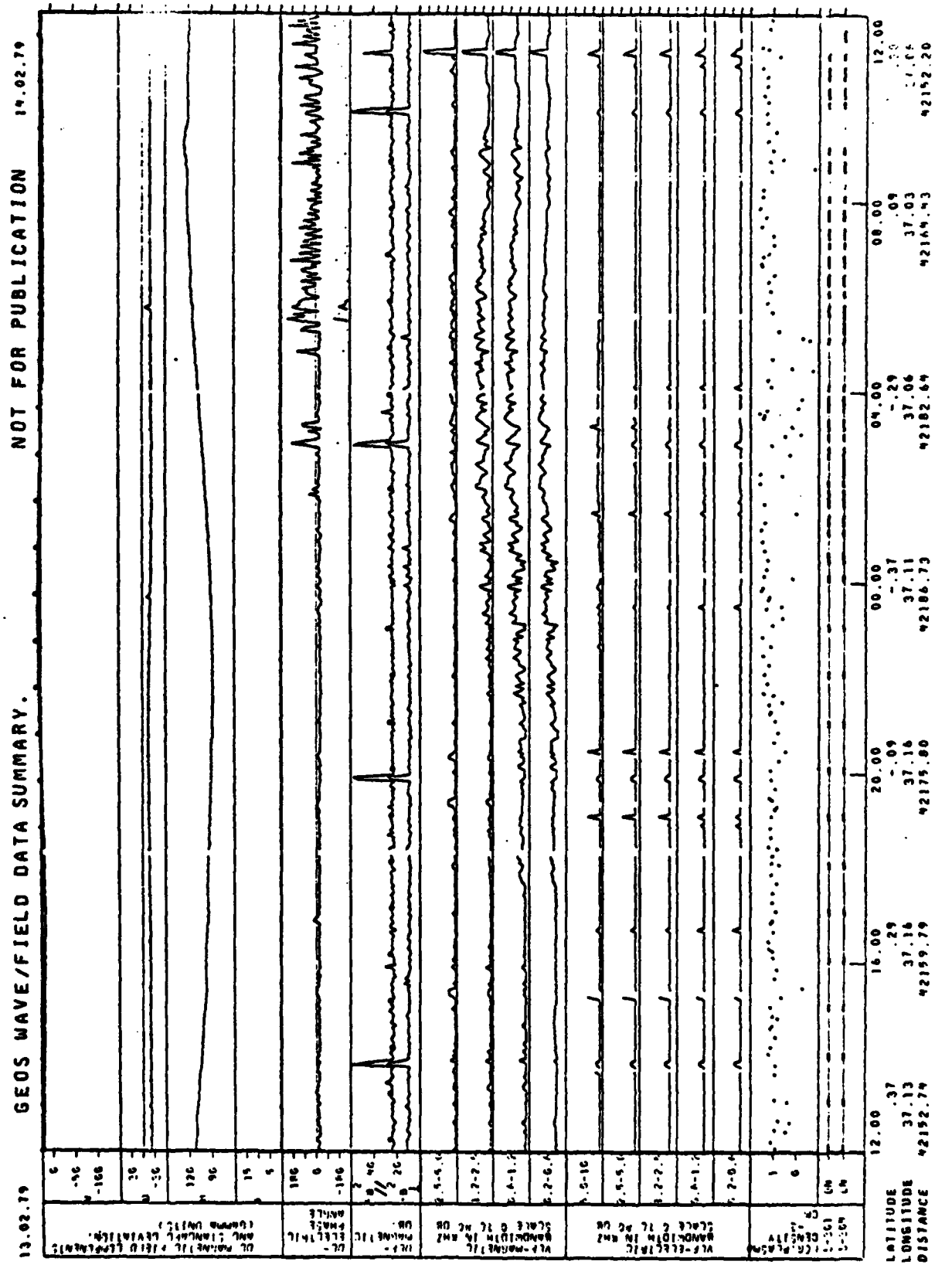

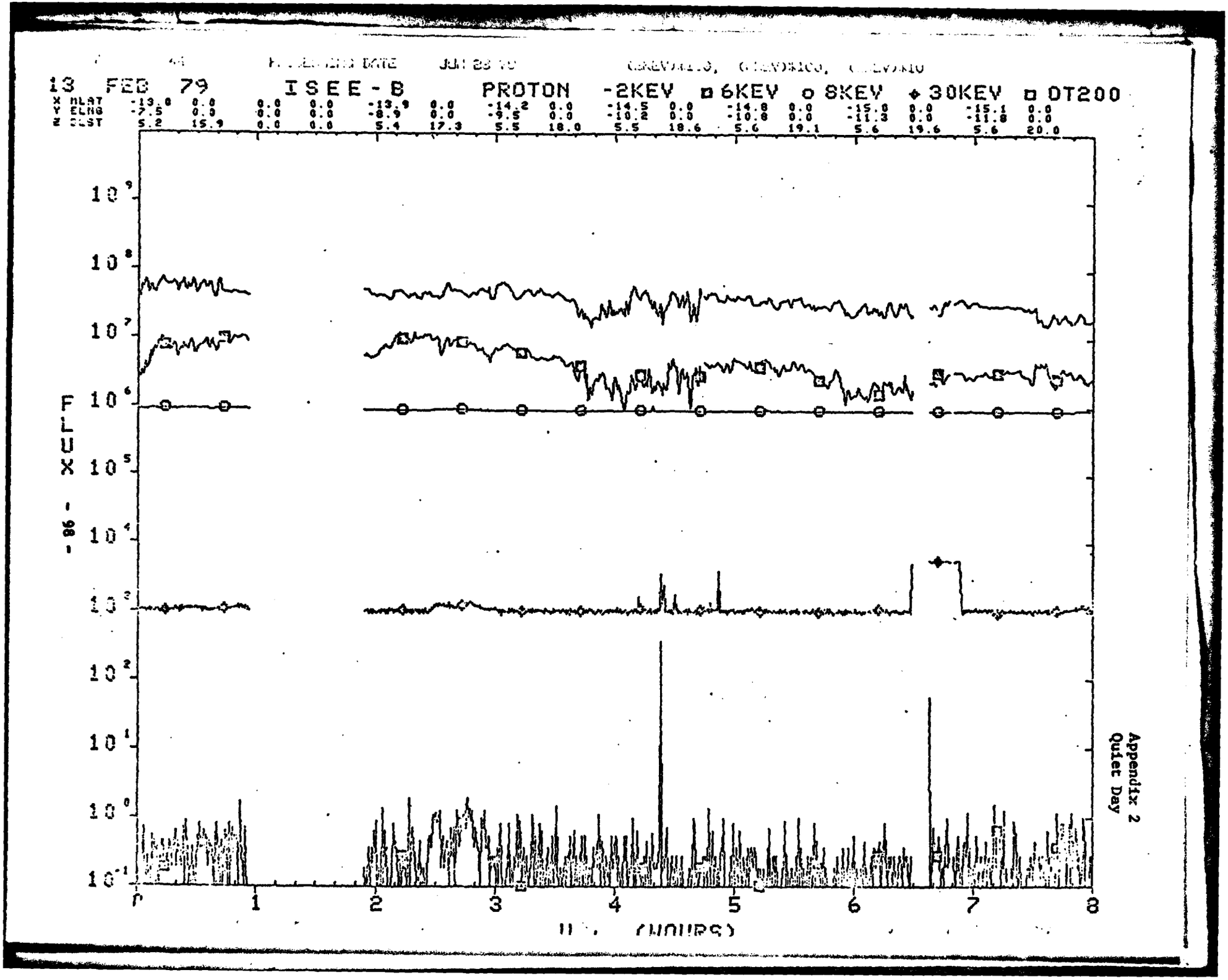

Appendix 2
Quiet Day

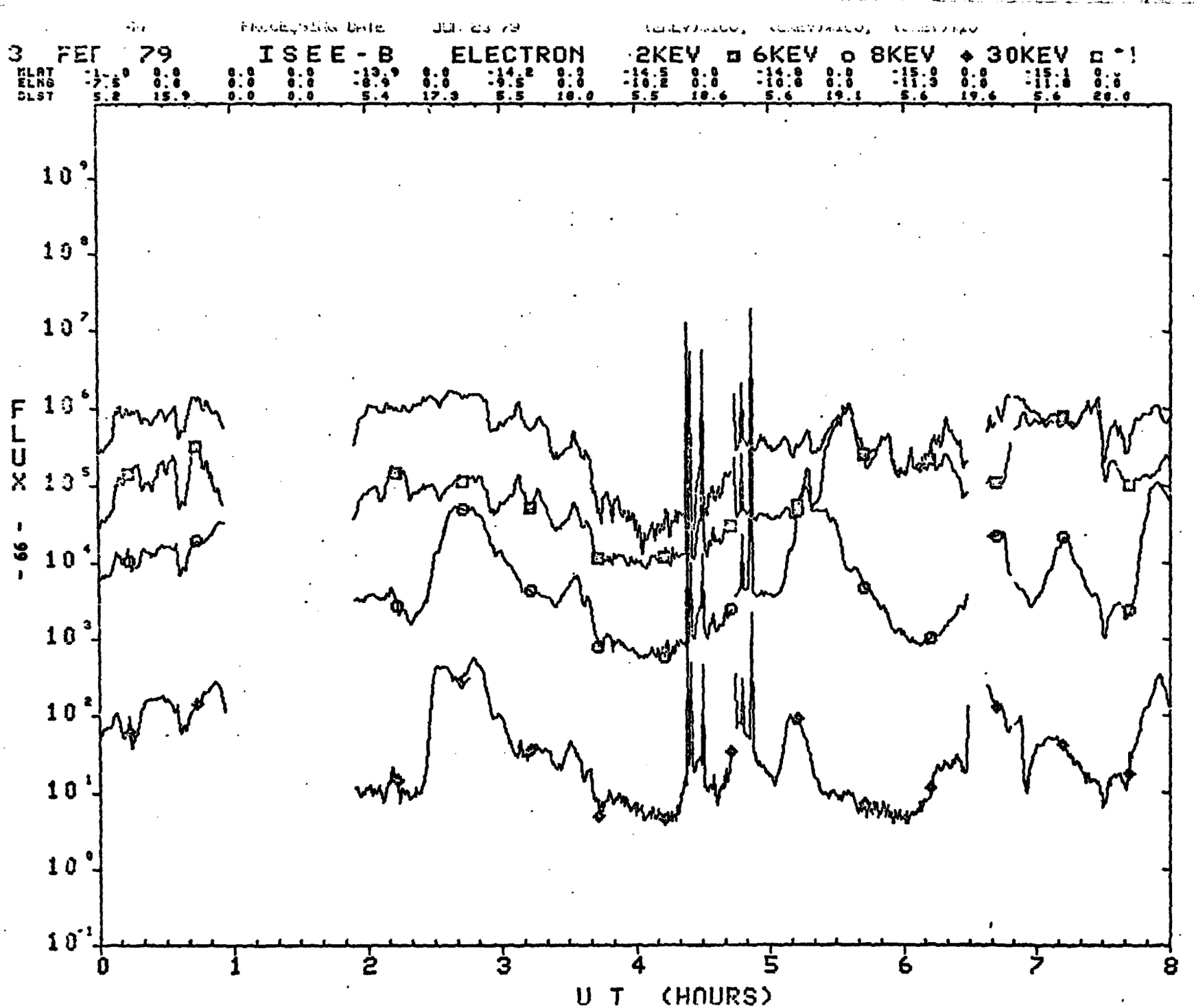

Appendix 2
Quiet Day

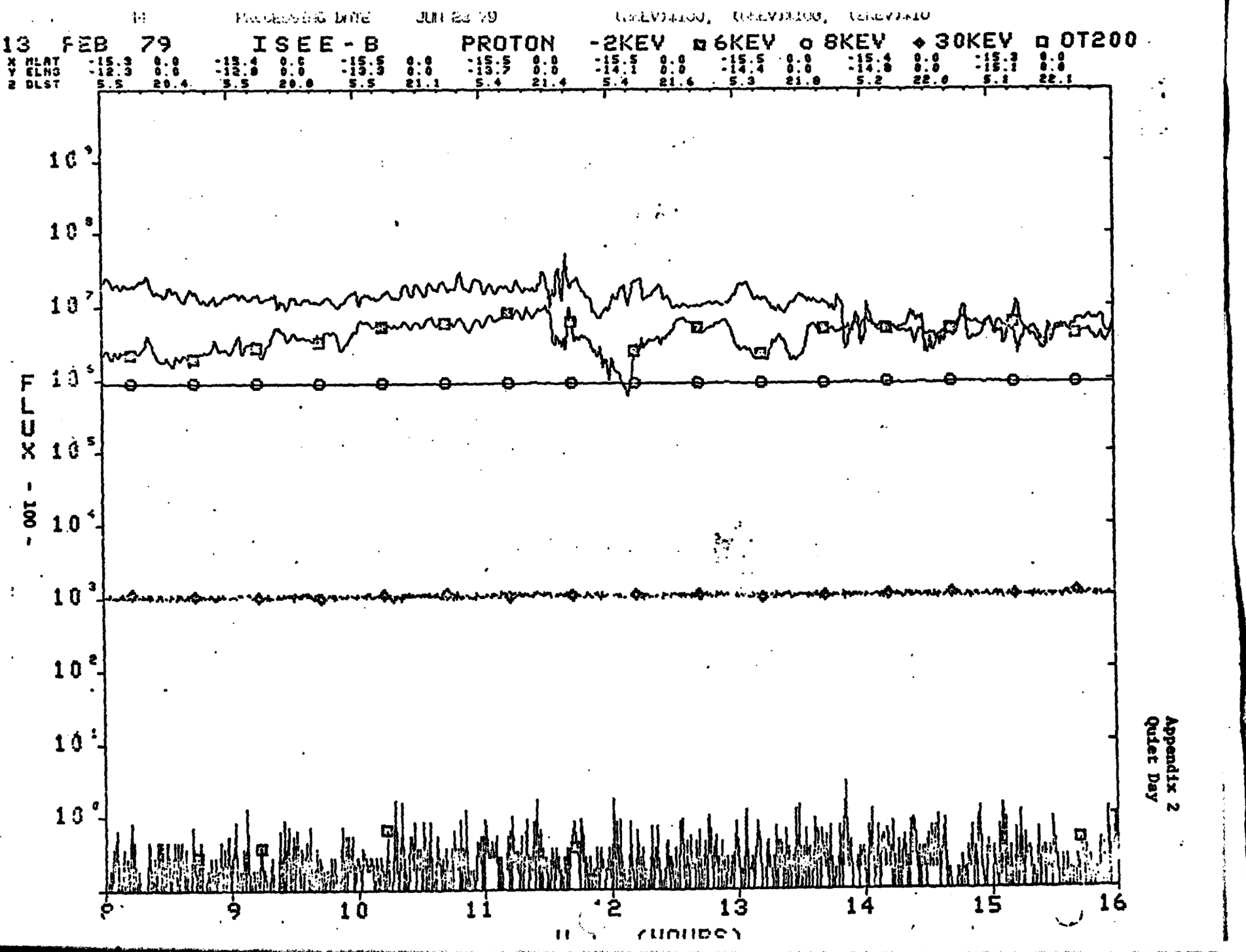

Appendix 2
Quiet Day

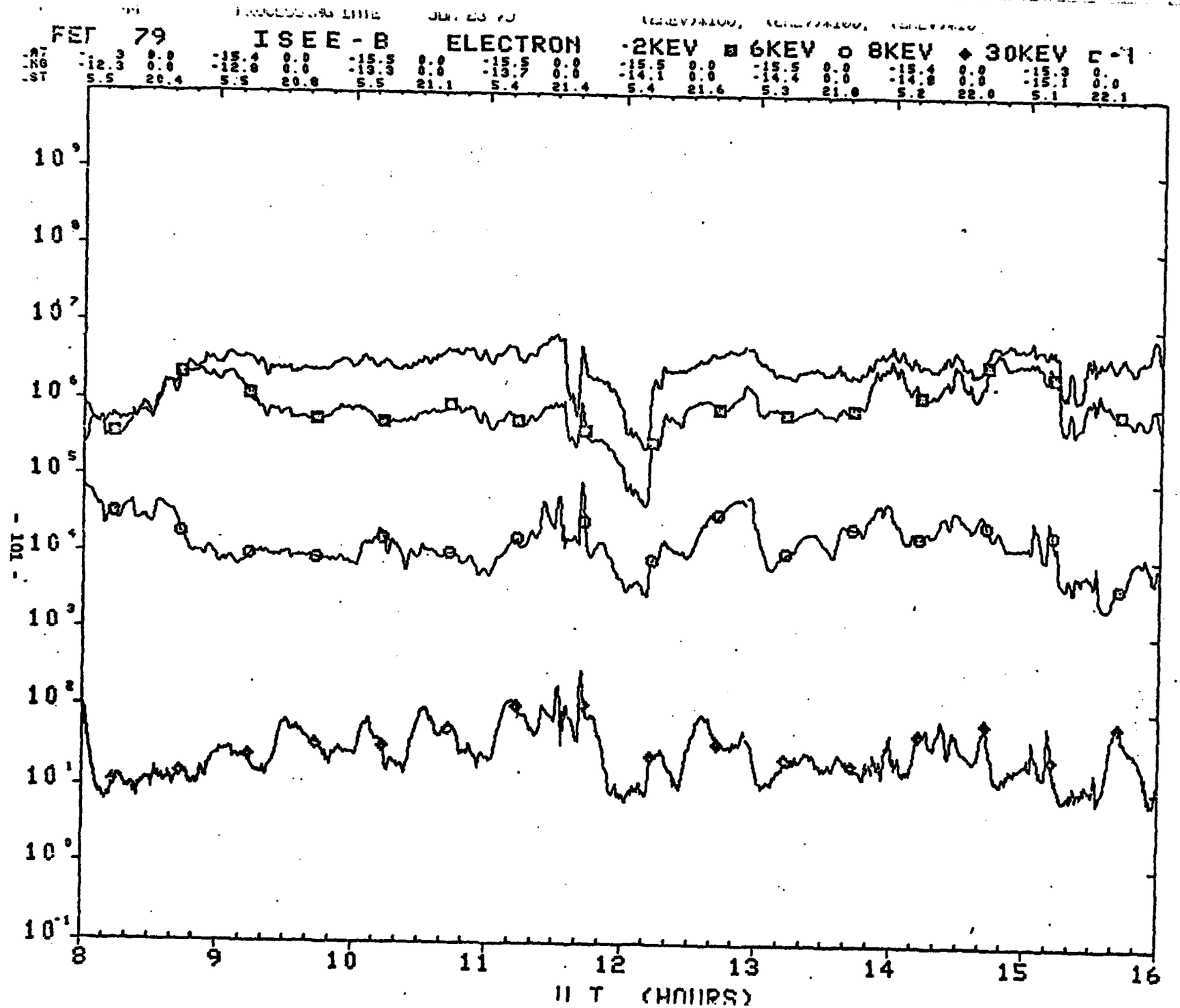
FEB 79
ISEE-B ELECTRON
2KEV 6KEV 8KEV 30KEV
10^9
10^8
10^7
10^6
10^5
10^4
10^3
10^2
10^1
10^0
10^-1
8
9
10
11
12
13
14
15
16
UT (HOURS)
- 101 -
Appendix 2
Quiet Day

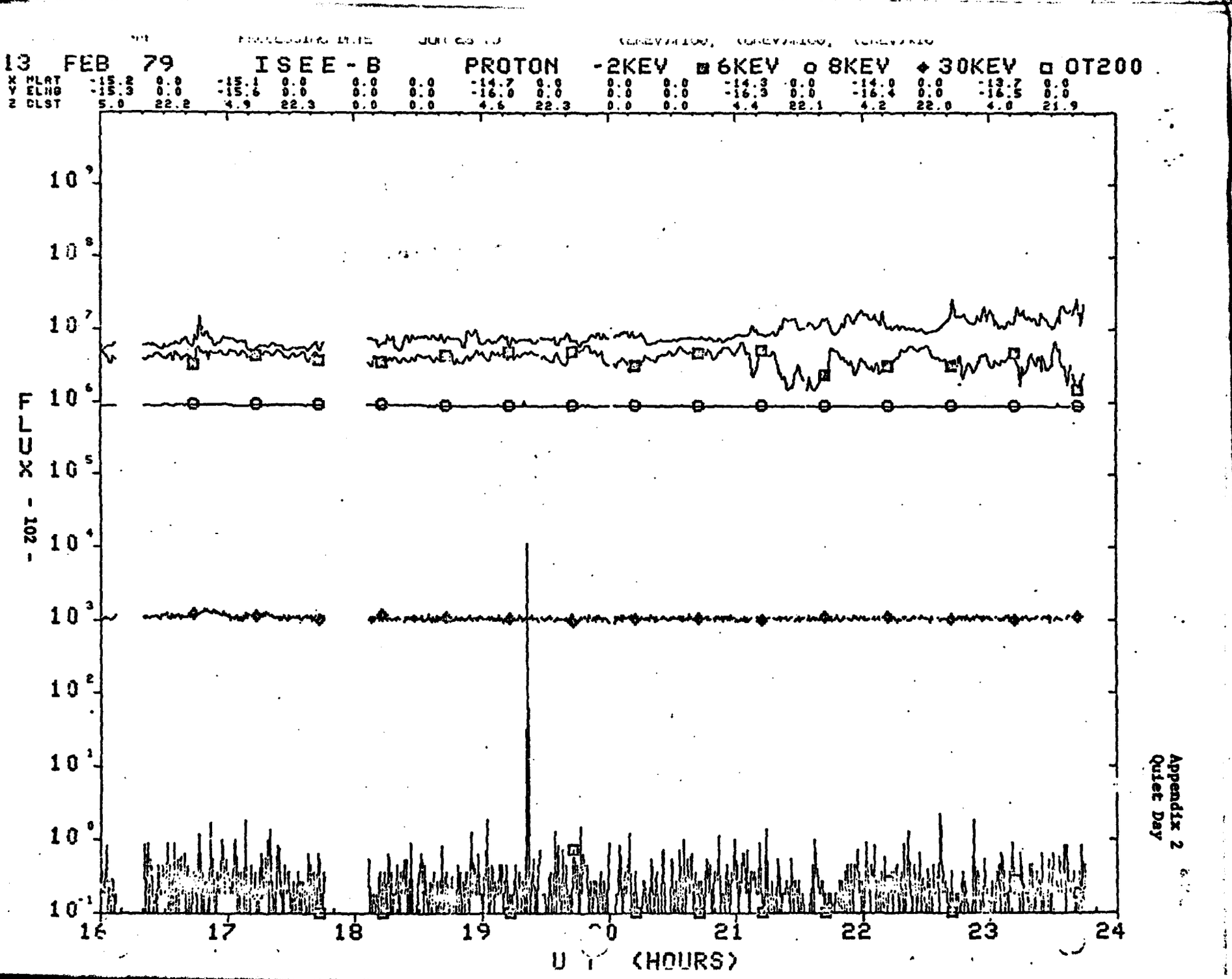
13 FEB 79 ISEE-B PROTON -2KEV 6KEV 8KEV 30KEV OT200
X MLAT -15.2 0.0 -15.1 0.0 0.0 0.0 -14.7 0.0 0.0 0.0 -14.3 0.0 -14.0 0.0 -13.7 0.0
Y ELNG -15.3 0.0 -15.6 0.0 0.0 0.0 -16.0 0.0 0.0 0.0 -16.3 0.0 -16.4 0.0 -16.5 0.0
Z GLST 5.0 22.2 4.9 22.3 0.0 0.0 4.6 22.3 0.0 0.0 4.4 22.1 4.2 22.0 4.0 21.9
FLUX - 102 -
16 17 18 19 20 21 22 23 24
U T (HOURS)
Appendix 2
Quiet Day

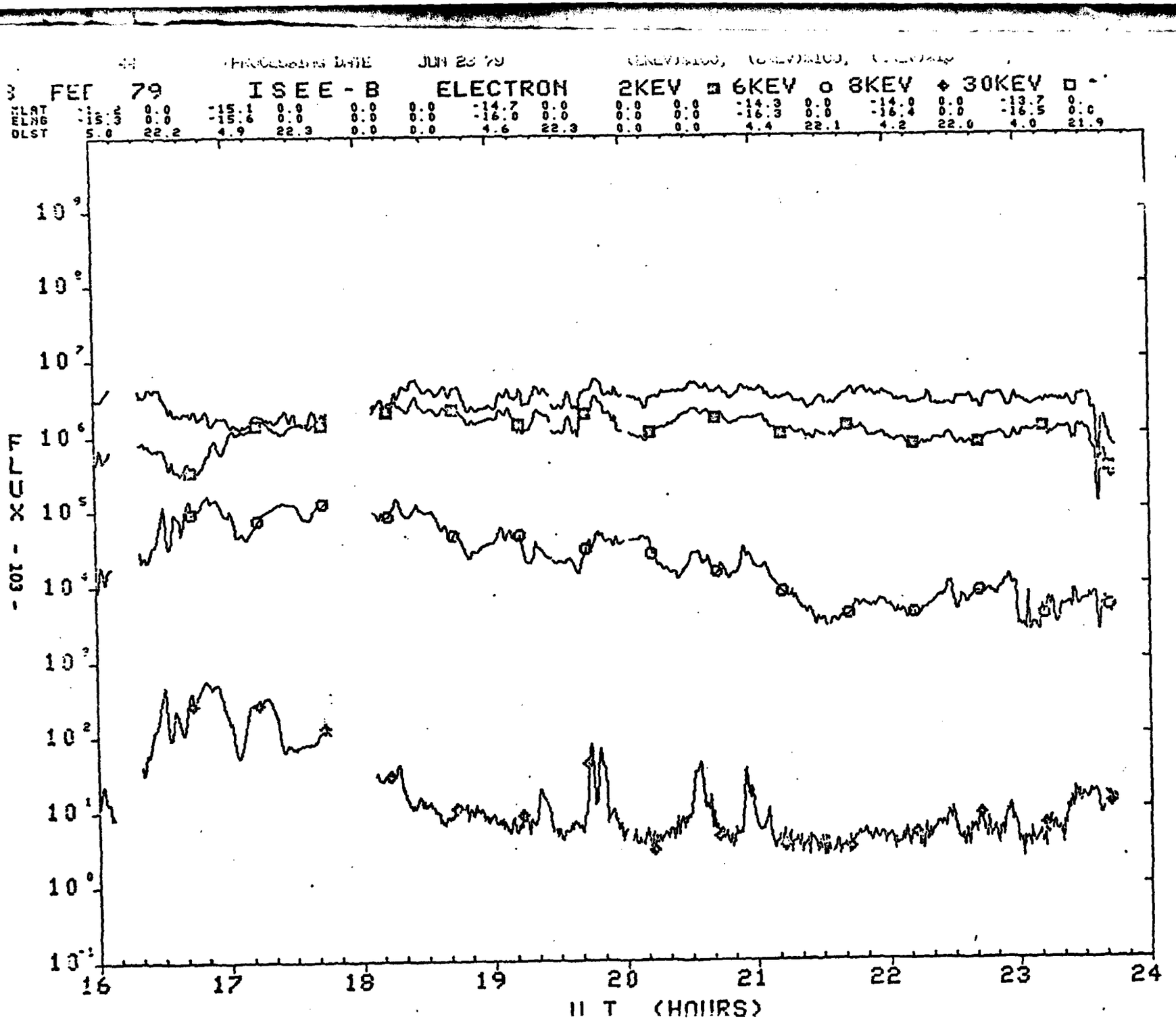

Appendix 2
Quiet Day

APPENDIX 2

Disturbed Day

February 22, 1979

$\Sigma Kp = 34$

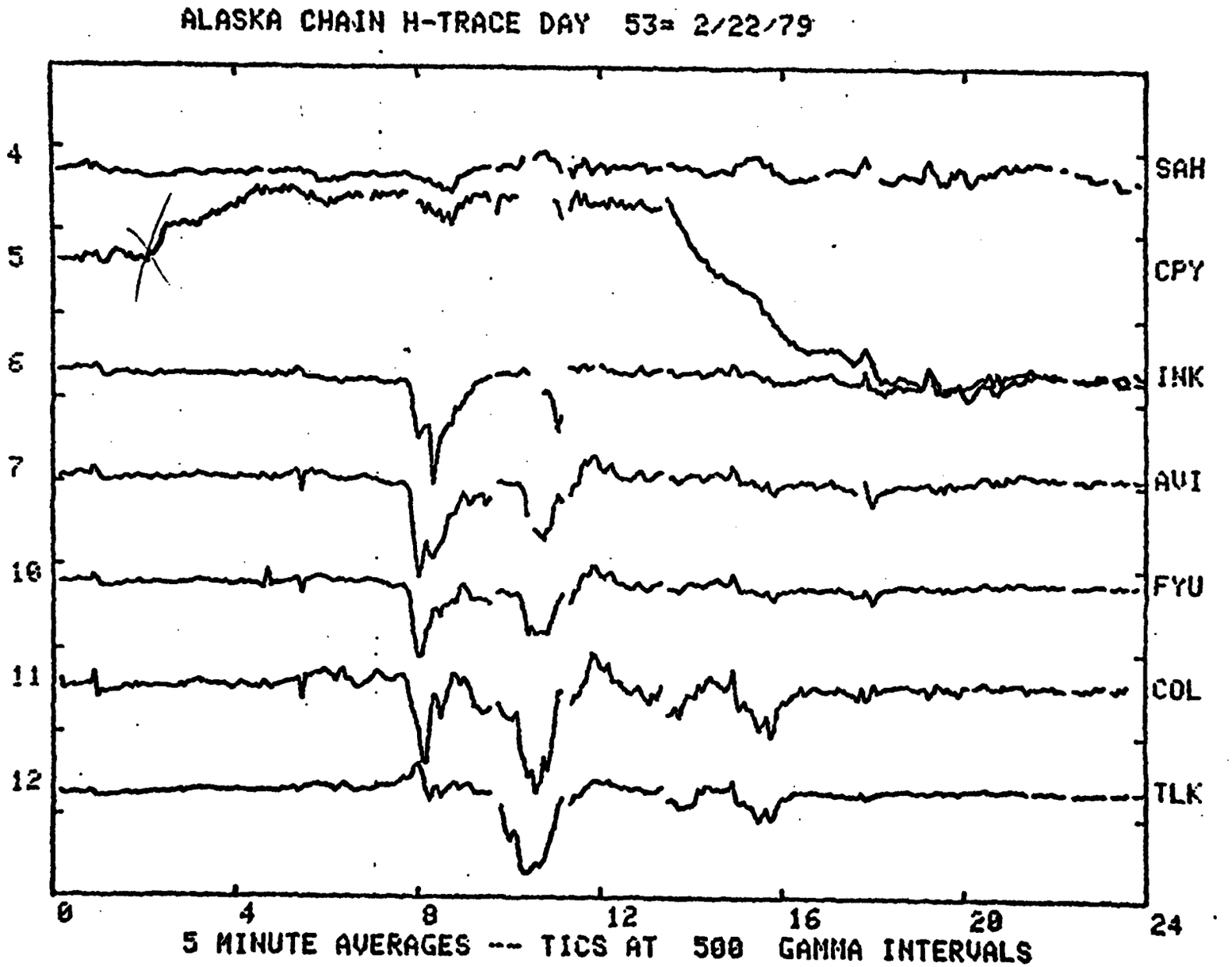

Appendix 2
Disturbed Day

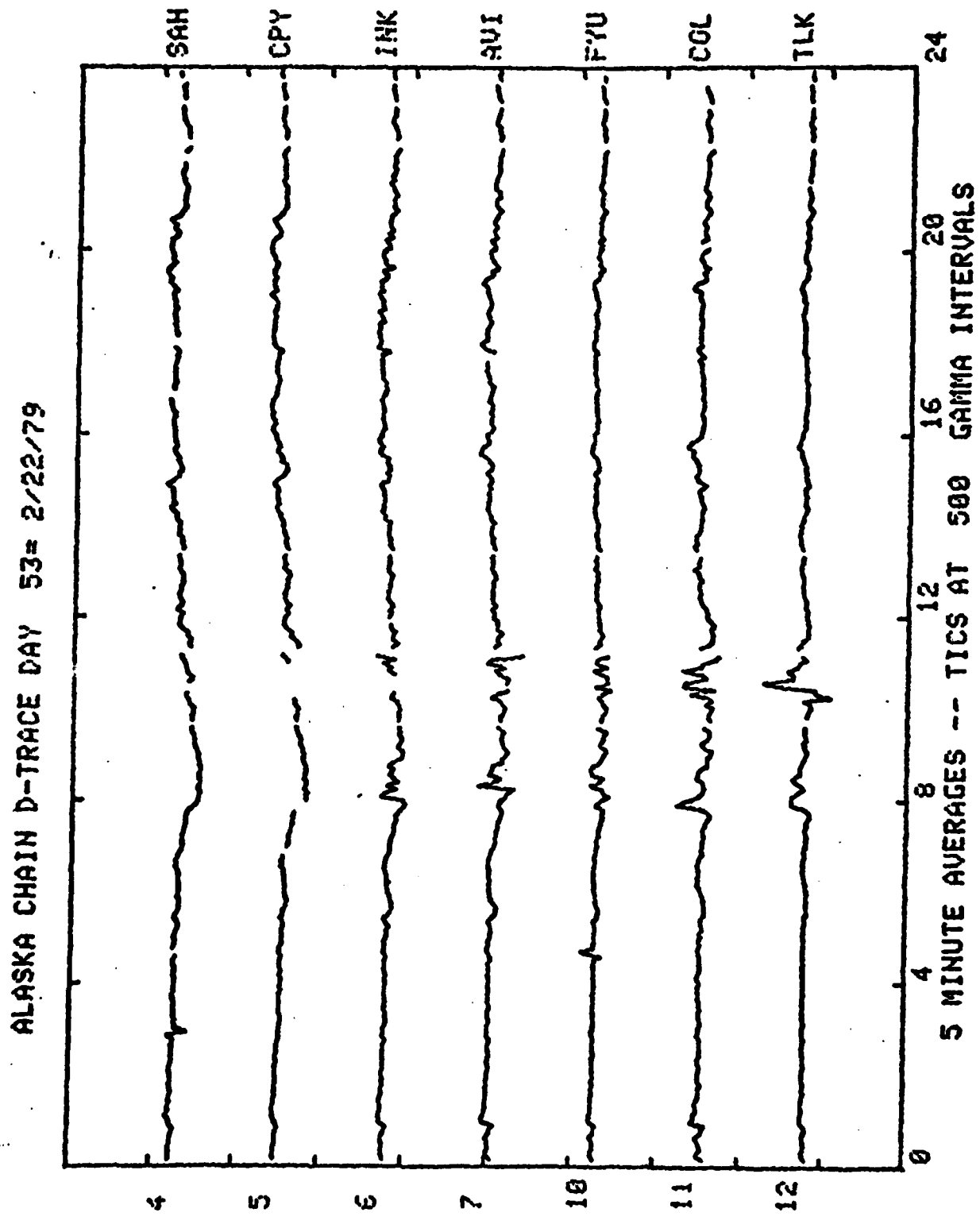
ALASKA CHAIN D-TRACE DAY 53= 2/22/79
SAH
CPY
INK
AVI
FYU
COL
TLK
4
5
6
7
10
11
12
0
4
8
12
16
20
24
5 MINUTE AVERAGES -- TICS AT 500 GAMMA INTERVALS

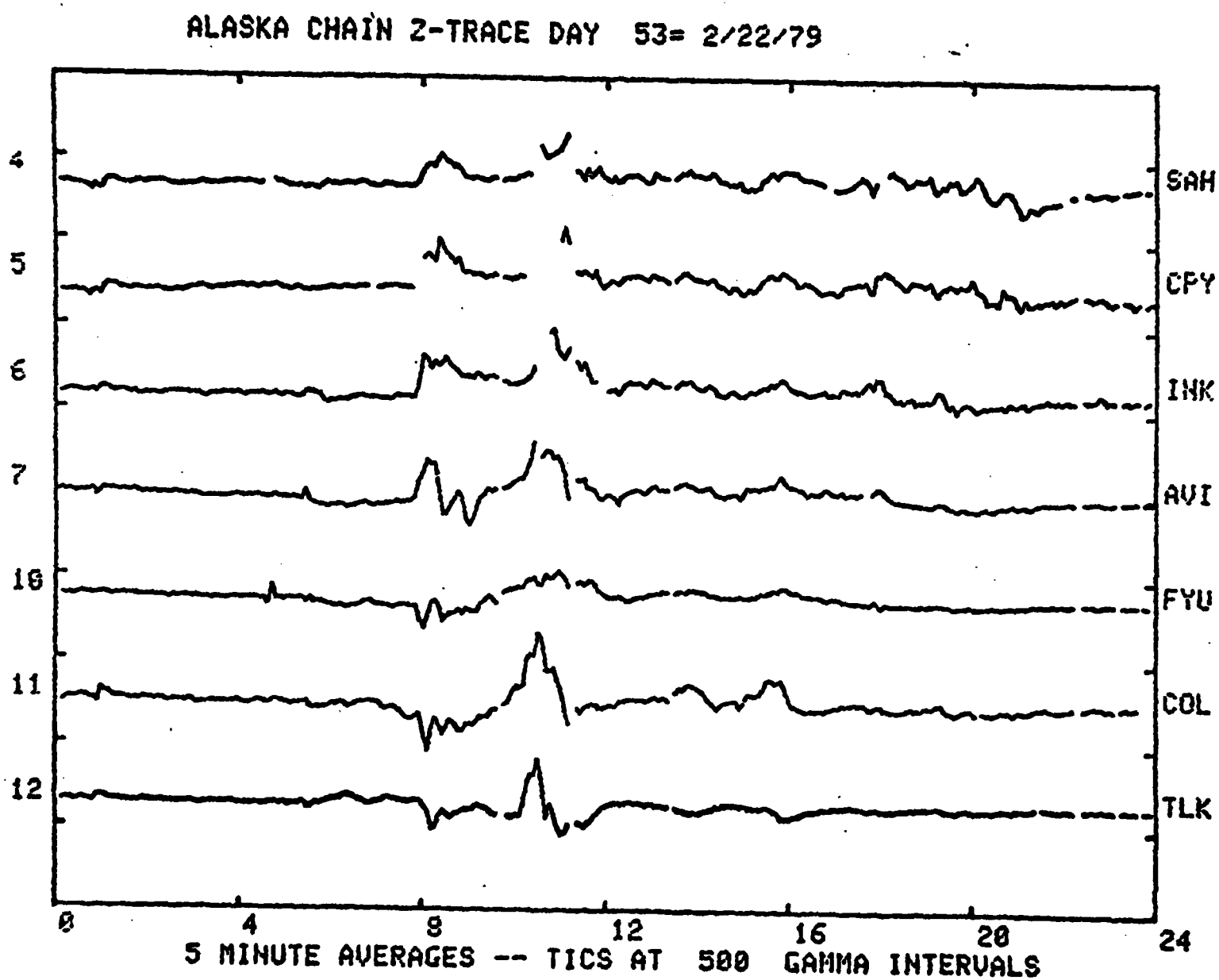
ALASKA CHAIN 2-TRACE DAY 53= 2/22/79
4
5
6
7
10
11
12
SAH
CPY
INK
AVI
FYU
COL
TLK
0
4
8
12
16
20
24
5 MINUTE AVERAGES -- TICS AT 500 GAMMA INTERVALS

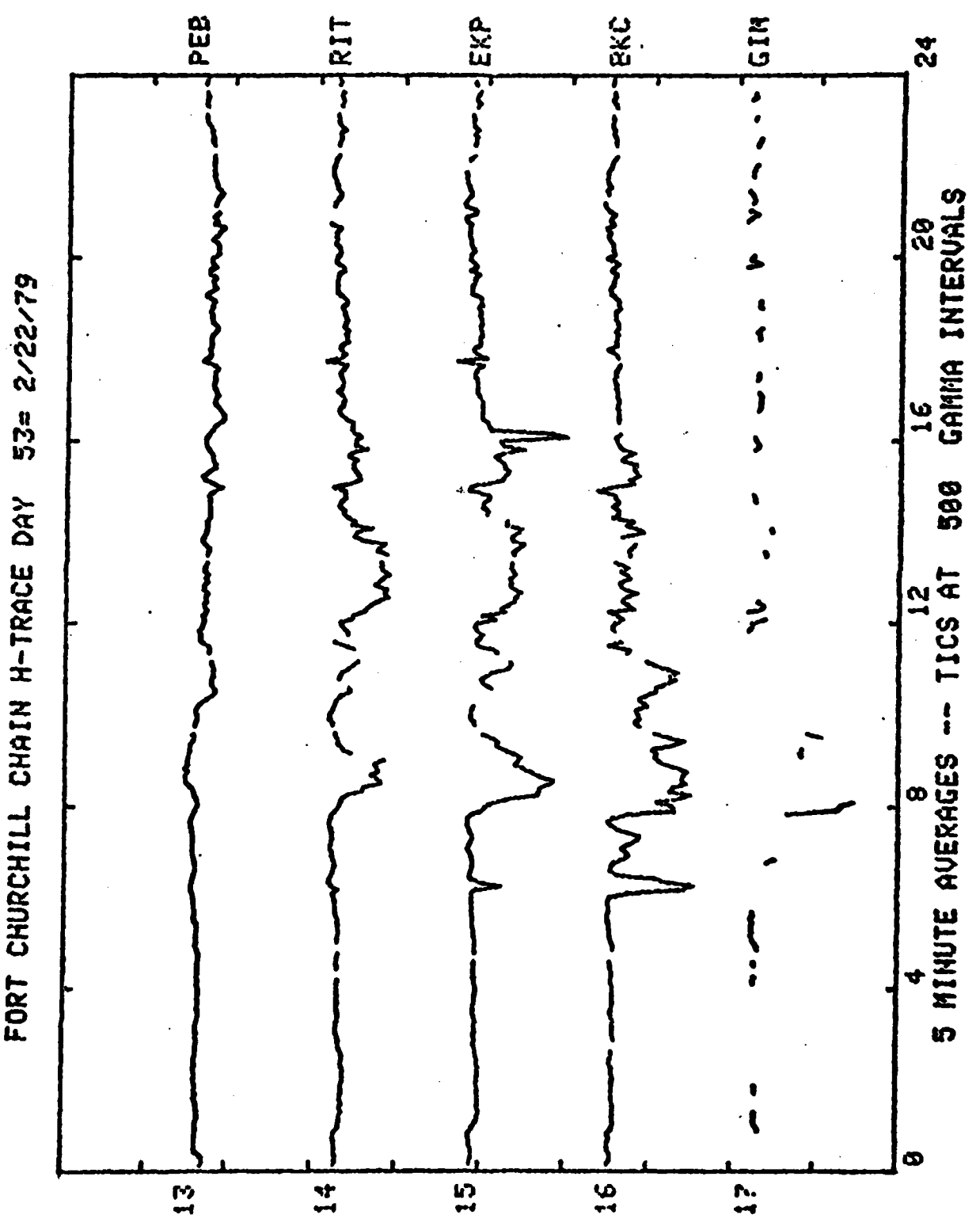
FORT CHURCHILL CHAIN H-TRACE DAY 53= 2/22/79
PEB
RIT
EKP
BKC
GIM
13
14
15
16
17
0
4
8
12
16
20
24
5 MINUTE AVERAGES -- TICS AT 500 GAMMA INTERVALS

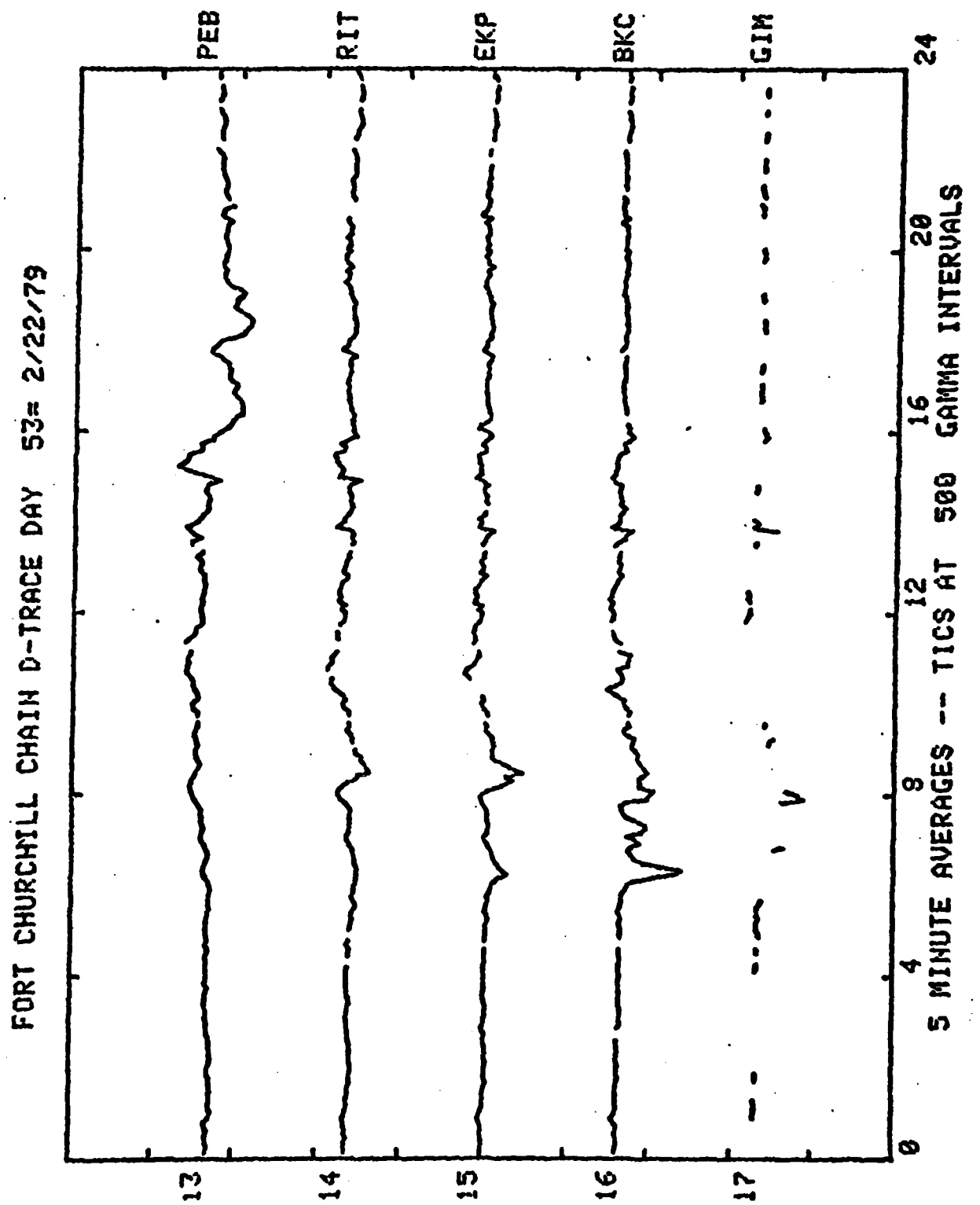
FORT CHURCHILL CHAIN D-TRACE DAY 53= 2/22/79
PEB
RIT
EKP
BKC
GIM
13
14
15
16
17
0
4
8
12
16
20
24
5 MINUTE AVERAGES -- TICS AT 500 GAMMA INTERVALS

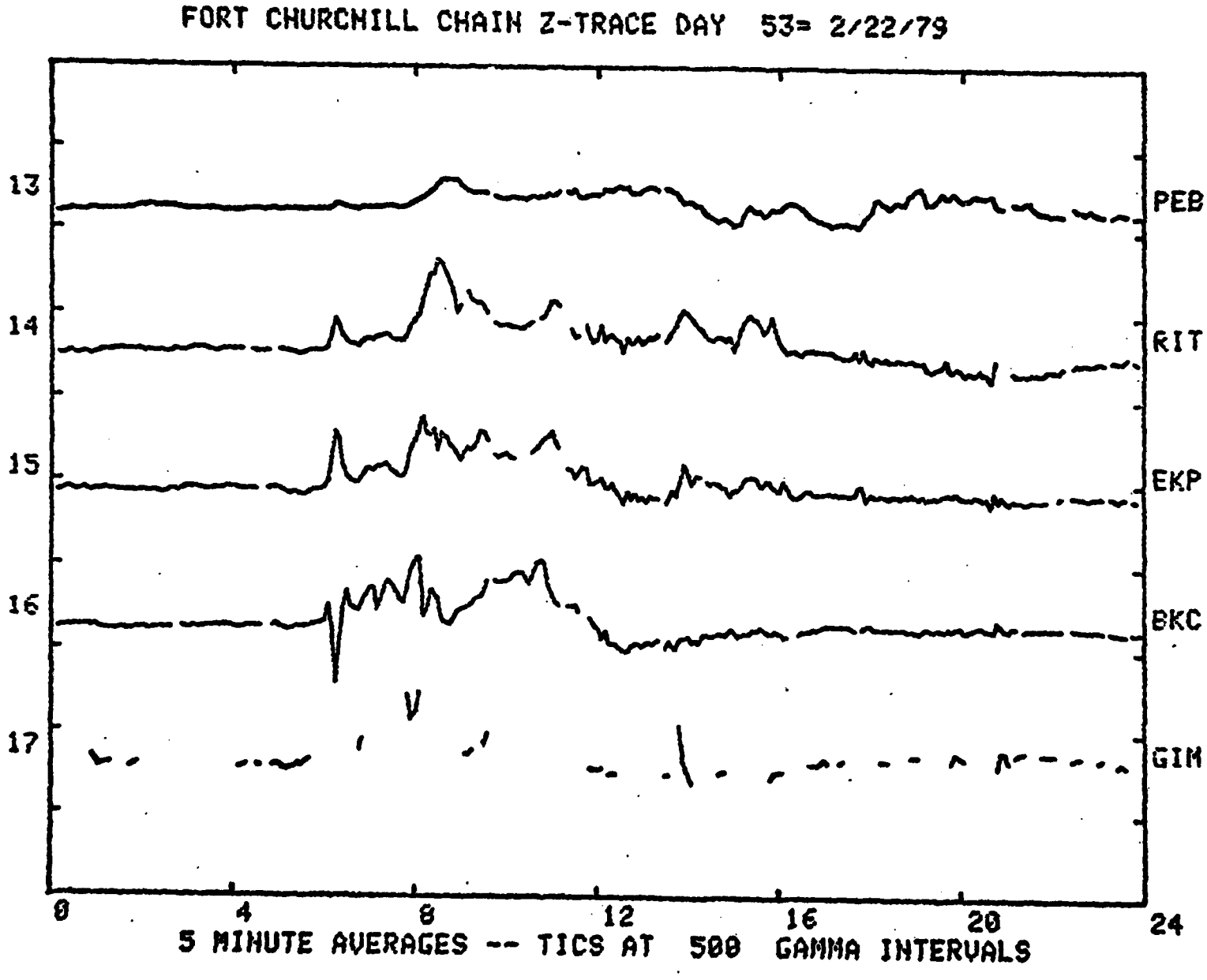

Disturbed Day

Appendix 2
Disturbed Day

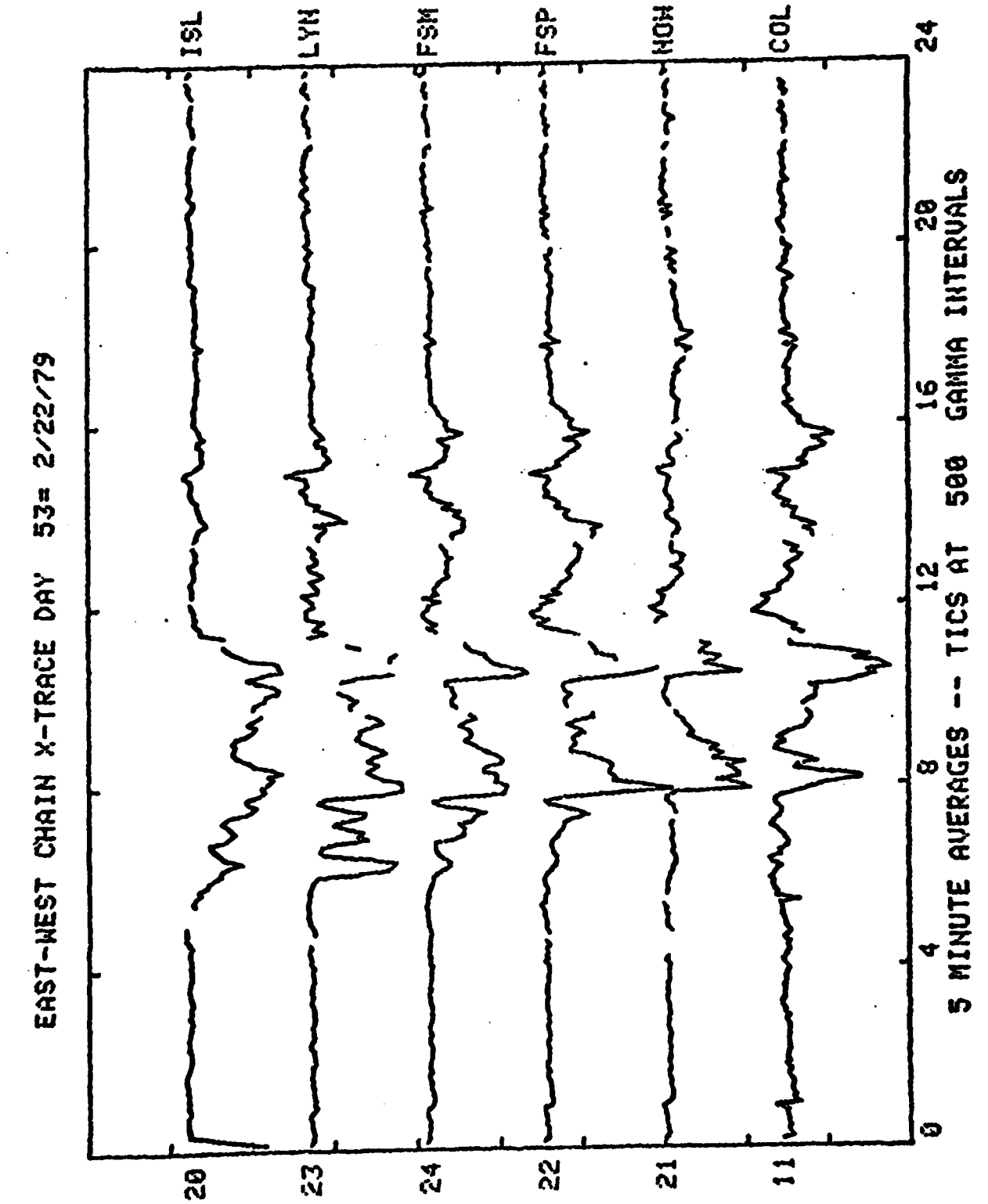

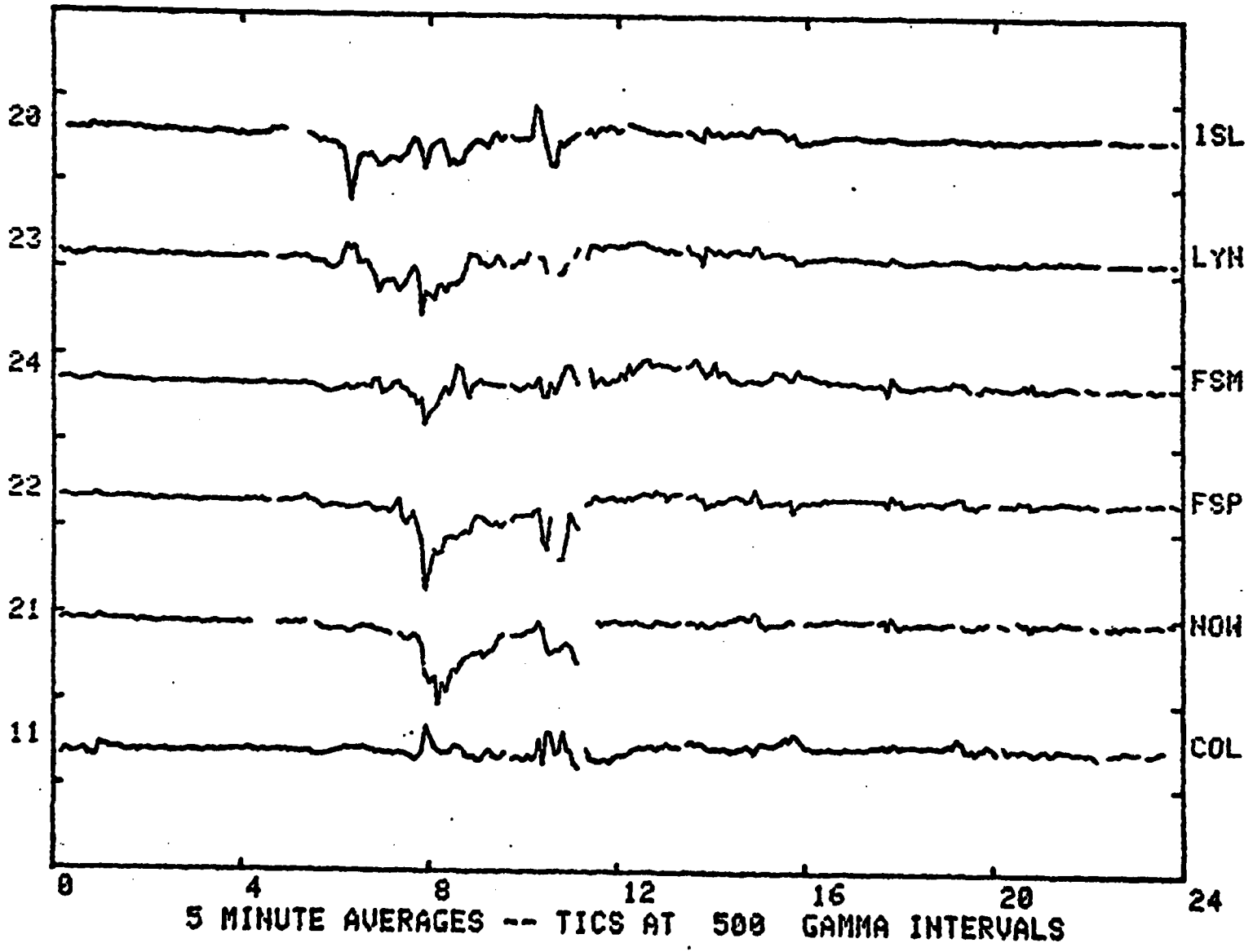

Appendix 2
Disturbed Day

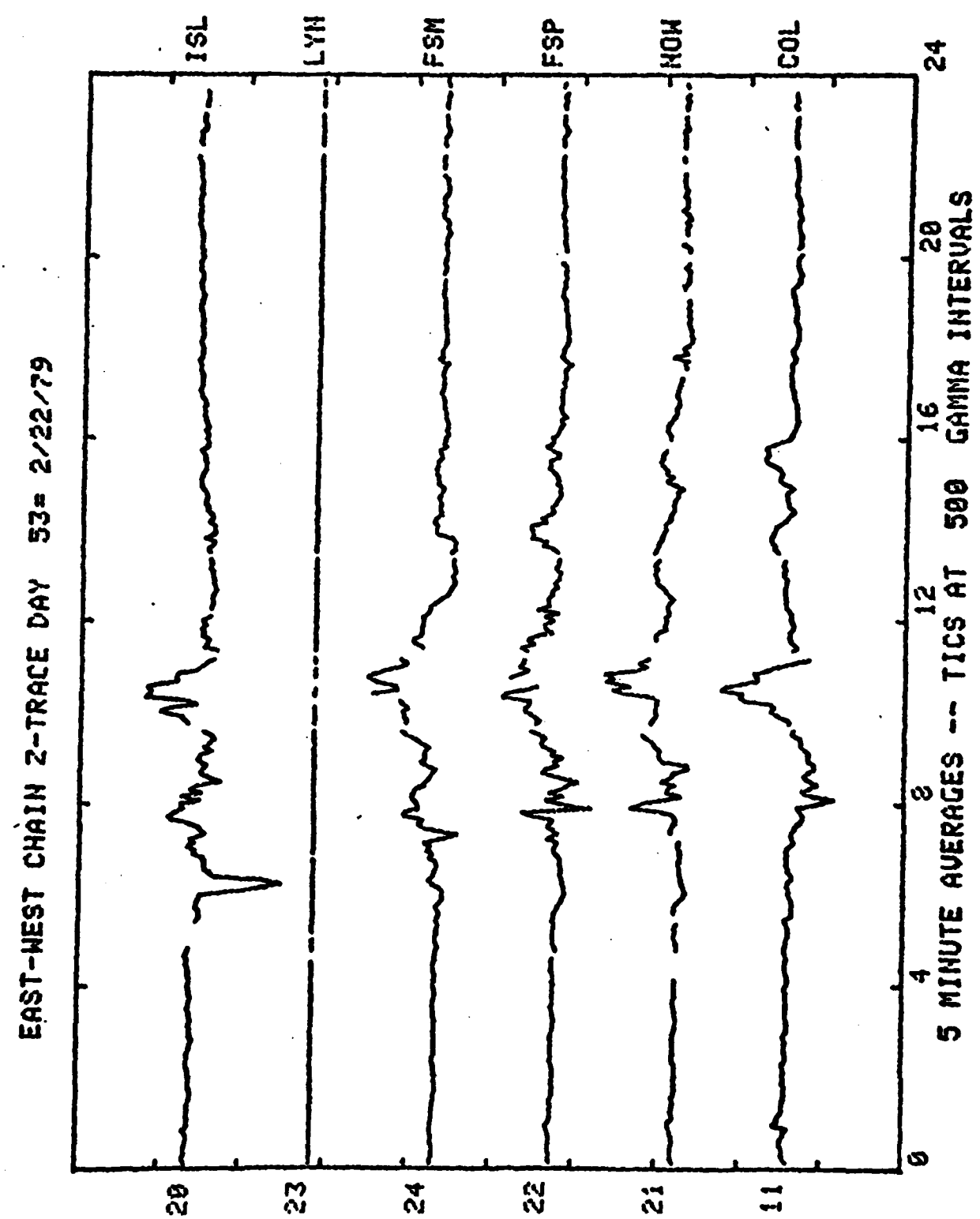
EAST-WEST CHAIN 2-TRACE DAY 53= 2/22/79
ISL
LYH
FSM
FSP
HOW
COL
0
4
8
12
16
20
24
5 MINUTE AVERAGES -- TICS AT 500 GAMMA INTERVALS
20
23
24
22
21
11

Appendix 2
Disturbed Day

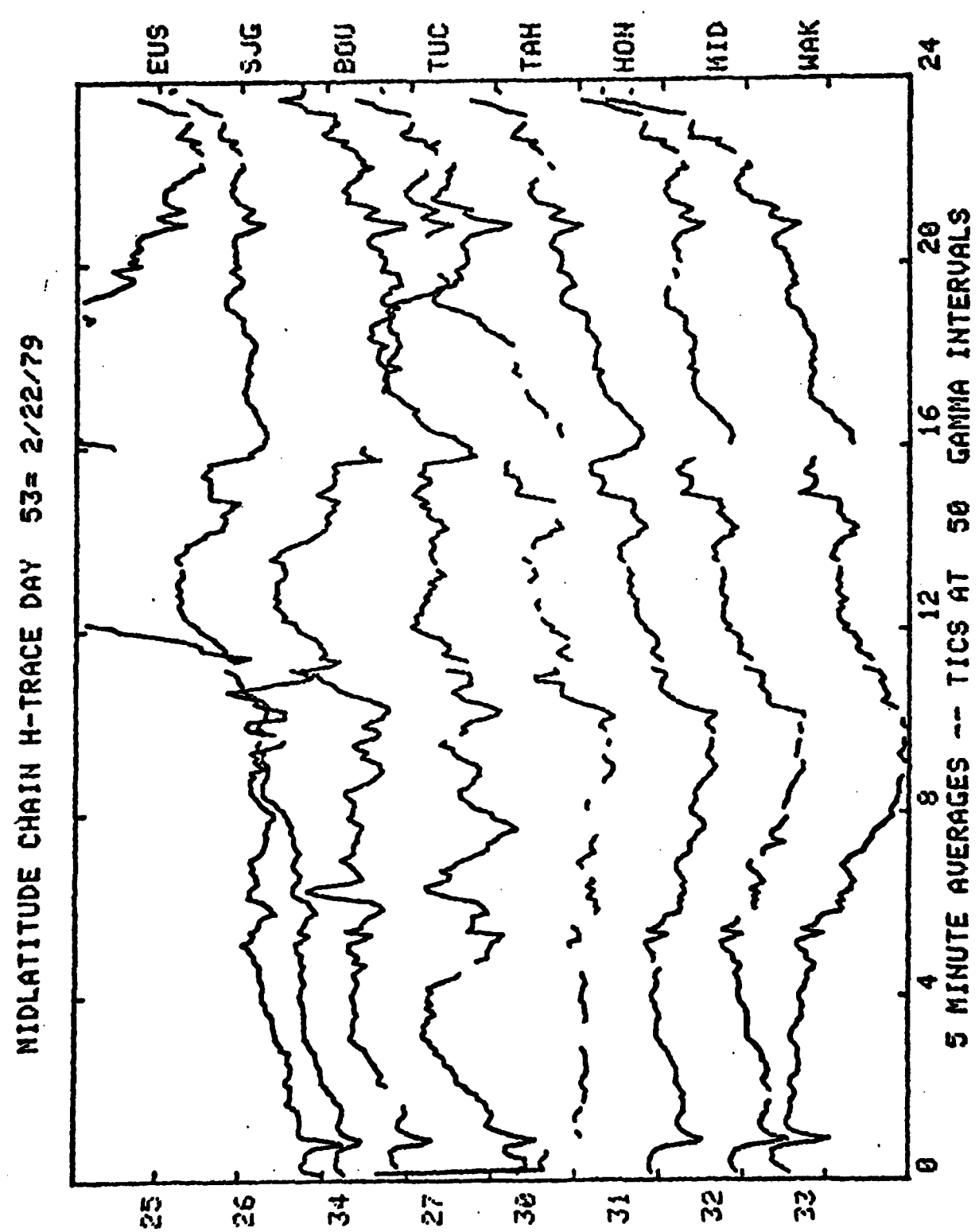

Appendix 2
Disturbed Day

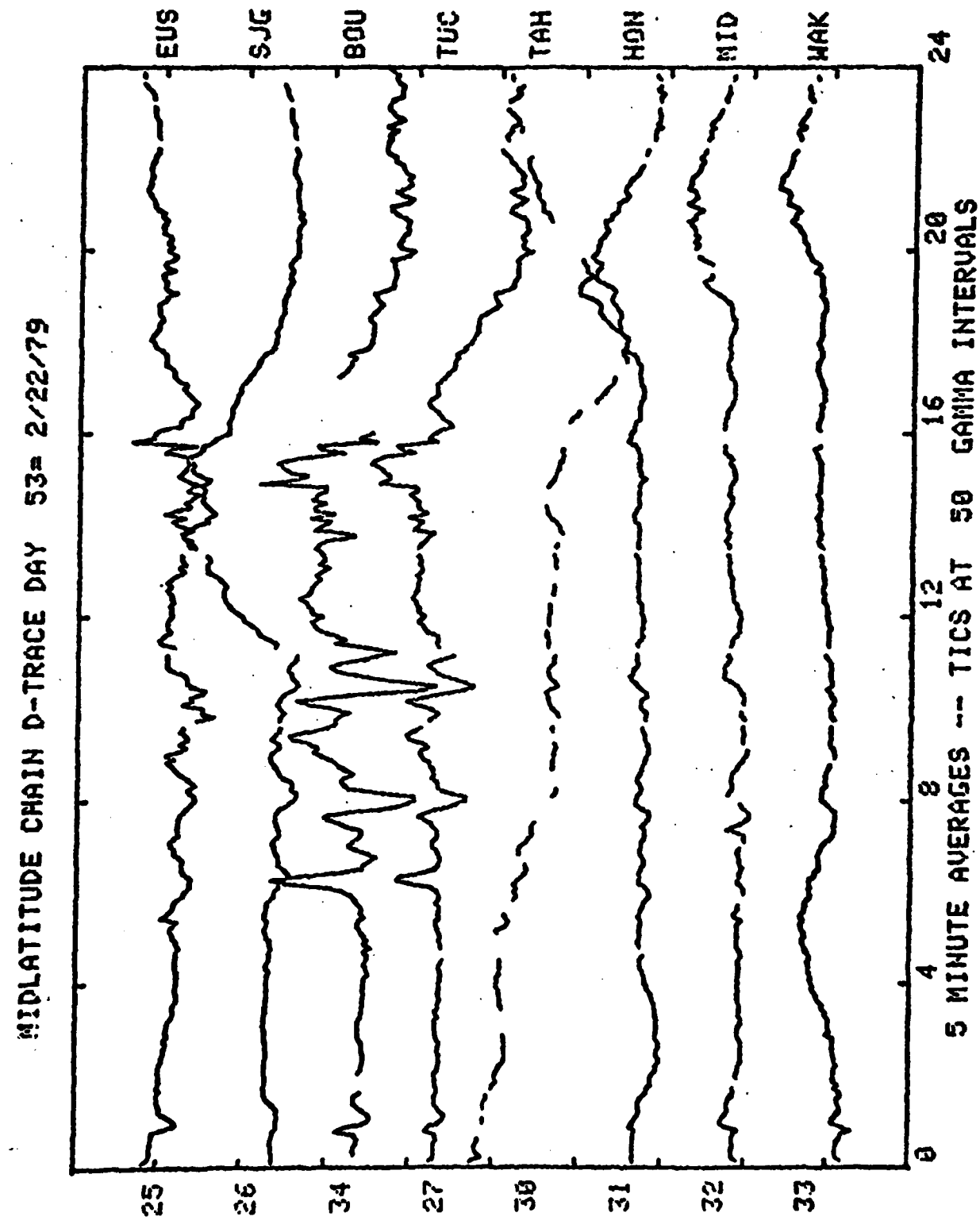

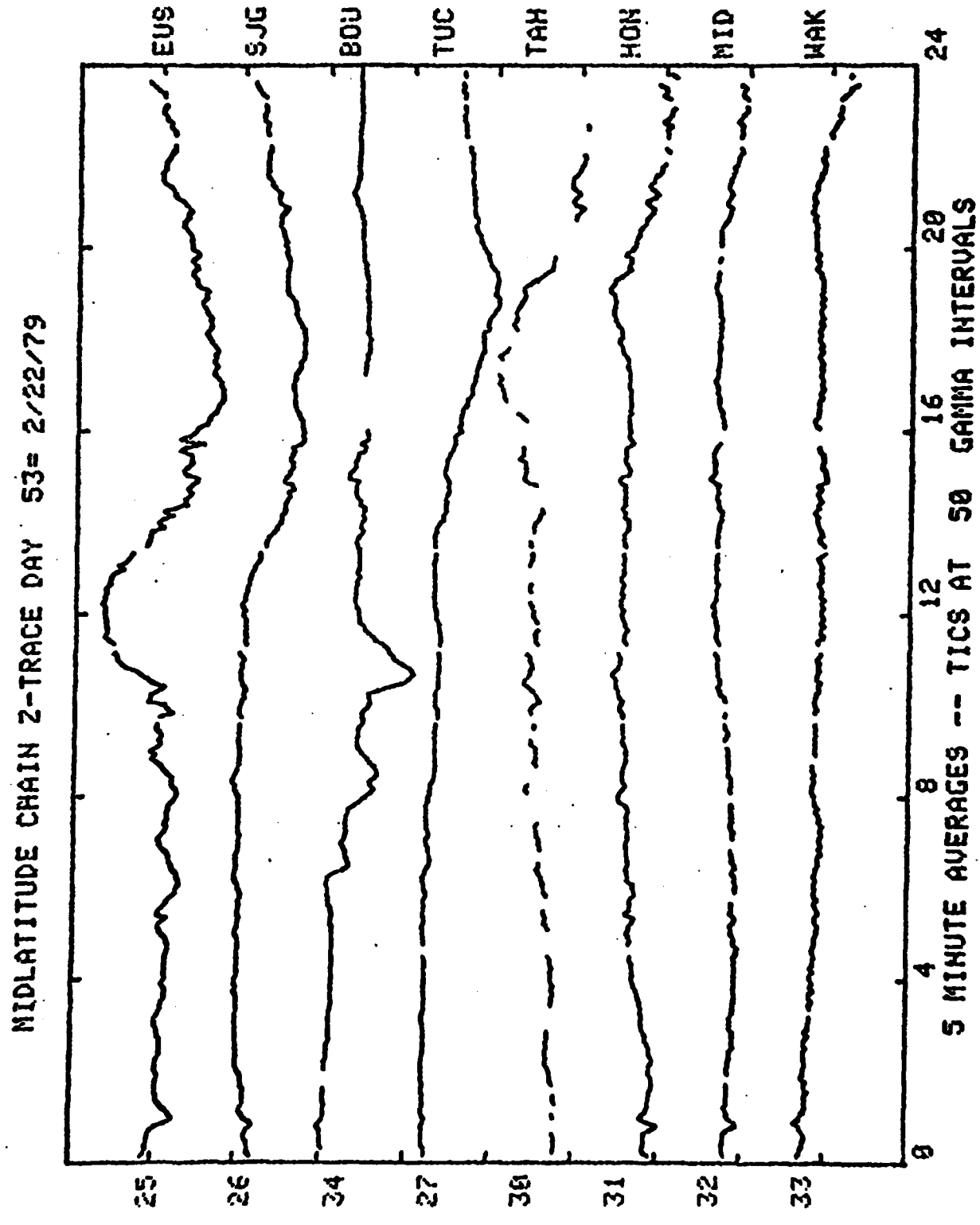
MIDLATITUDE CHAIN 2-TRACE DAY 53= 2/22/79
EUS
SJG
BOU
TUC
TAH
HON
MID
WAK
0
4
8
12
16
20
24
5 MINUTE AVERAGES -- TICS AT 50 GAMMA INTERVALS
25
26
34
27
30
31
32
33

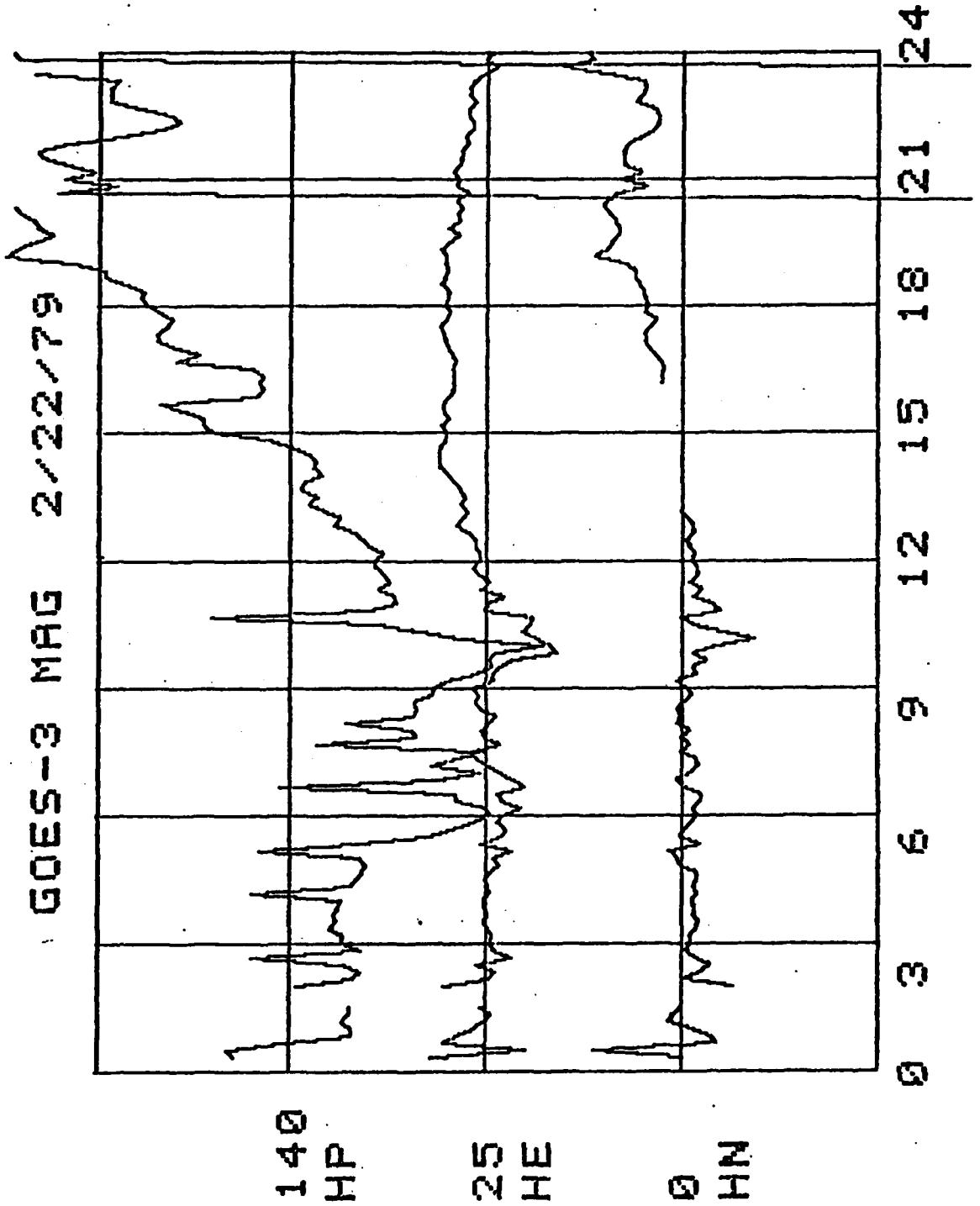
GOES-3 MAG 2/22/79
0 3 6 9 12 15 18 21 24
140 HP
25 HE
0 HN

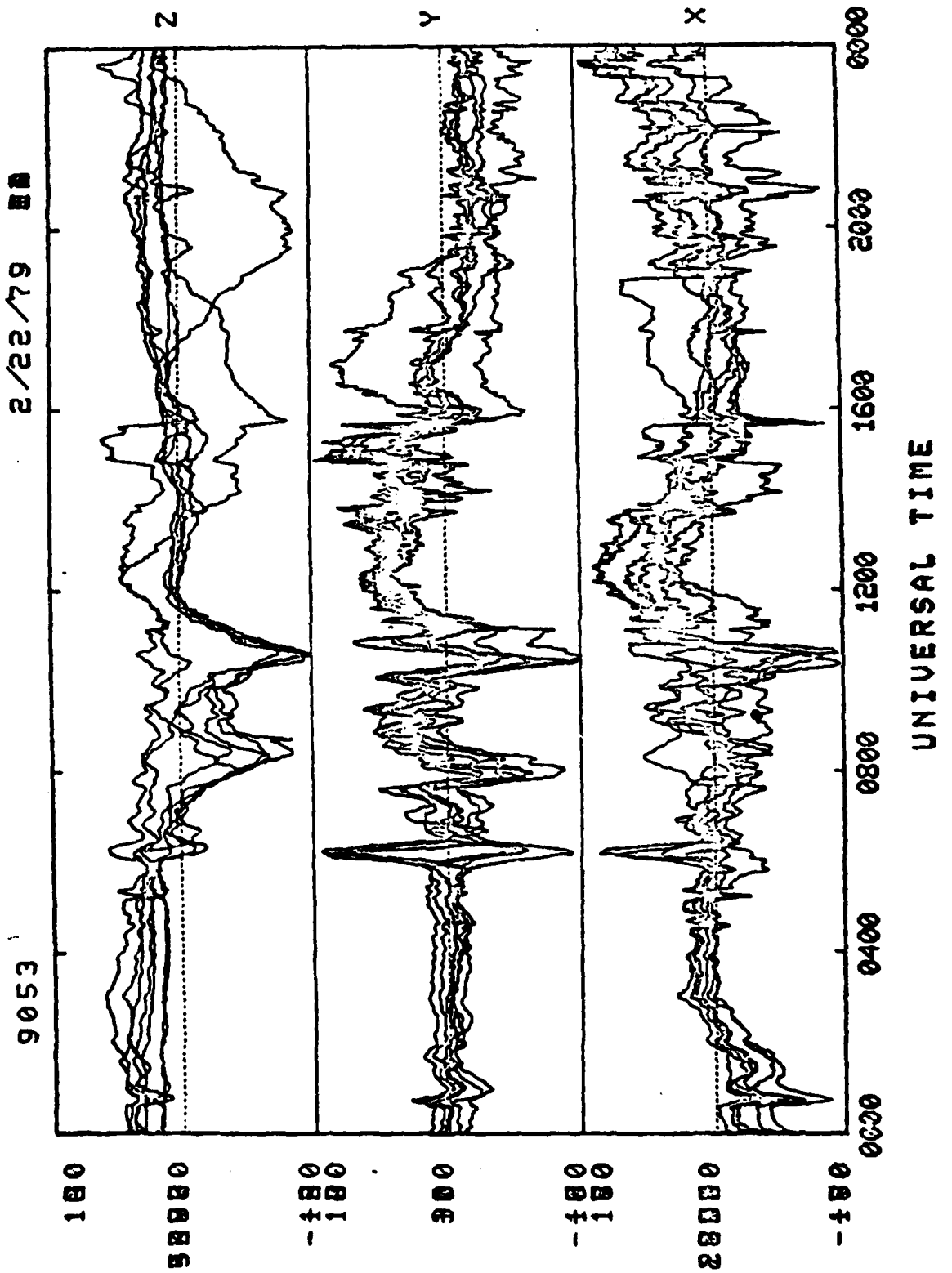
Z
Y
X
2/22/79
9053
UNIVERSAL TIME
0000
0400
0800
1200
1600
2000
0000
100
50000
-100
0
100
-100
0
100
-100
0

Appendix 2
Disturbed Day

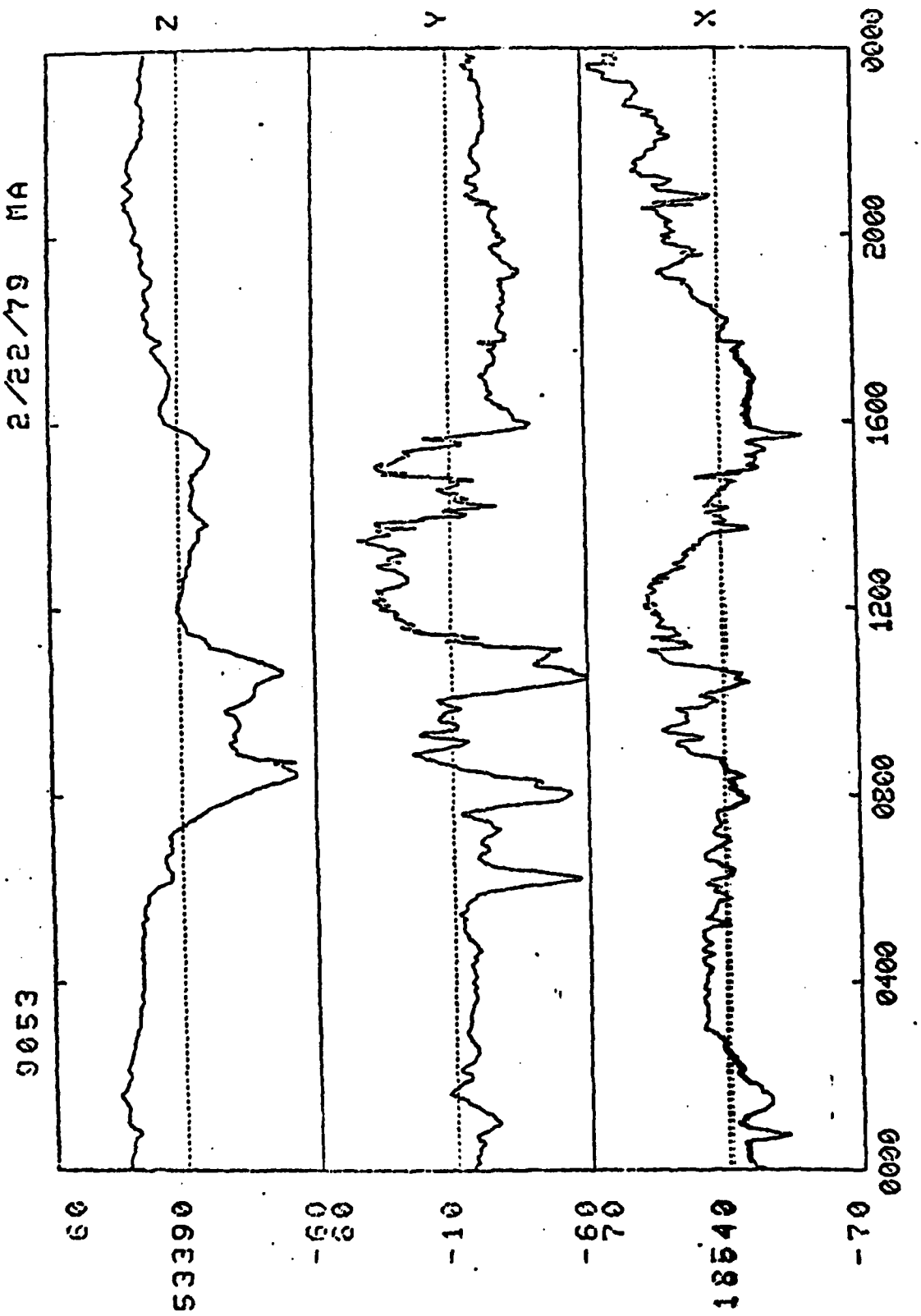

Appendix 2
Disturbed Day

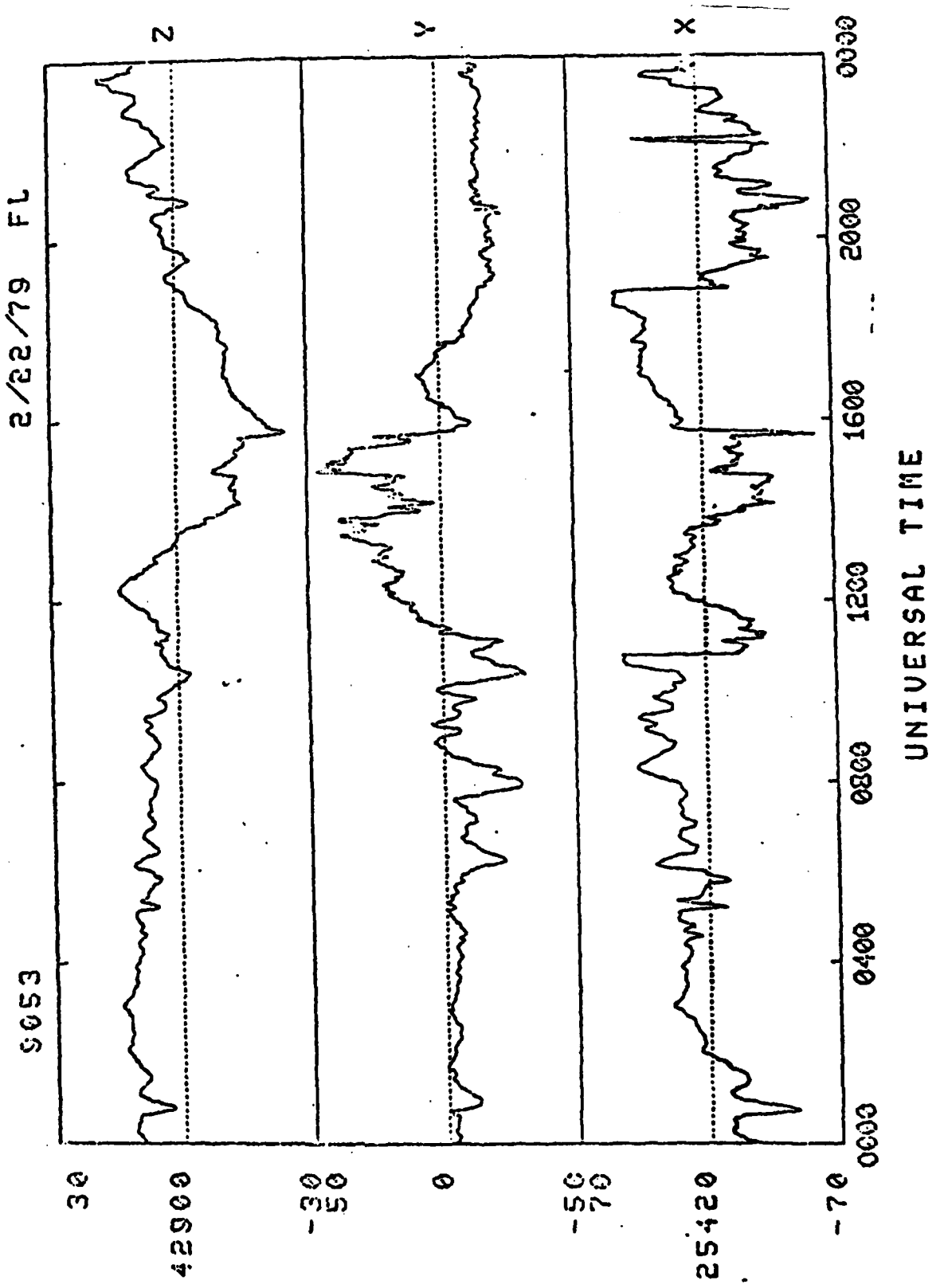

Appendix 2
Disturbed Day

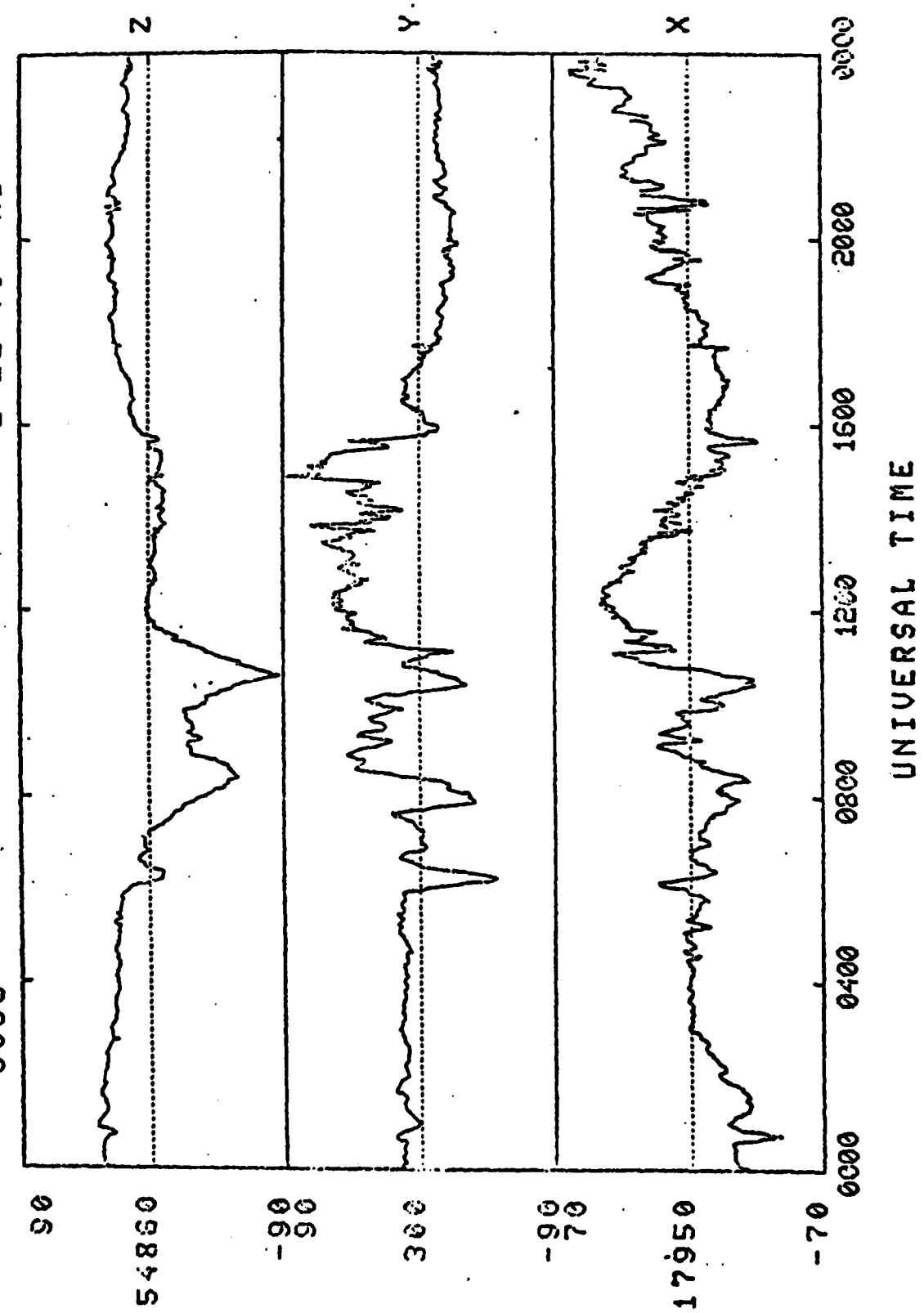

Appendix 2
Disturbed Day

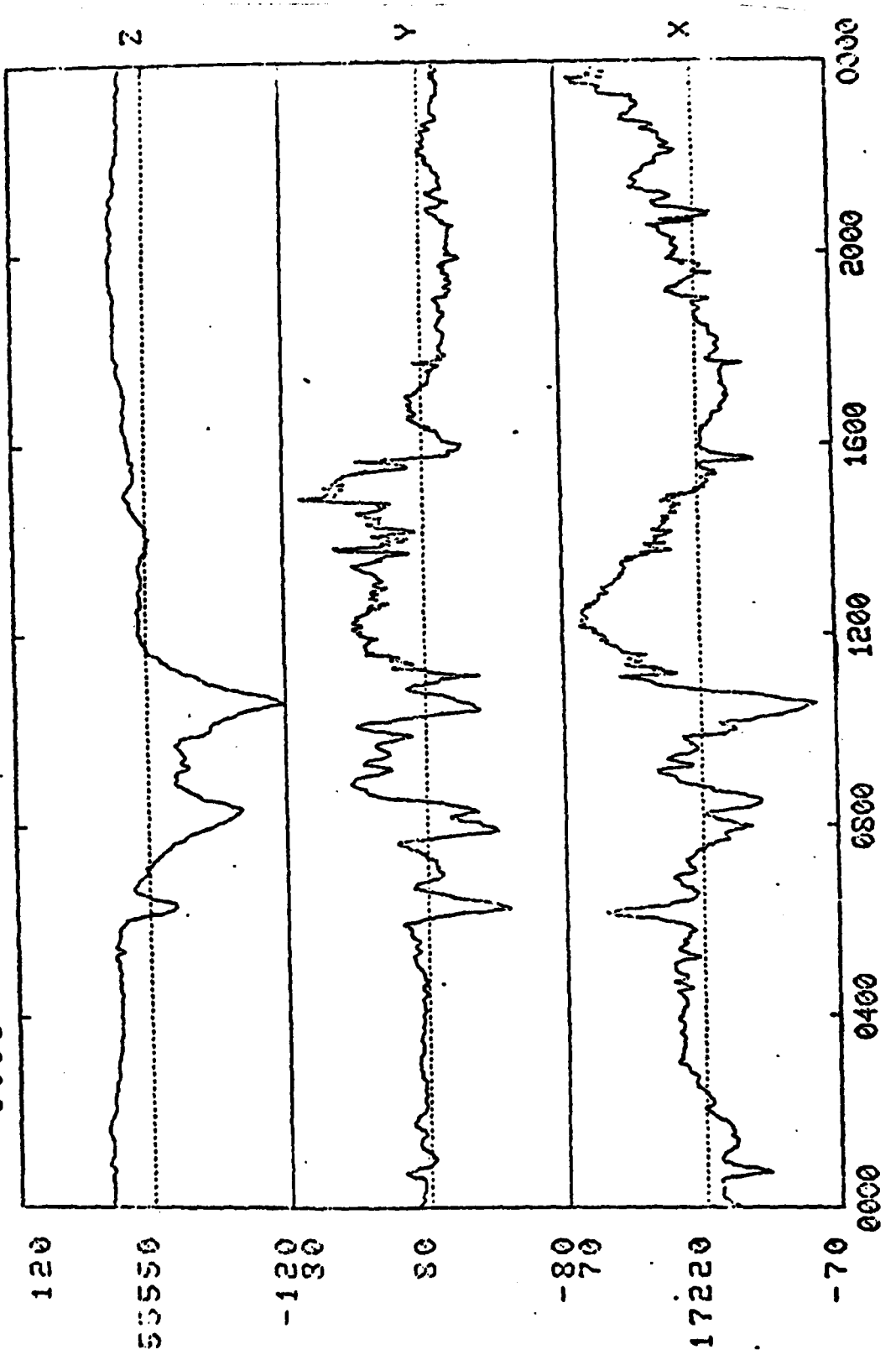

Appendix 2
Disturbed Day

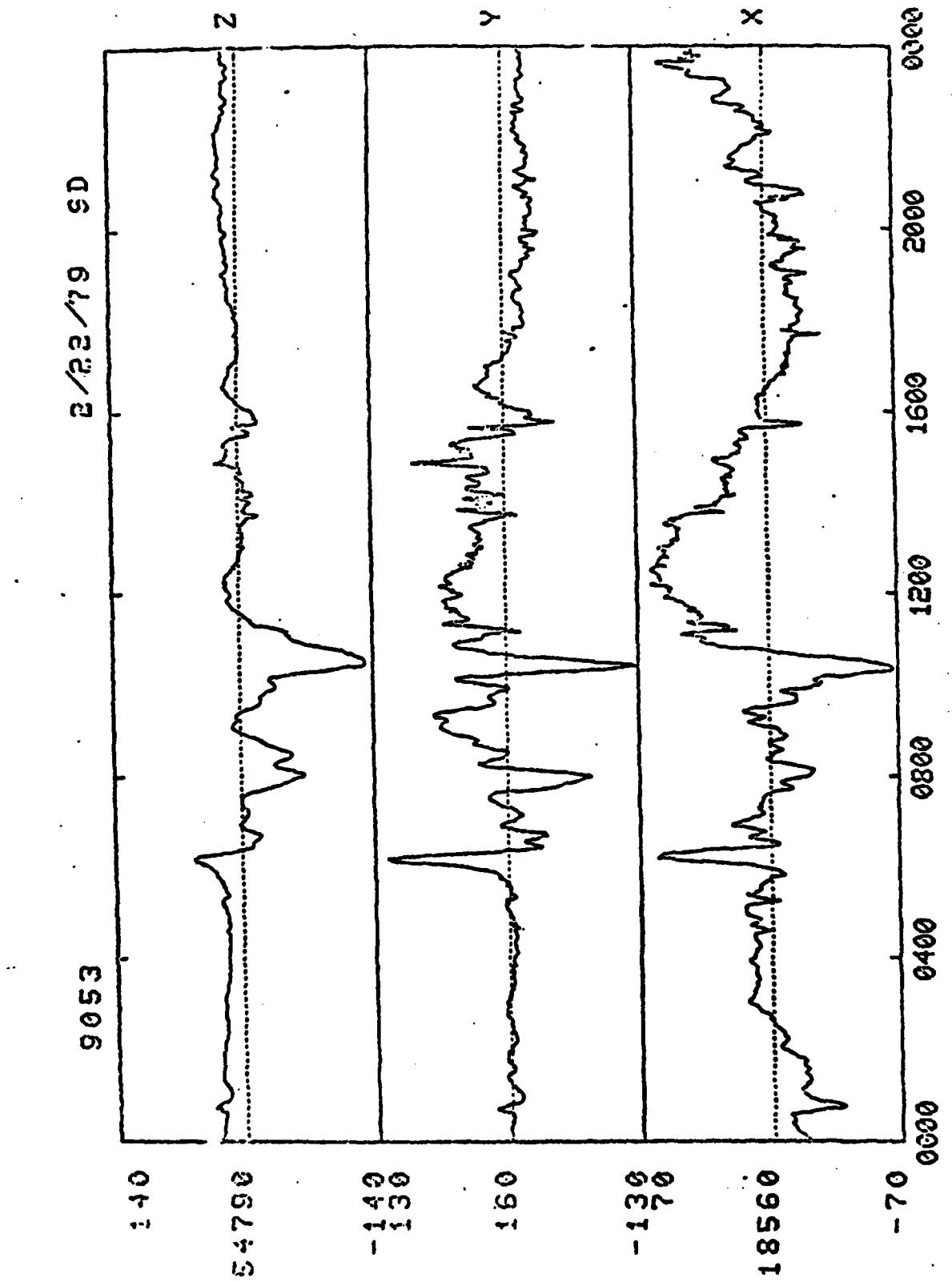

Appendix 2
Disturbed Day

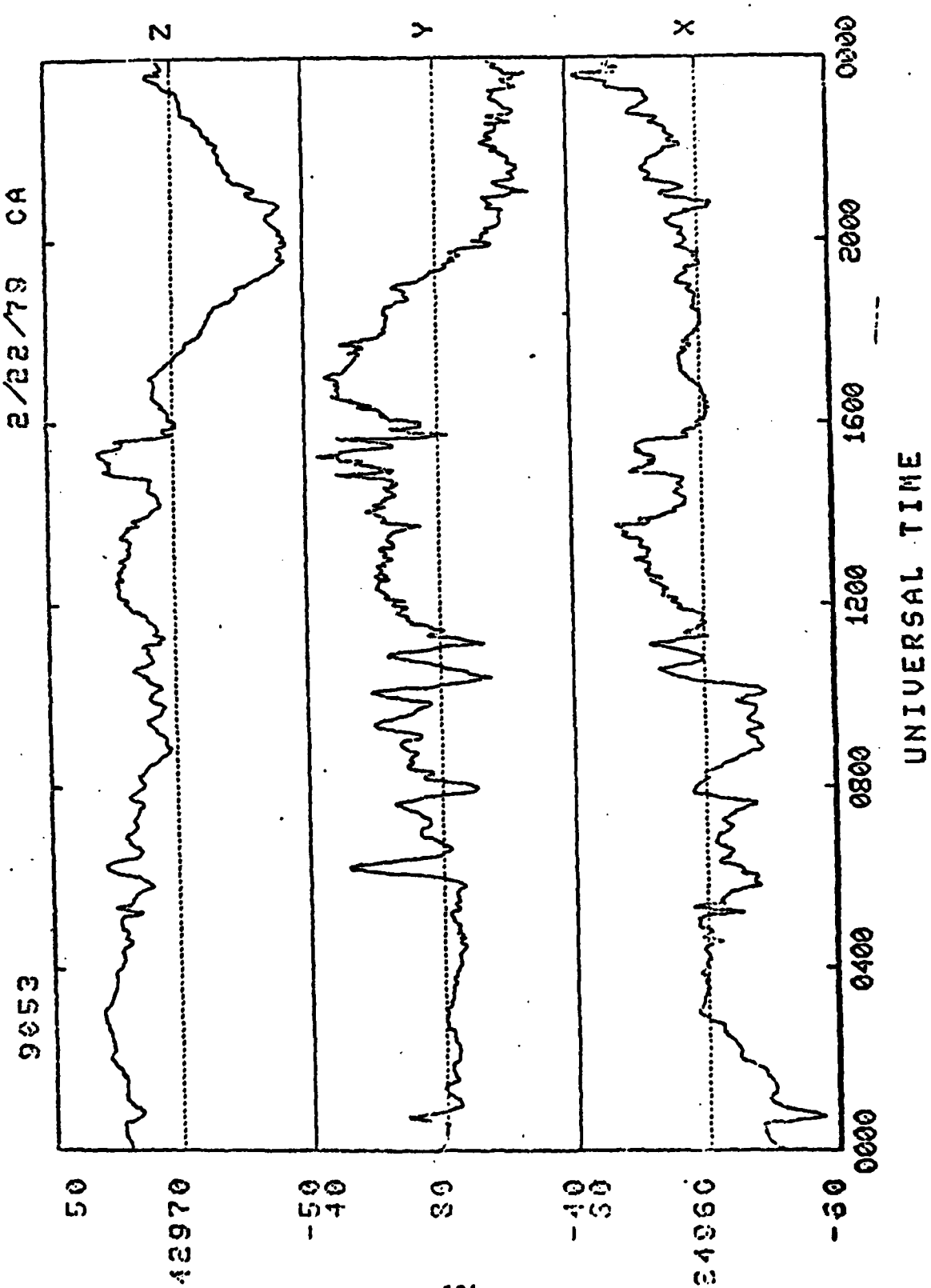

Appendix 2
Disturbed Day

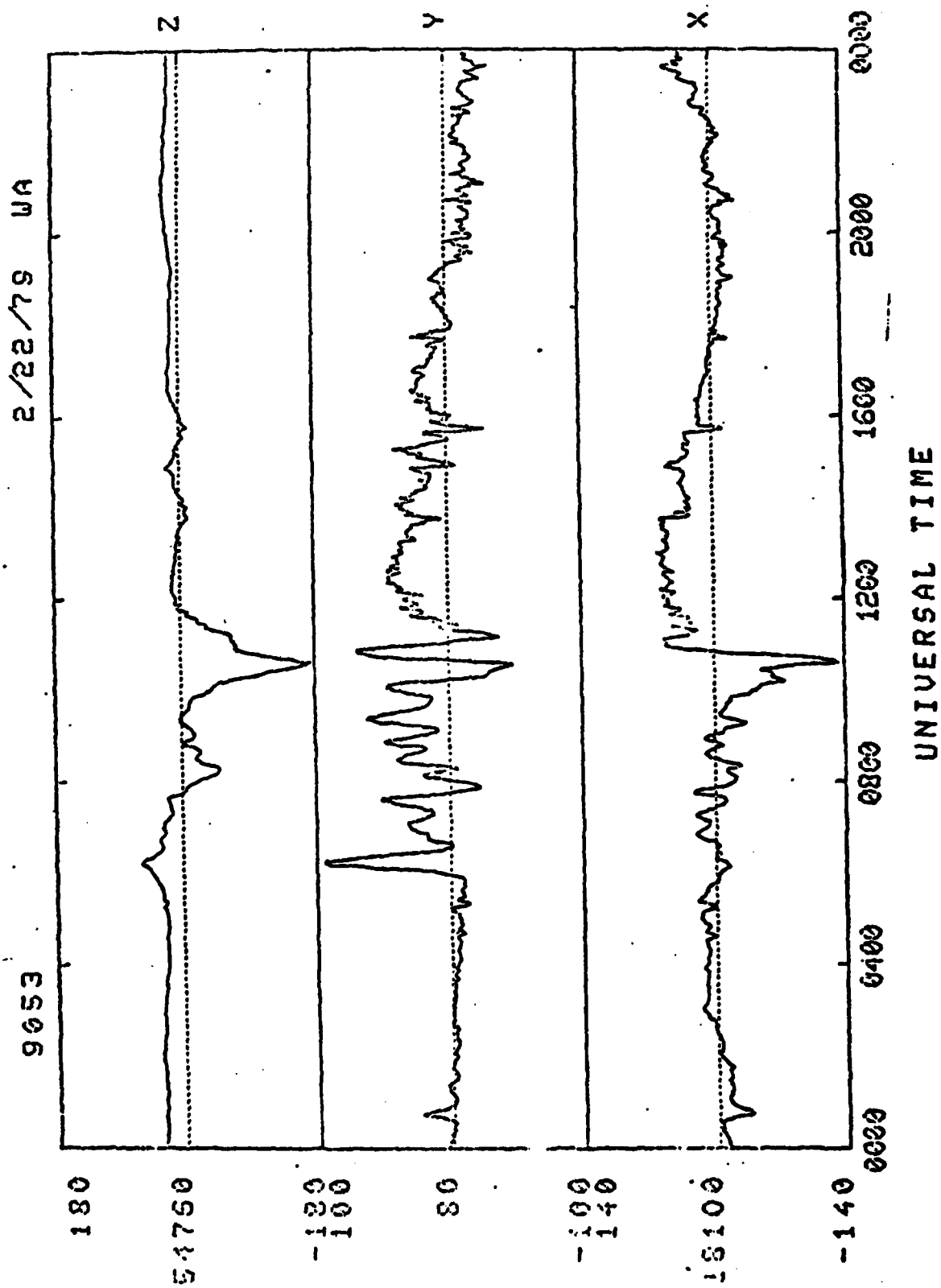

Appendix 2
Disturbed Day

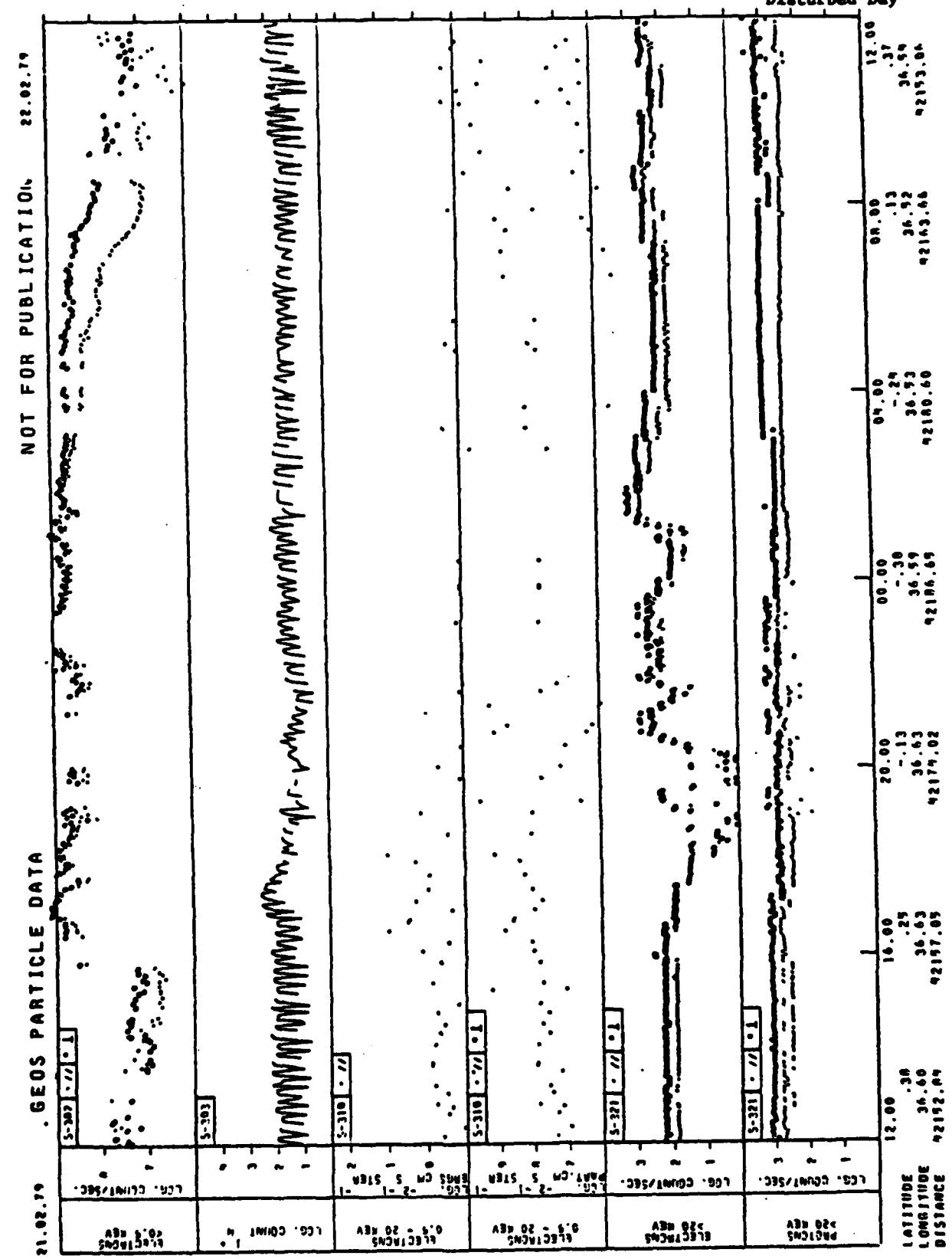

Appendix 2
Disturbed Day

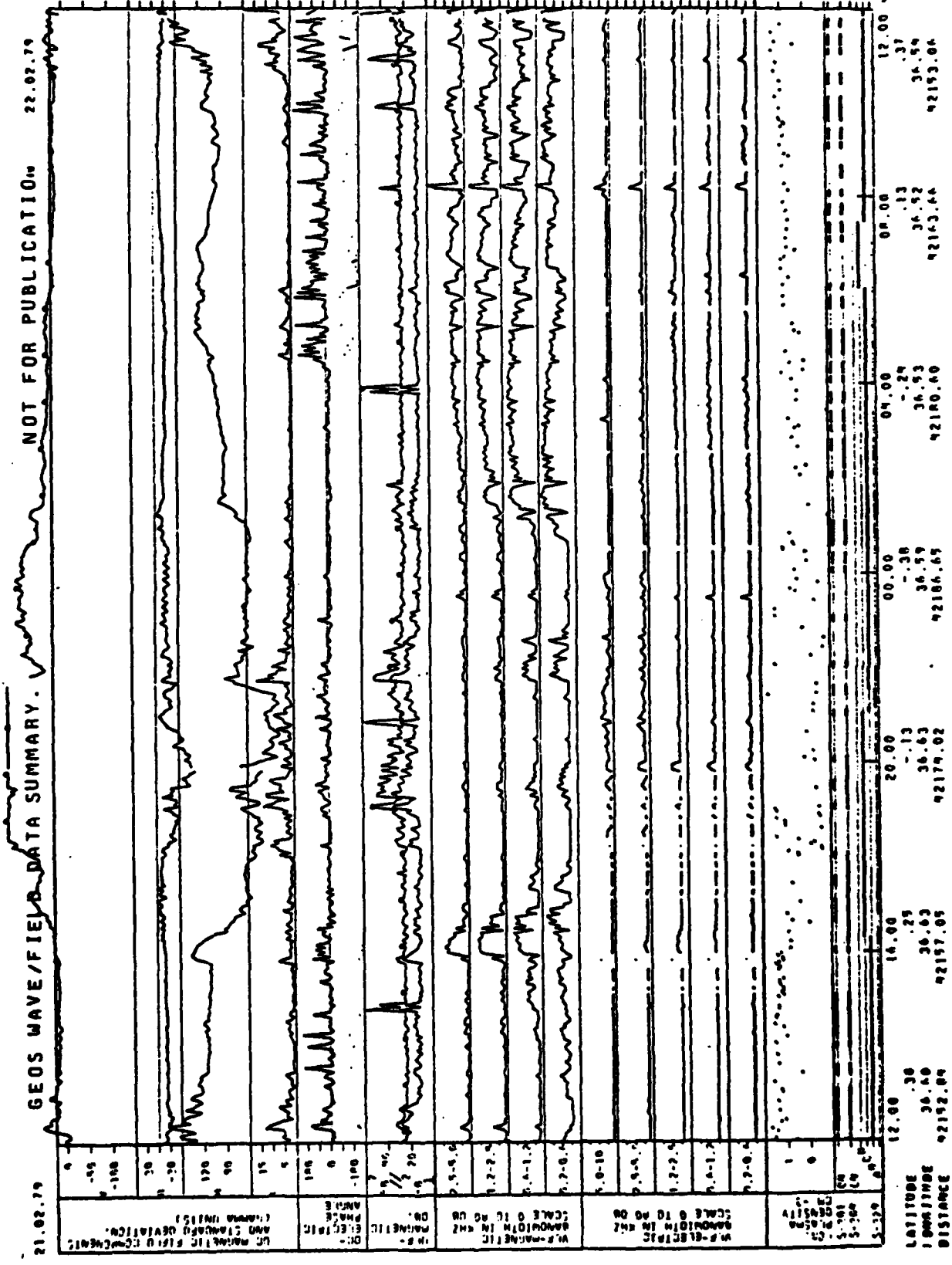

Appendix 2.
Disturbed Day

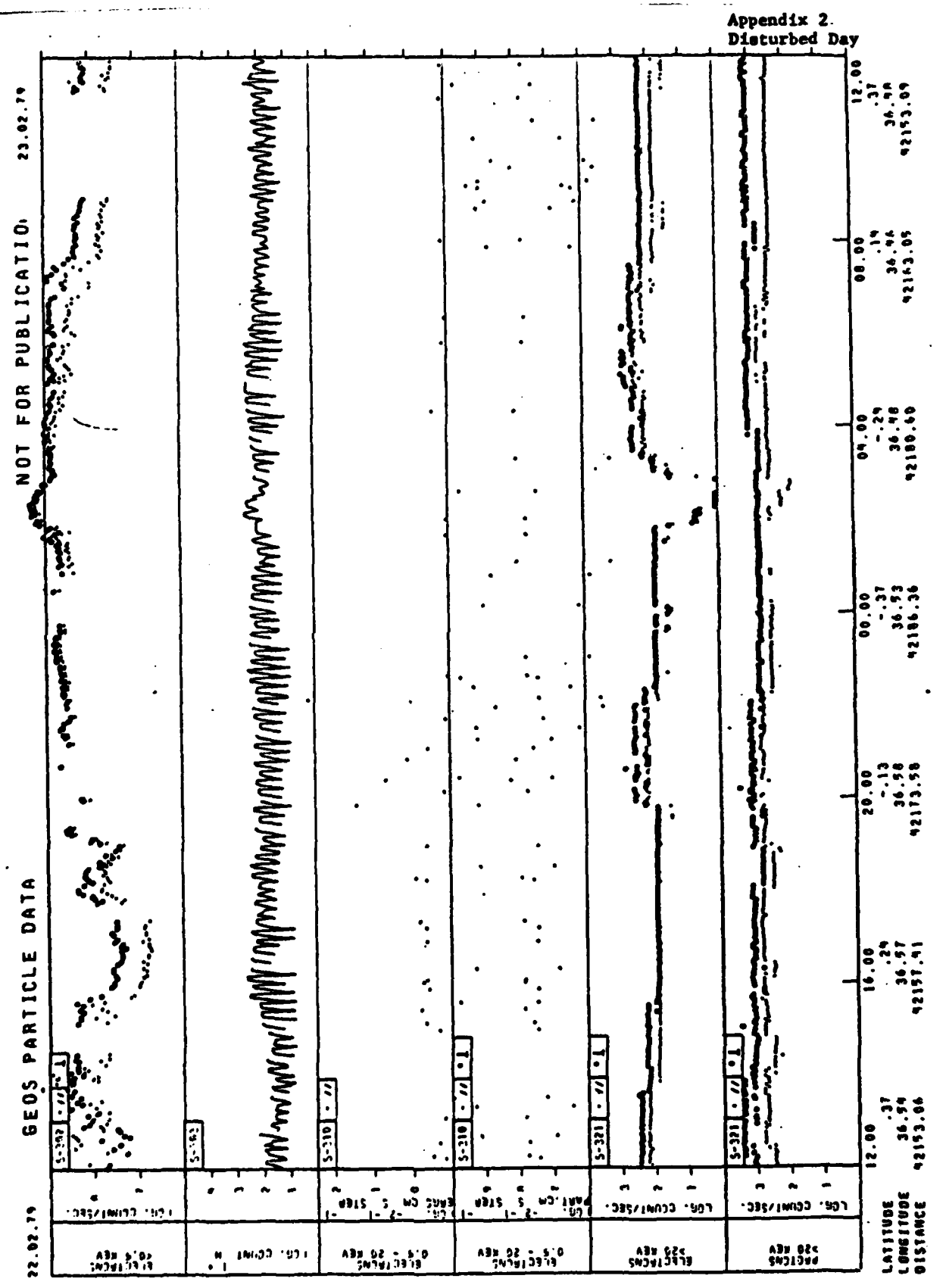

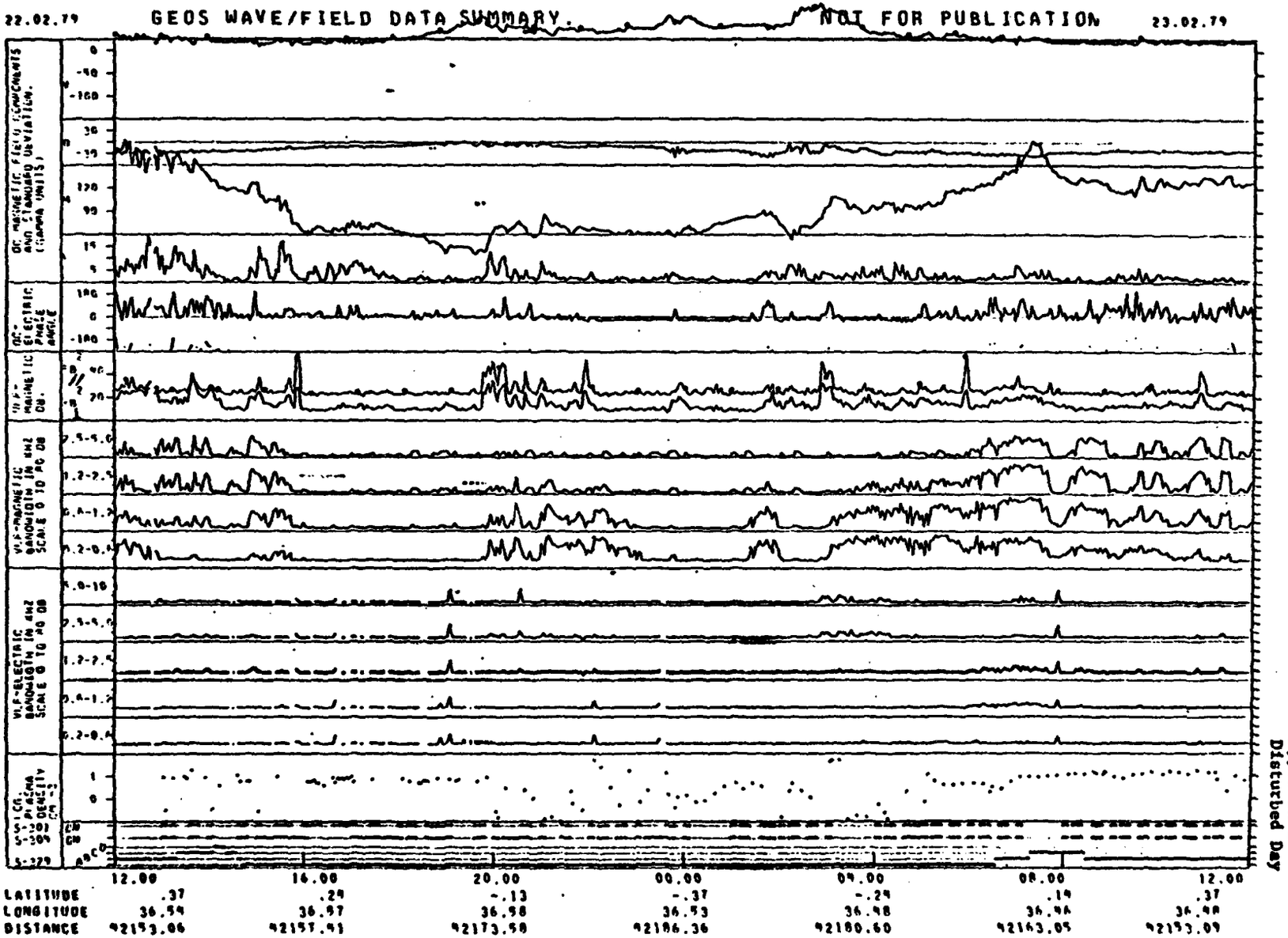

Appendix 2
Disturbed Day

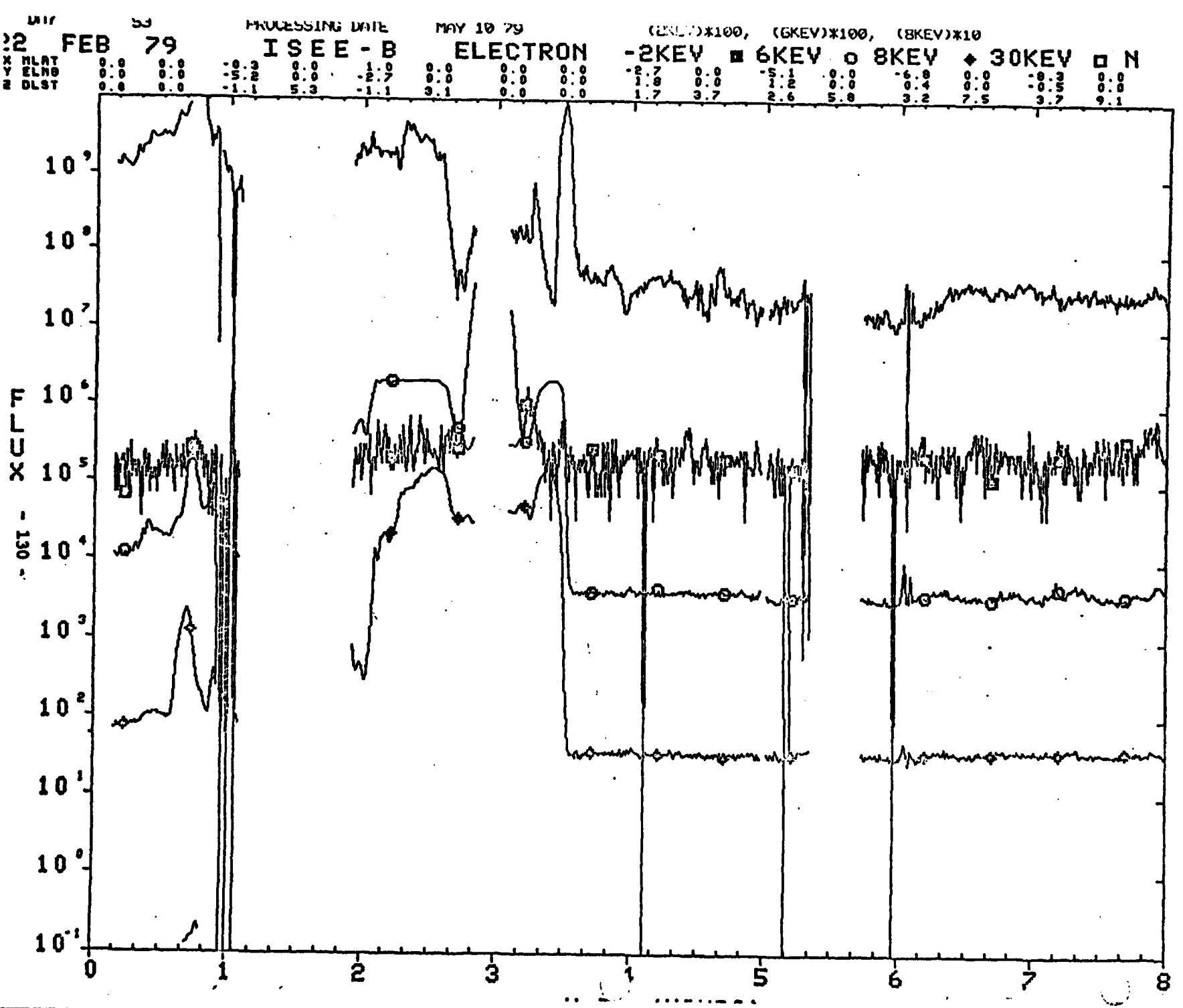
PROCESSING DATE MAY 10 79
12 FEB 79
ISEE-B ELECTRON -2KEV 6KEV 8KEV 30KEV N
(2KEV)*100, (6KEV)*100, (8KEV)*10
FLUX - 130 -
Appendix 2
Disturbed Day

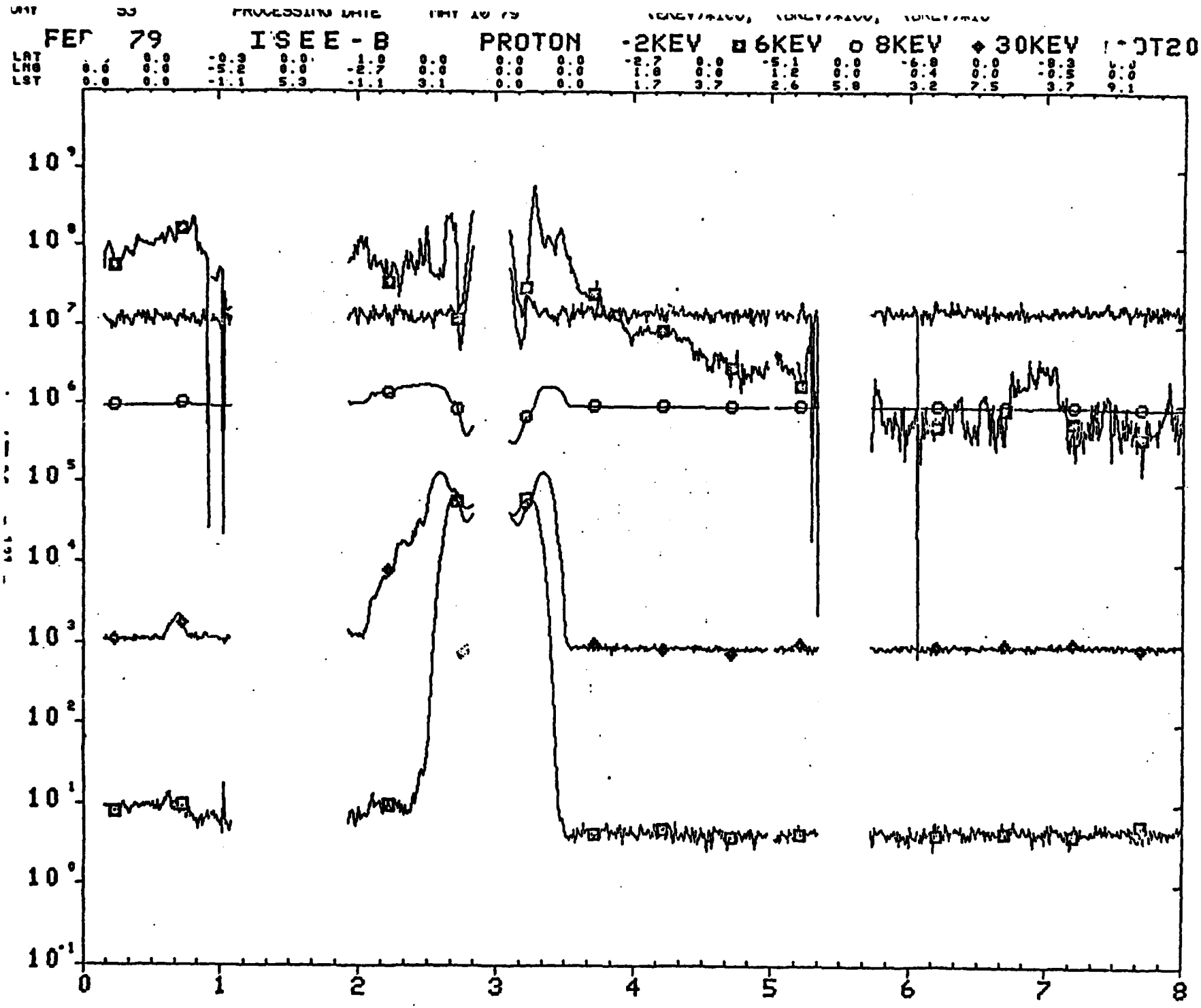

Appendix 2
Disturbed Day

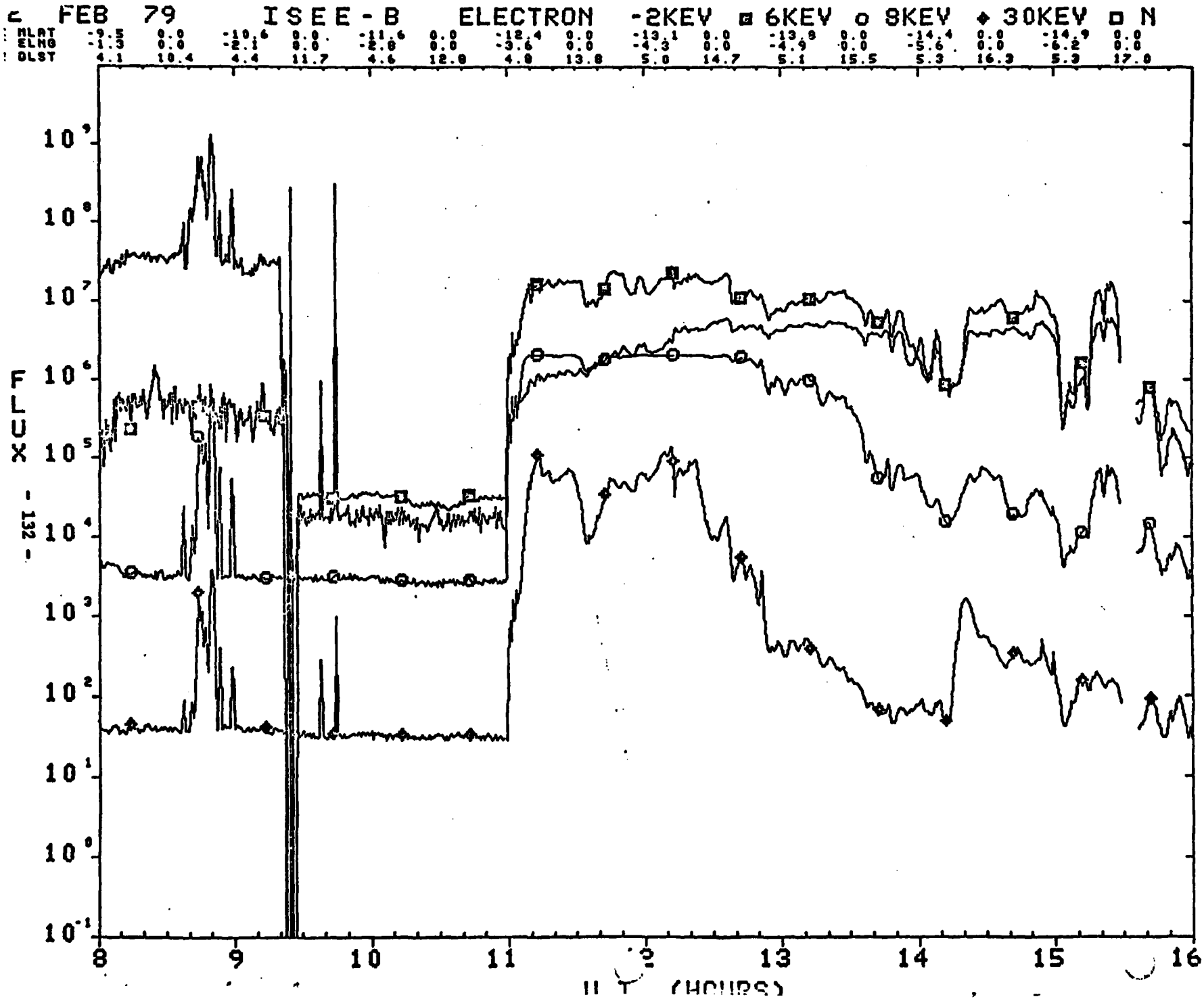

Appendix 2
Disturbed Day

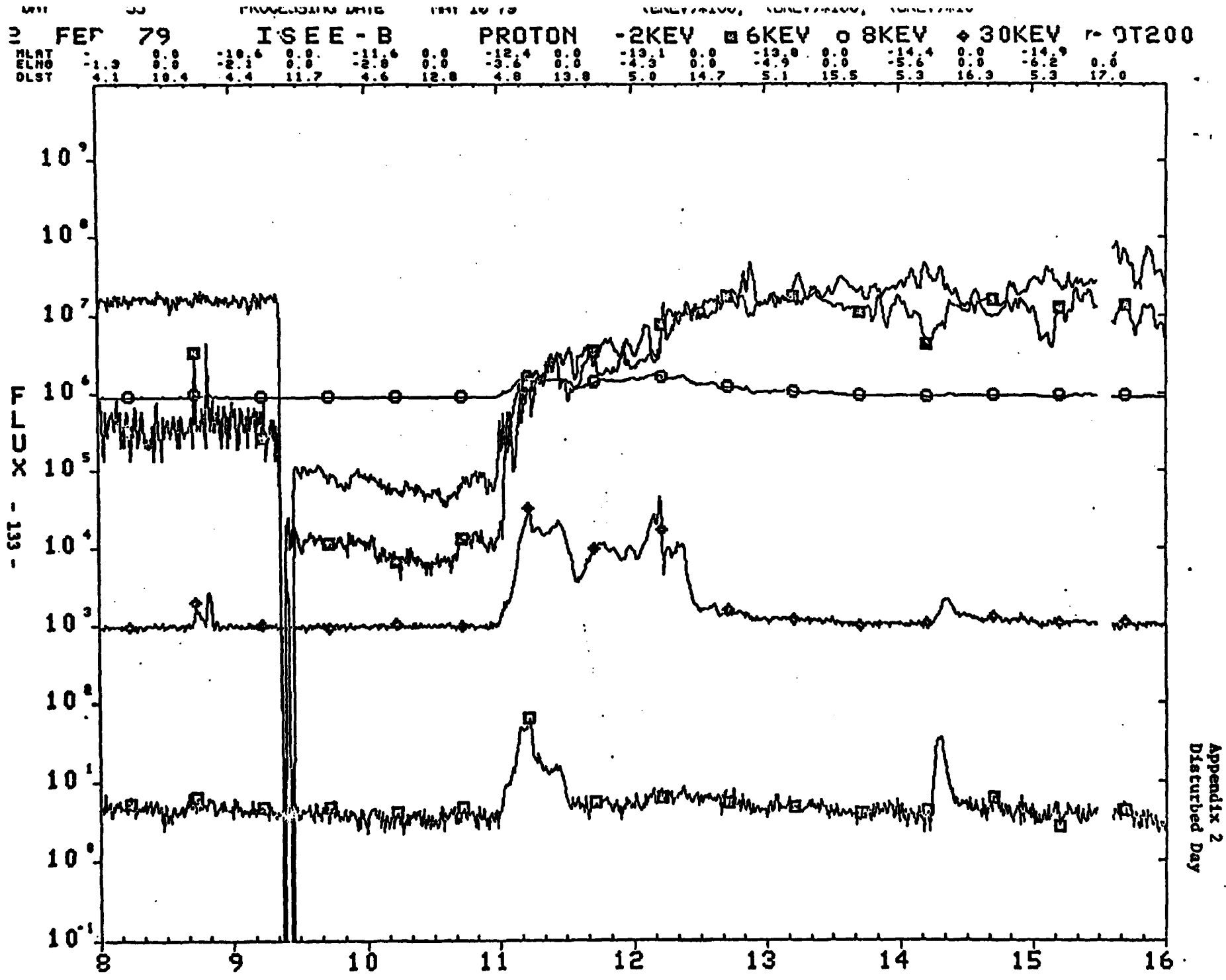

Appendix 2
Disturbed Day

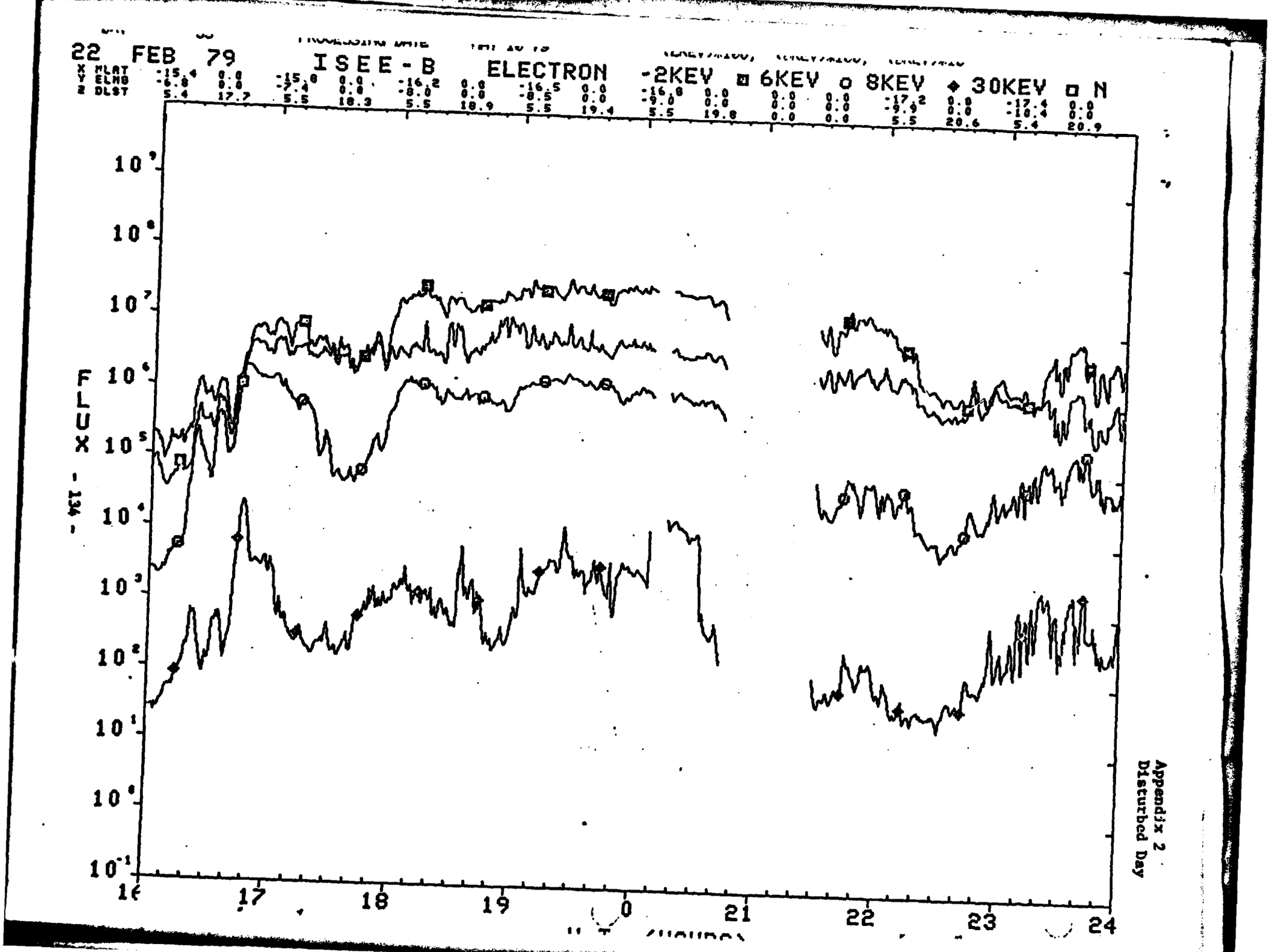
22 FEB 79
ISEE-B ELECTRON -2KEV 6KEV 8KEV 30KEV N
X MLAT
Y ELNG
Z DLST
FLUX - 134 -
Appendix 2
Disturbed Day

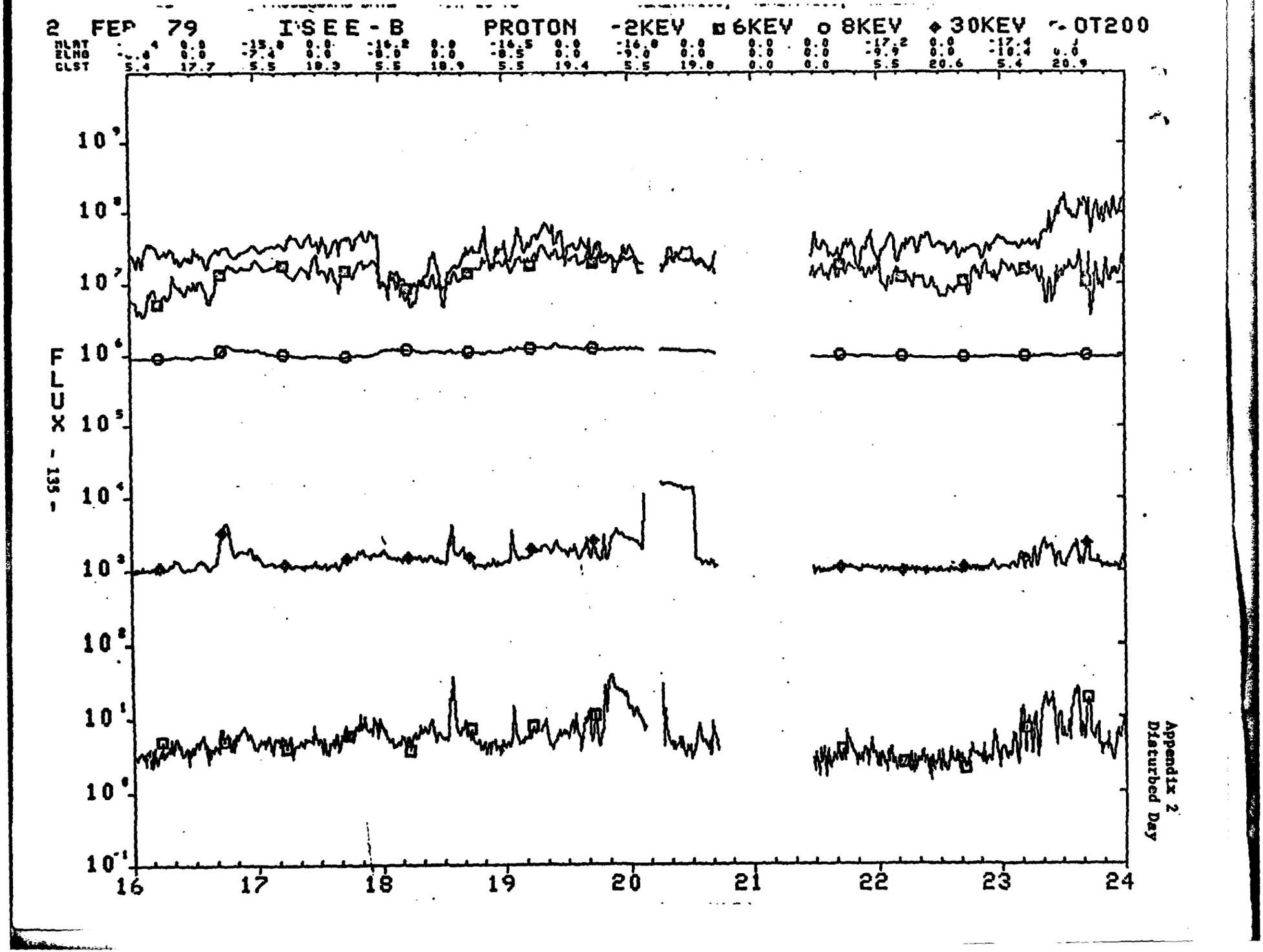
2 FEB 79 ISEE-B PROTON -2KEV 6KEV 8KEV 30KEV OT200
MLAT
ELNG
GLST
FLUX - 135 -
16
17
18
19
20
21
22
23
24
Appendix 2
Disturbed Day